Charles University

Second Faculty of Medicine

Doctoral study programme: Neurosciences

Mgr. Kateřina Štěpánková

Enhancing axon regeneration and neuroplasticity after spinal cord injury:
Bridging the gap between development and disease

Zvýšení regenerace axonů a neuroplasticity po poranění míchy:
Využití poznatků z vývoje centrálního nervového systému k léčbě jeho poranění

Dissertation thesis

Supervisor: MUDr. Lucia Machová Urdzíková, Ph.D.

Praha, 2024

Prohlášení:

Prohlašuji, že jsem závěrečnou práci zpracovala samostatně a že jsem řádně uvedla a citovala všechny použité prameny a literaturu. Současně prohlašuji, že práce nebyla využita k získání jiného nebo stejného titulu

Souhlasím s trvalým uložením elektronické verze mé práce v databázi systému meziuniverzitního projektu Theses.cz za účelem soustavné kontroly podobnosti kvalifikačních prací.

V Praze, 22.03.2024

Kateřina Štěpánková

……..

Podpis autora

Acknowledgment:

First and foremost, I want to express my gratitude to my supervisor, Dr Lucia Urdzíková Machová, for all that she has done for me over the last couple of years. I will be forever grateful to you for being a fantastic mentor and cheerleader for the project, never forgetting to point out the successes rather than the failures, and for all the learning opportunities you have provided me with during this time. You have given me so many opportunities to develop my skills and experience as an independent neuroscientist through your guidance, knowledge, advice and encouragement for progress. Your belief in me was more than enough to keep me going when I didn't think I could. Thank you so much for your support. It has truly been an honour.

Secondly, I would like to thank Associate Professor Pavla Jendelová, who gave me a wonderful opportunity to join the team when I was an inexperienced bachelor student with no vision of my

future scientific path, and also gave me her trust to carry out all the projects with some independence, allowing me to realise my own ideas within the projects. Then the massive thanks go to Professor James Fawcett and Dr Jessica Kwok for their amazing mentorship, guidance and broadening my scientific perspective, thank you both for giving me an amazing start to my scientific career, for all the encouragement and support that convinced me that science is the path I want to take even after completing my PhD.

Thanks also to all my colleagues in the Department of Neuroregeneration who have always been helpful and supportive, even when the science was against me. I apologise if I've missed any names here, but special thanks to Barbora Smejkalová, Lydia Knight, Katerina Havelíkova, Dr Dana Mareková, Dr Jana Svobodová Burianová and Dr Kristýna Árová for making the lab a vibrant and encouraging group for my research, but also for being amazing and lovely friends in the world outside the lab.

A very special word of thanks goes to the IT department at the Institute of Experimental Medicine, who always manage to save the day and have an amazing amount of patience with us scientists. Within the IT team, special thanks are due to Jakub Pjaták, who helped with the formatting of this thesis and provided moral support during the last two years of my PhD.

And finally, a very special thank you to all my amazing friends who have put up with me being a mess and using experiments/papers or dissertation as an excuse, but have still been there for me, and to my family, especially my mum and dad. Your unwavering support has not gone unnoticed. You've never stopped believing in me and that meant so much when I needed it most.

Enhancing axon regeneration and neuroplasticity after spinal cord injury:

Bridging the gap between development and disease

ABSTRACT

The precise wiring of the adult mammalian central nervous system (CNS) is determined during axon growth, guidance and neuroplasticity during and shortly after development. This intricate system is unable to regenerate when the adult spinal cord is injured. It's not well understood how to translate what is known about developmental processes into therapies for spinal cord injury (SCI). Therefore, effective therapies are difficult to find. This thesis aims to fill an important gap in our understanding of how developmental strategies for axonal growth and plasticity are exploited in SCI regeneration. In particular, we will contrast two approaches: (i) reducing the inhibitory environment that forms around the lesion, and (ii) exploiting the inhibitory environment for regeneration by forcing the overexpression of an appropriate integrin isoform in sensory neurons and allowing axons to grow on this environment. In this thesis, Aim 1, we used 4-methylumbelliferone (4-MU) to reduce the inhibitory environment formed around the lesion. The first step was to assess the potential adverse effects of long-term treatment. Using immunohistochemistry, proteomics, biomechanics, qPCR, behavioural tests and commercially available blood and urine tests, we found no irreversible adverse effects. Our next step was to test whether 4-MU could play a role in chronic SCI. 4-MU treatment reduced scarring after chronic SCI. However, the current dose was not sufficient to suppress SCI-induced CS-GAG upregulation. Further dose adjustment will be required to improve functional recovery after SCI. In Aim 2 of this thesis, the integrin adhesion molecule together with its activator was expressed in sensory neurons using a viral vector. The sensory pathway was partially restored in the presence of this adhesion molecule. Many axons regenerated from the thoracic lesion to the brainstem. This is a distance of 4-5 cm. Taken together, these findings have implications for our understanding of the developmental mechanisms of spinal cord regeneration.

Key words

4-methylumbeliferone, extracellular matrix, gene therapy, integrin, perineuronal nets, plasticity, regeneration, spinal cord injury

Zvýšení regenerace axonů a neuroplasticity po poranění míchy:
Využití poznatků z vývoje centrálního nervového systému k léčbě jeho poranění

ABSTRAKT

V průběhu vývoje centrálního nervového systému (CNS) a krátce po něm, dochází k růstu a vedení axonů, a zároveň k jeho plasticitě a tvorbě synaptických zapojení, které u dospělých savců pečlivě určují jeho přesné uspořádání a funkci. V dospělosti je tento proces ukončen a jistým způsobem zakonzervován. Po poranění míchy (*spinal cord injury*, SCI) dospělého jedince tento komplexní a složitý systém není schopen reagovat na poranění stejným způsobem, jako v období vývoje. Způsob, jak přenést poznatky o vývojových procesech do terapií po SCI, není dobře znám, což představuje obtížnost při hledání účinných léčebných postupů. V této práci se snažíme zaplnit důležitou mezeru v chápání toho, jak by bylo možné využít vývojové strategie růstu a plasticity axonů při regeneraci axonů po SCI, a to konkrétně dvěma přístupy: (i) Redukce inhibičního prostředí, které se tvoří okolo léze a (ii) naopak využitím inhibičního prostředí ve prospěch regenerace, a to vynucením nadměrné exprese příslušné izoformy integrínu v senzorických neuronech a umožnění růstu axonů po tomto prostředí. V této práci, pro cíl 1, jsme použili 4-methylumbeliferon (4-MU) ke snížení inhibičního prostředí vytvořeného kolem léze. Prvním krokem bylo posouzení možných nežádoucích účinků dlouhodobé léčby. Pomocí imunohistochemie, proteomiky, biomechaniky, qPCR, behaviorálních testů a komerčně dostupných testů krve a moči jsme nezjistili žádné nevratné nežádoucí účinky. Naším dalším krokem bylo otestovat, zda 4-MU může hrát roli při léčbě chronického SCI. Léčba 4-MU redukovala jizvu v chronické fázi SCI. Každopádně, námi prezentovaná dávka nebyla dostatečně účinná k potlačení SCI indukované upregulace CS-GAG. Ke zlepšení funkčního zotavení po SCI bude nutná další úprava dávky. V cíli 2 této práce byla adhezivní molekula integrín společně se svým aktivátorem exprimována v senzorických neuronech pomocí virového vektoru. V přítomnosti této adhezní molekuly došlo k částečné obnově senzorické dráhy. Mnoho axonů se regenerovalo z hrudní léze do mozkového kmene. Jedná se o vzdálenost 4-5 cm. Dohromady nám tyto výsledky pomáhají pochopit, jak by se vývojové mechanismy daly využít v regeneraci míchy po SCI.

Klíčová slova

4-methylumbeliferon, extracelulární matrix, genová terapie, integrín, perineuronální sítě, plasticita, regenerace, poranění míchy

LIST OF ABBREVIATIONS

4-MU	4-methylumbelliferone
5-HT	5-hydroxytryptamine
AAP	Assembly-activating protein
AAV	Adeno-associated virus
ACAN	Aggrecan
ADAM	A disintegrin and metalloproteinase
ADAMTS	A disintegrin and metalloproteinase with thrombospondin motifs
Apo-J	Apolipoprotein J
BBB test	Basso, Beattie, Bresnahan test
BBB	Blood-brain barrier
Bral1	Brain-specific link protein
BSCB	Blood-spinal cord barrier
CGRP	Calcitonin gene-related peptide
ChABC	Chondroitinase ABC
CLD	C lectin domain
CNS	Central nervous system
CPC	Cetylpyridium chloride
CS	Chondroitin sulfate
CSF	Cerebrospinal fluid
CSPG	Chondroitin sulfate proteoglycan
Ct	Cycle threshold
Ctrl	Cartilage link protein
CTRL	Control
DAPI	4',6-diamidino-2-phenylindole
DCM	Dichlormethane
DMSO	Dimethyl sulfoxide
DRG	Dorsal root ganglion
DSPG	Dermatan sulfate proteoglycan
ECM	Extracellular matrix
EGFR	Epidermal growth factor receptor
EtOH	Ethanol
FAK	Focal adhesion kinase
FN	Fibronectin

GAG	Glycosaminoglycan
Gal	D-galactose
GalNAc	N-acetyl-D-galactosamine
GAPDH	Glyceraldehyde-3-phosphate dehydrogenase
G-CSF	Granulocyte-colony stimulating factor
GFAP	Glial fibrillary acidic protein
GFP	Green fluorescent protein
GlcA	D-glucuronic acid
GlcN	D-glucosamine
GlcNAc	N-acetyl-D-glucosamine
GM-CSF	Granulocyte macrophage colony-stimulating factor
GSK3β	Glycogen synthase kinase 3 beta
HA	Hyaluronan, Hyaluronic acid
HABP	Hyaluronan-binding protein
HAPLN	Hyaluronan and proteoglycan link protein
HAS	Hyaluronan synthase
HSPG	Heparan sulfate proteoglycan
Iba-1	Ionized calcium binding adaptor molecule 1
IBA4	Isolectin B4
IdoA	L-iduronic acid
IFNγ	Interferon gamma
IgCAMs	Immunoglobulin superfamily cell adhesion molecules
IL	Interleukin
iPSC	Induced pluripotent stem cells
ITR	Inverted Terminal Repeat
JNK	c-Jun N-terminal kinase
KSPG	Keratan sulfate proteoglycan
MAG	Myelin-associated glycoprotein
MMP	Matrix metalloproteinase
MRI	Magnetic resonance imaging
NF200	Neurofilament 200
NG2	Neuron-glial antigen
NGAL	Neutrophil gelatinase-associated lipocalin
NgR	Nogo receptor

OMgp	Oligodendrocyte myelin glycoprotein
OPC	Oligodendrocyte precursor cell
PBS	Phosphate-buffered saline
PCR	Polymerase chain reaction
PDGF	Platelet-derived growth factor
PFA	Paraformaldehyde
PKC	Protein kinase C
PNN	Perineuronal net
PTEN	Phosphatase and tensin homolog
RAG	Regeneration-associated genes
RAR	Retinoic acid receptor
ROS	Reactive oxygen species
RPTPβ	Receptor-type protein tyrosine phosphatase beta
RT	Room temperature
SCI	Spinal cord injury
SOCS3	Suppressor of cytokine signaling 3
TIMP-1	Tissue inhibitor of metalloproteinases 1
TnC	Tenascin C
TNFα	Tumor necrosis factor alpha
TnR	Tenascin R
W/O	wash-out
WFA	Wisteria floribunda agglutinin
WHO	World health organization

TABLE OF CONTENTS

1. INTRODUCTION

1.1 Spinal cord Injury

A spinal cord injury (SCI) is a serious condition, often leading to severe morbidity and permanent disability, that can affect anyone at any time, especially in daily life. The spinal cord has three main functions: It sends motor commands from the brain to the body, it sends sensory information from the body to the brain, and it coordinates reflexes. When an injury occurs, i.e., damage to the axons of the nerves that run through the spinal cord, a loss of motor and sensory function occurs and ultimately leads to paralysis, the severity of which depends on the degree of injury. However, SCI brings with it a high degree of health complications and limitations in daily life, such as breathing problems, impaired bladder and bowel functions, disturbances of autonomic functions and impairment of sexual functions.

SCIs can occur when an external physical force causes an acute SCI (traumatic SCIs) or when an acute or chronic disease process, such as a neoplasm, infection or degenerative disc disease, causes a primary injury (nontraumatic SCIs). What traumatic and non-traumatic injuries have in common is that the injury is usually the result of severe trauma, and the primary injury is often irreversible (Ahuja et al. 2017). Accidents are the primary cause of SCIs in daily life, namely traffic accidents (more than 50%), falls (more than 24%), acts of violence (more than 17%) and extreme sports (more than 9%) (‘WHO’, n.d.). Traumatic lesions of the spinal cord axon projection pathways are not treatable. in human patients, although numerous research groups worldwide are investigating possible treatment strategies. The World Health Organisation (WHO) estimates that between 250,000 and 500,000 people suffer from SCI each year. They disproportionately affect patients under the age of 30, result in significant functional limitations for the rest of their lives, and put people at risk of multiple complications leading to increased morbidity and mortality. There is also an increasing incidence of SCI in elderly people in developed countries. This is due to advances in medicine, technology and health care that have increased life expectancy over the last 50 years. But longer life expectancy also means more chronic and acute diseases and higher medical costs. For these patients, SCI is a contributor to age-related functional decline and usually exacerbates pre-existing conditions. In addition, people over the age of 65 have shown an increased susceptibility to SCI. SCI adds to the list of complications that are common in this age group, such as osteoporosis, diabetes, heart disease and lung disease (Ikpeze and Mesfin 2017).

The pathophysiology of SCI involves primary and secondary mechanisms of injury. Although both mechanisms are involved in the neurological dysfunction at SCI. After the initial irreversible mechanical injury leading to necrosis and destruction of neuronal connections, several secondary processes take place that may last for several months until a lesion cavity forms. The location and severity of the spinal cord lesion are used to classify the consequences of injury. Current research efforts are focused on these processes, which are thought to be reversible or modulable to some degree. Such modulation would be beneficial to the patient as it would prevent degenerative damage to the spared tissue, which is known to progress over several months after the actual injury. Secondary processes include oedema, blood-spinal cord barrier (BSCB) disruption, ischaemia, inflammation, oxidative stress, glutamate excitotoxicity and apoptosis, all of which occur immediately after the mechanical insult. The molecular cascades in these processes are interconnected and proceed via positive feedback loops or through the use of different molecular and cellular elements at different time points (Oyinbo 2011). In terms of time, SCI can then be divided into the acute phase (< 48 hours), the sub-acute phase (48 hours to 14 days), the intermediate phase (14 days to 6 months) and the chronic phase (> 6 months) (Ahuja et al. 2017).

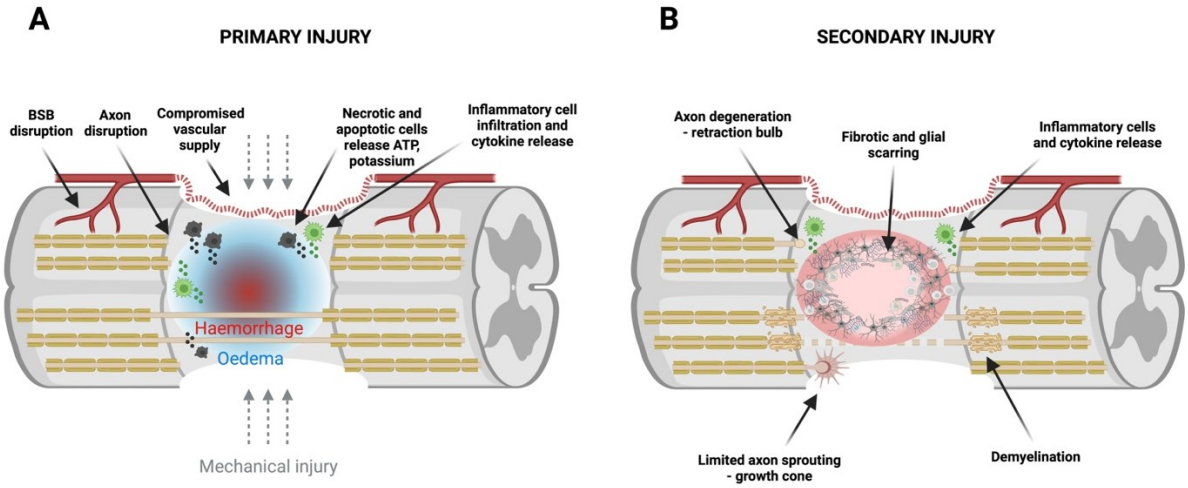

Fig. 1. Pathophysiology of spinal cord injuries. (**A**) Primary injury is caused by the initial external impact. The damage from mechanical injury causes cell death, axon transection, vascular compromise and disruption of the blood-spinal cord barrier (BSCB). Haemorrhage and oedema develop at the site of injury. Inflammatory cells begin to infiltrate, releasing cytokines that further activate the inflammatory cascade. (**B**) Secondary injury can last from minutes to months and years after the primary injury. Axonal and neuronal degeneration and demyelination occur. Some limited axonal sprouting also occurs, but regeneration efforts are hampered by the inhibitory extracellular matrix (ECM) environment formed at the lesion

site. Astrocytes and fibroblasts are activated and form a glial and fibrotic scar. Created with BioRender.com

The injury response following SCI resembles in many ways that of the developmental process. The first is axon guidance. During development, axons extend and navigate to form neural circuits, and after SCI, damaged neurons attempt to regrow axons and connect to new targets. It is also known that certain genes and pathways associated with neural development are reactivated following SCI. In the attempt to repair and regenerate damaged nerve tissue, this reactivation may play a role. Cell identity and function, both during development and in response to injury, may also change. There may be an attempt to recruit and activate different cell types, including stem cells, to participate in tissue repair after SCI. Finally, inflammation and activation of the immune system is part of the body's response to injury. There are also immune responses during development that affect how neural circuits form (Filous and Schwab 2018). However, the inflammatory response that follows a SCI can be either helpful or harmful. Despite these potential similarities, spinal cord regeneration in mammals is limited. Functional recovery after SCI is often only partial. In this thesis, we present a perspective on research in regenerative medicine that is inspired by the developmental mechanisms that facilitate regeneration after SCI.

1.2 Axotomy: cellular and molecular events after nerve injury

The SCI is often associated with axotomy that involves cutting or otherwise severing of an axon. When an axon is severed, there is an immediate influx of calcium at the injured axon tip (Bradke, Fawcett, and Spira 2012), the concentration of which exceeds 1 mM (Ziv and Spira 1995). This drastic increase in intracellular calcium is necessary for the initiation of axon regeneration, as neurons in a calcium-free environment are unable to initiate axon growth (Kamber, Erez, and Spira 2009; Ziv and Spira 1997). A retrograde first-wave injury signal transmits to the cell body through a backward propagating calcium wave, which is thought to lead to chromatin remodelling (Cho et al. 2013). This is the first communication between the injured tip and the soma. The cytoskeleton is remodelled (Yoo et al. 2003). After this initial burst of events, the soma undergoes chromatolysis, in which chromatin in the nucleus dissolves and disperses to the cell periphery as the cell body swells. Excitatory inputs are largely eliminated, leaving only inhibitory inputs as the main connection to the injured soma.

Local protein synthesis is necessary for the formation of the important retrograde signal, in which proteins such as importins and vimentin are translated locally in the injured axon (Yudin et al. 2008; Perry et al. 2012). Disruption of this signal attenuates the cellular response to injury (Yudin et al. 2008; Perry et al. 2012). The motor binding protein JIP, which interacts with Jun-N-terminal kinase (JNK), connects the axon vesicles to the injury signal and retrogradely transports the injury signal back along the microtubules(Abe et al. 2009). When the resting potential of the membrane is restored, the axon can form either a retraction bulb or a new growth cone (Fig. 2).

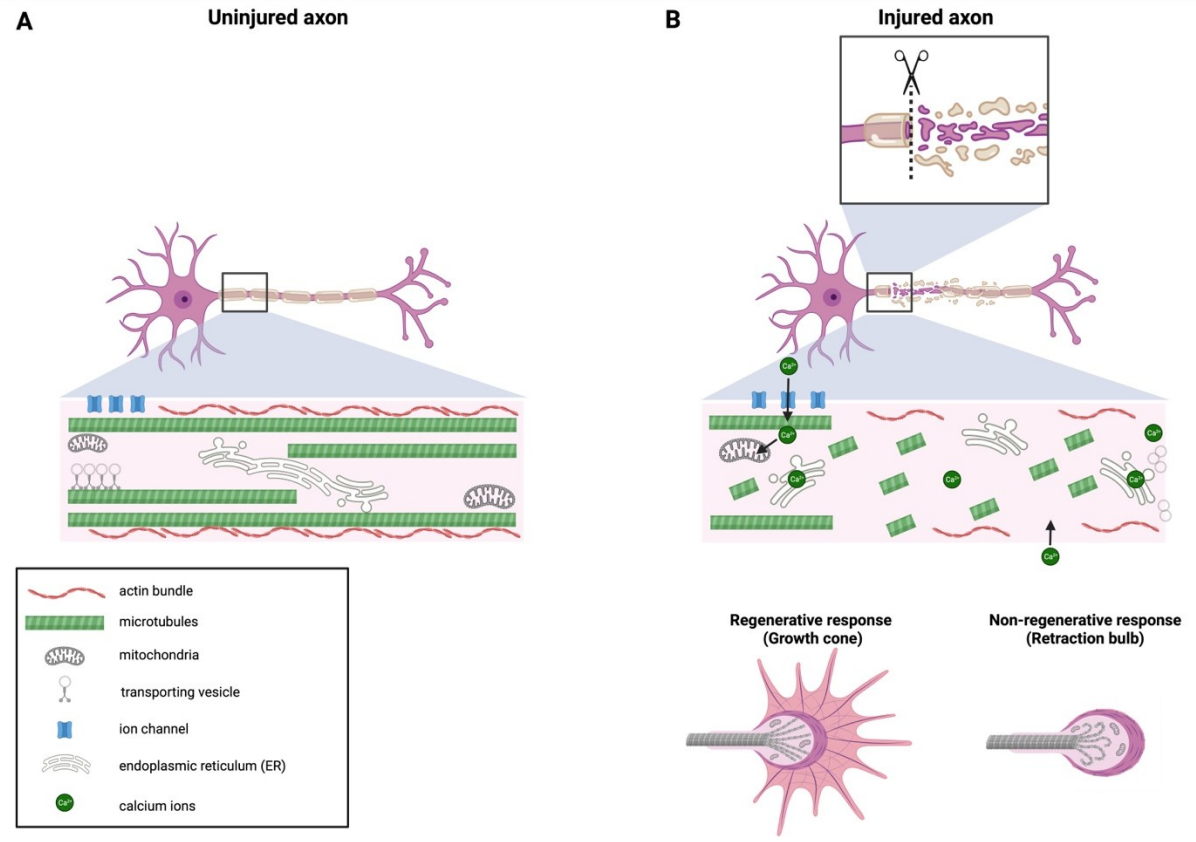

Fig. 2. Cytoskeletal organisation in growth cones and retraction bulbs in neurons. (**A**) Schematic representation of an uninjured axon. (**B**) Following axotomy, a series of cellular events occur at the site of axon injury, including rupture of the axon plasma membrane, calcium and ion influx, and cytoskeletal disassembly. Although the distal segment undergoes self-destructive degeneration, the fate of the proximal end depends largely on the type of axon and the nature of the injury. Regeneration-competent neurons follow the anabolic pathway. In these neurons, motile growth cones reform with reorganised cytoskeletons that will guide polarised extension. Regeneration incompetent neurons, however, follow the catabolic pathway, leading to the formation of retraction bulbs with highly disorganised microtubules and other organelles. Created with BioRender.com.

Retraction bulbs are thought to be the non-growing counterpart of growth cones, where growth failure is attributed to microtubule destabilisation (Ertürk et al. 2007). Within the axoplasm, calpain proteins are activated to cleave membrane spectrins, resulting in a brief proteolysis of the cytoskeleton (Czogalla and Sikorski 2005). This is thought to restructure the microtubule ends and is necessary for conversion to a growth cone (D. Gitler and Spira 1998; Daniel Gitler and Spira 2002). When the microtubules repolymerise, a brief realignment of polarities occurs. Vesicle transport resumes and selective traps are formed for anterogradely transported vesicles (Daniel Gitler and Spira 2002). Golgi vesicles, for example, can only be transported anterogradely. When the microtubules in the axon realign with the plus end outward, these vesicles remain trapped and therefore enable reconstruction of the growth cone.

The newly formed growth cone begins to recycle material, generating immediate replenishment, but ultimately local protein synthesis is necessary for the formation of the growth cone (Verma et al. 2005). The synthesis of proteins within the injured axon is a crucial event underlying regeneration, and faulty regulation of this process can lead to growth deficits (C. J. Donnelly et al. 2013).

After the formation of the growth cone, injured axons begin to regenerate or sprout. Previous studies have shown that axonal regeneration or sprouting is associated with the activation of genes related to axonal growth (Represa et al. 1993; Bendotti, Pende, and Samanin 1994; Mearow et al. 1994). Indeed, neurite outgrowth has been associated with the ability to express genes related to regeneration that are normally expressed during development (Skene 1989; van Niekerk et al. 2016).

Taken together, these results show that different growth forms are associated with different patterns of protein synthesis. Important studies have shown the importance of coordinated regulation of protein expression through the activation of specific signalling networks during axonal growth and regeneration.

1.3 The struggle to make CNS axons regenerate

Where axons can regenerate, as in peripheral nerves, they can restore function spontaneously. In the CNS, however, axon regeneration fails. This is the main reason why paralysis and loss of sensation are permanent in conditions such as SCI. Regeneration of

axons in patients with spinal cord injuries is one of the greatest hopes for restoring useful functions.

During development, neurons spread their axons throughout the nervous system and make connections to postsynaptic targets that are often quite distant from their origin. The ability of these young neurons to robustly extend their axons decreases dramatically in adulthood. This reduced intrinsic growth capacity is a key mechanism underlying the inability of adult CNS neurons to regenerate their axons after injury (Blesch and Tuszynski 2009; James W. Fawcett and Verhaagen 2018; Goldberg et al. 2002; Plunet, Kwon, and Tetzlaff 2002). The weak regenerative response after transection is not the only reason why CNS axons do not regenerate spontaneously; the environment surrounding CNS lesions also plays a crucial role in inhibiting axon growth.

Because CNS axons cannot regenerate spontaneously, sensory, motor and/or autonomic deficits are often permanent after CNS injury. Therefore, there is still a great unmet need for therapeutic strategies to improve the regeneration of injured CNS axons and thus improve function. Restoring regeneration and plasticity is therefore complex, and multiple inhibitory mechanisms must be considered. Regardless of the cause, we are now at a stage where the biology of regeneration failure is increasingly understood, and solutions are being found (James W. Fawcett 2020). To enhance axonal growth and promote functional recovery, the various intrinsic and extrinsic factors that control axon regeneration and navigation in the inhibitory environment of the central nervous system must be identified. In the next subsections, we will discuss some of the important extrinsic and intrinsic key factors that limit axon regeneration (Afshari, Kappagantula, and Fawcett 2009).

1.3.1 Extrinsic factors

The extrinsic factors are defined as the factors related to the environment. In other words, these factors can make it difficult for axons to navigate, create a physical barrier, send misleading signals and limit the resources axons need to grow. The extrinsic factors that negatively influence CNS axon regeneration are located in and around the lesion scar (Chew, Fawcett, and Andrews 2012; James W. Fawcett et al. 2012). Upon injury, astrocytes are activated and form a new glia limitans around the lesion area in order to re-establish the blood-brain barrier (BBB). Although the lesion area is usually referred to as a glial scar, it has a fibrous core surrounded by reactive astrocytes. This core is composed of infiltrating

fibroblasts and pericytes that have migrated from the dura mater and blood vessels, respectively (Klapka et al. 2005; Fagoe, van Heest, and Verhaagen 2014). The fibrous core consists of a collagen IV-containing matrix that serves as a scaffold for axon growth inhibitory molecules, such as chondroitin sulfate proteoglycans (CSPGs), and tenascins (Chew, Fawcett, and Andrews 2012; Klapka et al. 2005). The fibrous core contains inhibitors produced exclusively by astrocytes, in addition to molecules produced by fibroblasts, highlighting the role of the extracellular matrix (ECM) as a scaffold for soluble inhibitors (Vogelaar et al. 2015). Other inhibitors are not localized in the scar but in the white matter. Myelin components, like myelin-associated glycoprotein (MAG), Nogo, and oligodendrocyte myelin glycoprotein (OMgp) are very potent inhibitors of axon regeneration (J. K. Lee and Zheng 2012).

1.3.2 Intrinsic factors

Manipulations that remove or neutralise these inhibitory molecules, as described above, result in an enhanced anatomical regrowth of some types of axons. However, in most cases, only a small number of injured CNS axons are able to regenerate, which is consistent with the idea that the lack of regeneration in the adult CNS is an intrinsic property of the injured neurons. Therefore, if the severed axons themselves do not attempt to regenerate, there is little point in making the external environment of the axon more conducive to regeneration. In this part of the thesis, I will describe some of the most important intrinsic factors that influence the ability of axons to regenerate.

Unlike extrinsic factors, intrinsic factors include the genetic, physiological and pathological properties of a single neuron/axon. Axons from the PNS generally have a greater capacity for regeneration than those from the CNS. The lower regenerative capacity may have evolved as a protective mechanism to prevent overgrowth and the possibility of miswiring within the complex circuits of the CNS, with deleterious consequences for the higher vertebrate (Afshari, Kappagantula, and Fawcett 2009). During development, neurons display robust outgrowth capacity through a cell-intrinsic programme consisting of multiple pathways. Following connection establishment, adult CNS neurons have limited regenerative capacity due to reduced calcium changes, lack of increased histone acetylation, lack of robust expression of regeneration-associated genes (RAGs), limited local protein synthesis and the presence of inhibitors of axon regrowth (such as PTEN, SOCS3 and EFA-6). The lack of ability to regenerate neurons involves ineffective Wallerian degeneration (a

process of active degeneration of the distal end of axons as a result of injury), possible defects in injury signalling, lack of a robust response to injury, limited local synthesis capacity and the presence of inhibitors of axonal growth (Mar, Bonni, and Sousa 2014).

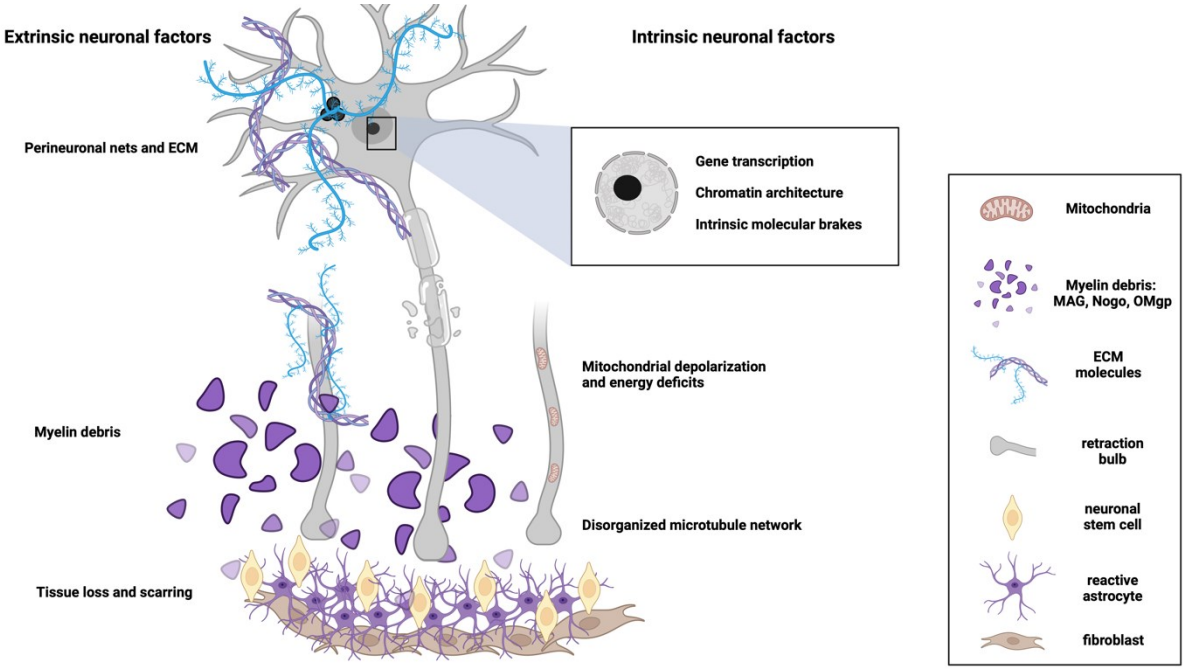

Fig. 3. Extrinsic and intrinsic mechanisms controlling axon regeneration. Schematic representation of extrinsic and intrinsic mechanisms controlling structural plasticity and axonal regeneration after CNS injury. Created with BioRender.com.

1.4 It all comes down to support - the role of the ECM in axon regeneration

As mentioned earlier, the CNS has little intrinsic regenerative capacity, although some functional recovery does occur. This occurs primarily in the form of sprouting, dendritic remodelling and changes in neuronal coding, firing and synaptic properties; elements collectively referred to as plasticity. An important approach to repairing the injured CNS is therefore to harness, promote and refine plasticity.

In adults, this is partially limited by the ECM. The ECM of the CNS is a major component of brain and spinal cord tissue. It consists of a dense substrate that occupies the space between neurons and glia and is estimated to account for 10-20% of the total brain volume (Nicholson and Syková 1998). It contains a variety of molecules, most of which are secreted by the cells of the CNS. While the ECM typically provides a supportive scaffold for CNS neurons, its role is not only structural but also beyond. The ECM is homeostatic, actively regulating and of great signalling importance, both directly via receptor or coreceptor-

mediated actions and via the spatial and temporal localisation of other signalling molecules. It also actively influences cell migration, axonal guidance and synaptogenesis during development and plays an important role in adult life in maintaining synaptic stability and limiting abnormal restructuring (Burnside and Bradbury 2014).

However, following CNS injury or disease, changes in the expression and composition of ECM components may prove detrimental to neuronal repair. Not only does the ECM provide an important environment to support a healing and/or regenerative response, but some molecules present in the ECM also restrict plasticity and limit healing. Therefore, an important therapeutic concept is to make the ECM environment more permissive by manipulating key components such as the inhibitory CSPGs, or to overexpress an appropriate isoform of ECM-binding receptors such as integrins, which binds the inhibitory molecules and uses them as a substrate, leading to an improvement in regeneration

The CNS ECM is rich in glycoproteins and proteoglycans. Fig. 4 shows the typical composition of the ECM and their interaction. The core component hyaluronan (HA; also known as hyaluronic acid or hyaluronate) forms the basic framework for the attachment of other glycoproteins and proteoglycans. These include above all tenascins and sulphated proteoglycans, which are stabilised by link proteins. These components may be arranged diffusely in the interstitial space or in condensed structures that include small 'axonal sheaths' encapsulating presynaptic terminal fibres and synaptic boutons, clustered matrix arrangements around nodes of Ranvier, and perineuronal nets (PNNs) surrounding the cell soma, proximal dendrites and axon initial segments of some neurons (Brückner et al. 1993; Celio et al. 1998). The density of PNNs varies: In the spinal cord, PNNs surround about 30% of motor neurons in the ventral horn, 50% of large interneurons in the intermediate grey and 20% of neurons in the dorsal horn (Lüth, Fischer, and Celio 1992; Brückner et al. 1996; 1994; Galtrey et al. 2008). The following section briefly describes the structure of some matrix components that are prominent and known to be relevant for plasticity and repair.

1.4.1 ECM structure and components

ECM is a complex network of molecules that provides structural support and guidance for developing neural cells. It is composed of proteins such as laminins, fibronectins and collagens. They form a scaffold-like structure that guides axon growth and synapse

formation. ECM proteoglycans and glycoproteins regulate cellular interactions, influencing neuronal migration, plasticity and overall CNS development (Karamanos et al. 2021).

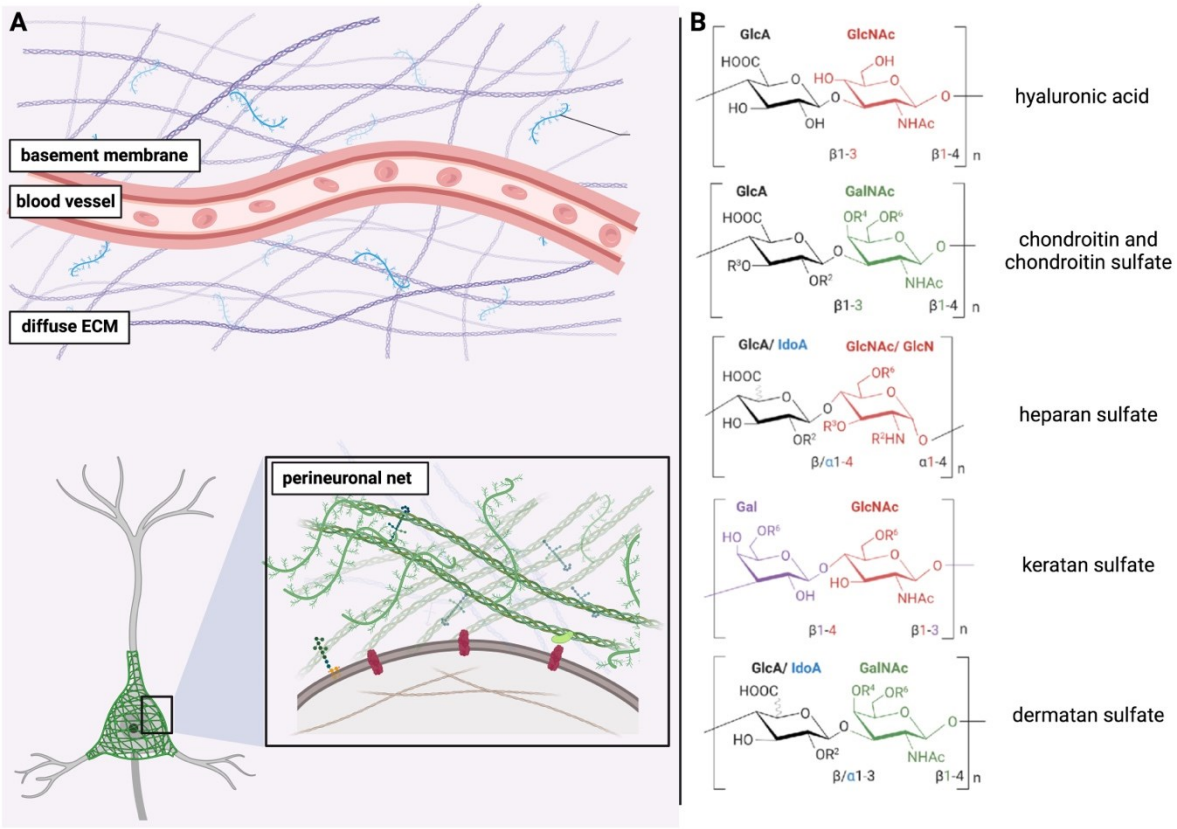

Fig. 4. Structure and components of the extracellular matrix and major glycosaminoglycans (GAGs). (**A**) In the CNS, the ECM is organised into basement membranes surrounding blood vessels, a diffuse interstitial matrix and condensed structures in the form of perineuronal nets surrounding the cell soma, proximal dendrites and axon initial segments of some neurons. (**B**) Structures of major GAGs: hyaluronic acid, keratan sulphate, chondroitin and chondroitin sulphate, dermatan sulphate and heparan sulphate. The monomers of the disaccharide building blocks are abbreviated as GlcA -D-glucuronic acid; GlcNAc -N-acetyl-D-glucosamine; Gal -D-galactose; GalNAc -N-acetyl-D-galactosamine; IdoA -L-iduronic acid; GlcN - D-glucosamine. Panel B is a modification of (Couto, Rodrigues, and Rodrigues 2022). Created with BioRender.com.

1.4.1.1 Laminin

Laminins, family of glycoproteins, are widely distributed in the CNS. They are heterotrimeric glycoprotein cell adhesion molecules and form the major non-collagenous glycoprotein of the basal laminae (Timpl et al. 1979). Through interaction with integrin and non-integrin receptors (such as syndecans, dystroglycans and lutheran blood group glycoprotein) (Durbeej 2010), laminin exerts a wide variety of important functions in the

CNS under both physiological and pathological conditions. The isoform diversity is achieved by the combinatorial expression of different α-, β- and γ-subunits, which form 15 unique laminin isotypes with different functions. However, the exact functions of each laminin molecule in CNS development and homeostasis are still largely unclear. The chains are arranged in a cruciform or T-shaped structure and contain globular (G) and rod-shaped domains that are required for self-assembly, polymerisation with neighbouring laminins and interaction with other molecules and receptors. Polymerisation of laminin occurs via interactions between the N-terminal G domains of the short arms and interactions with the cell surface are thought to occur predominantly via the longest arm through a tandem of five laminin G-like domains of the C-terminus of the α-chain (Hohenester and Yurchenco 2013; P. D. Yurchenco and Cheng 1993). Laminins are thought to be essential canonical adhesive and growth-promoting molecules that provide a substrate for neuronal migration and axonal pathfinding during development (Nirwane and Yao 2019).

1.4.1.2 Fibronectin

Fibronectin (FN) is a large dimeric protein consisting of three distinct tandem repeats (I, II and III). These repeats contain functional domains that, like laminin, enable polymerisation and interactions with other ECM components or cell surface receptors. Within the matrix, collagen interacts with FN I and II and heparan sulphate proteoglycans and tenascin interact with sites in FN III (Ingham, Brew, and Erickson 2004; Singh, Carraher, and Schwarzbauer 2010). The N-terminal type I repeats enable the self-interaction required for fibril formation, a process that is also cell-dependent, with matrix assembly controlled by receptors such as integrins that bind within FN III (Schwarzbauer 1991). The association of cytoplasmic integrin domains with the cytoskeleton via adaptor proteins (such as focal adhesion kinase) also suggests that fibronectin plays a central role in migration, morphogenesis and proliferation (Pankov and Yamada 2002).

1.4.1.3 Collagen

In the systemic ECM, the most common matrix components are members of the collagen family, which provide the structural integrity of the parenchyma and contribute to the stability and biomechanical properties. There are several types of collagens, of which approximately 90% are fibril-forming following the association of multiple triple helixes and contribute to the tensile strength of common systemic connective tissues and cartilage (Gelse, Pöschl, and Aigner 2003). In contrast, the most important collagen in CNS ECM is

basal laminae collagen IV. It forms a more flexible triple helix that polymerises itself into a network and serves as a scaffold for the integration of laminin and fibronectins into a planar basement membrane; a matrix meshwork that is additionally interconnected via other glycoproteins and sulphated proteoglycans (Peter D. Yurchenco 2011). In the injured brain and spinal cord, collagen IV, along with types I and III (Matthews et al. 1979; Weidner, Grill, and Tuszynski 1999), is the predominant fibrous element of scar tissue (Hermanns, Klapka, and Müller 2001), in which cells located near the lesion release chains of protocollagens that self-assemble into a dense network (Timpl and Brown 1996).

1.4.1.4 Hyaluronan

Hyaluronan (HA) is an anionic, non-sulphated glycosaminoglycan and one of the main components of ECM. HA is evolutionarily conserved and found in abundance throughout the body. As a simple linear polysaccharide, HA exhibits a variety of biological functions. HA interacts with various molecules to maintain tissue homeostasis and organise the structure of the ECM. HA is widely distributed in both the diffuse matrix and PNNs. HA is a long linear polysaccharide consisting of repeating, non-sulphated N-acetylglucosamine and glucuronic acid disaccharide units linked by β1-4 and β1-3 bonds. HA forms the matrix architecture into which proteoglycans and glycoproteins are non-covalently incorporated (Fraser, Laurent, and Laurent 1997). It is known to bind to the extracellular receptors CD44 and CD168 (Toole 1990; Aruffo et al. 1990); however, results from in vitro modelling suggest that HA is anchored within PNNs to the neuronal cell surface via its synthesising enzyme hyaluronic acid synthase (HAS) (Kwok, Carulli, and Fawcett 2010; Sarama Sathyaseelan Deepa et al. 2006). In mammals, there are three HAS enzymes (HAS1,2,3), which are transmembrane proteins that produce HA on the inner surface of the plasma membrane and eject nascent HA from the cell (Maloney et al. 2022). Due to its biophysical properties and contribution to the structural integrity of the ECM, it plays a key role in cell proliferation and morphogenesis together with receptor interactions on the cell surface (Toole 2001). Cell receptor activation has far-reaching consequences, including proliferation (Bourguignon et al. 1997), cytoskeletal reorganisation (Oliferenko et al. 2000) and regulation of inflammation (Jiang, Liang, and Noble 2007), and its linkage with other matrix components enables a complex network of protein-protein interactions (Zacharias and Rauch 2006).

1.4.1.5 Tenascins

Tenascins are a family of four similar glycoproteins (tenascin-C, -R, -X and -W), but only two of them are found on CNS ECM - tenascin-C (TnC) and tenascin-R (TnR) (Chiquet-Ehrismann 2004). TnC forms hexamers consisting of a central globular core surrounded by six identical polypeptide arms. TnC is expressed in neuronal and non-neuronal tissues during development and repair and specifically in areas of neurogenesis and plasticity in adulthood (Šekeljić and Andjus 2012). TnC is known to bind to cell surface integrins, immunoglobulin cell adhesion molecules (IgCAMs), annexin II and the transmembrane receptor protein tyrosine phosphatase β (RPTPβ), and to interact with fibronectin and sulphated proteoglycans (Šekeljić and Andjus 2012; Jakovcevski et al. 2013) . TnR forms mainly trimeric structures that have a similar consecutive arrangement of domains as TnC. TnR is not found in the systemic ECM. It is synthesised exclusively in the CNS and secreted by oligodendrocytes and some neurons, where it contributes to the formation of PNN (F. S. Jones and Jones 2000).

1.4.1.6 Hyaluronan and proteoglycan link protein (HAPLN)

There are four members of the link protein family: cartilage link protein (Crtl1 [HAPLN1]), brain-derived link proteins 1 and 2 (Bral1 [HAPLN2], Bral2 [HAPLN4]) and HAPLN3 (Spicer, Joo, and Bowling 2003). In the CNS, Crtl1 plays a crucial role in the formation and stability of CSPG and HA complexes (Kwok, Carulli, and Fawcett 2010). In addition, PNNs are also stabilised by Bral2, while perinodal ECM has been reported to be associated with higher concentrations of Bral1. Ctrl1 is thought to classically binds the CSPGs aggrecan and neurocan, while Bral2 localises with the CSPG brevican (Bekku et al. 2003; R. A. Asher et al. 1995).

1.4.1.7 Sulphated proteoglycans

Proteoglycans consist of a core protein covalently bound to negatively charged glycosaminoglycan (GAG) chains, which in turn are differently sulphated. Depending on the combination of constituent sugars, GAGs are classified as heparan sulphate (HSPG), keratan sulphate (KSPG), dermatan sulphate (DSPG) or chondroitin sulphate (CSPG).

In HSPG, DSPG and CSPG GAG, synthesis is initiated in the Golgi by the sequential addition of four monosaccharides [xylose, two molecules of Gal and GlcA] to form a linker tetrasaccharide. In KSPG, the GAGs are derived from N- or O-linked oligosaccharides. Unbranched polysaccharide chains are then elongated by repeated alternate addition of an

amino sugar and GlcA. In HSPG and KSPG, the amino sugar is N-acetylglucosamine; in CSPG and DSPG, the amino sugar is N-acetylgalactosamine (GalNAc). The crucial step in the synthesis of chondroitin sulphate and dermatan sulphate GAGs is the epimerisation of GlcA to its stereoisomer iduronic acid; the presence of iduronic acid leads to the synthesis of dermatan sulphate. GAG chains are additionally variably sulphated by sulphotransferase enzymes (Iozzo and Schaefer 2015). CSPGs are described in more detail owing to their importance for CNS plasticity and repair.

1.4.1.8 Chondroitin sulphate proteoglycans

CSPGs are a well-studied family of CNS ECM molecules. They are known to play an important role in preventing nerve growth and limiting plasticity after CNS injury. Members of the CSPG family involved in the response to CNS injury include the lecticans, NG2, phosphacan and the small leucine-rich proteoglycans decorin and biglycan. The structure of a CSPG consists of a protein core covalently linked to one or more simple GAG chains, which have distinct roles in the biological function of the CSPG (Laabs et al. 2007; Bukhari et al. 2011). Several studies emphasised the important role of GAG chains in neuronal growth inhibition and regeneration (Geissler et al. 2013; Laabs et al. 2007; Carulli et al. 2010; Difei Wang et al. 2011; H. J. Lee et al. 2012). It has also been suggested that most of the functions of the CSPGs are mainly carried out by the chondroitin sulphate moieties, while the core proteins act as a scaffold (Laabs et al. 2007).

1.4.1.9 Lecticans

The neural ECM includes the CSPG of the lectican family of proteins, which are the most abundant family of CSPG in the CNS (Geissler et al. 2013; Bekku and Oohashi 2010). Members of the lectican family include aggrecan, versican, neurocan and brevican. They all have a G1 domain at the N-terminus and a G3 domain at the C-terminus. The G1 domain contains an HA-binding region and an immunoglobulin-like loop that interacts with the HA and the link protein to form stable. ternary complexes in the ECM. The G3 domain contains epidermal growth factor receptor (EGFR) repeats (both EGFR and calcium-binding EGFR), a C lectin domain (CLD) and a complement binding protein-like motif. The CLD is involved in mediating interactions with other matrix components and has a conserved expression in all lecticans. These include ligands with multimeric affinity for CLD, such as tenascins, presumably enabling cross-linked matrix assembly (Lundell et al. 2004). The affinity of such interactions can also be regulated by alternative splicing of other G3 domains (Day et al.

2004). In addition, aggrecan contains a G2 domain, which has a similar composition to the tandem repeats within G1 but is not thought to confer any additional interaction with HA (Kiani et al. 2002; Howell and Gottschall 2012). Based on the incorporation of two GAG-binding domains, termed GAG-α and GAG-β, versican has four differently glycosylated splice variants. V0 isoform contains both GAG-α and GAG-β regions, V1 contains only GAG-β and V2 contains only GAG-α. V3 lacks GAG-binding domains and therefore CS chains. V2 has been suggested to be specifically involved in the structuring of the perinodal ECM during development (Dours-Zimmermann et al. 2009). Lectican expression levels and locations change during development, culminating in organised, stable. and abundant distribution in healthy adult ECM.

1.4.1.10 NG2

In the healthy CNS, NG2 is found on the surface of developing and adult oligodendrocyte precursor cells (Levine, Reynolds, and Fawcett 2001). A single transmembrane segment separates a large extracellular domain from a short cytoplasmic tail. This can be cleaved at sites close to the outer plasma membrane and released into the ECM as the entire ectodomain. From a structural and functional point of view the extracellular part can be further subdivided into three domains; N-terminal globular domain 1, an extended central non-globular domain 2 and the juxtamembrane domain 3. The central domain 2 contains GAG attachment sites. It also interacts with collagen V and VI (Tillet et al. 1997; Stallcup 2002). Depending on whether the ectodomain is cleaved or not, domains 1 and 3 are likely to be differentially accessible for interaction with the ECM and neurons (Ughrin, Chen, and Levine 2003; A. M. Tan, Zhang, and Levine 2005). After CNS injury, the proliferation of NG2+ive cells has been observed at the site of injury (Levine 1994). These represent a mixed population of cells including oligodendrocyte precursors, meningeal cells and macrophages. The collective effect of these cells is increased NG2 expression (Bu, Akhtar, and Nishiyama 2001; McTigue, Tripathi, and Wei 2006; L. L. Jones et al. 2002; Hampton et al. 2004).

1.4.2 The role of the ECM in regulating CNS plasticity during development

The ECM is a critical regulator of CNS plasticity during development. The ECM can be thought of as a supportive environment that shapes the way nerve cells grow, connect and change. CNS plasticity refers to the ability of the CNS to change and adapt. The ECM plays a role in this by influencing the strength of synapses and the ability of neurons to adapt their connections. It's as if the ECM holds the reins on how much the CNS can change at different

stages of its development. During postnatal development, the CNS goes through critical periods when it's particularly open to learning and change. Through the gradual maturation of ECM composition, the ECM helps to control these periods as the neural circuit approaches its adult form (Barros, Franco, and Müller 2011; Long and Huttner 2021). An understanding of the mechanisms by which the critical period is initiated and terminated will inform approaches aimed at re-activating plasticity in order to promote repair after injury (Nahmani and Turrigiano 2014). As the critical period closes, the ECM undergoes significant changes (Burnside and Bradbury 2014). The formation of the PNN coincides with the end of the critical period (Mirzadeh et al. 2019). Correspondingly, there is an upregulation of aggrecan and HA as the critical period closes (Carulli, Rhodes, and Fawcett 2007). CSPG expression is also associated with critical period closure (Lander et al. 1997). In addition, a developmental increase in the ratio of four- to six-sulphated CSPGs has been shown to close the critical period for plasticity and is associated with the expression of the homeoprotein Otx2 and the associated transcriptional activation of mature firing dynamics (Sugiyama et al. 2008; Miyata et al. 2012). Put simply, the ECM forms the framework for the developing CNS. It provides guidance for axons, supports synapse formation, influences plasticity and even influences recovery from injury. To unravel the mysteries of brain development and find ways to improve recovery from CNS injury, understanding how the ECM works is crucial.

1.4.3 The ECM after injury

Following injury to the CNS, there are dramatic changes in the composition of the ECM. This, in turn, is likely to be influenced by the nature of the injury, depending on which cells are subsequently localised at the site of injury. For example, after blunt trauma that disrupts the BBB but leaves the dura intact (such as contusive SCI), glia cells are generally considered to be the main source of scar matrix deposition, whereas penetrating SCI results in greater fibroblast invasion across the disrupted meninges (Silver and Miller 2004). Fig. 5 shows the typical cell recruitment and expression of ECM components after penetrating SCI compared to blunt trauma in the CNS (focus on CSPG expression after SCI).

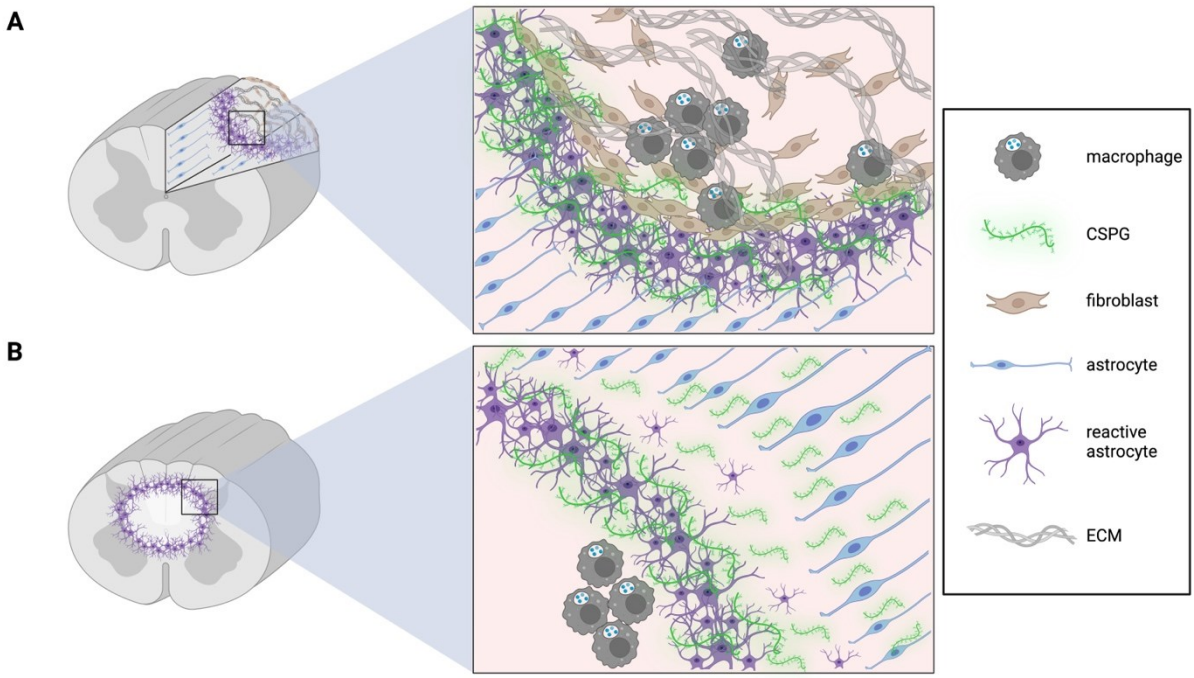

Fig. 5. The glial scar. Immune cells, including macrophages, invade the lesion through the disrupted BBB following CNS injury. Astrocytes undergo morphological changes, closing the BBB and spatially isolating core damage and inflammation from spared tissue. Specifically, the synthesis and release of inhibitory chondroitin sulfate proteoglycans (CSPGs) into the ECM are upregulated. (**A**) A lesion of the spinal cord that has penetrated the dura. Fibroblasts are also proliferating from the damaged meninges. (**B**) A spinal cord contusion injury in which the dura mater remains intact. A fluid-filled cavity forms after phagocytosis of necrotic tissue and cellular debris, surrounded by a sparing rim of white matter. Meningeal fibroblast invasion is not prominent after this type of non-penetrating trauma, but fibroblasts may be derived from perivascular sources or from infiltrating Schwann cells (not shown in this diagram). Fig. 5 is a modification of (Burnside and Bradbury 2014). Created with BioRender.com.

1.4.3.1 Glial scar

After CNS injury, a cascade of secondary pathology is triggered by primary axonal and vascular damage. BBB permeability is increased and a neuroinflammatory response is initiated with upregulation of local pro-inflammatory cytokines and chemokines (D. J. Donnelly and Popovich 2008). This activates predominantly astrocytes as well as microglia and oligodendrocyte precursor cells (OPCs) to form the glial component of the injury response and develop a glial scar. The main cellular components of the glial scar are reactive astrocytes. Reactive astrocytes are characterised by increased glial fibrillary acidic protein

(GFAP) expression. They proliferate and exhibit changes in gene expression and morphology. Classically, they are thought to undergo hypertrophy and extend overlapping processes leading to persistent scar formation (Sun and Jakobs 2012). This is also associated with increased expression of TnC (Y. Zhang et al. 1997; Laywell et al. 1992) and, in particular, sulphated proteoglycans (Morgenstern, Asher, and Fawcett 2002). Molecular triggers of reactive astrogliosis after CNS trauma include cytokines, trophic factors and some molecules upregulated as a result of oxidative stress (John, Lee, and Brosnan 2003; Sofroniew 2009). A particular mechanism proposed to directly induce astrocytic CSPGs synthesis is the extravasation of fibrinogen and TGF across the disrupted BBB (Schachtrup et al. 2010). Reactive astrocytes have important roles in the restoration of extracellular homeostasis and the release of pro- and anti-inflammatory cytokines after injury, but it is their role in scar formation that has a direct impact on the organisation and composition of the ECM in regions of CNS injury (Silver and Miller 2004).

There are important healing and protective aspects to the glial scar. However, despite the beneficial role of glial scar formation in the maintenance of homeostasis and the sealing of areas of CNS damage, it has also been associated with failure of regeneration (James W Fawcett and Asher 1999). This has been attributed in part to the presence of the dense configuration of reactive astrocytes that form a physical barrier to growth cone progression, but also to the accumulation and persistence of a number of inhibitory ECM molecules, particularly CSPGs (Fitch and Silver 2008; James W. Fawcett et al. 2012). In addition to astrocytes, microglia and OPCs are contributors to the glial scar. Microglia are ubiquitously distributed as a resting population and are the resident immune cells within the CNS. Upon injury, they proliferate, morphologically change, release cytokines, ROS, free radicals and acquire a phagocytic phenotype (Davalos et al. 2005; Streit, Walter, and Pennell 1999). OPCs also proliferate after CNS injury. They exhibit hypertrophy with elongated cell processes. They up-regulate the expression of the α-receptor for platelet-derived growth factor (PDGF) and CSPGs, in particular NG2 (Levine 1994; Z. J. Chen et al. 2002).

1.4.3.2 Fibrotic scar

A general feature of scar formation in all organs across a range of pathologies is the generation of collagenous tissue and ECM proteins derived from fibroblasts (Gurtner et al. 2008). Following injury to the CNS, the cell populations that contribute to a fibroblast phenotype are likely to be mixed. Meningeal fibroblasts are known to contribute to scar

formation and secrete collagen (particularly types I, III and IV) (Matthews et al. 1979; Weidner, Grill, and Tuszynski 1999), fibronectin and laminin (Shearer and Fawcett 2001). Endothelial cells may contribute (Schwab et al. 2001) and one study has implicated type A pericytes in the division, migration and formation of stromal cells that contribute to lesion core fibrosis (Göritz et al. 2011). In a spinal contusion model (nonpenetrating injury with intact dura), collagen1α1 cells were also identified as a source of perivascular fibroblasts distinct from pericytes (Soderblom et al. 2013). An infiltrating Schwann cell scar component has also been documented. This feature has been further characterised in post-mortem human tissue following particularly severe maceration-type spinal injury and is associated with collagen IV, laminin and fibronectin deposits surrounding the glial scar (Armin Buss et al. 2007).

1.4.3.3 CSPGs are upregulated in the ECM following injury

There is a general up-regulation of CSPGs in the ECM following injury to the CNS (Moon et al. 2002; Plant, Bates, and Bunge 2001). CSPGs are known to inhibit axon regeneration (McKeon, Höke, and Silver 1995; Snow, Brown, and Letourneau 1996; Morgenstern, Asher, and Fawcett 2002; Smith-Thomas et al. 1994; L. L. Jones, Margolis, and Tuszynski 2003), and various sulfated GAG chains are responsible for much of their inhibitory effect, although aspects of the CSPG core protein are also known to possess inhibitory properties (Ughrin, Chen, and Levine 2003; Lemons et al. 2003). To date, receptors that have been reported to mediate CSPG inhibition include RPTPσ (Yingjie Shen et al. 2009; Fry et al. 2010) and the related leucocyte common antigen-related phosphatase (LAR) (Fisher et al. 2011), the EGF receptor (Koprivica et al. 2005) and the Nogo receptors NgR1 and NgR3 (Dickendesher et al. 2012). Pathways involved in CSPG inhibition include the canonical Rho/ROCK signalling pathway (Monnier et al. 2003), protein kinase C (PKC) (Sivasankaran et al. 2004), Akt/GSK3β (Dill et al. 2008) and via impaired phosphorylatory cascades in integrin signalling (C. L. Tan et al. 2011).

1.4.3.4 Targeting of extracellular matrix may be beneficial for functional recovery after SCI

Removal or disruption of CSPGs can be achieved by inhibiting their synthesis, enzymatic degradation, antibody neutralisation or pharmacological targeting of effector molecules. The bacterial enzyme chondroitinase ABC (ChABC) is most commonly used for enzymatic modification of CSPGs. It catalyses the degradation of the glycosidic linkages between the

CS-GAGs of CSPGs, releasing them from the CSPG core protein (Prabhakar, Capila, et al. 2005; Prabhakar, Raman, et al. 2005). The beneficial effects of ChABC delivery have been replicated by many independent laboratories in various injury models (Bradbury and Carter 2011). The positive results obtained with the use of ChABC in rodents have been further confirmed in larger animals.

There are endogenous proteins that can also influence matrix composition. These could be used therapeutically. These include matrix metalloproteinases (MMPs), a disintegrin and metalloproteinases (ADAMs) and a disintegrin and metalloproteinase with thrombospondin motifs (ADAMTS) (Troeberg and Nagase 2012). MMPs, ADAMs and ADAMTS have been suggested to play a beneficial role in CNS injury through the degradation of CSPGs (Burnside and Bradbury 2014). Ultimately, removing CSPGs has been consistently shown to be beneficial for nearly two decades, and it is possible to see the next steps in translating CSPG-targeted therapies to the clinic.

Independent laboratories (M. S. Chen et al. 2000; T. GrandPré et al. 2000) have reported growth of CNS axons and recovery of limb function following the use of anti-Nogo-A antibodies. Interestingly, co-delivery of anti-Nogo-A antibodies and ChABC is more effective than either treatment alone in improving functional recovery following SCI, suggesting that removing multiple inhibitory factors is beneficial (Zhao et al. 2013). Nogo receptor antagonist NEP1-40 originally enhanced corticospinal tract and serotonergic fibre growth after thoracic dorsal hemisection in rats with striking results (Tadzia GrandPré, Li, and Strittmatter 2002). Promising results from the last 30 years of preclinical research on Nogo-A and anti-Nogo-A antibodies have led to the first human intrathecal application of anti-Nogo-A antibodies in a phase I human clinical trial for cervical SCI (Kucher et al. 2018), and further trials of NOGO intervention are currently underway (NCT03935321:'NISCI - Nogo Inhibition in Spinal Cord Injury (NISCI)', n.d.; NCT03989440: AXER-204 in Participants With Chronic Spinal Cord Injury (RESET)', n.d.).

1.5. Unlocking axonal resilience: integrins and intrinsic mechanisms of axon regeneration

As we have already seen, in the adult spinal cord there is very little regeneration of damaged axons after an injury. However, unlike the previous section which focused on the role of the extrinsic environment, to get the full story we should also discuss the neurons themselves.

When the axon is injured, the retraction bulb is formed and there is limited axon sprouting due to the low intrinsic growth capacity. But this is not the case during development; at this stage, axons have a much greater intrinsic growth capacity (Liu et al. 2011). They are able to grow towards their targets using the extrinsic cues that guide the growth cone as it extends over cells and through the extracellular matrix. One of the molecules involved in this process is the family of receptors known as integrins. Integrins are cell surface proteins that bind to molecules in the ECM and transduce external signals that regulate the cytoskeleton and activate intracellular signalling pathways that modulate axonal growth. This subsection discusses the intrinsic mechanisms regulating axon regeneration from an integrin perspective only (Eva et al. 2012).

1.5.1 Integrin structure, activation, and interactions

The integrin family is involved in a wide range of processes, including tissue development (Danen and Sonnenberg 2003), neuronal development (Gardiner 2011) the immune response (Means and Luster 2010), cancer (Wenjun Guo and Giancotti 2004), synaptic plasticity (Park and Goda 2016) and axonal regeneration in the PNS (Gardiner 2011; Eva and Fawcett 2014). Integrins are a heterodimeric family of receptors. They are composed of an alpha and a beta subunit. It is the combination of these subunits that determines the specificity of their binding to the ECM (Hynes 2002; Myers, Santiago-Medina, and Gomez 2011). They are complex receptors that are bi-directional in that affinity for the ligand is strictly regulated by inside-out activation, whereas binding of activated integrin to its ligand results in outside-in signalling (Hynes 2002) (Fig. 6A). Integrins can, however, be inactivated by inhibitory molecules in the CNS (F. Hu and Strittmatter 2008; C. L. Tan et al. 2011). This inactivation can be overcome by activation from the inside out, which can be achieved in several ways. For example, in non-neuronal cells, the presence of talin and kindlins, which bind to the C-terminus of integrins, can regulate the affinity of integrins to the ECM (Anthis and Campbell 2011; Ye, Kim, and Ginsberg 2012; Moser et al. 2009). Talin-mediated activation alters the structure of the transmembrane domain of the β1 integrin, inducing a conformational change in the extracellular domain and thereby increasing its ability to bind to ligands (Askari et al. 2009). This is facilitated by kindlin proteins. Their combined action forces the integrins into a high-affinity state (Fig. 6B). Talin is also dependent on activation by signalling molecules, so that the inside-out activation of integrins is complex and ultimately controlled by a large number of signalling molecules, including calcium ions, diacylglycerol, Rap1, phosphatidylinositol 4,5-bisphosphate and calpain (Anthis and Campbell 2011; Moser et al.

2009). How integrins in axons are regulated by talin and kindlins is not fully understood, but talin is reportedly present at growth cone filopodia tips (Myers, Santiago-Medina, and Gomez 2011; Renaudin et al. 1999). Furthermore, brain and cultured central and peripheral neurons showed that the expression of kindlin-1 and kindlin-2 are important for the regulation of integrin activation and axon growth (C. L. Tan et al. 2012). Once bound to their ligands, integrins alter cell behaviour by triggering outside-in signalling and binding to the cytoskeleton in an adhesion complex. These focal adhesion complexes are known as point contacts on growth cones (Renaudin et al. 1999). The focal adhesions have been well characterised. They consist of scaffold proteins such as talin, vinculin and paxillin, which link the complex to the actin cytoskeleton, and numerous signalling and adaptor molecules such as focal adhesion kinase (FAK) and Src, which regulate the complex and transmit outside-in signals (Huttenlocher and Horwitz 2011; Parsons 2003). All the key components of focal adhesions listed above are present in growth cone point contacts (Renaudin et al. 1999), so it is therefore likely that integrins at the growth cone function in a similar way to other cellular locations, although they may be subject to growth cone-specific regulation. Finally, integrin function is further regulated through transport, which is a major determinant of adhesion, spread, migration and cancer invasion (P. Caswell and Norman 2008; M. C. Jones, Caswell, and Norman 2006; Margadant et al. 2011; Pellinen and Ivaska 2006).

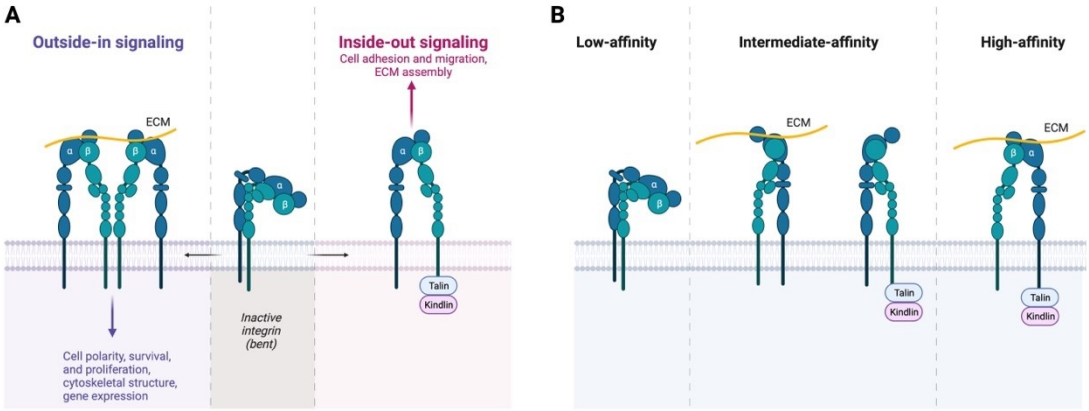

Fig. 6. (**A**) shows that the integrin family of cell adhesion receptors is involved in bidirectional signalling, with inside-out signalling activating integrin ligand binding and outside-in signalling mediating cellular responses triggered by integrin ligand binding, leading to cell spreading, retraction, migration and proliferation. (**B**) Integrin function is structurally regulated. The schematic shows the three different conformations of the integrin. In its low affinity state, the integrin is sharply bent, and the headpieces are close to the plasma membrane. In the intermediate affinity state, the ECM ligands or cytoplasmic proteins lead

to a complete extension of the extracellular domains. However, the separation of the cytoplasmic leg domains is the hallmark of the open high affinity activated integrin. Created with BioRender.com.

1.5.2 Relationship between integrin and regeneration

Neurons in which integrins are localised in axons are also the neurons that have been shown to regenerate most readily. It is therefore of interest to have a link between the subcellular localisation of integrins and the regenerative capacity of the nervous system (Nieuwenhuis et al. 2018). As mentioned above, integrins play a crucial role in coordinating the development of the CNS and PNS. Axon growth is a specialised form of cell migration, and for any cell to migrate, the growth tip must have an adhesion molecule that recognises an environmental ligand and is linked to signalling and cytoskeletal mechanisms. Successful axon extension is due in large part to a discrete balance of integrin and ECM expression that occurs during development. As the CNS develops, different integrins are expressed by numerous neuronal populations. Not only are they involved in axon initiation and development, but they are also required for the correct formation of neuronal architecture through interactions with their ligands (Liu et al. 2011) These ligands are differentially expressed throughout the CNS. However, in the adult CNS, especially in response to injury, neurons are less likely to express high levels of integrins compared to their developing counterparts, leaving neurons without the necessary receptors to regrow through a lesioned environment that is often characterised by highly upregulated ECM (Hammarberg et al. 2000; L. S. Jones 1996; Pinkstaff et al. 1999). Interestingly, axon growth could be seen as a specialised form of cell migration.

All cell migration has to follow the same biological rules. For any cell to migrate, it must have receptors on its surface that are capable of binding to molecules in its surroundings, and these receptors must be linked to intracellular signalling pathways and the dynamic cytoskeleton. Cell surface receptors are trafficked to and from the surface by endosomal trafficking machinery. Integrins are the key receptors for ECM molecules and regenerating axons need to penetrate the glial ECM. In the adult CNS, the major ECM glycoprotein is Tn-C, which is upregulated at sites of injury in the brain and spinal cord. The integrin that allows cells to migrate on Tn-C is α9β1, and this integrin is expressed in the CNS during embryonic development, but it is then downregulated in the adult and is not upregulated after injury.

When Fawcett's group at Cambridge started working in this area, the first question they asked was whether expressing α9β1 in adult neurons would promote axon regeneration. They found that neurons transfected in vitro grew long axons on Tn-C, but when the same idea was tried *in vivo*, there was much less regeneration. An adeno-associated virus (AAV) vector was used to transfect sensory neurons with α9β1 and when the dorsal root was injured, only a small increase in regeneration was seen (compared to control). The reason for the difference between *in vitro* and *in vivo* regeneration turned out to be that the major inhibitory molecules of the adult CNS (not present in the in vitro model) all inactivate integrins, preventing them from binding to Tn-C and signalling (J. W. Fawcett 2017; Cheah et al. 2016). The next steps in their experiments were therefore to overcome the inactivation of integrins by CSPGs and NogoA. This was done by transducing neurons with kindlin-1 to prevent integrin inactivation. This allowed the axons to overcome the inhibitory environment after CNS injury, together with transduction with α9β1 integrin. When α9β1 and kindlin-1 were delivered to the C6 and C7 dorsal root ganglia and the roots crushed, the regenerating axons were able to overcome the inhibitory environment. The regenerated sensory axons grew all the way up the spinal cord to the medulla, making connections in the correct layers of the dorsal horn along the way. This is a previously unattained level of regeneration, and the new connections worked: the animals regained the sense of pain and touch (J. W. Fawcett 2017; Cheah et al. 2016). A prerequisite for this is that the neurons are able to transport integrins and kindlin down their axons to the site of the axotomy so that they can take part in the regeneration and extension of the axon growth cone. For dorsal root ganglion (DRG) neurons, this does not seem to be a problem, as almost all molecules expressed in the cell bodies appear to be transported down the axons (J. W. Fawcett 2017). This raises the question of whether the overexpression of α9β1 in the (dorsal root ganglion) DRG would lead to the same functional recovery after SCI.

Taken together, this suggests that forced expression of an appropriate integrin that interacts with available molecules in the ECM has the potential to alter the intrinsic ability of an axon to grow, as expression of a single subunit of a growth-promoting integrin can allow growth in an otherwise inhibitory environment. For example, expression of α9 integrin together with its activator kindlin-1 allows axon growth over tenascin-C in vitro and some sensory axon regeneration after dorsal root crush in the spinal cord *in vivo* (Cheah et al. 2016).

1.6 Strategies for spinal cord regeneration

As previously discussed, SCI involves extensive processes ranging from nervous cell death to vasculature changes and ECM remodelling (Hilton, Moulson, and Tetzlaff 2017; Bradbury and Burnside 2019). This occurs as a time-dependent cascade of complex biological processes which may take months to years after injury (A. Buss et al. 2004; Meldrum 2000; D. J. Donnelly and Popovich 2008). Some spontaneous recovery is observed in experimental animal models and less so in humans (Curt et al. 2008; Hilton et al. 2016). However, the endogenous repair mechanisms are of minor importance and the recovery remains incomplete (J. W. Fawcett et al. 2007; Gregoire Courtine et al. 2008). Furthermore, by reactivating processes that trigger axon growth during development, axon regeneration is possible in the adult CNS. In fact, there is a remarkable communication between the growth machinery that is present during development and the components that are present in the adult. This machinery has been found to be severely inhibited by growth inhibitors in the adult CNS, and releasing this inhibition appears to be a way of triggering axon regeneration (Winter, He, and Jacobi 2022). On the basis of the pathology of SCI and the development, researchers have identified several targets for developing potential therapeutic interventions. These can be described as the '7 Rs'. Firstly, the Reduction of secondary damage (Badhiwala et al. 2018; Ditor et al. 2007; Feldblum et al. 2000; Baptiste and Fehlings 2006; Mao et al. 2017; Thuret, Moon, and Gage 2006) which mainly involves the pharmacological agents that suppress the immune system or inhibit key pathways involved in inflammation. Cell transplants have the potential to fill in the lesion and thus Replace the injured tissue (Griffin and Bradke 2020; Assinck et al. 2017). The Resupply of neurotrophins, which help neurons to survive, develop and function may improve neuronal survival and direct axonal growth (Griffin and Bradke 2020). It is controversial whether it is appropriate to target Remyelination following SCI. The myelin sheath of myelinated axons increases the speed of action potential transmission. The importance of this property is obvious in multiple sclerosis, but researchers have recently questioned whether pathophysiological oligodendrocyte support and remyelination contributions are relevant for functional recovery after SCI (Duncan et al. 2020). Following SCI, there are widespread acute oligodendrocyte death and axonal demyelination, and remyelination has been suggested to be important to protect axons from further degeneration and improve conduction (Norenberg, Smith, and Marcillo 2004; Nave 2010b; 2010a; Almad, Sahinkaya, and McTigue 2011). Two approaches are available: Transplanting cells that can directly differentiate into oligodendrocytes or promoting the recruitment and differentiation of

endogenous OPCs (Tetzlaff et al. 2011; Karimi-Abdolrezaee and Eftekharpour 2012; K. A. Irvine and Blakemore 2008; Duncan et al. 2020). With regard to remyelination, there are still doubts as to whether therapeutic targeting of oligodendrocyte remyelination is a worthwhile target for clinical translation. Rehabilitation is important in pruning and refining circuits that are relevant to the specific motor task (Mang et al. 2013). In addition, rehabilitation stimulates local neurotransmitter production (Côté et al. 2011), modulates several neurotransmitter systems (Edgerton et al. 2004) and promotes compensatory relay network sprouting (Grégoire Courtine et al. 2009). In addition, several studies have demonstrated an important role for rehabilitation in regeneration and plasticity (Loy and Bareyre 2019). In mice, rats and cats, different forms of rehabilitation can improve recovery of motor function after SCI (Loy and Bareyre 2019). The Removal of the inhibitory molecules and the Regeneration by targeting the intrinsic mechanism of the neuron have already been mentioned in the previous chapters.

1.7 Current research and new and experimental therapies

New and experimental therapies are not only about novel therapeutics, but also about how to deliver something that is already known, or how to make existing therapies more stable. or easier to use in human patients. The routes and methods of delivery of therapeutics are of paramount importance in SCI therapies and research. Not only is it essential to understand the underlying mechanisms and propose effective treatments, but it is also critical to determine how these therapies will be delivered to animal models and humans. Choosing the appropriate route of administration, such as intravenous, intrathecal or local injections, plays a key role in ensuring targeted delivery of the therapeutic agent to the injured spinal cord. In addition, the development of innovative delivery systems, such as nanoparticles or gene therapy vectors, but also to find a drug that can be administered orally, thus providing a completely non-invasive route of administration. It can increase the precision and efficiency of treatment. In SCI research, this careful consideration of delivery methods is critical to bridging the gap between promising laboratory findings and their practical application in clinical settings, ultimately aiming to improve the quality of life of people affected by SCI.

Areas of active research that have the potential to transform the field of spinal cord care include the following (Khan and Ahmed 2022): for example, the stem cell research, particularly using induced pluripotent stem cells (iPSCs) and neural stem cells, has received considerable attention. These cells have the potential to differentiate into a variety of neural

cell types and to promote the regeneration of tissues (Wen Guo et al. 2022). Moreover, the advances in gene therapy, such as the use of adeno-associated viral (AAV) vectors, have attracted interest as a promising system for transgene delivery to the CNS due to their safety profile and long-term gene expression (Stepankova, Jendelova, and Machova Urdzikova 2021). Pharmacological therapy is another potential intervention. Research into novel drugs that target specific molecular pathways for neural repair, neuroprotection, reduction of inflammation and manipulation of inhibitory extrinsic factors at the lesion site has made considerable progress (Moretti et al. 2023).

1.7.1 AAV-mediated gene therapy

In recent years, adeno-associated virus (AAV)-mediated gene therapies have gained clinical interest for the treatment of a wide range of neurodegenerative and neuromuscular diseases, such as amyotrophic lateral sclerosis (Cappella et al. 2019), Alzheimer's disease (Rafii et al. 2018; Hara et al. 2004; J. Zhang et al. 2003; Fukuchi et al. 2006), Parkinson's disease (Leff et al. 1999; Y. Shen et al. 2000; Keeler and Flotte 2019), Huntington's disease (B. D. Dufour et al. 2014), spinal muscular atrophy (Pattali, Mou, and Li 2019), and others. In SCI, gene therapy has been used to remove scar tissue and allow new cord-muscle and cord-brain connections to form (Taha 2010; Bo et al. 2011; Rowland et al. 2008; Franz, Weidner, and Blesch 2012; Uchida et al. 2014). Adeno-associated virus (AAV) vectors have emerged as a potential solution for the above diseases.

Although there is potential for the treatment of SCI and preclinical studies have demonstrated its use in rodent models of SCI, AAV-mediated gene therapy for SCI is still in its infancy. Therefore, there has been no successful clinical translation to date and research in this area needs to be further developed and optimised.

The simple goal of all gene therapies, which is also true of AAV-mediated gene therapies, is to safely deliver nucleic acid cargo into cells, which has lagged behind the identification of disease-associated genes.

In simple terms, AAV is a protein coat that surrounds and protects a small single-stranded DNA genome of about 4.8 kb. AAV is a member of the parvovirus family and is dependent on co-infection with other viruses, mainly adenoviruses, for replication. Initially serologically differentiated, hundreds of unique AAV strains have been identified in

numerous species through molecular cloning of AAV genes. Their single-stranded genome contains three genes: Rep (replication), Cap (capsid) and aap (assembly). Through the use of three promoters, alternative translation start sites and differential splicing, these three genes give rise to at least nine gene products. These coding sequences are flanked by inverted terminal repeats (ITRs) that are required for replicating and packaging the genome. The Rep gene encodes four proteins (Rep78, Rep68, Rep52 and Rep40) that are required for viral genome replication and packaging, while Cap expression gives rise to the viral capsid proteins (VP; VP1/VP2/VP3), which form the outer capsid envelope that protects the viral genome and are actively involved in cell binding and internalisation. It is estimated that the viral envelope is made up of 60 proteins that are arranged in an icosahedral structure with the capsid proteins in a molar ratio of 1:1:10 (VP1:VP2:VP3). The aap gene, which overlaps the cap gene in an alternate reading frame, encodes the assembly-activating protein (AAP). This protein is located in the nucleus and is thought to provide a scaffolding function for capsid assembly (Berns and Bohenzky 1987; Balakrishnan and Jayandharan 2014; Warnock, Daigre, and Al-Rubeai 2011).

Although there is much more to the biology of wild-type AAV, much of which is not fully understood, this is not the form that is used to generate gene therapeutics. Recombinant AAV (rAAV), which lacks viral DNA, is essentially a protein-based nanoparticle engineered to traverse the cell membrane, where it can ultimately traffic and deliver its DNA cargo into the nucleus of a cell. In the absence of Rep proteins, ITR-flanked transgenes encoded within rAAV can form circular concatemers that persist as episomes in the nucleus of transduced cells (Choi, McCarty, and Samulski 2006). During vector production, the ITRs are required to direct genome replication and packaging. The remaining wt-AAV protein coding sequences are replaced by the therapeutic gene expression cassettes. When the viral coding sequence is completely replaced, it increases the packaging capacity of AAV vectors. It also contributes to their low cytotoxicity and immunogenicity after in vivo delivery (Dan Wang, Tai, and Gao 2019; Verdera, Kuranda, and Mingozzi 2020). Because recombinant episomal DNA does not integrate into host genomes, it will eventually be diluted over time as the cell undergoes repeated rounds of replication. This will eventually result in the loss of the transgene and transgene expression, with the rate of transgene loss dependent on the turnover rate of the transduced cell. These characteristics make rAAV ideal for certain gene therapy applications. Following is an overview of the practical considerations for the use of rAAV as a gene therapy agent, based on our current understanding of viral biology and the state of

the platform. The final section provides an overview for how rAAV has been incorporated into clinical-stage gene therapy candidates, as well as the lessons learned from those studies that can be applied to future therapeutic opportunities.

In general, there are a number of different routes of administration. Depending on the specificity of the AAV serotype and its ability to migrate from the periphery to the spinal cord, there are several non or minimally invasive ways to deliver the vector, e.g., intramuscular, intraneural and intravenous. The intrathecal route can also be considered minimally invasive. It is used to deliver the viral vector to brain cells. Following viral injection directly into the cerebrospinal fluid (CSF), AAV vectors can cross the BBB and expression can proceed directly to brain cells without requiring direct delivery to the brain (Fischell and Fishman 2021). Direct delivery, on the other hand, involves an invasive surgical procedure that targets a specific area of tissue in the spinal cord. This type of intervention is known as the intraparenchymal route of delivery of a viral vector (Fig. 7) (Hardcastle, Boulis, and Federici 2018).

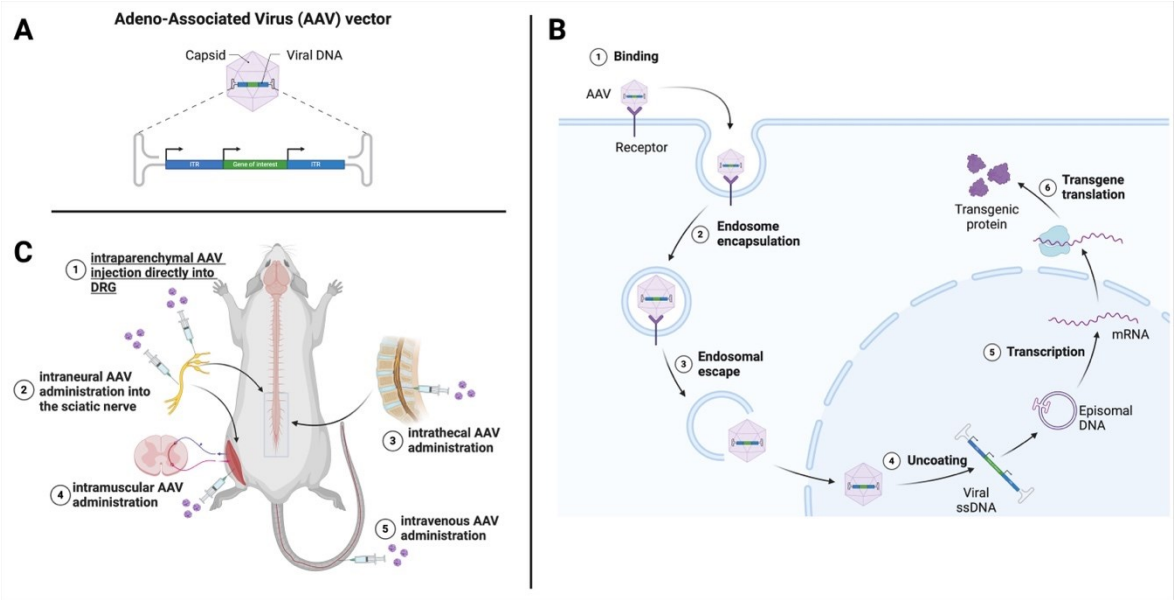

Fig. 7. (**A**) shows the schematic representation of the AAV vector that can be used for any gene therapy purpose. (**B**) shows the diagram of how the AAV vector infection occurs after delivery of the AAV vectors, and (**C**) shows the schematic representation of the possible routes of administration of the AAV vectors. Created with BioRender.com.

1.7.2 Oral treatment

In general, finding an oral treatment that allows regeneration after SCI would be an absolute game changer for SCI patients. Oral treatment offers potential advantages for spinal cord injured patients. Compared to treatments that require injections or surgery, oral medications are often more convenient and easier to administer. This may have a positive effect on patient compliance and overall treatment adherence. The avoidance of invasive procedures can reduce the risk of complications, infections and other adverse effects associated with surgery. An oral treatment may eliminate the need for surgery or injections, resulting in a simpler and less risky treatment process. Compared to treatments that require specialised medical procedures, oral medicines may be more accessible to a wider population. This could make the treatment more widely available to people with spinal cord injuries, regardless of where they live or whether they have access to medical facilities. If well tolerated and safe, oral treatment could allow outpatient management, reducing the need for prolonged hospitalisation. Last but not least, oral medications can be more easily combined with other oral treatments or therapies, allowing a comprehensive and multifaceted approach to managing SCI (Alqahtani et al. 2021).

According to the research, recently published in the British Journal of Clinical Pharmacology, oral treatments do not appear to be impossible for SCI patients. KCL-286 is a new drug being developed as a therapeutic intervention for spinal cord injuries. KCL-286 is an orally available agonist that activates the retinoic acid receptor (RAR) β2, a transcription factor that stimulates axonal outgrowth, and has recently been tested in Phase 1 clinical trials. The results showed that KCL-286 was well tolerated by healthy volunteers at doses that exceeded the potentially clinically relevant plasma exposure levels based on pre-clinical in vivo models. Target engagement demonstrated that the drug candidate activates its receptor. These results support the continued development of KCL-286 to treat SCI (Goncalves et al. 2023, 1).

2. AIMS AND HYPOTHESIS

In the introductory section of this thesis, we mentioned the difficulties that axons face in regenerating in the mature CNS. Regeneration in the adult mammalian CNS is unsuccessful due to reduced intrinsic regenerative capacity of affected neurons, myelin-associated inhibitory factors and components of the glial scar (Silver and Miller 2004). This basically leads to two main therapeutic approaches. In simple terms, we can either remove the inhibitory environment in the CNS and thus increase plasticity, or we can use the inhibitory environment in favour of regeneration by over-expressing the right isoform of a molecule that can bind to the inhibitory environment around the lesion site and thus allow axons to pass through the lesion and thus promote regeneration.

2.1 Novel oral therapy for SCI: removing the inhibitory CSPGs to improve regeneration and plasticity

As discussed earlier, enzymatic removal of CSPG and PNN by ChABC has been shown to reopen a critical window to enhance plasticity and promote functional recovery in several models of SCI (Yousefifard et al. 2022). The use of ChABC, however, has several drawbacks. The main drawback to the use of this bacterial enzyme is its thermal instability and short half-life, which requires multiple or continuous intrathecal administration, potential body immune response and difficult dosing (Z. Chen, Li, and Yuan 2015). In addition to ChABC, an attempt has been made to find an oral treatment that could replace ChABC in its use. A subset of 245 compounds known for their CNS penetration and oral bioavailability were tested. None of these 245 compounds showed sufficient ability to overcome CSPG inhibition (Keough et al. 2016).

Our aim was to find another molecule that could be used as a replacement for ChABC after SCI. One of the candidates, a small molecule, 4-methylumbelliferone (4-MU), already approved by the FDA and EMA for use in human patients, which can down-regulate PNNs and reactivate neuroplasticity to improve memory (Dubisova et al. 2022). 4-MU is a well-known inhibitor of the synthesis of HA (Nagy et al. 2015; 2019). Previous studies have shown that 4-MU inhibits the production of UDP-glucuronic acid (UDP-GlcA) (Galgoczi et al. 2020), a key substrate for HA production, and the expression of hyaluronan synthase (HAS), UDP-glucose pyrophosphorylase (an enzyme involved in the biosynthesis of UDP-glucose) and UDP-glucose dehydrogenase (an enzyme that converts UDP-glucose to UDP-glucuronic acid) (Kakizaki et al. 2004; Kultti et al. 2009). Interestingly, UDP-GlcA and some

other GAGs including dermatan and heparan sulphates are also substrates for the synthesis of chondroitin sulfate (CS). This means that in addition to the inhibition of HA synthesis, there should also be an inhibition of CSPG synthesis after 4-MU treatment. This suggests that 4-MU may be sufficient not only to disrupt the PNNs around spinal neurons and thus allow sprouting axons to make the new synaptic connections, as the PNNs would not prevent synaptic formation, but also to reduce the scar (where astrocytes produce a huge amount of HA and the CSPGs are upregulated) (Fig. 8).

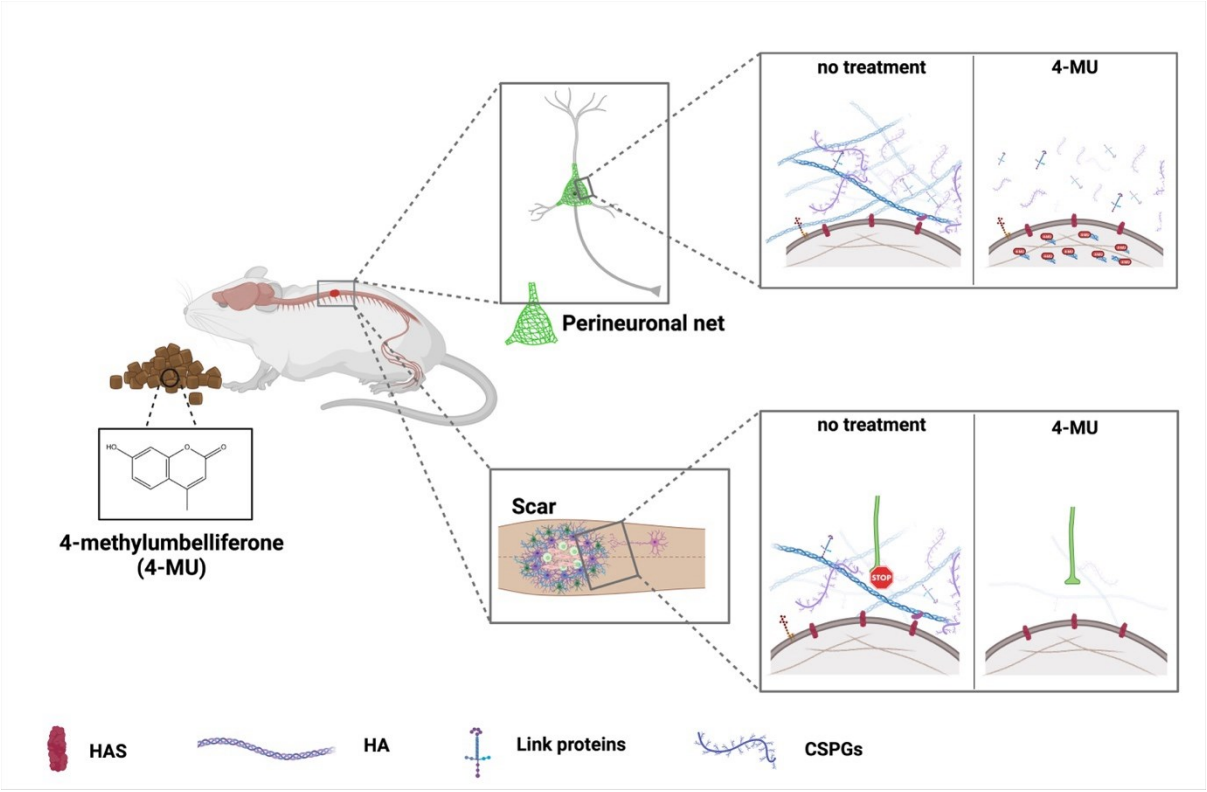

Fig. 8. Graphical summary for aim 1. 4-MU is a small molecule, a derivative of coumarin, that reduces HA and CSPGs - the main components of PNNs, but also the majority of the scar surrounding the spinal lesion. Created with BioRender.com.

As 4-MU is administered orally, we expected the drug to have a systemic effect, and we also expected that if we were to use this drug to observe functional improvements after SCI, we would need to administer the drug long-term. We decided to do a pharmacological study first to see if the dose of 1.2 g/kg/day was safe for long-term use in rats (Fig. 9). Then we did a study in rats with SCI to assess its effect on chronic SCI (Fig. 10). The choice of the chronic phase of SCI was mainly on the basis of the clinical relevance of the potential use of the treatment. As the acute phase is more associated with trying to keep the patient safe, leaving little room for any additional treatment beyond what is needed to keep the patient alive, the mechanism of action may also be contraindicated for other physical complications.

2.1.1 Pharmacological assessment of the low dose of 4-MU

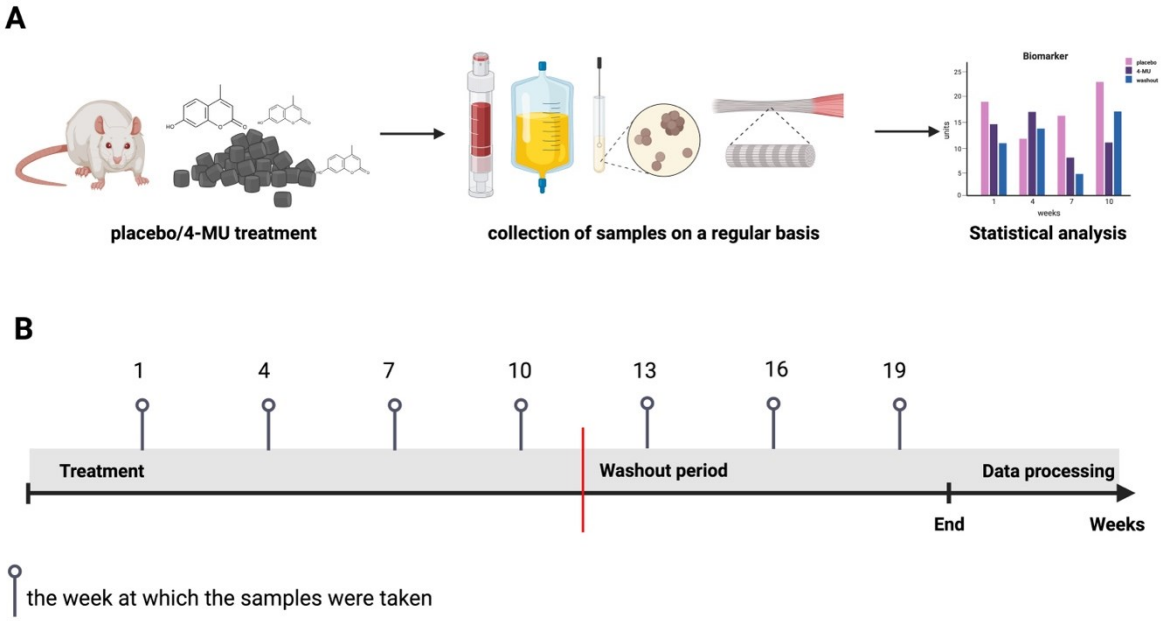

Fig. 9. Graphical summary for aim 1.1. (**A**) Pharmacological evaluation and biomechanical analysis of animals treated with placebo, animals treated with 4-MU and after a wash-out period. Animals were treated for 10 weeks, and blood and urine samples were collected every 3 weeks and sent to SYNLAB for analysis. After 10 weeks, the placebo-treated animals and half of the 4-MU-treated animals were sacrificed. The remainder of the 4-MU-treated animals were kept for a further 9 weeks to observe the wash-out effect. (**B**) Graphical representation of the experimental timeline. Created with BioRender.com

2.1.2 Effect of the low dose of 4-MU on SCI at the chronic stage

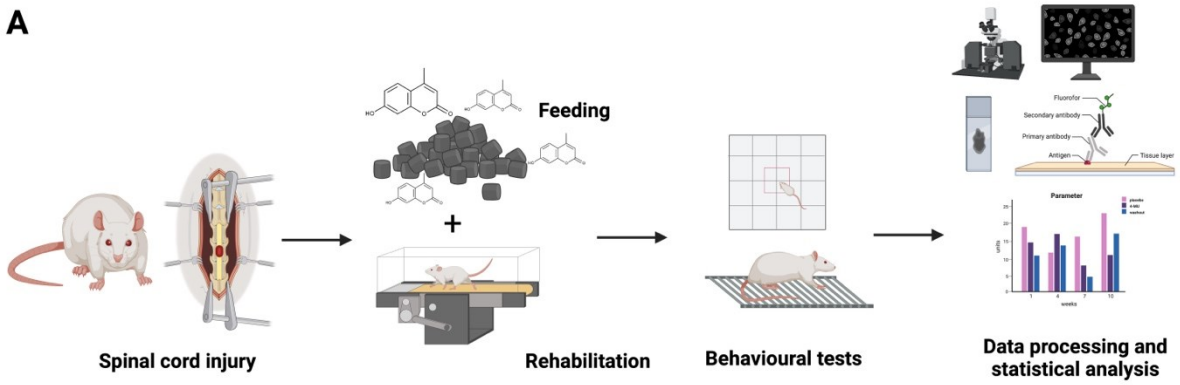

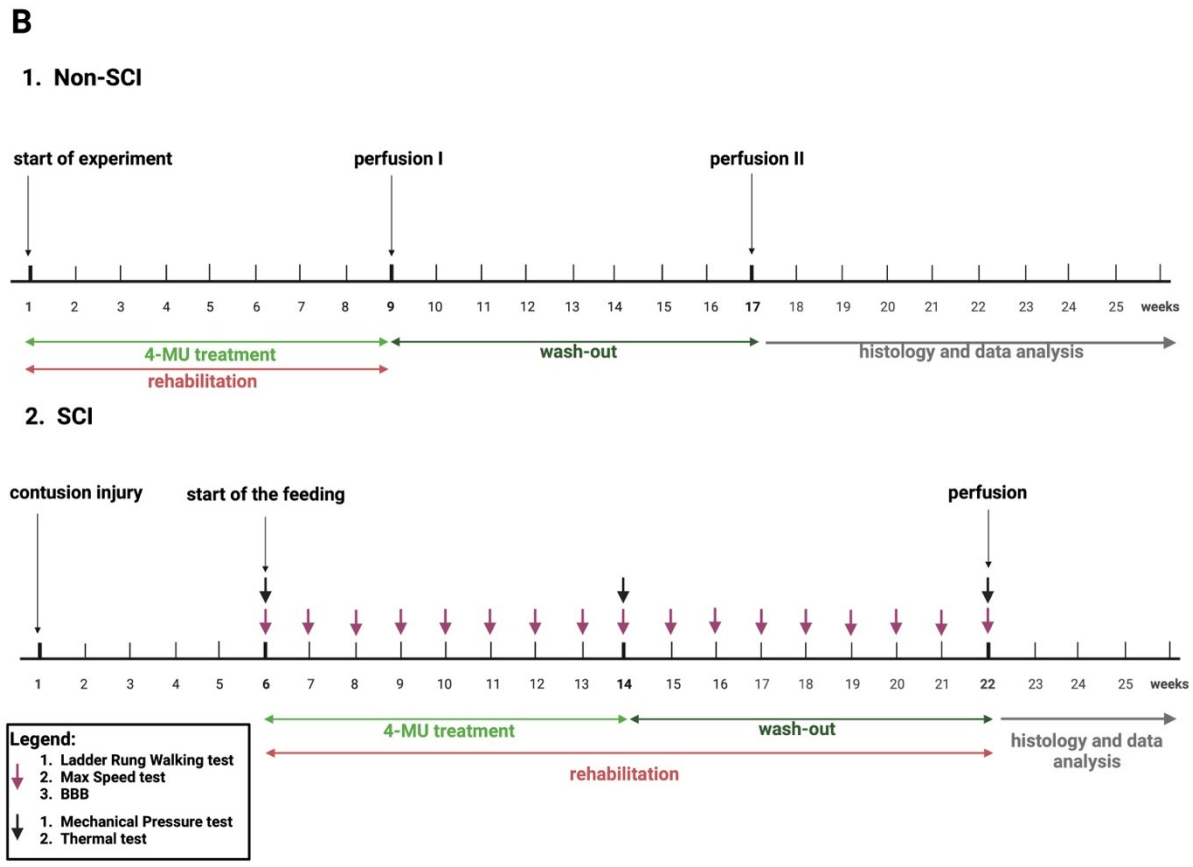

Fig. 10. Graphical summary for Aim 1.2. (**A**) Schematic of the study in spinal cord injured rats to evaluate the 4-MU-mediated effect on chronic SCI. (**B**) Graphical representation of the experimental time course. Firstly, we wanted to observe whether the rehabilitation itself had any effect on PNNs in the spinal cord in order to better interpret the SCI data in the next step. We then performed SCI in healthy rats and waited 6 weeks for the glial scar to form, as we hypothesised that glial scar reduction would be one of the 4-MU-mediated effects. The placebo and 4-MU treatments were accompanied by rehabilitation to refine the newly sprouting axons and enable them to make new connections in the task-specific manner. Created with BioRender.com

2.2 Using AAV-mediated overexpression of integrin α9 for sensory pathway reconstruction after SCI

Only when the axonal tracts connecting the brain and spinal cord regenerate and restore motor and sensory connections can full recovery from SCI occur. In the mammalian spinal cord, neither sensory nor motor axons can regenerate spontaneously. This is partly because the axons lack a suitable. adhesion molecule that allows them to interact with the damaged spinal cord. We therefore tried to overexpress an integrin adhesion molecule and its activator in sensory neurons using a viral vector. After dorsal root crush, we have already seen that

overexpression of the integrin α9 with its activator kindlin-1 can allow axon regeneration (Cheah et al. 2016).

In this aim, adult female rats received a spinal cord lesion at the T10 level and, at the same time, injections of AAVs into DRGs at the L4,5 level. The three experimental groups received different AAV injections, 1) AAV-GFP (*green fluorescent protein*, GFP group), 2) AAV-kindlin-1-GFP (kindlin group), 3) AAV-kindlin-1-GFP + AAV-α9 -V5 (α9-K1 group). AAV-GFP (provides a control for AAV injection, AAV-kindlin-1-GFP shows the effect of activating integrins endogenously expressed in DRG neurons, AAV-kindlin-1-GFP + AAV-α9 -V5 is the regeneration-inducing treatment with the tenascin-binding integrin and its activator. Animals underwent sensory behavioural testing for 12 weeks and were killed for histology at week 13. Prior to this, some animals received electrical stimulation of the sciatic nerve to upregulate cFOS in spinal cord neurons (Fig. 11). Our question was whether this approach would allow sensory axons to regenerate through the SCI (not just dorsal root crush) to the brainstem and restore sensation.

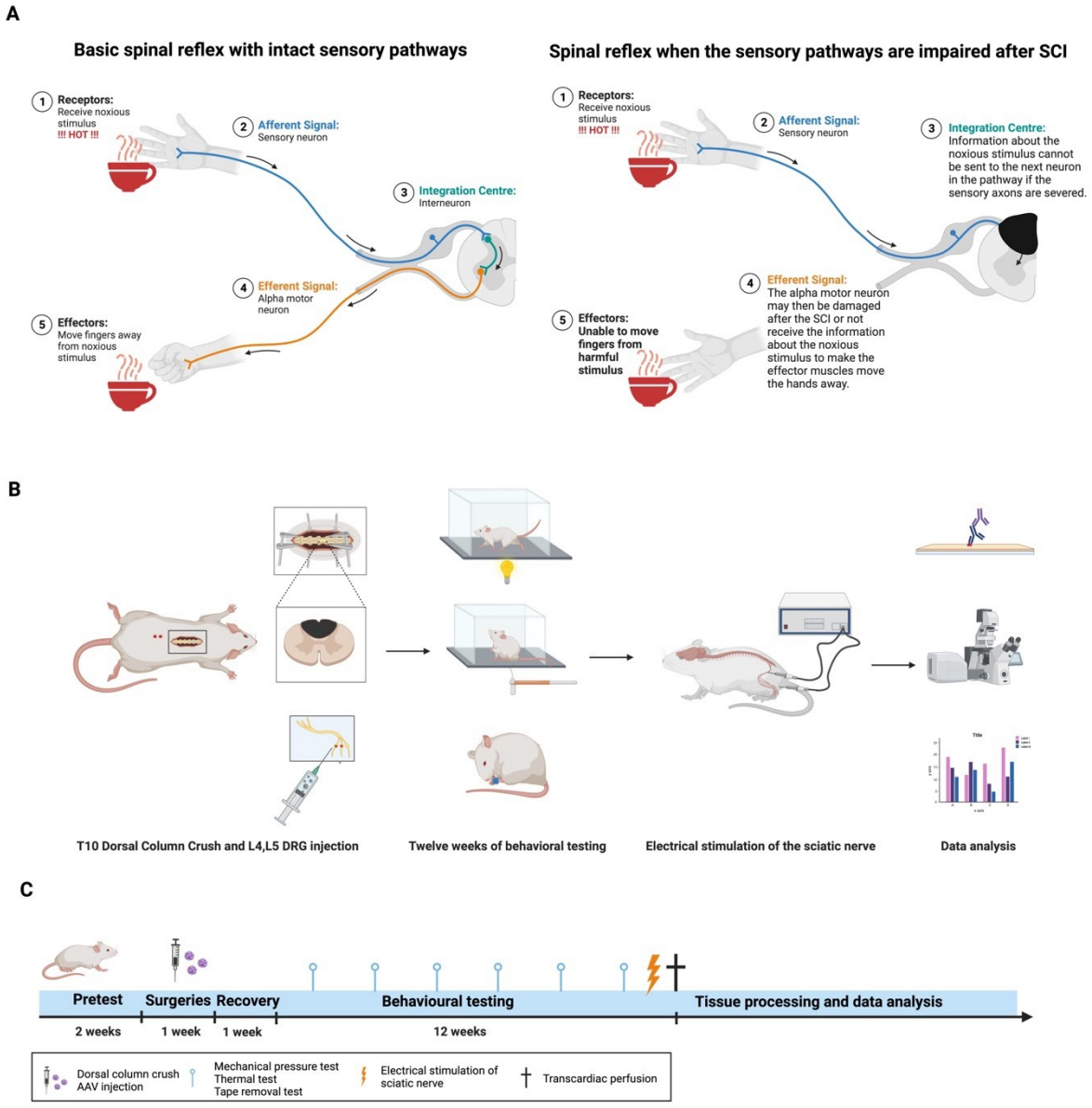

Fig. 11. Graphical summary for Aim 2. SCI is about much more than not being able to walk. The ascending (sensory) pathways are more likely to be affected when the spinal cord is injured. The (**A**) schematic shows the basic withdrawal reflex and what happens when the ascending spinal pathways are damaged. We hypothesised that the regenerative approach to reconstructing the sensory pathways might be a little easier to achieve because the sensory neurons are not directly in the spinal cord and are further away from the injury site. In addition, DRGs innervate characteristic skin areas (dermatomes) that can be tested with behavioural tests - L4, L5 dermatomes are considered skin areas including parts of thighs, knees, legs and paw pads (Whitman, Launico, and Adigun 2024). (**B**) Schematic representation of Objective 2. The DRGs L4 and L5 were injected with AAV (GFP only, Kindlin-1 only and Integrin α9-Kindlin-1 in a 3:1 ratio) and the dorsal column crush was

performed simultaneously with the direct DRG injection. The animals were then tested for 12 weeks - the battery of sensory behavioural tests was selected, and the animals' hind limbs were regularly tested every two weeks. Prior to sacrifice, 3 randomly selected animals from each group were anaesthetised with urethane and the sciatic nerve was electrically stimulated to induce cFOS expression. All animals were then sacrificed, and the tissues processed and analysed. (**C**) Graphical representation of the experimental time course. Created with BioRender.com

3. METHODS

3.1. Experimental animals

Ten-week-old healthy female Wistar rats (n = 24; 250 ± 30 g) were used for the pharmacological evaluation of potential 4-MU-mediated adverse effects. Rats were obtained from Janvier Labs (CS 4105 Le Genest Saint-Isle; Saint-Berthevin Cedex-53941 France). Only female rats were used in this study to reduce the potential confounding effect of rapid weight gain observed in male rats in a long-term study. The animals were randomly divided into 3 groups (n = 8 per group): a placebo group, a treated group (4-MU) and a wash-out group. For the entire duration of the experiment, the rats were housed in pairs under standard conditions with a 12-hour light and 12-hour dark cycle. The rats had access to tap water and food ad libitum. After 10 weeks of treatment with 4-MU, animals from the placebo and 4-MU groups were sacrificed. Animals in the wash-out group survived for another 9 weeks.

8-week-old female Wistar rats (n=55, 250-300 g) were included in the study. The study focused on the effect of 4-MU in the treatment of SCI in its chronic stage. The animals were obtained from Janvier Labs (CS 4105 Le Genest Saint Isle; Saint Berthevin Cedex 53941 France). 40 animals were used for the histochemical and biochemical evaluation of the dose effect of 1.2 g/kg/day 4-MU in 4-MU fed/non fed combined with/without rehabilitation groups. This was done to follow up the previous part and to study the effect of rehabilitation on the level of perineuronal nets. This dose was chosen because our aim was to test whether a lower dose of 1.2 g/kg/day body weight would be effective in reducing inhibitory ECM while minimising consumption of 4-MU for potential adverse effects of long-term treatment for SCI. These animals were divided into 5 groups (8 rats per group) using simple randomisation - placebo, placebo + exercise/rehabilitation, 4-MU, 4-MU + rehabilitation and 4-MU with a planned 2-month post-treatment period (wash-out group). Based on our previous experiments, we expected an effect size of ≥ 1.7. A power calculation of $\alpha = 0.05$, number of groups = 5, total sample size of 8 is required for each experimental group. Histochemical and biochemical evaluation of treatment was then performed on uninjured animals. 18 animals underwent spinal cord contusion, 3 animals with a BBB score of less than 8 one week after injury were excluded. Feeding started 6 weeks after SCI, when the chronic phase was fully established. Half of the animals received chocolate chow with 4-MU (1.2 g/kg/day) (treatment group) and the other half received chocolate chow without any treatment (placebo group). Both the placebo and treatment groups received daily treadmill exercise. Feeding was stopped after 8 weeks, but daily rehabilitation continued for

a further 8 weeks. The rats were housed in pairs in cages with a 12-hour light/dark cycle under standard conditions (temperature (22 ± 2 °C) and humidity (50 ± 5 %)).

The final part of the work involved 8-week-old female Lister-Hooded rats (n=36; 150-175 g). Rats were purchased from Envigo. Rats were randomly assigned to three experimental groups (GFP only, Kindlin-1 only and alpha9-Kindlin-1) prior to surgery. Rats were housed in groups of three in cages with a 12-hour light/dark cycle and standard conditions of temperature (22 ± 2°C) and humidity (50% ± 5%). Rats had free access to tap water and food ad libitum.

3.2 SCI surgeries

All procedures were performed in accordance with relevant guidelines and regulations. All animal procedures were approved by the Ethics Committee of the Institute of Experimental Medicine of the Academy of Sciences of the Czech Republic (ASCR) and were performed in accordance with Act No. 77/2004 of the Czech Republic (ethics approval number: 13/2020). A power calculation based on previous studies was performed prior to the experiment to estimate the number of animals required. All work was performed in accordance with European Commission Directive 2010/63/EU and ARRIVE guidelines. Every effort was made to minimise pain and distress.

For each objective, the choice of SCI model was different. The simple reason for this is the specific research questions being investigated as well as practical considerations, particularly the postoperative care of the animals. In Aim 1, the contusion injury model was used to investigate whether the systemic manipulation with ECM can promote any kind of regeneration after SCI. Contusion models resemble most human SCIs, which are often caused by trauma such as car accidents or falls. However, in Aim 2 we used the dorsal column crush model as a specific type of SCI model. This model focuses on damage to the dorsal columns of the spinal cord to specifically simulate injury to sensory pathways. The use of the dorsal column crush model was based on the research objective of a potential therapeutic intervention to promote regeneration and recovery of sensory function.

3.2.1 Contusion model of SCI

A commercially available Infinite Horizon SCI device (IH-0400 Spinal Cord Impactor device; Precision Systems and Instrumentation, Lexington, KY, USA) was used to induce

moderate thoracic spinal cord contusion. Rats were first anaesthetised with 5% (v/v) isoflurane in the anaesthetic chamber. During surgery, anaesthesia was maintained at 1.8-2.2% in 0.3 L/min oxygen and 0.6 L/min air. Prior to surgery, the animals were injected subcutaneously with buprenorphine (Vetergesic® Multidose, 0.2 mg/kg body weight). Laminectomy was performed under sterile conditions at the Th8/Th9 level with spinal stabilisation at Th7 and Th10 using Adson tissue forceps. Animals were subjected to a moderate contusion injury at 200 kdyn. For the first two weeks after injury, the rats` urinary bladders were checked for urine retention and manually emptied when needed. If signs of inflammation and/or pain were observed, the rats were treated with antibiotics and/or analgesics. After surgery, the animals were randomly assigned a number and then randomly assigned to the placebo or 4-MU group. The experimenter was blinded to the treatment group during behavioural analysis. The identity of the animals and their treatment group was not revealed until after the analysis. No animals were excluded from the study; exclusion was based on the BBB results at 4- and 7-days post-surgery, the target BBB at 7 days post-surgery was 8. 1 animal in the SCI group died 5 weeks after SCI for unknown reasons. No other animal had to be humanely killed during the experiment.

At the end of the experiments, half of the rats from each group received a lethal dose of intraperitoneal ketamine (100mg/kg) and xylazine (20mg/kg), intracardially perfused with 4% paraformaldehyde (PFA) in 1X phosphate-buffered saline (PBS), and post fixation in the same solution for 24 hours. A subset of rats were killed with a lethal dose of ketamine (100mg/kg) and xylazine (20mg/kg), after which spinal cord brain were dissected and snap-frozen on dry ice before storage at -80°C for subsequent qPCR and GAGs extraction.

3.2.2 Dorsal column crush

Dorsal column crush was performed using fine Bonn forceps (Fine Science Tools). SCI was performed under inhalational anaesthesia with isoflurane (1.8-2.2%; Baxter Healthcare Pty Ltd; cat. no. 26675-46-7) at 0.3 L/min oxygen and 0.6 L/min air. Buprenorphine (Vetergesic® Multidose) was administered subcutaneously to all animals at a dose of 0.2 mg/kg body weight. The laminectomy was performed at the T10 level (depending on the group). Small incisions were made in the dura using a sharp edge of U100 syringe needle (B Braun Omnican 50 syringe; cat. no. 9151117S), and the dorsal columns were crushed using fine Bonn forceps (Fine Science Tools). The tips of the Bonn forceps were held on either side of the dorsal columns where the small cuts were made, pressed down 1 mm into the

spinal cord and then held tightly together for 15 seconds. This lesion, as shown in many previous studies, results in a complete transection of the dorsal columns down to the level of the spinal canal. The muscles and skin were sutured together immediately after the injury. At the end of survival, animals were anaesthetised intraperitoneally with lethal doses of ketamine (100 mg/kg) and xylazine (20 mg/kg). An exception was made for the three randomly selected rats from each group, which were euthanised with a lethal dose of urethane (see the cFOS stimulation section for more information). All animals were then perfused intracardially with 4% PFA in 1X PBS. The night after surgery, two animals (one from each cohort) died. In this study, two animals had to be humanely euthanised from the thoracic injury cohort for welfare reasons.

3.3 Therapeutical interventions

3.3.1 4-MU treatment

2.5% (w/w) 4-MU was added to a chocolate-flavoured rat chow (Sniff GmbH, Germany) and prepared for use. This percentage would provide rats with 1.2 (± 0.2) g/kg/day of 4-MU if the diet was consumed ad libitum. This amount was estimated from our pilot study. Rats were maintained on the 4-MU diet for 8-10 weeks. Food consumption was measured on a weekly basis to monitor dose consumption.

3.3.2 AAV-mediated gene therapy

3.3.2.1 Preparation of AAV1 vectors

The plasmids AAV-SYN-α9-V5 and AAV-CMV-kindlin1-GFP were scaled and sequenced prior to AAV1 packaging as described previously (Hermens et al. 1999). To produce viruses, HEK293T cells were transfected with the individual expression and helper genes and cultured for three days. The transfected cells were then lysed. This was done by three freeze-thaw cycles. After centrifugation, the crude lysate was ultracentrifuged at 490000 x g, 16°C for 70 min using a type 70Ti rotor (Beckman) through an iodixanol gradient (15%, 25%, 40% and 60%). The virus was then collected for concentration on an Amicon Ultra-15 device (Millipore). The virus titre was then determined by real-time quantitative PCR at 2.34 × 1012 GC/ml for AAV1-α9-V5 and 4.99 × 1012 GC/ml for AAV1-kindlin1-GFP. AAV1-SYN-GFP was purchased from Vigene (distributed by Charles River). The titre was diluted from 2.0 × 1013 GC/ml to 2.0 × 1012 GC/ml.

3.3.2.2 Direct injection into the DRGs

Injections into the DRGs were carried out prior to the SCI, however this was done on the same day and in quick succession. Using sterilised surgical instruments, two DRGs (L4 and L5) were exposed on the left side and 1 µL of viral vector at a working titre of 2 x 1012 GC/ml was manually injected using a Hamilton syringe with custom-made needles (Hamilton; specification: 33-gauge, 12 mm, PST3). Anaesthesia and analgesia were administered to the animals as described in the SCI surgery section.

3.4 Behavioural tests

The behavioural tests were performed at different time points. The experimental paradigm is shown in the experimental plans with each of the objectives (Fig. 9, 10, 11). The time points were chosen to ensure that the animals did not learn the task independently of reflexes. They were also chosen to give the most informative value for each of the objectives. Animals were placed in the testing room at least 30 minutes prior to testing to allow for adaptation. Each rat was measured at least 3 times prior to surgery to provide a baseline for each test.

3.4.1 Basso, Beattie and Bresnahan (BBB) test

The locomotor ability of the rats was assessed using the Basso, Beattie and Bresnahan (BBB) open field test (Basso, Beattie, and Bresnahan 1995). The rats were placed in an arena. The arena was surrounded by a rectangular enclosure. The results were scored on a range of 0-21 points; from a complete lack of locomotor ability (0) to a healthy rat-like locomotor ability (21).

3.4.2 Ladder Rung Walking test

The ladder rung walking test was used to assess advanced locomotor skills. The animals were placed on a horizontal ladder 1.2 m long. The ladder had irregularly spaced rungs. A dark box, which was preferred by the rats, was placed at the end of the ladder. The rats crossed the ladder 3 times consecutively and all attempts were recorded by camera. Hind paw placement on the rungs, as previously described by Metz and Whishaw (Metz and Whishaw 2009) from all three videos, was scored using a seven-point scale (0-6 points). The scoring scale used by Metz and Whishaw was divided into three categories: 0-2; 3-4; 5-6. The videos were then scored and the percentage of steps that fell into each of the 3 categories

was calculated. Prior to SCI, all animals were pretrained. The rats were tested weekly for 16 weeks, starting 6 weeks post-SCI.

3.4.3 Maximum speed test

As part of the 4-MU experiment, a maximum speed test was performed. Maximum speed was tested weekly, starting 6 weeks after SCI. The treadmill speed started at 20 cm/s and increased by 2 cm/s every 10 seconds. The treadmill was stopped, and the last value recorded when the animal was unable to walk at a given speed.

3.4.4 Treadmill rehabilitation

Treadmill training accompanied the 4-MU treatments in the pharmacological assessment experiments and the SCI treatment. It started 6 weeks after SCI and took place 5 consecutive days per week for 16 weeks. The training consisted of 10 minutes of running, 20 minutes of rest and 10 minutes of running. The speed of the treadmill was 16-18 cm/s in the first and second weeks and 20 cm/s in the remaining weeks of the training period. Some of the rats were trained even after the 4-MU treatment was stopped. This was done to further evaluate the effect of 4-MU on non-SCI and SCI animals.

3.4.5 Rotarod

Motor performance and motor coordination were assessed using the rotarod. Prior to rotarod training (ROTA-ROD 47700, UGO BASILE S.R.I.), rats were habituated to remain on a stationary drum for 60 s and pre-trained at 5 rpm for 120 s. In the test phase, animals were tested for 300 s with increasing acceleration from 5 to 10 rpm for the first 180 s and then for a further 120 s with acceleration of 10 rpm on three different days after training. The time it took for the rat to fall from the rotary bar was recorded.

3.4.6 Grip test

The forelimb grip strength test was designed to assess neuromuscular function by determining the maximum force developed by a rat. A device (BSGT2S; Harvard Apparatus, Holliston, MA, USA) was used to measure forelimb grip strength. The experimenter pulled horizontally on the tail of the rat grasping a metal grid attached to the apparatus. The maximum muscle force was recorded as the force applied to the grid before the rat lost its grip. Over the course of a week, the test was repeated on three different days.

3.4.7 Thermal test - Plantar test

Thermal hyperalgesia after SCI and/or during treatment was assessed by the thermal test. Animals were habituated for approximately 30 min in an acrylic box of the standard Ugo Basile apparatus (Ugo Basile, Comerio, Italy). A portable. infra-red lamp was then placed directly under the foot pad of the hind paw, always in the same position. Once the lamp had been placed, a thermal radiant stimulus was applied. The apparatus was connected to a device that automatically recorded the time (in seconds) between starting the stimulus and withdrawing the paw. Both hind paws were tested five times. If the animal did not respond within 30 s or became wet, the attempt was terminated. After excluding the highest and lowest readings, the average of the three readings was taken.

3.4.8 Mechanical pressure test - Von Frey test

The mechanical pressure test was an assessment of mechanical allodynia after SCI and/or during treatment. Animals were habituated for 15 min in an enclosure with a metal mesh floor. A Von Frey rigid tip coupled to a force transducer (IITC Life Science, California, USA) was applied to the foot pad of the hind paw with a gradual increase in pressure until the animal withdrew its paw. The maximum amount of pressure was recorded in grams. Both hind paws were tested five times. The trial was terminated if the animal did not respond within 90 g. The average was calculated from three values after exclusion of the highest and lowest value.

3.4.9 Tape Removal test

For the tape removal test, each rat was trained for 5 sessions. After surgery, the rat was tested every two weeks. The rat was then removed from its home cage and placed in an empty test cage. It was habituated for 15 minutes. A small piece of adhesive tape (approximately 1 square centimetre) was applied to the paw of each rat. Three trials, with at least 3 minutes between each trial, were performed on each hind paw, left (experimental) and right (internal control). Left and right paws were tested simultaneously. The time at which the animal noticed the tape for the first time and the time at which the animal removed the tape were recorded. The tape was removed and a time of 5 min was recorded if the rat had not noticed/removed the tape after 5 min. The paper tape (TimeMed Labeling Systems, Inc.; Fisher Scientific; cat. no. NC9972972) was used for this test.

3.5 Immunohistochemistry

10-40 µm sections (free-floating and mounted on glass slides) were permeabilized with 0.5% (v/v) Triton X-100 in 1X PBS for 20-80 min. If the primary antibodies were biotinylated, endogenous biotin was blocked using an avidin/biotin blocking kit (Abcam; cat. no. ab64212) to reduce non-specific background. After permeabilisation and/or avidin/biotin blocking, the tissue was blocked in ChemiBLOCKER (1:10; Millipore cat. no. 2170), 0.3 M glycine, 0.2% (v/v) Triton X-100 in 1X PBS for 2 h. The sections were then incubated with labels and/or primary antibodies as indicated in Tab. 1. Fluorescence-conjugated secondary antibodies were used to detect primary antibodies after washes. Goat anti-host antibody or the streptavidin anti-host antibody of the respective primary antibody/marker conjugated with Alexa Fluor 405, 488, 594 and 647 (1:300; 2 h; room temperature (RT)).

3.6 Tissue clearing for lightsheet microscopy

Four randomly selected DRGs from each group were dehydrated through an ethanol (EtOH) dilution series (30%, 50%, 70%, 100%) with 2% Tween20 (Sigma-Aldrich, cat. no. P1379) and then delipidated in dichloromethane (DCM) with EtOH (2:1). Samples were then rehydrated through serial EtOH dilutions (70%, 50%, 30%) with 2% Tween20. Samples were then permeabilized through a solution containing 0.2% Triton v PBS, 0.3M glycine, 10% dimethyl sulfoxide (DMSO). Samples were blocked in 0.2% Triton v PBS, 0.3M glycine, 10% DMSO and 10% ChemiBLOCKER (2 days, 37°C). After blocking, DRG samples were incubated in the blocking solution with added primary antibodies: anti-GFP (Invitrogen, cat. no. 11122, 1:400, 2 days, 37°C) and anti-V5 (Invitrogen, cat. no. R96025, 1:400, 2 days, 37°C). Secondary antibodies (1:300) were prepared in blocking solution and applied at 37°C for 3 days. Samples were then rehydrated using the same EtOH dilution series as above and cleared in ethyl cinnamate (Sigma-Aldrich, cat. no. 112372) for 2 hours at RT. After clearing and imaging, DRGs were rehydrated in EtOH dilutions (100%, 70%, 50%, 30%), washed in PBS and cryoprotected in sucrose solution (10%, 20%, 30%), sectioned as described above and re-used for transduction efficiency analysis.

Tab. 1. Table showing the primary antibodies used in the experiments.

1° Antibody/labelling agent	Epitope	Host	Dilution, Incubation	Company
Biotinylated *Wisteria floribunda* agglutinin (WFA)	Chondroitin sulfate in the PNNs	N/A	1:150, 24 h	Sigma-Aldrich cat. no. L1516
Biotinylated Hyaluronan Binding protein (b-HABP)	Hyaluronan	N/A	1:150, 24 h	Amsbio cat. no. AMS.HKD-BC41
Anti-ACAN	Aggrecan	Rabbit polyclonal IgG	1:150, 24 h	Sigma-Aldrich cat. no. AB1031
Anti-GFAP-Cy3	Glial fibrillary acidic protein	Mouse monoclonal IgG	1:800, 24 h	Sigma-Aldrich cat. no. C9205
Anti-ChAT	Choline acetyltransferase	Mouse monoclonal IgG	1:600, 72 h	Invitrogen cat. no. MA5-31383
Anti-5-HT	5-hydroxytryptamine	Mouse monoclonal IgG	1:400; 24 h	Invitrogen cat. no. MA5-12111
Anti-synapsin	Synapsin	Rabbit polyclonal	1:100; 48 h	Novus Biologicals cat. no. NB300-104
Anti-Nestin	Nestin	Mouse monoclonal IgG1	1:300, 48 h	Chemicon cat. no. MAB353
Anti-NG2	Neural/glial antigen 2	Rabbit polyclonal IgG	1:300, 48 h	Chemicon cat. no. AB5320
Glial fibrillary acidic protein	Glial fibrillary acidic protein	Chicken polyclonal IgY	1:300, 48 h	Abcam cat. no. ab4674
Anti-CS-56	Chondroitin Sulfate	Mouse monoclonal IgM	1:100, 24 h	Sigma-Aldrich cat. no. C8035
Anti-IBA1	Ionized calcium-binding adapter molecule 1	Rabbit polyclonal IgG	1:300, 48 h	FUJIFILM Wako Pure Chemical Corporation cat. no. 019-19741
Anti- Collagen 1a	Collagen, type I	Mouse monoclonal IgG1	1:200, 48 h	Abcam cat. no. ab6308
4′,6-Diamidino-2-phenylindole dihydrochloride (DAPI)	Nucleic acid staining	N/A	1:3000, 15 mins	Invitrogen cat. no. D1306
Anti-GFP	Green fluorescent protein (GFP)	Rabbit polyclonal IgG	1:800, 72 h	Invitrogen cat. no. A-11122
Anti-GFP	Green fluorescent protein (GFP)	Chicken polyclonal IgY	1:800, 72 h	Invitrogen cat. no. A-10262
Anti-V5	V5 tag	Mouse monoclonal IgG2a	1:800, 72 h	Invitrogen cat. no. R960-25
Anti c-FOS	c-FOS protein	Mouse monoclonal IgG1	1:500, 48 h	Abcam cat. no. ab208942
Anti-NF200	Neurofilament 200	Rabbit polyclonal IgG	1:800, 72 h	Sigma-Aldrich cat. no. N4142
Anti-IBA4	Isolectin B4	N/A	1:800, 72 h	Sigma-Aldrich cat. no. L2140
Anti-CGRP	Calcitonin gene related peptide	Rabbit polyclonal IgG	1:800, 72 h	Sigma-Aldrich cat. no. PC205L
Anti-βIII tubulin	βIII tubulin	Rabbit monoclonal IgG	1:1000, 72 h	Cell Signaling cat. no. 5568
Anti-laminin	Laminin	Rabbit polyclonal IgG	1:800, 72 h	Abcam cat. no. ab11575
Anti-TnC	Tenascin-C	Rabbit polyclonal IgG	1:500, 48 h	Kindly provided by Faissner Lab, Bochum, Germany

3.7 GAGs isolation

Prior to incubation with acetone to remove lipids, frozen brains and spinal cords were first weighed. Samples were then dried and minced before Pronase treatment (15 mg Pronase per hemisphere, (Roche, #11459643001) in 0.1M Trizol hydrochloride (Sigma-Aldrich, #T3253), 10mM calcium acetate (Millipore, #567418), pH 7.8). Samples were homogenised in Pronase solution using a Potter Elvehjem tissue homogeniser. Remaining protein

fragments were removed by precipitation with trichloroacetic acid (Sigma-Aldrich, #T6399). Supernatant containing GAGs were collected and stored on ice. After neutralisation with 1M Na2CO3 (Sigma-Aldrich, #S7795) to pH 7.0, GAGs were isolated using ethanol precipitation. The recovered GAGs were redissolved in 0.3ml deionised water. GAG concentration was determined by cetylpyridium chloride (CPC) turbidity measurement. A standard curve was generated from 1 µg/µl CS A (Sigma-Aldrich, #C9819) (Kwok, Foscarin, and Fawcett 2015). Briefly, the diluted sample was mixed with 0.2% (w/v) CPC and 133 mM MgCl2 (Sigma-Aldrich, #M2670) at a 1:1 ratio. The absorbance was measured at 405 nm using a spectrophotometer with a plate reader (FLUOstar® Omega, BMG LABTECH).

3.8 RT-PCR

Quantitative real-time PCR (qPCR) was used for the quantitative evaluation of gene transcript levels in spinal cord treated with or without 4-MU. RNA was isolated using the RNeasy Mini Kit (QIAGEN, #74804) according to the manufacturer's protocol. The quantity of isolated RNA was quantified using a NanoPhotometer© P330 (Implen, Munich, Germany). Subsequently, reverse transcription of RNA to complementary DNA (cDNA) was performed using TATAA GrandScript cDNA Synthesis Kit (TATAA Biocenter, #AS103c) in a T100TM thermal cycler (Bio-Rad, Hercules, CA, USA) according to the manufacturer's protocol. For qPCR, TaqMan® Gene Expression Assays (Life Technologies by Thermo Fisher Scientific, Waltham, MA, USA) were used for HAS1 (Rn01455687_g1), HAS2 (Rn00565774_m1), HAS3 (Rn01643950_m1) and the glyceraldehyde-3-phosphate dehydrogenase (GAPDH) (Rn01775763_g1), all purchased from Applied Biosystems and used as recommended by the manufacturer. Amplification was performed on the qPCR cycler (QuantStudio® 6 Flex PCR System, Applied Biosystems® from Thermo Fischer Scientific, Waltham, MA, USA). The same cycling conditions were used for all amplifications: 2 min at 50 °C, 10 min at 95 °C, followed by 40 cycles of 15 s at 95 ◦C and 1 min at 60 °C. Expression was calculated using the threshold cycle value (Ct) and the 2-ΔΔCt method. Expression was normalised to the control group. Each of the qPCR experiments were carried out in duplicate. The Ct values of each of the measured conditions were normalised to the GAPDH. The 2-ΔΔCt values were then expressed as described by Livak and Schmittgen (Livak and Schmittgen 2001).

3.9 Haematology and Biochemistry

Animals were anesthetised with an inhalant mixture of isoflurane and air (3 v/v% isoflurane, AbbVie, Chicago, IL, USA), with an inflow of 300 mL/min, and kept under anaesthesia for the entire duration of the blood sample collection. Blood was collected from the retro-orbital venous sinus by inserting an autoclaved Pasteur pipette tip into the medial canthus of the eye under the nictitating membrane. The pipette tip was positioned between the eyeball and the bony orbit of the eye. Blood was collected every 3 weeks (in the 1st, 4th, 7th, 10th week of the experiment in all three groups and in weeks 13, 16, 19 in the wash-out group). Blood samples were collected into BD Microtainer® blood collection tubes. Blood samples for haematological analysis were collected in anticoagulant tubes containing K2EDTA (cat. no. 365974), and the following parameters were assessed: red blood cells count, haemoglobin, haematocrit, white blood cell count and relative number of white blood cells. Blood samples for biochemical analysis were collected in a serum-separating tube (cat. no. 365963), and the following serum parameters were determined: sodium, potassium, calcium, phosphorus, urea, creatinine and total bilirubin. Results were evaluated by Synlab (Munich, Germany). While the animal was still under anaesthesia, urine was collected. The rat was held over a Petri dish, and by manual pressure on the lower abdominal area, urine was squeezed out of the bladder. The urine was collected with a syringe into an Eppendorf tube (1.5 mL). In every sample, levels of glucose and proteins were assessed. Urine was evaluated by Synlab (Munich, Germany) as blood samples.

3.10 Proteomics

For assessment of renal toxicity, urinary proteins were assessed using the Kidney Toxicity 5-Plex Rat ProcartaPlex™ Panel 2 (Invitrogen cat. no. EPX050-30125-901). Prior to transcardial perfusion, urine samples were collected manually from each rat and stored at -80°C. The Rat Kidney Toxicity 5-Plex ProcartaPlex Panel 2 allows analysis of 5 protein targets, albumin, cystatin, clusterin (Apo-J), NGAL and TIMP-1, in a single well using Luminex xMAP technology to determine potential nephrotoxicity in drug studies. Samples were measured in accordance with the manufacturer's protocol.

The Th Complete 14-Plex Rat ProcartaPlex™ Panel (Invitrogen cat. no. EPX140-30120-901) was used to assess the T helper response. This panel allows 14 protein targets to be analysed in a single well using Luminex xMAP technology. The targets are IL-1α; G-CSF; IL-10; IL-17A; IL-1β; IL-6; TNFα; IL-4; GM-CSF; IFNγ; IL-2; IL-5; IL-13; IL-12p70.

Samples were analysed on Bio-Plex 200 systems (Bio-Rad, Hercules, CA, USA) according to the manufacturer's protocol.

3.11. Biomechanics

Biomechanical evaluation was performed in collaboration with the Czech Technical University, Prague, Faculty of Mechanical Engineering, Department of Mechanics, Biomechanics and Mechatronics, Radek Sedláček's group.

3.11.1 Bending Bone Strength Measurement

The mechanical properties of rat femurs were measured using a three-point bending test. Femurs were excised, cleaned of soft tissue and frozen to preserve them. After defrosting, bone was rehydrated in physiological saline solution at 8°C for 24 hours before testing. Prior to testing, the specimens were stored for 2 hours at room temperature (23°C ± 2°C). The biomechanical servo-hydraulic testing system MTS Mini Bionix 858.02 and a special fixture were used for the three-point bending test. To apply the load to the medial part of the rat femur, the specimens were placed on two rounded bars 13 mm apart. The upper part of the fixture was used to load the specimen at a constant rate of 2.0 mm/min until it broke. Furthermore, the mechanical testing was performed at room temperature (23°C ± 2°C). From the ultimate force F_{max} (N) and the Young's modulus of the bone W_{omin} (mm^3), the flexural strength σ_{omax} (MPa = N x mm-2) was calculated. The ultimate force (the force at failure) is the maximum load that a specimen can withstand before it breaks. And from the geometric parameters of the bone section that were measured, the bending modulus of the bone was determined after destruction. From the load curve in the graphical dependence of force on displacement, the external stiffness of the bone S [N x mm-1] and the energy required to break the bone U [mJ] were obtained. The direction of the tangent in the linear region of the load curve was used to obtain the external stiffness of the bone. The area under the load curve up to the maximum force was used to calculate the energy of deformation.

3.11.2 Skin tensile test

The mechanical properties were evaluated by carrying out uniaxial tensile tests on rectangular strips of the skins (the width of the specimens was 8 mm, and the thickness was 0.8 - 1.0 mm). The determination of the tensile strength and the Young's modulus of the skin at a defined deformation was the methodology of the experiment. The evaluation parameters were the tensile modulus of elasticity E, determined at two values of the relative longitudinal

deformation - at 5 % (E5) and at 10 % (E10). These values were obtained from the dependence of true stress on relative deformation as the direction of the tangent of the linear portion of the load curve. The tensile test was performed using the MTS Mini Bionix 858.02 biomechanical servohydraulic testing system and pneumatic jaws. The video extensometer automatically determined the reference length and strain of the specimens using contrasting marks on the surface of the specimens. Specimens were mounted on pneumatic grips and loaded to fracture at a constant speed of 20.0 mm/min.

3.11.3 Tendon tensile test

To assess the mechanical properties of rat tendons, destructive tensile tests were performed to evaluate their strength. The tendons were frozen for preservation and, after thawing, hydrated in physiological saline at 8°C for 24 h prior to the test. Prior to testing, the samples were stored for 2 hours at room temperature (23°C ± 2°C). Rat tendon samples were supplied in a bone-to-muscle configuration, i.e., the tendon was dissected on one side with a piece of muscle and on the other side with a piece of bone. This configuration made it possible to secure the tendon in the pneumatic jaws during the test. Prior to testing each specimen, the muscle was frozen by immersion in liquid nitrogen for 5 seconds. Careful attention was paid that the tendon does not become frozen with the muscle. Tensile testing was performed using the MTS Mini Bionix 858.02 biomechanical servohydraulic testing system and pneumatic jaws. The tendons were clamped between two metal clamps mounted in pneumatic grips. This ensured a constant force and a strong, stable. grip of the specimens as the cross section changed. The grips were fitted with a diamond-tipped cutting edge. The specimens were loaded at a constant rate of 10.0 mm/min until they were destroyed. The evaluation parameters were the maximum force and the maximum stress (i.e., the strength), the strength being calculated from the relationship $\sigma max = F_{max} / S$ [MPa].

3.12 cFOS stimulation

Three animals from each group were terminally anaesthetised with urethane (Sigma Aldrich; cat. no. U2500) at a dose of 1.5 g/kg for the AAV gene therapy experiments. The sciatic nerve was then exposed. The stimulating electrode was inserted into the nerve and the ground electrode was inserted into the muscle close to it. Stimulation consisted of 10 stimulus trains, as previously described by Bojovic et al. (Bojovic, Bramham, and Tjølsen 2016), with a stimulus duration of 0.5 ms at an amplitude of 7.2 mA, a frequency of 100 Hz, a train

duration of 2 s and an 8 s interval between trains. Single subdermal needles (Rhythmlink) were used as electrodes, and animals were perfused 2 h after electrical stimulation.

3.13 MRI

To assess the completeness of the dorsal column lesion, ex vivo MRI imaging was performed: After transcardial perfusion, 2 cm long injured spinal cord samples were harvested, post-fixed in 4% PFA in PBS (over 2 nights) and then transferred to PBS with 0.002% azide in a small plastic tube (1.5 ml) with a cap. The spinal cord was then visualised ex vivo using a 7T preclinical MRI scanner (MRS*DRYMAG 7.0T, MR Solutions, Guildford, UK). The scanner was equipped with a mouse head resonator coil. Three high-resolution sequences were acquired: Axial T2-weighted turbo spin-echo sequence, repetition time TR = 4000 ms, turbo factor TF = 8, echo interval TE = 8 ms, effective TE = 40 ms, number of acquisitions AC = 16, acquisition time approximately 17 min. The acquisition matrix was 128 × 128, field of view FOV = 10 x 10 mm2, 20 slices, slice thickness 0.5 mm without gap. A similar T2-weighted turbo spin-echo sequence was used for sagittal slices (TR=3000 ms, TF=8, TE=8 ms, effective TE=40 ms, AC=16, acquisition time 13 min) with modified geometry: matrix 128 × 256, FOV=10 × 20 mm2, 15 slices, slice thickness=0.3 mm without gap. An axial T1-weighted image was acquired with a 3D gradient echo sequence, TR=10ms, flip angle 20°, TE=3.3ms, number of acquisitions AC=16, acquisition time 11 min. The matrix was 128 × 128 × 32, FOV = 10 × 10 × 16 mm3 (providing axial slices of 0.5 mm thickness). MRI was performed in collaboration with the Centre for Advanced Preclinical Imaging (CAPI) in Prague.

3.14 Microscopy and image analysis

For Aim 1.1, to assess changes in HA and ACAN/CSPGs in organ sections, samples were observed and imaged using a Zeiss LSM 880 Airyscan microscope (Carl Zeiss AG; Oberkochen, Germany). For all organs, three replicate sections were imaged on a Zeiss LSM 880 confocal microscope and analysed in FIJITM.

For Aim 1.2, staining was imaged on a LEICA CTR 6500 microscope using FAXS 4.2.6245.1020 software (Tissue Gnostics, Vienna, AT). Images were analysed using ImageJ™ (NIH, Bethesda, MD, USA) for the total number of cells in the ventral horns with WFA+ive signal, ACAN+ive signal and the number of co-localised cells. The intensity of HABP was analysed using HistoQuest 4.0.4.0154 software (Tissue Gnostics). 5-HT, nestin,

GFAP, NG2, CS-56, collagen 1a, and Iba-1 were imaged using a Zeiss LSM 880 confocal microscope. Synapsin was imaged with an Olympus FV10i confocal microscope (Olympus Life Science, Waltham, MA, USA). The intensities of the above markers were measured using ImageJ™ (mean grey value or integrated density). Results were compared between the 4-MU and placebo groups. The particle analysis function in FIJI software was used to quantify Iba-1 positive.

For Aim 2., Confocal imaging was carried out using a Zeiss LSM880 Airyscan microscope and light sheet imaging was carried out using a Zeiss Lightsheet Z.1 microscope. Images were analysed semi-automatically using NIH ImageJ or, if necessary, manually using the reticle in the eyepiece of the microscope. The light sheet data were processed using the Huygens software (Scientific Volume Imaging, The Netherlands, http://svi.nl) and the Imaris microscopy image analysis software (Oxford Instruments). The unprocessed data and metadata are archived by the authors, and the images used for analysis were not manipulated. For the submitted images, the curves were adjusted in all images and across the images. In order to make the axons better visible in the thesis, an unsharp mask was used. The graphics editor Affinity (© 2023 Serif (Europe) Ltd) was used. The Affinity V2 Universal Licence was kindly purchased by the Second Faculty of Medicine, Charles University Grant Agency, Project No. 320421.

The experimental conditions, including immunohistochemistry and microscopy, were identical for images where intensity measurement and comparison were performed. The stained sections were imaged using the same laser power, gain and airy units. The appropriate microscope for the intended analysis of each marker was first discussed with the Core Facility at IEM CAS.

3.15 Statistics

For Aim 1.1, data are expressed as means ± SEM of N independent measurements. One-way ANOVA (HABP and ACAN intensity, behavioural test, proteomics, bone marrow evaluation, biomechanical test) or two-way ANOVA (CS-56 and HABP intensity, haematological, serological and biochemical parameters, glycosuria and urinary proteins) was used to assess the significance of the difference between the means of two or three groups of data. Statistical significance was defined as a p-value < 0.05. The statistical analysis was carried out using the GraphPad Prism 9 software package.

For Aim 1.2, data were processed, and statistical analysis performed using GraphPad Prism (GraphPad Software). Various statistical tests were used for the analysis of the effect of 4-MU treatment on chronic SCI in rats. For astrogliosis, HABP, WFA, ACAN, 5-HT, synapsin intensity in SCI cohorts, BBB and ladder rung walking test, two-way ANOVA followed by Sidak's multiple comparison test was used. For intensity of HABP, number of cells wrapped by PNNs in intact spinal cords and gene expression of has genes, two-way ANOVA followed by Dunnett's multiple comparison test was used. For two-way ANOVA, various post-hoc tests were used. To specifically test the 4-MU effect and/or rehabilitation effect against a reference group (placebo without rehabilitation) in the results of the non-SCI cohorts, the Dunnett's test was used. Except in two cases where Tukey post hoc test was used for PCR evaluation because individual gene expression values were related to untreated control without rehabilitation and for maximum speed test. All possible pairs of means were compared using the Tukey test. For SCI cohort results, Sidak's multiple comparisons were used. These are recommended for pairwise group comparisons. One-way ANOVA followed by Dunnett's test for multiple comparisons was used to assess the total amount of GAGs. All data presented in graphs are expressed as arithmetic means. Standard errors of the mean are included. Significance was determined as follows: ns-not significant, *$p < 0.05$ **$p < 0.01$ ***$p < 0.001$ and ****$p < 0.0001$. The data have not been tested for normality. No outlier test was performed.

For Aim 2., the data are expressed as mean ± SEM. Tukey's one- or two-way multiple comparison test was used to determine statistical differences between groups. A p-value of 0.05 was considered significant for all statistical analyses. GraphPad Prism (GraphPad 9 and after the update, 10 Software) was used for data processing and statistical analysis.

The statistical tests and appropriate post-hoc tests used in the individual analyses are also indicated in the results sections above the respective figures.

4. RESULTS

4.1 4-MU treatment at a dose of 1.2 g/kg/day is safe for long-term usage in rats

4.1.1 Body-wide downregulation of HA at 1.2 g/kg/day dose of 4-MU

HA is not only one of the most important polysaccharide components of the extracellular matrix, it also plays a key role in the regulation of a large number of cellular processes and in the organisation of the tissue architecture (Kobayashi, Chanmee, and Itano 2020). Here, we investigated potential adverse effects of long-term systemic administration of 4-MU at 1.2 g/kg/day. The brain, spinal cord, spleen, liver and kidney were subjected to immunohistochemical analysis for hyaluronan-binding protein (HABP) and aggrecan (ACAN) or CSPGs (CS-56), respectively (Fig. 12 and 13). A significant downregulation of staining intensity was observed in the tissues. This confirmed the effect of 4-MU in reducing HA and CS.

4-MU treatment in healthy animals reduced the intensity of both ACAN- and HABP+ive signals in the brain by almost 50% (ACAN: 46.16 ± 6.23%, n = 3; p = 0.0128; HABP: 44.26 ± 5.71%, n = 3, p = 0.0141; Fig. 12 A-D). After 9 weeks of wash-out, the intensity had not returned above 83% (ACAN: 79.1 ± 2.02%, n = 3; p = 0.1287; HABP: 72.9 ± 4.07%, n = 3, p = 0.0956; Fig. 12 A-D). In the spinal cord, the fluorescent signal decreased even more after 4-MU treatment (ACAN: 42.35 ± 4.62%, n=3; p=0.0012; HABP: 63.26 ± 4.07%, n=3, p=0.00015; Fig. 12 E-H). After 9 weeks of wash-out, the aggrecan signal had returned to almost 90% (ACAN: 89.7 ± 2.08%, n = 3; p = 0.2911). Spinal HA levels returned to baseline (HABP: 45.29 ± 11.19%, n = 3, p = 0.9932; Fig. 12 E-H), contrasting with the positive ACAN signal. Aggrecan was chosen as a marker of PNNs.

We decided to replace aggrecan with CS-56 for visualisation in kidney, spleen and liver sections in order to stain for CSPGs in other organs. The treatment with 4-MU shows different effects in the organs of healthy animals. In the liver, our results show a significantly reduced CS-56 positive signal (25.56 ± 1.13%, n = 3; p = 0.0173, Fig. 13). However, the HABP positive signal did not show a significant difference even after 4-MU treatment. In the spleen, no significant changes were observed between the three groups (Fig. 13). Within the kidney, we observed an increase of CS-56 fluorescence intensity (31.23 ± 7.64%, n = 3; p=0.0018) and a decrease of HABP fluorescence intensity (44.88 ± 4.08%, n = 3, p=0016; Fig. 13). After the 9-week wash-out period, CS-56 positive signal remained low in the liver

compared to healthy controls (p = 0.0009), in contrast to the kidney samples where CS-56 positive signal remained high after the wash-out period (p = 0.0247).

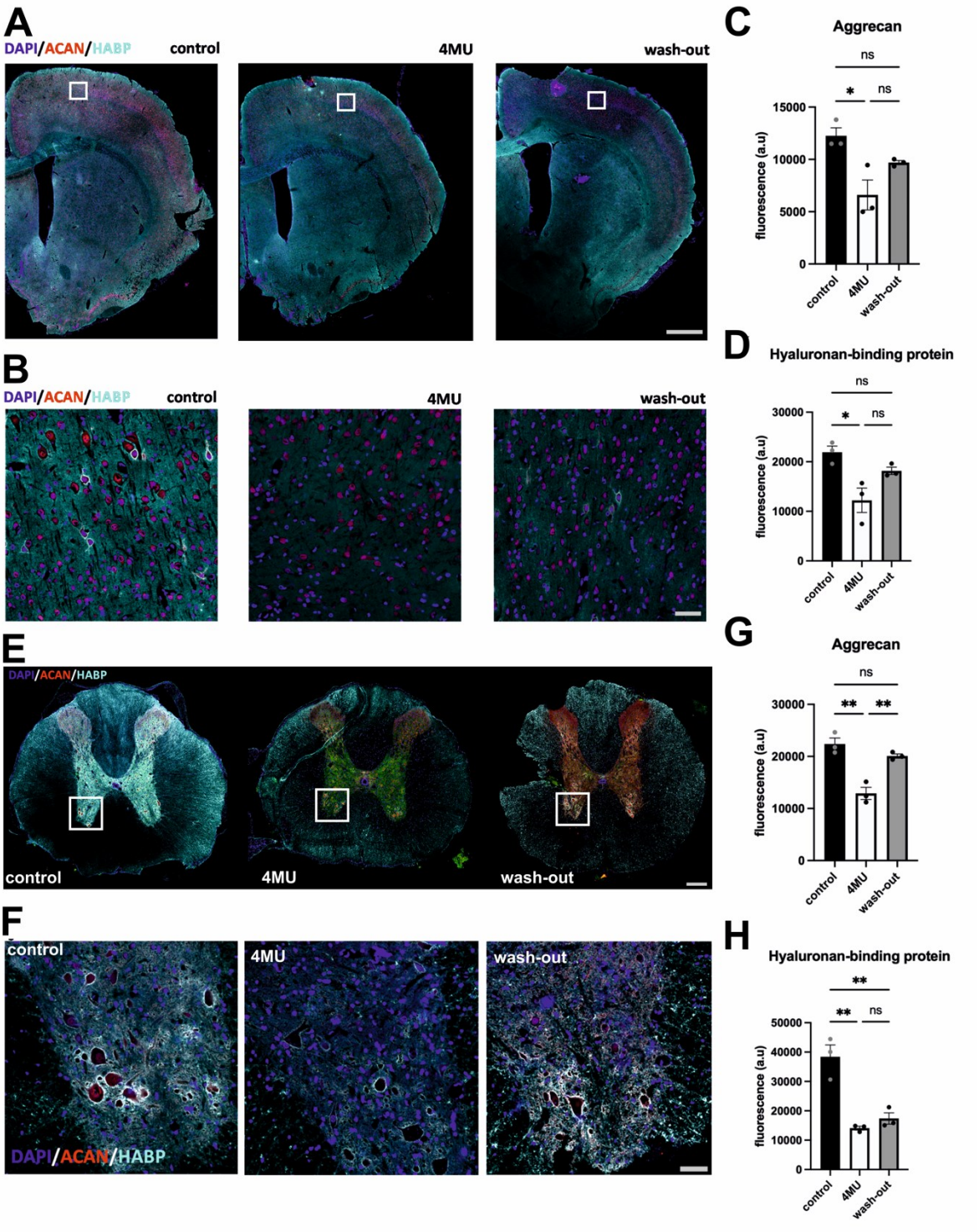

Fig. 12. After 10 weeks of treatment, 4-MU at a dose of 1.2 g/kg/day downregulates HA and PNNs in the brain and spinal cord. (**A**) Representative confocal images showing HA and ACAN positive areas in brain slices from placebo, 4-MU and 9-week wash-out animals. Scale bar: 1000 µm. (**B**) Representative confocal images showing a detail of the cortex of the brain. In 4-MU-treated animals, HA and ACAN positivity is reduced in comparison to

untreated controls and partially returns after the 9-week wash-out period. Scale bar: 50 µm. (**C, D**) Quantification of the signal of ACAN and HABP in the cerebral cortex. Values are mean ± SEM for n = 3 in each group. (**E**) Representative confocal images showing HA, ACAN and DAPI positive areas in spinal cord sections from placebo, 4-MU and 9-week wash-out animals. Scale bar: 200 µm. (**F**) Detail of the ventral horns of the spinal cord in representative confocal images. The 4-MU-treated animals showed a lower HA and ANCA positivity than the untreated controls, which partially returned after 9 weeks. Scale bar: 50 µm. (**G, H**) Quantification of ACAN- and HABP+ive signals in spinal grey matter. Values are expressed as mean ± SEM; *$p < 0.05$, **$p < 0.01$ by one-way ANOVA with Tukey's multiple comparison test, n=3 in each group; ns = not significant.

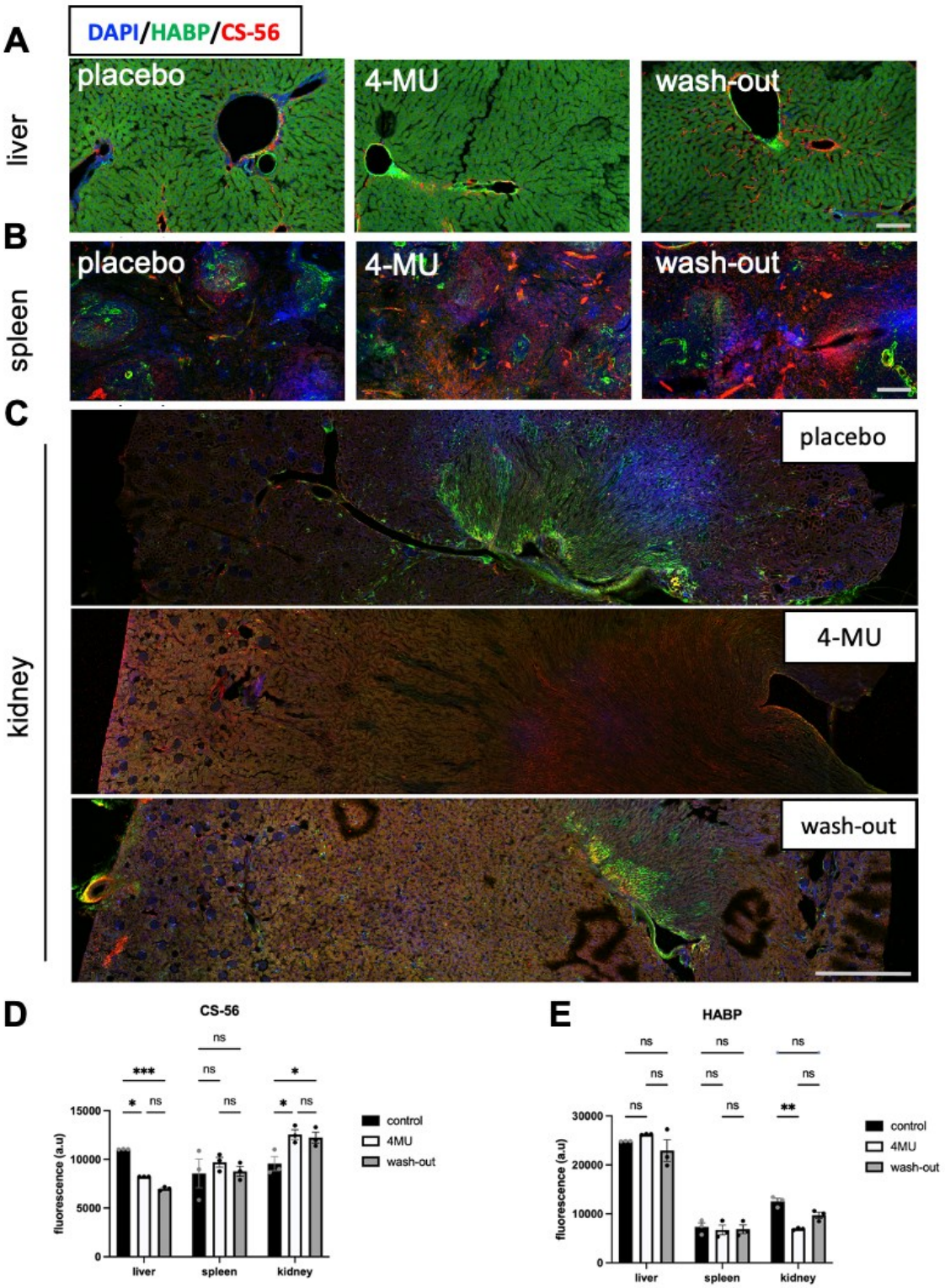

Fig. 13. Systemic downregulation of HA and CSPGs was observed after administration of 4-MU at a dose of 1.2 g/kg/day. Representative confocal images of HA- and CSPG+ive areas in (**A**) liver (100µm), (**B**) spleen (200µm) and (**C**) kidney (1000µm) in placebo-fed, 4-MU-fed and 9-week wash-out animals, demonstrating the downregulation of both markers and the return of signal after 9 weeks of wash-out (**D, E**) Quantification of CS-56 and HABP positive signals in renal, splenic and liver sections. Values are mean ± SEM, *p < 0.05, **p

< 0.01, ***p < 0.001 by two-way ANOVA with Tukey's multiple comparison test, n=3 in each group. ns = no significance.

4.1.2 No adverse effects on haematological or biochemical parameters were observed with long-term administration of 4-MU at a dose of 1.2 g/kg/day

To investigate whether long-term treatment with 1.2 g/kg/day 4-MU affected any of the haematological parameters, we focused on the following parameters: leukocytes, haemoglobin, haematocrit, erythrocytes, erythrocyte distribution width, platelets, reticulocytes, neutrophils, lymphocytes, monocytes, eosinophils, basophils and neutrophils (Fig. 14). Data are presented in Tab. 2. The haematology parameters of all three groups were compared with the benchmark values ("Clinical Laboratory Parameters for Crl:Wi (Han) rats", Charles River Laboratories International, 2008). Except for absolute and relative monocyte counts, where data was outside the reference range, all parameters were within the reference range. Monocyte counts increased in all three groups without significant differences.

The next step was to test the biochemical parameters of the blood and the blood serum. Following parameters were monitored: sodium, potassium, calcium, phosphorus, creatinine, urea (Tab. 3) and markers associated with liver injury (total bilirubin, bile acids, AST, ALT, ALP) (Fig. 14). We focused primarily on liver function tests to monitor potential liver injury, as almost all drug classes can cause drug-induced liver injury (David and Hamilton 2010). At week 7 of 4-MU treatment, significant differences in measured ALT levels were observed between the wash-out group (1.189 ± 0.080 µkat/L) and placebo (0.886 ± 0.097 µkat/L). In addition, we observed slightly higher ALT enzyme values (1.005 ± 0.133 µkat/L) than the reported reference values (0.3-0.75µkat/L) throughout the experiment.

4-MU has been shown to increase bile acid secretion and is used to treat cholestasis (Hoffmann et al. 2005). Therefore, after treatment with 4-MU, we checked the concentration of bile acids. We observed a significantly higher level of bile acids in the blood 4 weeks after treatment in comparison to the control group (4-MU 79.36 ± 29.67 µmol/L, wash-out 96.36 ± 28.69 µmol/L vs. control 14.15 ± 3.11 µmol/L; $p = 0.0014$ and $p < 0.0001$, respectively). At week 7, bile acid levels remain high in the treated group, although significance is observed only in the wash-out group, reflecting possible physiological adaptation to 4-MU after long-term treatment (4-MU 46.07 µmol/L, wash-out 71.37 ± 10.78 µmol/L vs. 21.296

± 12.803 μmol/L; p = 0.38 and p = 0.0235, respectively). For the remaining haematological markers of liver injury, our data showed no other significant differences between groups.

Tab. 2. Table showing haematological test results from the first and last week of treatment and after the washout period. The table also shows normal physiological values for the parameters shown.

PARAMETERS	UNITS	placebo		4-MU		wash-out			PHYSIOLOGICAL RANGE
		1st week	10th week	1st week	10th week	1st week	10th week	19th week	
leukocytes	10^9/l	10.625 ± 0.717	7.572 ± 0.986	8.950 ± 0.734	7.286 ± 0.419	8.400 ± 0.310	8.100 ± 0.745	5.729 ± 0.370	**1.39-7.49**
haemoglobin	g/l	148.750 ± 1.925	148.714 ± 5.022	151.250 ± 1.292	141.571 ± 6.778	149.625 ± 2.352	129 ± 25.974	148.857 ± 3.066	**137-168**
hematocrit	l/l	0.429 ± 0.007	0.445 ± 0.015	0.437 ± 0.008	0.404 ± 0.018	0.421 ± 0.010	0.446 ± 0.009	0.408 ± 0.009	**0.32-0.5**
erythrocytes	10^12/l	7.553 ± 0.113	7.744 ± 0.258	7.641 ± 0.171	7.201 ± 0.270	7.408 ± 0.169	7.930 ± 0.221	7.197 ± 0.180	**7.07-9.03**
erythrocytes-mean volume	fl	56.825 ± 0.258	57.486 ± 0.463	57.213 ± 0.319	56.014 ± 0.705	56.875 ± 0.432	56.417 ± 0.655	56.814 ± 0.796	**48.9-57.9**
erythrocytes - colorant	pg	19.500 ± 0.327	19.286 ± 0.421	19.750 ± 0.453	19.714 ± 0.421	20.000 ± 0.327	19.500 ± 0.224	20.715 ± 0.421	**17-20**
Red Cell Distribution Width	%	13.525 ± 0.205	13.871 ± 0.467	13.563 ± 0.078	13.443 ± 0.194	13.763 ± 0.224	13.783 ± 0.201	14.114 ± 0.192	**10.5-14.9**
thrombocytes	10^9/l	796.500 ± 61.632	710.714 ± 203.150	740.000 ± 62.309	963.429 ± 155.209	1181.625 ± 127.863	1151.667 ± 155.749	1023.143 ± 161.486	**638-1177**
reticulocytes (abs)	10^9/l	234.857 ± 15.277	236.286 ± 37.150	285.625 ± 17.267	213.000 ± 15.205	220.000 ± 12.821	246.000 ± 23.058	193.286 ± 13.928	**129.8-383.7**
reticulocytes(relat)	%	2.807 ± 0.185	3.033 ± 0.622	3.035 ± 0.178	2.670 ± 0.216	2.751 ± 0.141	2.785 ± 0.203	2.349 ± 0.122	**1.7-4.7**
neutrophils (abs)	10^9/l	1.240 ± 0.248	0.621 ± 0.220	0.688 ± 0.137	0.363 ± 0.115	0.528 ± 0.098	0.317 ± 0.160	0.800 ± 0.155	**0.15-1.5**
lymphocytes (abs)	10^9/l	8.609 ± 0.595	6.236 ± 0.891	7.443 ± 0.604	6.157 ± 0.402	7.053 ± 0.322	6.942 ± 0.676	4.370 ± 0.280	**0.82-5.66**
monocytes (abs)	10^9/l	0.575 ± 0.130	0.614 ± 0.175	0.678 ± 0.152	0.711 ± 0.120	0.736 ± 0.166	0.793 ± 0.148	0.404 ± 0.090	**0.02-0.16**
eozinophils (abs)	10^9/l	0.150 ± 0.030	0.084 ± 0.037	0.085 ± 0.022	0.060 ± 0.030	0.061 ± 0.020	0.027 ± 0.025	0.133 ± 0.032	**0.01-0.15**
basophils (abs)	10^9/l	0.026 ± 0.006	0.006 ± 0.003	0.018 ± 0.006	0.007 ± 0.004	0.011 ± 0.005	0.007 ± 0.007	0.013 ± 0.006	**0.0-0.03**
neutrophils (relat)	%	11.313 ± 1.963	7.957 ± 2.849	7.813 ± 1.461	5.271 ± 1.801	6.350 ± 1.238	3.933 ± 2.099	13.943 ± 2.404	**7.1-33.2**
lymfocytes (relat)	%	81.288 ± 1.487	82.357 ± 2.903	83.375 ± 0.778	84.186 ± 1.231	83.950 ± 1.235	85.800 ± 1.480	76.600 ± 2.398	**62.2-90**
monocytes (relat)	%	5.813 ± 1.747	8.469 ± 1.931	7.650 ± 1.561	9.514 ± 1.297	8.825 ± 2.111	9.783 ± 1.658	6.943 ± 1.362	**0.8-3.9**
eozinophils (relat)	%	1.350 ± 0.246	1.057 ± 0.486	0.950 ± 0.224	0.943 ± 0.465	0.750 ± 0.256	0.333 ± 0.314	2.314 ± 0.475	**0.5-4.5**
basophils (relat)	%	0.238 ± 0.060	0.071 ± 0.036	0.200 ± 0.050	0.086 ± 0.055	0.125 ± 0.056	0.083 ± 0.083	0.200 ± 0.069	**0-0.8**

Tab. 3. Table showing blood biochemistry test results from the first and last week of treatment and after the washout period. The table also shows normal physiological values for the parameters shown.

PARAMETERS	UNITS	placebo		4-MU		wash-out			PHYSIOLOGICAL RANGE
		1st week	10th week	1st week	10th week	1st week	10th week	19th week	
sodium	mmol/l	141.750 ± 0.675	141.250 ± 0.590	142 ± 0.526	141.714 ± 0.286	141.750 ± 0.491	141.125 ± 0.441	139.429 ± 0.297	**142-151**
potassium	mmol/l	4.748 ± 0.186	4.708 ± 0.115	4.711 ± 0.130	4.769 ± 0.089	4.794 ± 0.088	4.591 ± 0.136	5.344 ± 0.124	**3.82-5.55**
calcium	mmol/l	2.549 ± 0.027	2.556 ± 0.037	2.621 ± 0.011	2.533 ± 0.018	2.480 ± 0.018	2.516 ± 0.015	2.511 ± 0.025	**2.4-2.8**
phosphorus	mmol/l	1.875 ± 0.097	1.450 ± 0.053	2.036 ± 0.044	1.436 ± 0.050	1.769 ± 0.057	1.444 ± 0.070	1.221 ± 0.092	**1.6-3.45**
urea	mmol/l	5.538 ± 0.342	6.250 ± 0.370	5.025 ± 0.121	5.286 ± 0.137	5.400 ± 0.073	5.950 ± 0.321	5.886 ± 0.260	**2.05-4.1**
creatinine	μmol/l	23.000 ± 1.210	23.375 ± 1.133	22.875 ± 0.515	28.714 ± 0.918	25.625 ± 0.754	34.125 ± 0.766	29.714 ± 1.392	**17-44.2**
total bilirubin	μmol/l	1.888 ± 0.156	2.543 ± 0.177	2.00 ± 0.149	2.300 ± 0.076	2.088 ± 0.132	2.163 ± 0.299	2.786 ± 0.209	**0.89-2.64**
ALT	μkat/l	0.914 ± 0.035	1.043 ± 0.089	0.959 ± 0.058	0.809 ± 0.038	1.014 ± 0.029	0.960 ± 0.050	1.303 ± 0.162	**0.3-0.75**
AST	μkat/l	2.054 ± 0.268	3.270 ± 0.401	2.120 ± 0.115	2.031 ± 0.240	2.511 ± 0.371	2.050 ± 0.198	2.836 ± 0.353	**1.24-2.4**
ALP	μkat/l	2.660 ± 0.178	1.922 ± 0.262	2.401 ± 0.148	1.698 ± 0.266	2.883 ± 0.249	2.144 ± 0.148	2.544 ± 0.230	**1.034-3.84**
bile acids	μmol/l	16.741 ± 3.895	14.686 ± 5.142	12.839 ± 3.482	26.920 ± 5.333	13.388 ± 3.005	45.110 ± 7.712	32.841 ± 8.941	**2.00-10.00**
proteins	g/l	60.688 ± 1.286	63.150 ± 1.433	60.700 ± 0.716	60.171 ± 0.879	60.038 ± 0.666	61 ± 0.745	51.757 ± 0.847	**55-77**
albumin	g/l	32.600 ± 0.638	35.386 ± 0.731	32.125 ± 0.382	33.733 ± 0.506	32.900 ± 0.498	30.075 ± 3.999	33.929 ± 0.513	**24-48**

Alanine Aminotransferase (ALT)

nominal range: 0.3 – 0.75 µkat/L

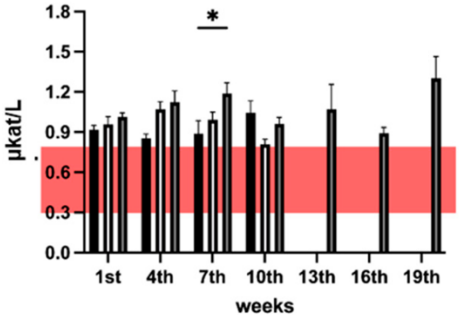

Aspartate Aminotransferase (AST)

nominal range: 1.24 – 2.65 µkat/L

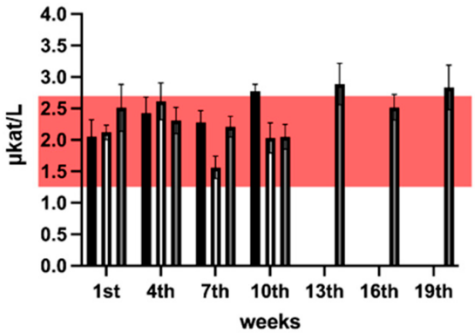

Alkaline Phosphatase (ALP)

nominal range: 1.04 – 3.84 µkat/L

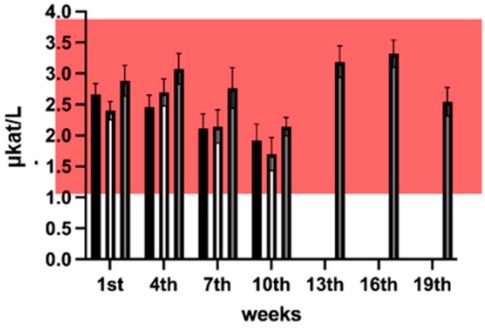

Albumin

nominal range: 24 – 48 µkat/L

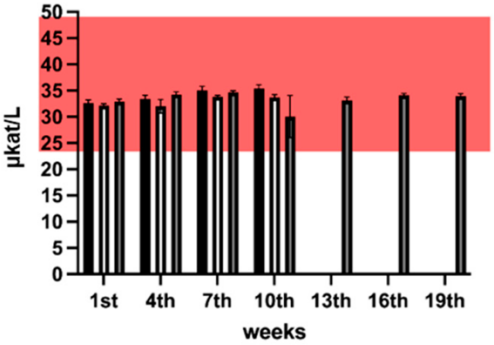

Proteins

nominal range: 55 – 77 µkat/L

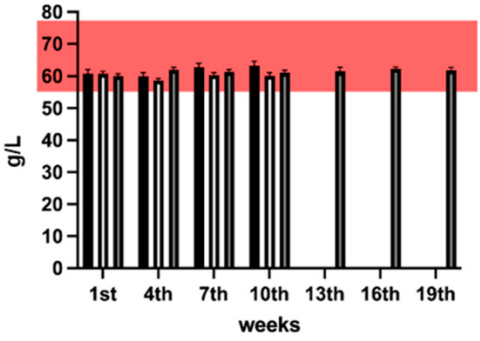

Total bilirubin

nominal range: 0.89 – 2.64 µkat/L

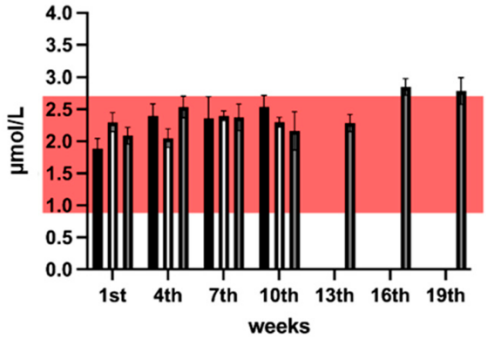

Bile acids

nominal range: 2 – 20 µkat/L

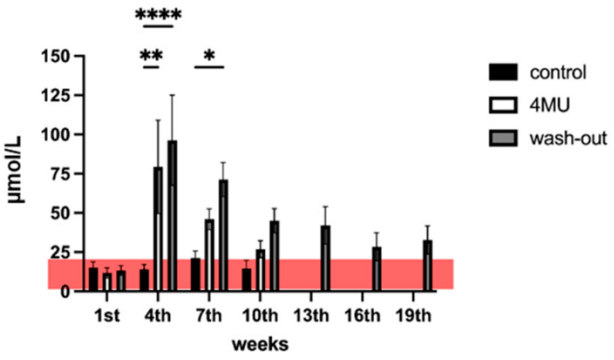

Fig. 14. After long-term treatment with 4-MU at a dose of 1.2 g/kg/day, liver function tests do not indicate any liver damage. The nominal range of each test is indicated by the pink box in each graph. $p < 0.05$, ** $p < 0.01$, **** $p < 0.0001$ by two-way ANOVA with Tukey's multiple comparison test, n= 5 - 7.

The results suggest that no serious adverse changes in blood haematological or biochemical parameters were induced by long-term treatment with 4-MU. Serum glucose, cholesterol, triacylglycerol and iron levels were also assessed. See Tab. 4 for the data. After 10 weeks of treatment with 4-MU at a dose of 1.2 g/kg/day, no renal impairment was observed. Glucose and protein levels were analysed every three weeks on the basis of histochemical changes in the kidneys. Glycosuria is usually associated with impaired renal filtration and is an abnormal amount of glucose in the urine. Compared to the placebo group (0.032 ± 0.011 g/L), glycosuria was observed in the 4-MU-treated group (0.443 ± 0.167 g/L) and in the wash-out group (0.424 ± 0.155 g/L) at week 4 (Fig. 15). At weeks 7 and 10, urine glucose levels remained slightly elevated in both the 4-MU-treated and wash-out groups compared to reference values. However, there was no significant difference from the placebo group. Urine glucose levels returned to the normal physiological range (Fig. 15) during the wash-out period.

Tab. 4. Table showing blood serum test results from the first and last week of treatment and after the washout period. The table also shows normal physiological values for the parameters shown.

PARAMETERS	UNITS	placebo		4-MU		wash-out			PHYSIOLOGICAL RANGE
		1st week	10th week	1st week	10th week	1st week	10th week	19th week	
glucose in serum	mmol/l	6.803 ± 0.228	6.605 ± 0.505	6.943 ± 0.483	6.408 ± 0.618	6.616 ± 0.274	11.579 ± 3.868	8.313 ± 0.377	4.23-9.714
cholesterol	mmol/l	2.210 ± 0.092	2.481 ± 0.117	2.086 ± 0.065	3.472 ± 1.491	2.094 ± 0.052	1.986 ± 0.096	2.190 ± 0.056	0.62-1.89
triacylglycerides	mmol/l	1.280 ± 0.139	1.717 ± 0.299	1.213 ± 0.100	1.355 ± 0.190	1.400 ± 0.156	1.716 ± 0.214	1.580 ± 0.217	0.22-1.30
iron	µmol/l	54.988 ± 2.540	66.468 ± 5.425	58.888 ± 5.130	51.533 ± 4.759	54.850 ± 3.650	56.686 ± 3.955	61.486 ± 7.198	

Elevated levels of protein in the urine, known as proteinuria, are often associated with kidney damage. At week 1 (0.179 ± 0.064 g/L) and week 10 (0.179 ± 0.038 g/L) of the sampling period, proteins outside normal physiological values were observed in the 4-MU-treated and wash-out groups (Fig. 15), as well as in the placebo group. Only at week 7, compared to the 4-MU-treated (0.271 ± 0.057 g/L) and wash-out (0.313 ± 0.052 g/L) groups, was there a significant difference in the placebo group (0.103 ± 0.030 g/L). Protein levels did not return to physiological levels during wash-out (Fig. 15).

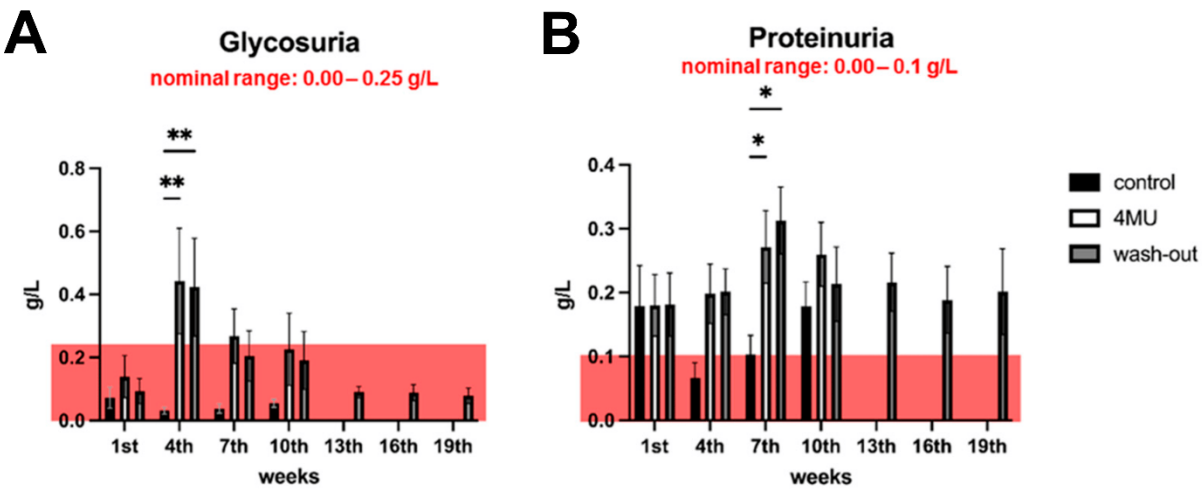

Fig. 15. After 1.2 g/kg/day of 4-MU treatment, glycosuria and proteinuria do not indicate severe renal damage. Changes in urinary glucose (**A**) and protein (**B**) during 4-MU treatment are shown in the bar graphs. The nominal range of each assay is indicated by the pink box in each graph. Data are expressed as means ±SEM. *p<0.05, **p<0.01 by two-way ANOVA with Tukey's multiple comparison test, n=7.

The Rat Kidney Toxicity 5-Plex ProcartaPlex Panel 2 (Invitrogen, cat. no. EPX050-30125-901) was used to further investigate the effect of drug metabolism on renal injury. Five urinary biomarkers were selected for assessment of nephrotoxicity (Fig. 16): clusterin, cystatin C (Cys-C), neutrophil gelatinase-associated lipocalin (NGAL), urinary tissue inhibitor of metalloproteinases-1 (TIMP-1) and albumin. Clusterin is usually associated with tubulointerstitial kidney lesions and drug-induced damage is evidenced by reduced gene and protein expression. Under physiological conditions, Cys-C is filtered. It is completely reabsorbed and catabolised in the proximal tubule. Acute kidney injury leads to increased urinary Cys-C. NGAL, an iron-transporting protein, increases its urinary excretion after nephrotoxic and ischaemic insults. It is therefore one of the biomarkers of acute kidney injury (Makris et al. 2009). TIMP-1 levels are low in healthy kidneys but have been shown to increase significantly in models of renal disease. TIMP-1 levels are also associated with the extent of fibrosis (X. Zhang et al. 2006). The final marker studied was albumin. Albumin is a well-established diagnostic and prognostic marker for assessing the severity of glomerular disease in the progression of chronic kidney disease. Our results showed that compared to the placebo (19.903 ± 2121 pg/mL) and 4-MU-treated (18.115 ± 647 pg/mL) groups, the wash-out group (12.861 ± 1442 pg/mL) had significantly reduced levels of clusterin. Cys-C, NGAL, TIMP-1 and albumin levels were not significantly different between groups.

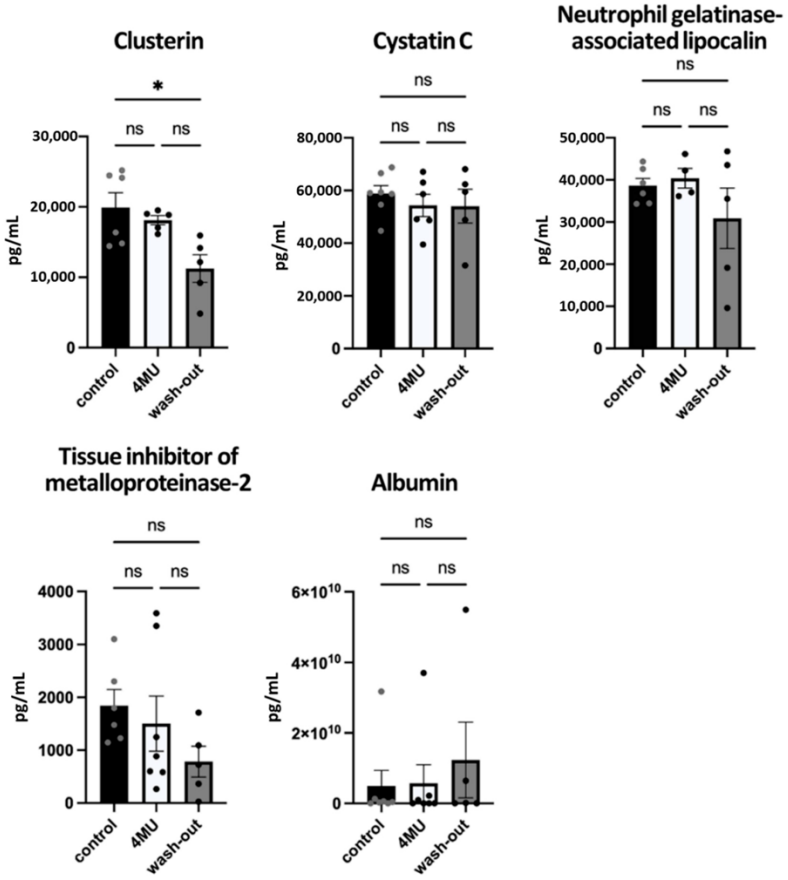

Fig. 16. Assessment of nephrotoxicity using urinary biomarkers. Levels of urinary markers of renal injury are shown as bar graphs. Data expressed as mean ± SEM; * $p < 0.05$ by one-way ANOVA with Tukey's multiple comparison test, n=4-7. ns = not significant.

4.1.3 1.2 g/kg/day dose, 4-MU increases blood serum levels of IFN-γ, IL10 and IL12p70 after 10 weeks of daily administration, but levels return to baseline during wash-out period

There is evidence that HA regulates cytokine release (Nagy et al. 2015). We therefore investigated whether 4-MU-mediated inhibition of HA synthesis would affect this process. The levels of 14 cytokines (IFN-γ, IL10, IL12p70, IL13, IL2, IL17a, IL4, IL5, IL6, IL1α, IL1β, TNF-α, GM-CSF and G-CSF) in blood serum were measured using the Complete 14-Plex Rat ProcartaPlex™ Panel (Invitrogen, cat. no. EPX140-30120-901). However, we could only detect six. The other eight markers were either negative or were below the limit of detection of the kit. Our results indicate that the levels of IFN-γ, IL-10, IL-12p70 and G-CSF were significantly elevated in the 4-MU-treated animals compared to the placebo control group, whereas in the wash-out group the levels decreased back to control levels. In addition, after the wash-out period, the levels of all the markers affected by the 4-MU

treatment returned to the levels of the healthy controls. The levels of IL13 and IL2 did not change significantly when compared to the control group (Fig. 17).

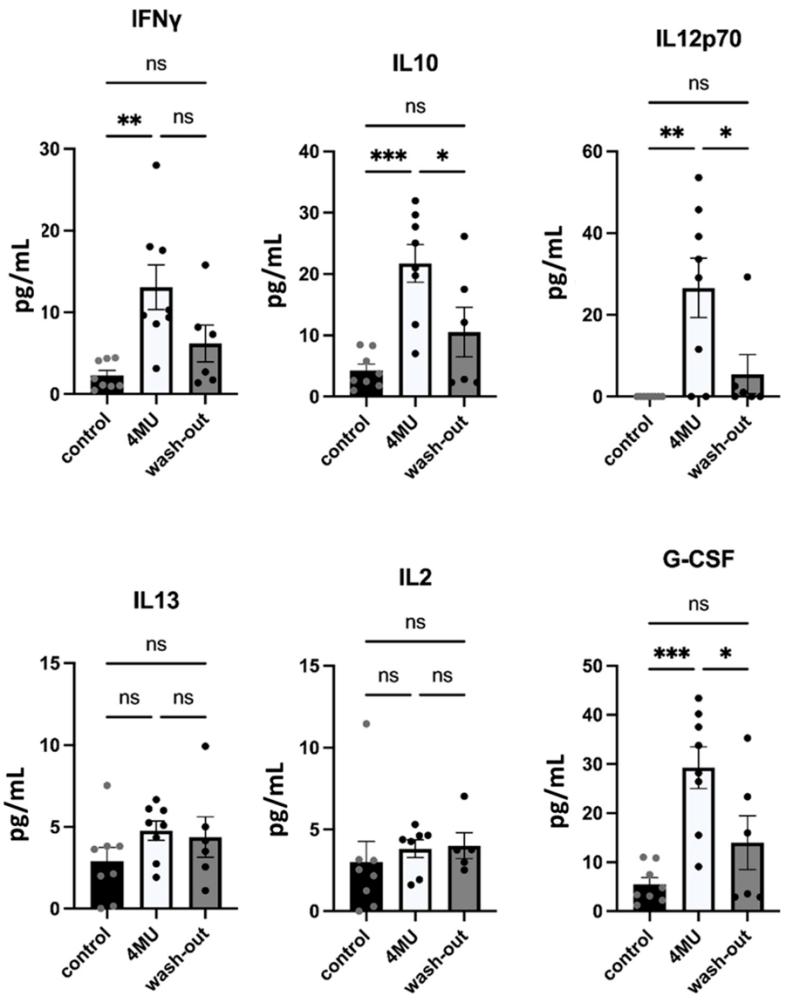

Fig. 17. After long-term treatment with 4-MU, serological levels of cytokines and interleukins were measured. The bar graphs show the levels of the cytokines and interleukins that were detected. Data are expressed as mean ± SEM; *p<0.05, **p<0.01, ***p<0.001 by one-way ANOVA with Tukey's multiple comparison test, n=5 to 8. ns = not significant.

4.1.4 1.2 g/kg/day dose of 4-MU does not affect animal behaviour

Two behavioural tests were used to determine the possible behavioural changes that 4-MU might have on the muscle strength and locomotor functions of the rats (Fig. 18). The grip strength test was used to assess neuromuscular function. It determined the maximum force that the animal could produce. Animals in the wash-out group had a significant reduction in the isometric contraction force of the forelimb compared to the placebo control group, but the reduction was mild. Motor function and forelimb-hindlimb coordination were assessed using the rotarod. Between the groups, no significant changes were observed.

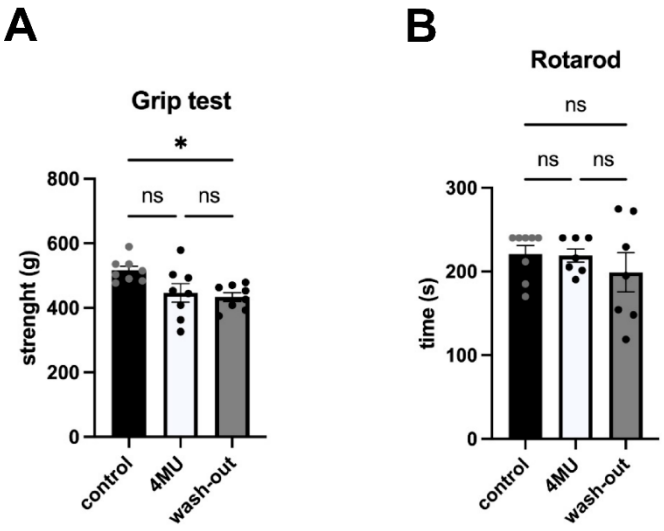

Fig. 18. Results between placebo, 4-MU and wash-out groups showed no changes in motor function after 10 weeks of 4-MU treatment, but significant differences were observed in forelimb strength between placebo and wash-out groups. (**A**) shows the results of the grip strength test and (**B**) shows the results of the rotarod test. For easy identification of each data point, different coloured dots are used. Data expressed as mean ± SEM; *p < 0.05 by one-way ANOVA with Tukey's multiple comparison test. ns = not significant.

4.1.5 Long-term 4-MU treatment at the current dose does not affect the biomechanical properties of tendons and skin, but does affect the biomechanical properties of bone

To further characterise the systemic effect mediated by 4-MU, we decided to investigate the biomechanical properties of bones, skin and tendons after long-term 4-MU treatment. Our results suggest no significant changes in the measured parameters, except for the external stiffness of the bones, where we observed a significant reduction in the stiffness of the measured femurs. External stiffness represents the resistance to deformation under the applied load. These results suggest that the reduced level of HA and GAGs in the bones leads to a reduction in the water content, making the bones less resistant to deformation (Tab. 5). In addition, bone itself, being composed of not only inorganic minerals but also organic proteins and, of course, water, has a complex chemical and material composition at the microscopic level. Considering bone as an organic-inorganic composite, the ratio between these must be taken into account when it comes to the biomechanical properties of bone tissue. If the ratio is shifted towards being more organic or more inorganic, then the mechanical properties will change significantly (Luo and Amromanoh 2021).

Tab. 5. The biomechanical properties of the bones, skin and tendons in the control group, the 4-MU group and the wash-out group. Data are expressed as mean ± SEM; **p<0.01, ***p<0.001 by one-way ANOVA with Dunnett's multiple comparisons test (n=14-28). The significant difference (two stars in red) shown in the external bone stiffness is expressed as 4-MU treated animals compared to CTRL (i.e., healthy untreated animals). CTRL = control, W/O = wash-out.

BONES		
Bending strenght [Nmm-2]	CTRL	158,8 ± 2,847
	4-MU	153,1 ± 3,435
	W/O	156,6 ± 4,331
External stiffness [N/mm]	CTRL	726,7 ± 18,09
	4-MU	**617,0 ± 25,97** **
	W/O	801,1 ± 27,55
Energy [mJ]	CTRL	66,72 ± 2,983
	4-MU	60,34 ± 2,013
	W/O	63,321 ± 3,554
TENDONS		
Maximum force [N]	CTRL	20,11 ± 2,673
	4-MU	14,75 ± 1,746
	W/O	23,56 ± 3,708
Maximum stress [N/mm]	CTRL	20,11 ± 2,673
	4-MU	14,75 ± 1,746
	W/O	23,56 ± 3,708
SKIN		
Young modulus E5 (5%) [mJ]	CTRL	9,326 ± 1,113
	4-MU	13,57 ± 1,856
	W/O	10,43 ± 1,240
Young modulus E10 (10%) [mJ]	CTRL	16,43 ± 2,910
	4-MU	16,06 ± 2,702
	W/O	16,79 ± 3,704

4.2 4-MU at a dose of 1.2 g/kg/day reduces glial scar but is insufficient to induce functional recovery after chronic SCI

4.2.1 Although 4-MU reduces GAG synthesis and PNN in the uninjured spinal cord, 4-MU at a dose of 1.2 g/kg/day is not sufficient to downregulate the increased production of chondroitin sulphates after SCI

We have seen in our previous experiments that 4-MU mediates a downregulation of HA in the spinal cord, but we wanted to investigate this downregulation in more detail and after 8 weeks of feeding and the effect of rehabilitation on the ECM in uninjured animals.

Adult rats were fed 4-MU at a dose of 1.2 g/kg/day on a daily basis for 8 weeks, and some of them were then subjected to a wash-out period of 8 weeks. GAGs were extracted from the dissected spinal cords. The total amount of HA and GAGs was quantified by turbidity

assay (Kwok, Foscarin, and Fawcett 2015) (Fig. 19A). The results showed that 4-MU treatment alone (0.09 ± 0.81 mg/g; n=4; p=0.0086) and 4-MU plus daily treadmill training (0.17 ± 0.16 mg/g; n=4; p=0.0113) significantly reduced GAG levels compared to placebo (2.02 ± 0.70 mg/g; n=4). In the treated animals, rehabilitation did not affect the efficacy of 4-MU in downregulating GAG synthesis. Interestingly, daily treadmill exercise alone also showed a modest but non-significant reduction in GAG levels compared to placebo (1.06 ± 0.16 mg/g; n=4; p=0.2555), suggesting that rehabilitation (or exercise) may independently reduce GAG levels. In the wash-out group, the total amount of GAGs (0.93 ± 0.40 mg/g; n = 4; p = 0.1734) recovered to a level similar to that of the rehabilitation group, suggesting a partial return of GAGs (Fig. 19A). In comparison to the placebo group, the 4-MU and/or rehabilitative effect on GAGs levels was tested.

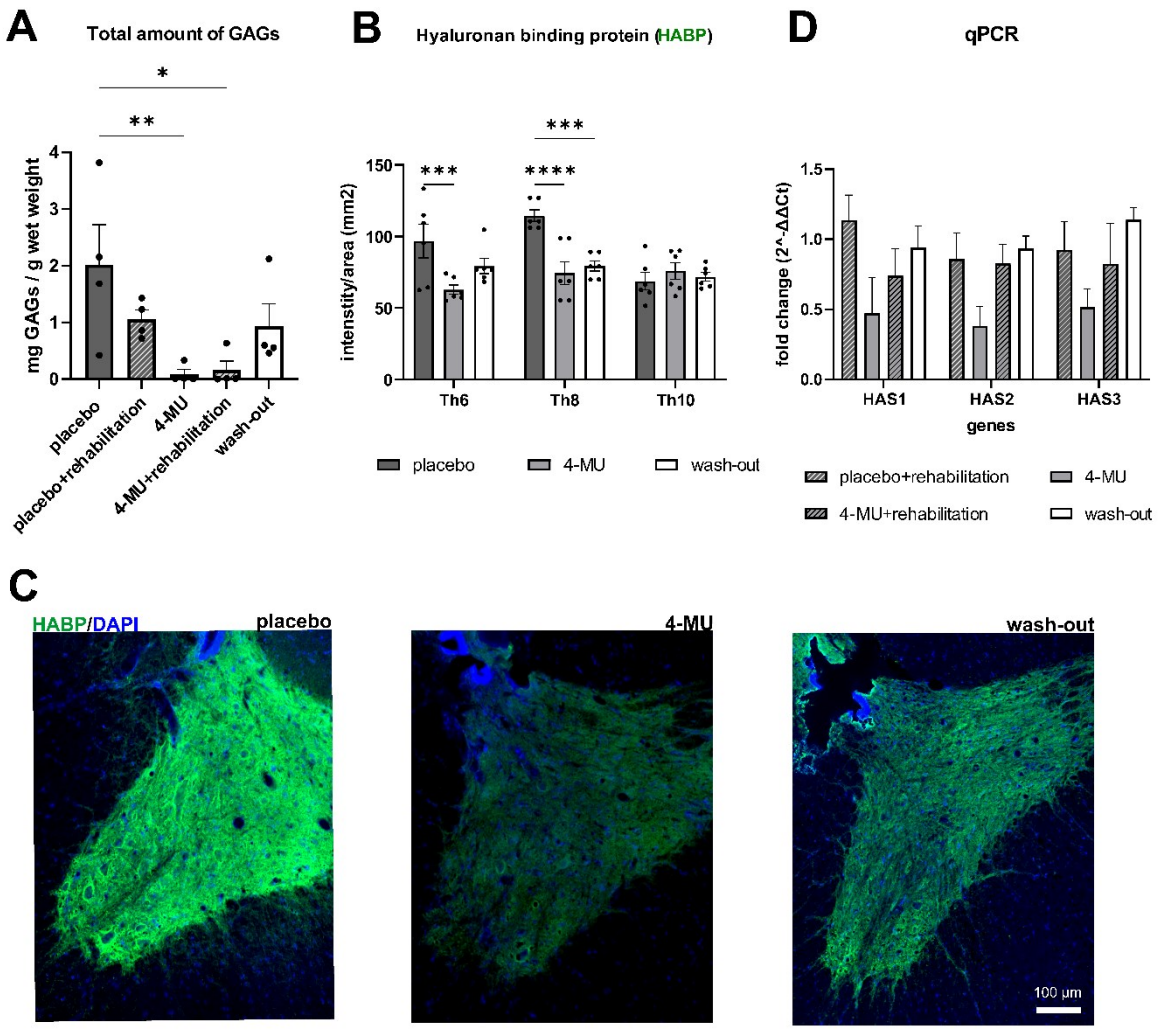

Fig. 19. 4-MU reduces HA and CSPG synthesis in non-SCI animals even after 8 weeks of feeding. (**A**) Bar graph showing the total amount of GAGs extracted from frozen spinal cords after the feeding of 4-MU or placebo and after the wash-out period. Values are

presented as mean ± SEM; * $p < 0.05$, by one-way ANOVA, Dunnett's post-hoc test. (n = 4 animals per group). (**B**) Quantification of (**C**). Bar graph shows mean intensity per grey matter area with individual data points. HistoQuest software from TissueGnostics was used to calculate intensity. Values are presented as mean ± SEM; *$p < 0.05$, **$p < 0.01$ by two-way ANOVA, Dunnett's post-hoc test. (n = 3 animals per group, 2 images per animal). (**C**) After 8 weeks of feeding and after 8 weeks of wash-out, representative fluorescence images showing differential HABP + signal intensity in grey matter (Th8) in the placebo, 4-MU-treated and wash-out groups. Scale bar 100 μm. (**D**) Bar graph showing the fold change in the expression of hyaluronan synthase (HAS) 1, 2, 3 genes (as 2^-ΔΔCt). Normalised to the placebo-treated animals without rehabilitation. qRT-PCR was used to determine 2^-ΔΔCt values. Values are presented as mean ± SEM; two-way ANOVA, Tukey post-hoc test in all 4 groups (n = 4 animals per group).

We also quantified the degree of HA downregulation using HABP staining (Fig. 19 B, C). Sections at Th6 and Th10 and around the level of Th8, the focus of subsequent experiments, were subjected to histochemical staining. In the 4-MU-treated group, the intensity of HABP was significantly decreased at Th8 (74.32 ± 12.81; n = 3; $p < 0.0001$) and Th6 sections (68.68 ± 4.20; n = 3; $p = 0.0007$) compared to the placebo group (at Th8, 114.53 ± 6.36, n = 3 and at Th6, 114.57 ± 10.97, n = 3). At the Th10 level, there was no significant difference between the 4-MU and placebo groups. After 8 weeks of wash-out, HA remained at low levels at Th8 (79.37 ± 5.57; n = 3; $p = 0.0005$) and Th6 (83.24 ± 11.00; n = 3; $p = 0.0962$) compared to the placebo group, with some tendency for HA production to return, but not to reach the level of the placebo group (Fig. 19 B, C).

Quantification of HAS mRNA expression in spinal cord samples by qPCR (Fig. 19D) did not show a significant down-regulation of HAS gene expression in the 4-MU group. However, clear trends of downregulation of HAS gene expression were observed in the 4-MU group compared to all other groups. In the wash-out group, HAS gene expression reached placebo levels in combination with the rehabilitation group, suggesting a recovery of normal GAGs expression after the wash-out period.

We next investigated the effect of 4-MU treatment (at a dose of 1.2 g/kg/day) on PNNs in the ventral horns. This was done by co-staining for WFA and ACAN. WFA is a widely used marker of PNNs and has been shown to specifically label the N-acetyl-D-galactosamine

residue at the terminal ends of chondroitin sulphate chains (Testa, Prochiantz, and Di Nardo 2019; Reichelt et al. 2019). ACAN is a major PNN component. It has been reported to be superior in labelling PNN+ive motor neurons in the spinal cord (Sian F. Irvine and Kwok 2018). Spinal cord sections from all 5 groups were stained for WFA (Fig. 20) and ACAN (Fig. 20) and the number of positive cells was counted in the ventral horns up to the central canal (Fig. 20). Similar to the biochemical assays, 4-MU treatment and treadmill exercise independently reduced the total number of WFA+ive cells in the spinal ventral horns (Fig. 20). The combination of both induced a greater down-regulation, but this did not reach significance. We also observed that the number of WFA+ive and ACAN+ive neurons returned to control levels after the wash-out period. PNNs have previously been shown to encapsulate α-motoneurons in the spinal cord. Using anti-ChAT antibody, we observed reduced PNNs around ChAT+ive neurons in uninjured thoracic spinal cords after 4-MU treatment (Fig. 20). This suggests that the current dose of 4-MU at 1.2 g/kg/day or rehabilitation can effectively reduce PNNs in the uninjured spinal cord.

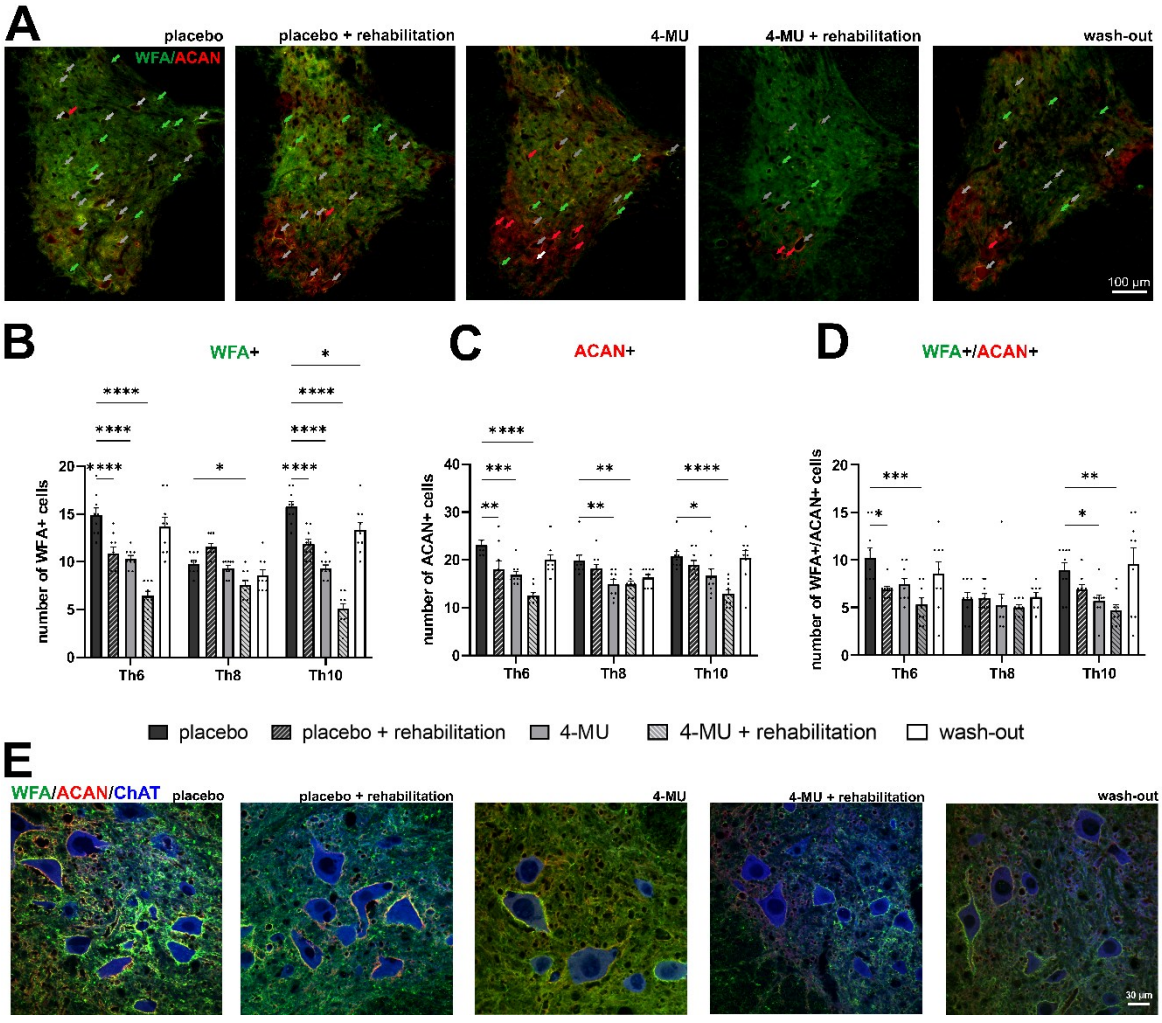

Fig. 20. Down-regulation of PNNs after 8 weeks of 4-MU feeding in uninjured animals, with or without daily treadmill training, and the re-appearance of PNNs after 8 weeks of wash-out period. (**A**) Representative fluorescent images showing *Wisteria floribunda agglutinin* (WFA) and aggrecan (ACAN) positive PNNs around cells in the ventral horns and their colocalization (WFA+ive /ACAN+ive) in thoracic spinal cord (Th8) in uninjured animals in all 5 groups after 8 weeks of feeding and after 8 weeks of wash-out period. Green arrows indicated the WFA+ive PNNs enwrapped cells; red arrows indicated ACAN positive PNNs enwrapped cells and grey arrows indicated cells where WFA/ACAN positive signal colocalizes. Scale bar 100 μm. (B–D) Quantitative analysis of WFA positive or ACAN positive PNNs. Data showed mean ± SEM (n = 3 animals per groups, 3 sections per animal). *p < 0.05, **p < 0.01, ***p < 0.001, ****p < 0.0001, two-way ANOVA, Dunnett's multiple comparison. (E) Representative confocal images showing WFA positive and ACAN positive PNNs surrounding ChAT positive motoneurons in the thoracic rat spinal cord (Th8) in placebo, 4-MU treated and wash-out group in ventral horn. Scale bar 30 μm.

Having found that a dose of 4-MU of 1.2 g/kg/day in combination with rehabilitation was effective in reducing PNNs in the spinal cord, we next investigated whether this dose was sufficient to reduce the increased expression of inhibitory ECM in the injured spinal cord. Rats were subjected to a moderate SCI induced by a 200 kdyn impact at the Th8 level of the spine. Six weeks after injury, the animals were randomly divided into two groups. The groups received a daily diet containing 4-MU or placebo for 8 weeks. In addition, both groups received task-specific rehabilitation for the 16 weeks concurrent with the oral 4-MU treatment (i.e., 8 weeks during 4-MU treatment and 8 weeks after) in order to prime appropriate re-connection from the potentially enhanced neuroplasticity (Fig. 21).

First, we evaluated the amount of HA within the spinal cord (Fig. 21) using HABP. In the 4-MU-treated group (40.78 ± 6.30), there is a significant reduction in HA around the lesion, rostrally (up to 5 mm) and caudally (1 and 5 mm) from the lesion compared to the placebo group (72.46 ± 6.46). After 4-MU treatment, we observed a trend towards lower HA levels throughout the spinal cord. Even after an 8-week wash-out period, the intensity remained reduced.

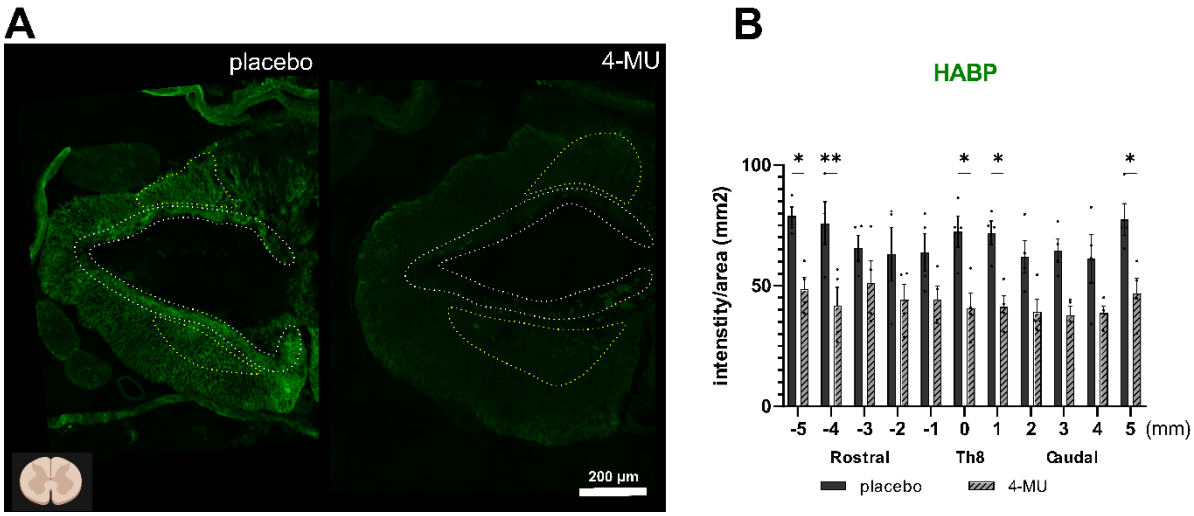

Fig. 21. After chronic SCI, 8 weeks of 4-MU treatment and 8 weeks of wash-out combined with daily rehabilitation, HABP intensity remained reduced. (**A**) Representative fluorescence images showing differential HABP+ signal intensity in placebo and 4-MU-treated SCI rats after 8 weeks of feeding and 8 weeks of wash-out. Intensity per section throughout the spinal cord is shown as a bar graph. The border of the cavity is indicated by white dotted lines. Spared grey matter is represented by yellow dotted lines. Due to injury variability and individual animal characteristics, the area of spared grey matter varies between animals. 3 animals were excluded because of the BBB test 1 week after injury (i.e., animals with a BBB test score below 8 were not included in this study). The diagram in the lower left-hand corner shows the orientation of the cross-sections, which were created using BioRender.com. Scale bar 200 µm; (**B**) Quantification of (**A**). Individual data (n = 3 animals per group) are shown with their mean ± SEM. Two-way ANOVA, Sidak's multiple comparison test, *$p < 0.05$, **$p < 0.01$.

We then assessed the level of PNNs and CSPGs using WFA and ACAN. Our results showed no significant difference between the 4-MU-treated and placebo groups after a further 8 weeks of no treatment but daily rehabilitation (Fig. 22). These results are consistent with our data from uninjured animals where PNNs reappeared after 8 weeks of wash-out (Fig.s 22). The strong upregulation of CSPGs after SCI made the dose of 1.2 g/kg/day of 4-MU insufficient to suppress their production in the injured spinal cord.

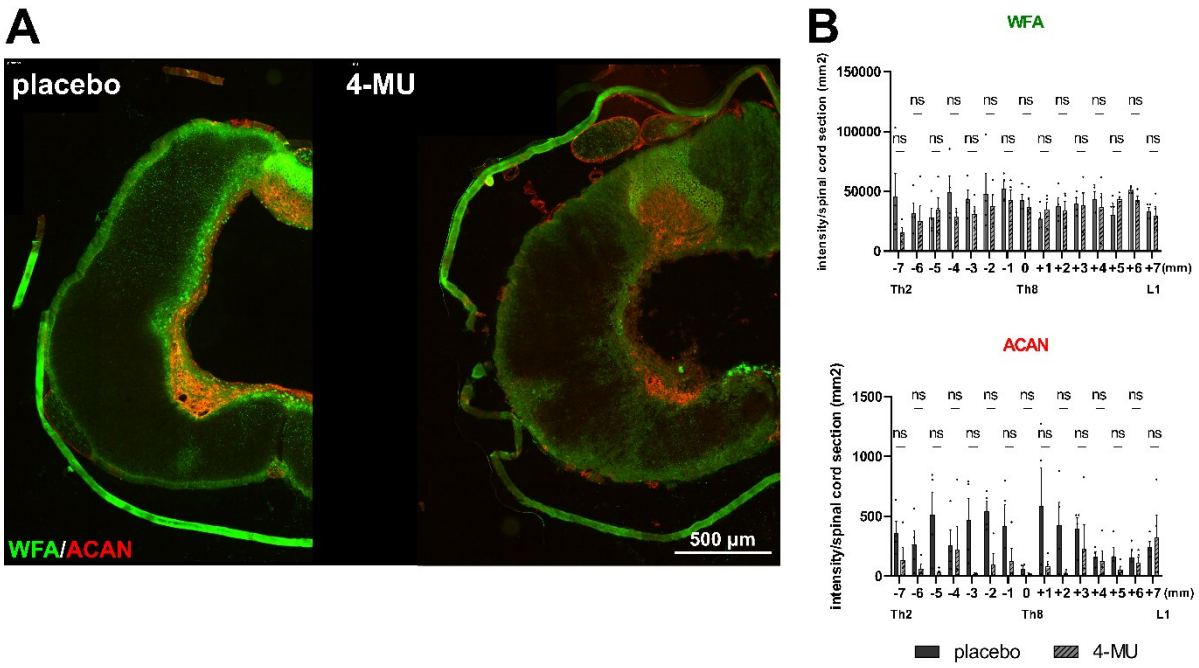

Fig. 22. Immunofluorescent double staining of WFA and ACAN suggested that 4-MU at the current dose of 1.2 g/kg/day was not sufficient to downregulate the increased production of chondroitin sulphates after SCI. (**A**) Representative fluorescence images showing the area of WFA+ive (in green) and ACAN+ive (in red) around the centre of the lesion. (**B**) Quantitative analysis of WFA or ACAN intensity. Bar graphs show the intensity per section over the entire spinal cord. The centre of the lesion is marked as level 0. Individual data points and their mean ± SEM are presented (n=4 animals per group). ns by two-way ANOVA, Sidak's multiple comparison test.

To further investigate changes in the extracellular matrix around the lesion site, we have examined the levels of CSPGs (Fig. 23). Using the CS-56 antibody, which recognises CS-GAG chains, we observed a significant down-regulation of CS-56 signal at the lesion epicentre in the 4-MU-treated group in comparison to the placebo group. This contrasts with the WFA and aggrecan staining shown in Fig. 23, where no significant change could be observed. As CS-56 is specific for the chondroitin sulphate type A and C enriched sequence (Sarama S Deepa et al. 2007), our results suggest that there is a differential regulation of the sulphation pattern around the lesion site after 4-MU treatment. The mechanism by which 4-MU induces such changes is not well understood.

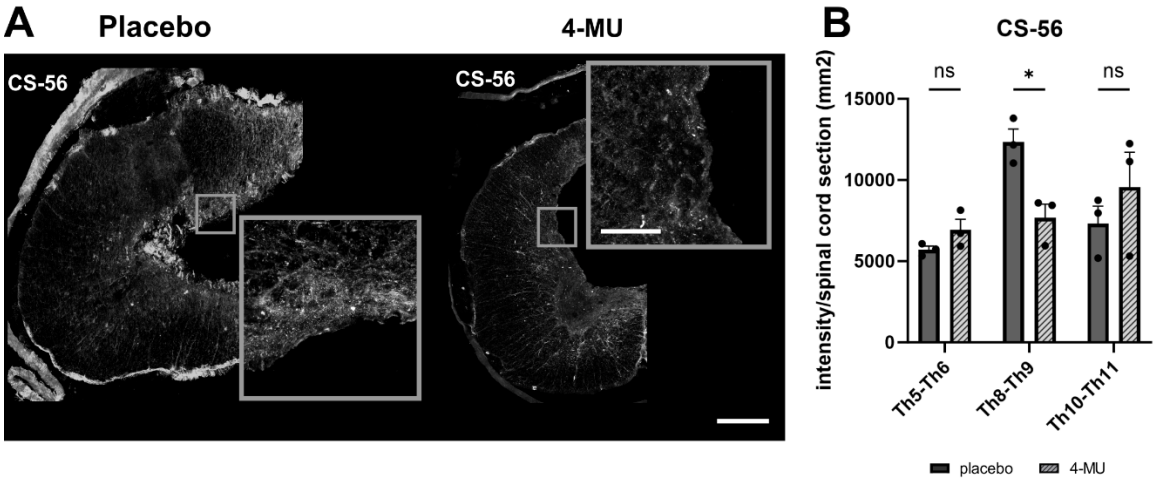

Fig. 23. 4-MU treatment alters CS-56+ive signal around the lesion scar (Th8-9), but not above (Th5-6) or below (Th10-11) the lesion. (**A**) To investigate changes in CS sulfation, the effect on CS-56+ive signal was examined. The representative confocal images show the 4-MU-mediated changes in CS-56 signal intensities between groups. The insets are high magnification views of the staining. The scale bar is 200 µm for the overview image and 50 µm for the insets. (**B**) Quantification of (A). Intensities per section over the entire spinal cord are shown as bar graphs. Individual data are presented as mean ± SEM (n = 3 animals per group). *p < 0.05 by two-way ANOVA, Sidak's multiple comparison test.

4.2.2 4-MU at 1.2 g/kg/day reduces glial scar in chronic SCI

HA is upregulated by astrocytes in neuroinflammation (R. Asher et al. 1991; Struve et al. 2005; Back et al. 2005) and is produced by both neurons and glia in the CNS. In the mouse model of experimental autoimmune encephalomyelitis, 4-MU has previously been shown to reduce astrogliosis in the brain parenchyma (Hedwich F. Kuipers et al. 2016). Given our observation of HA downregulation around the lesion cavity, we next focused on the effect of 4-MU on the glial scar after SCI. A quantitative analysis of the GFAP+ive area was carried out to assess the glial scar surrounding the lesion cavity on cross sections (Fig. 24). A significant decrease in astrogliosis was observed in the 4-MU treatment group at a dose of 1.2 g/kg/day in comparison to the placebo group. The average peak in the middle of the lesion was 1.49 ± 0.51% (n=4) in the 4-MU groups and 6.1 ± 1.94% (n=4) in the placebo groups (Fig. 24). Note also that GFAP staining in the periphery of 4-MU sections appeared brighter than in the placebo control groups. We therefore analysed the pixel intensity between the two groups. No significant difference was observed.

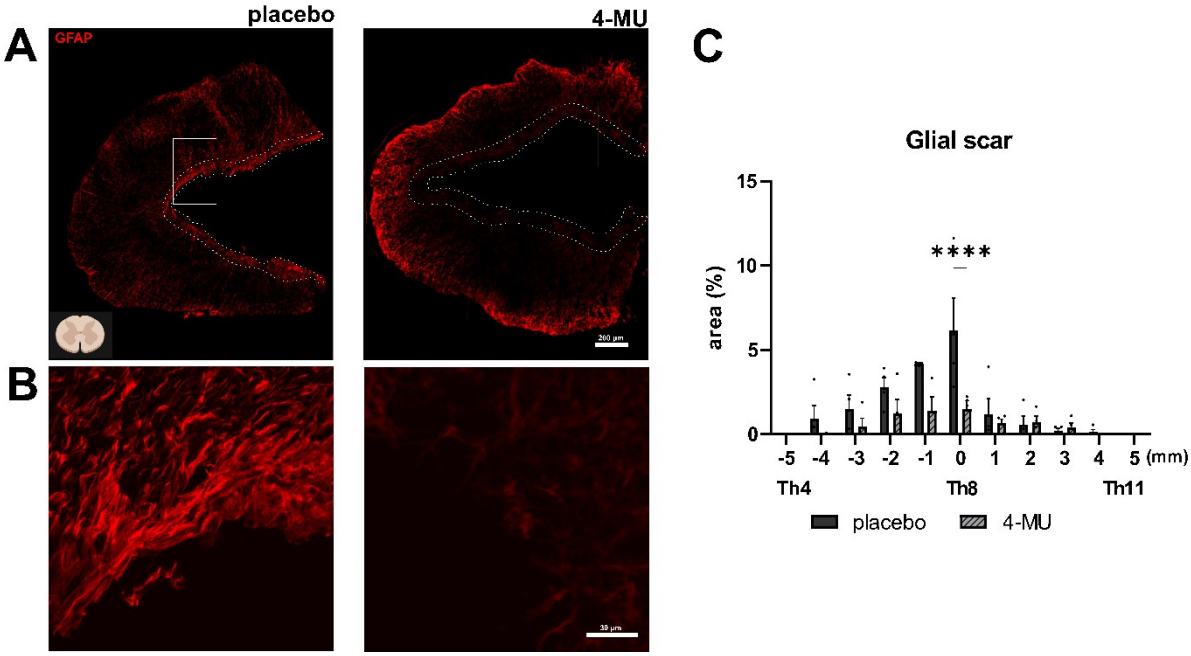

Fig. 24. The area of glial scar around the lesion site was reduced by 4-MU treatment. (**A**) Representative fluorescence images of the lesion epicentre staining for GFAP in chronic SCI treated with 4-MU and placebo. Dotted lines indicate the lesion cavity boundary in the 4-MU-treated group and the GFAP+ive area in the placebo-treated group. (B) Magnified images showing structural changes in GFAP+ive scar tissue after 4-MU treatment compared to placebo-treated animals. Scale bar: 30µm; (C) Bar graph showing the area of glial scar around the central cavity in the GFAP-stained images using ImageJ software. Values are presented as mean ±SEM; **** $p<0.0001$ by two-way ANOVA, Sidak post hoc test. (n= 4 animals per group).

4.2.3 4-MU at a dose of 1.2 g/kg/day has an effect on astrocytes, immune cells and OPCs, but not on fibroblasts/meningeal cells in the contusion model of chronic SCI

To determine whether 4-MU affects GFAP expression only in scarring astrocytes or in the astrocytes themselves, we used nestin immunohistochemistry to compare the behaviour of GFAP+ive cells around the lesion epicentre (Th8-Th9), inferior (Th10-Th11) and superior (Th5-Th6) to the lesion (Fig. 25). Compared to placebo, intensity measurements showed a reduction in signal for both nestin and GFAP after 4-MU treatment. This is an indication that there is a reduction in astrocyte proliferation and activation.

Next, we looked at microglia/macrophages and oligodendrocyte progenitor cells (OPCs) to see how they were affected by 4-MU treatment. We used the ionised calcium-binding adaptor molecule 1 (Iba-1) as a microglia/macrophage specific calcium-binding protein (Fig.

25). Compared to the placebo group, we observed a significantly higher number of Iba-1 positive cells at the lesion site after 4-MU. This is an indication that 4-MU mediates the infiltration of microglia and macrophages in this area.

We then examined the changes in OPC with neuronal glial antigen 2 (NG2) and observed a significant increase in NG2 signal after long-term treatment with 4-MU followed by a two-month wash-out period (Fig. 24). As NG2-expressing OPCs may either: (i) contribute to scar formation in response to bone morphogenic protein (BMP) secretion by activated astrocytes, or (ii) self-renew and facilitate regeneration, further experiments will be required to confirm their functions at the lesion site. Nevertheless, these results are evidence that treatment with 4-MU is effective in the modulation of the cellular composition around the lesion area.

The levels of collagen 1a produced by meninges or fibroblasts were also examined. At the lesion site and away from the lesion, there was no significant change in the presence of collagen 1a+ive cells.

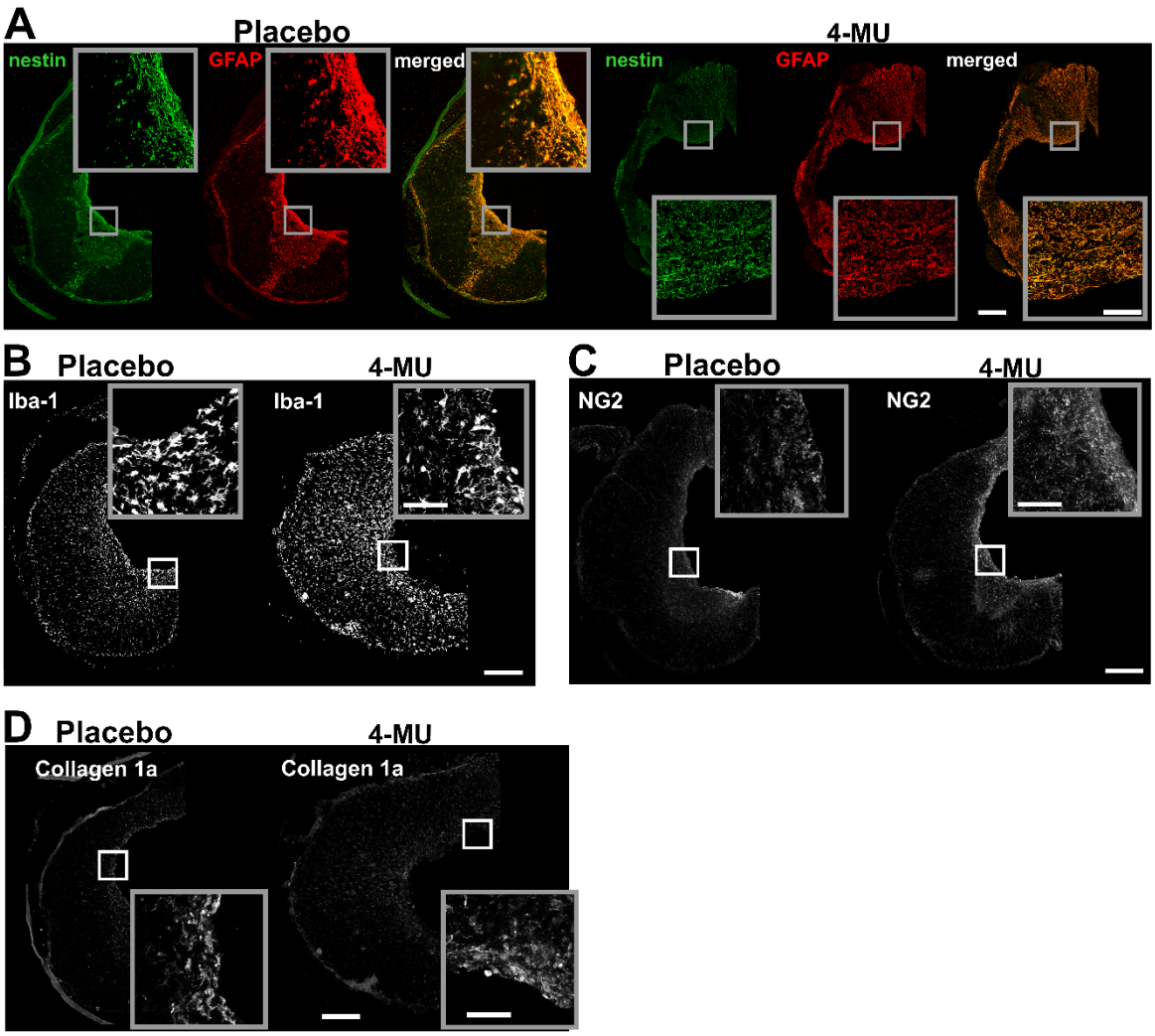
A
Placebo
4-MU
nestin
GFAP
merged
nestin
GFAP
merged
B
Placebo
4-MU
Iba-1
Iba-1
C
Placebo
4-MU
NG2
NG2
D
Placebo
4-MU
Collagen 1a
Collagen 1a
F
Nestin
GFAP
Iba-1
NG2
Collagen 1a
intensity/spinal cord section (mm2)
Iba-1 +ve cells/mm2
ns
*
****
***
Th5-Th6
Th8-Th9
Th10-Th11
placebo
4-MU

Fig. 25. Treatment with 4-MU leads to changes in the cell and ECM composition around the lesion scar (Th8-9), above the lesion (Th5-6) and below the lesion (Th10-11). (**A-D**) Representative confocal images showing the 4-MU-mediated effect on scarring cells and components using different markers - (**A**) nestin and GFAP were used for visualisation of scarring astrocytes. (**B**) Iba-1 was used to visualise microglia/macrophages. (**C**) NG2 for visualisation of oligodendrocyte precursor cells (OPCs). (**D**) Collagen 1a for visualisation of meninges and fibroblasts. All insets show an enlarged view of the staining area. Scale bar 200 μm for the overview image and 50 μm for the insets. (**F**) Quantification of (**A-E**). Except for Iba-1 staining, where the number of Iba-1 positive cells per mm was counted, bar graphs show intensities per section throughout the spinal cord. Individual data are presented as mean ± SEM (n = 3 animals per group). $p < 0.05$, **$p < 0.01$, ***$p < 0.001$, ****$p < 0.0001$, by two-way ANOVA, Sidak's multiple comparison test.

4.2.4 4-MU at a dose of 1.2 g/kg/day promotes the sprouting of serotonergic fibres at a distance from the injury, but has no effect on the density of synapses around the site of the lesion

The results in Fig. 21 and 22 show that while a dose of 1.2 g/kg/day is able to reduce HA and glial scar, the levels of CSPGs remain similar to untreated injured controls after SCI (Fig. 19 and 20), and that there are sulphation modifications on the CS-GAG chains. Serotonin (5-hydroxytryptamine; 5-HT) is a major neurotransmitter in the mammalian spinal cord. It plays an essential role in the control of sensorimotor functions. We therefore sought to determine whether 4-MU treatment alters serotonergic innervation. We observed that after 8 weeks of treatment with 4-MU, followed by a 2-month wash-out period and rehabilitation, there was a significant increase in 5-HT+ive puncta in the ventral horns above the lesion in the 4-MU-treated group (259.25 ± 12.3) compared to the placebo group (208.58 ± 4.06), and below the lesion in the 4-MU-treated group (270.67 ± 15.17) compared to the placebo group (203.96 ± 6.01) (Fig. 26). The results suggest that 4-MU treatment leads to downregulation of HA and promotes long-term synaptic plasticity after chronic SCI in combination with rehabilitation during the 8-week wash-out period. We stained two levels above and below the lesion for the presynaptic marker synapsin and measured the number of synaptic contacts within the ventral horns to determine whether there was a difference in overall synaptic density (Fig. 26). 4-MU-treated animals had a trend towards an increase in synaptic density in the area above the lesion, but with no significant difference (Fig. 26). Below the lesion,

probably due to the lack of CS reduction as observed in Fig. 22, there is no change in synaptic density measurements.

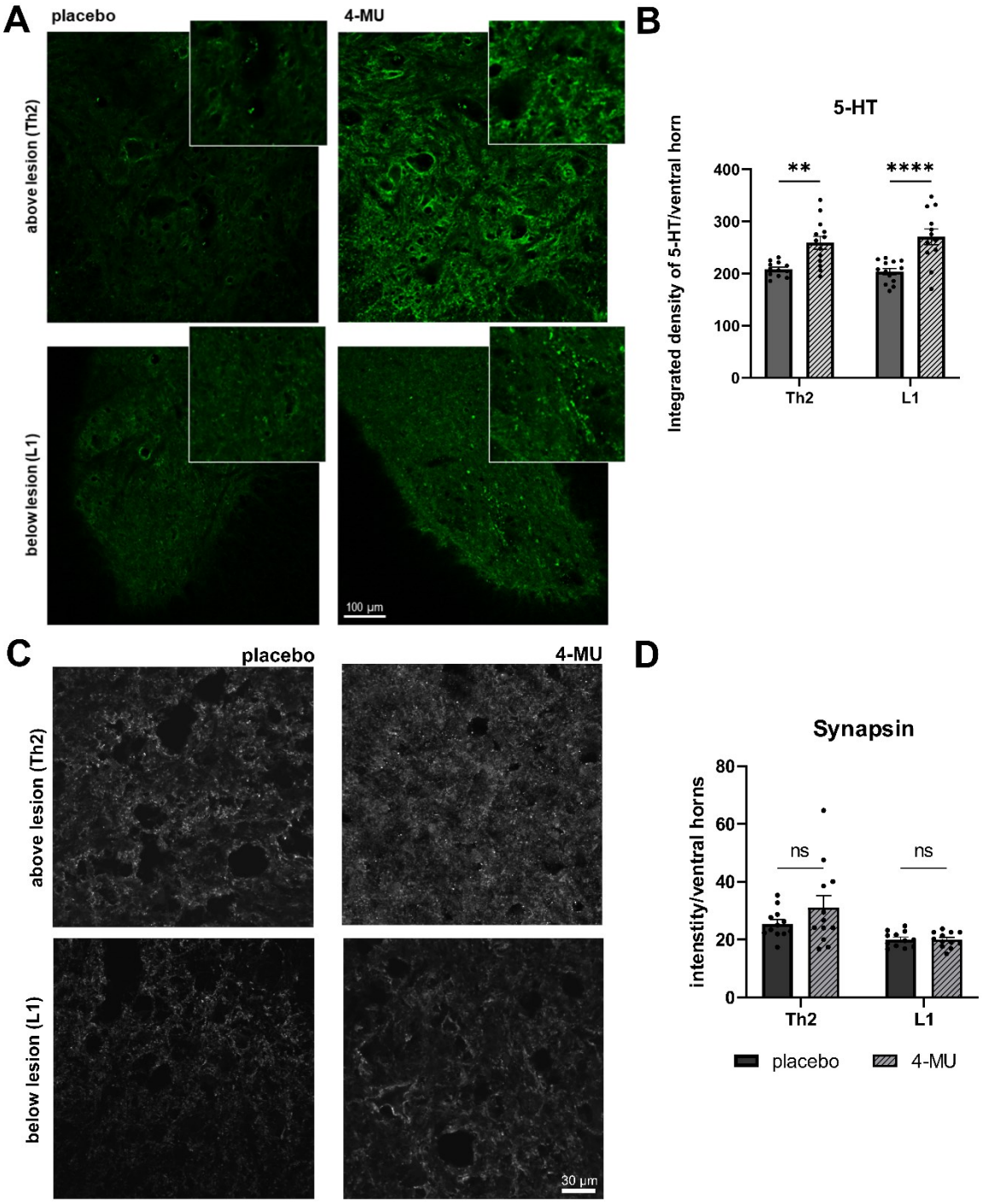

Fig. 26. Treatment with 4-MU increases the number of serotonergic fibres far from the site of injury, but does not increase the number of synapses at the site of injury after chronic SCI. (**A**) Representative confocal images staining for 5-hydroxytryptamine (5-HT) in the ventral horn over and under the lesioned area in the placebo and 4-MU-treated groups in chronic SCI. Insets show enlarged stained areas. Scale bar 100 µm; (**B**) Bar graph showing

the integrated density of the 5-HT+ive signal in the ventral horns, using the ImageJ™ software. Values are mean ± SEM (n=4 animals per group; 2-3 sections per animal); **p < 0.01, ****p < 0.0001 by two-way ANOVA, Sidak's multiple comparison test. (**C**) Representative detailed confocal images of the ventral horn above and below the injury, staining for synapsin in the 4-MU-treated and placebo groups at the chronic stage of SCI. Scale bar 30 μm; (**D**) Bar graph showing the intensity measured per region (in pixel) on the ventral horn with ImageJ software. Data presented as mean ± SEM (n = 4 animals per group; 3 sections per animal); ns>0.05 by two-way ANOVA, Sidak's multiple comparison test.

4.2.5 4-MU at a dose of 1.2 g/kg/day is not sufficient to improve functional recovery in the chronic phase of SCI

We tested whether axonal sprouting induced by 4-MU and daily rehabilitation would lead to functional recovery in the chronic stage of SCI, based on biochemical results showing that 4-MU abolishes plasticity-limiting perineuronal networks. To test this, the full battery of behavioural tests was performed, including the weekly BBB test, the maximum speed test and the ladder rung walking test. This was combined with daily treadmill rehabilitation to assess their locomotor abilities. In order to assess changes in thermal and mechanical sensation, two sensory tests were chosen, the mechanical pressure test and the thermal test. These two tests were carried out three times - before the feeding with the 4-MU pellets/placebo pellets, at the end of the feeding period and at the end of the whole experiment. There were no significant differences or indications of a trend towards improvement at any time point. This suggests a lack of 4-MU mediated recovery (Fig. 27).

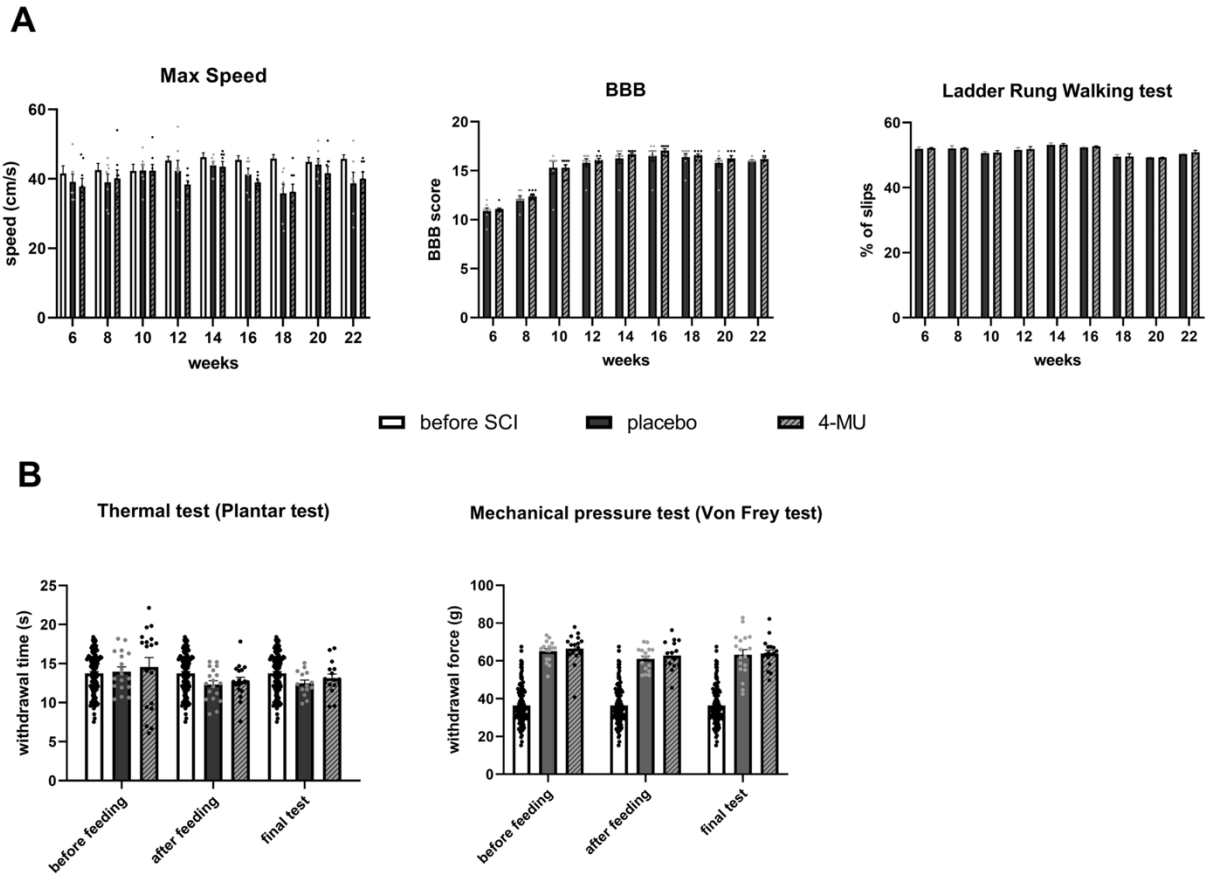

Fig. 27. After chronic SCI, treatment with 4-MU at the current dose does not result in functional recovery. The animals were tested on a weekly basis for their ability to reach the highest possible speed on the treadmill (max speed), for locomotion in the open field test (Basso, Beattie, Bresnahan-BBB), for dexterity (ladder rung walking test) and for sensory function (plantar and von Frey tests). And for the sensory function (plantar test and von Frey test) at the three different time points of the experiment. (**A**) Bar graphs show the results of behavioural tests to assess the rats' locomotion - maximum speed (max speed), BBB, ladder-rung walking test. The data show a spontaneous recovery in both groups following the first 2 weeks of daily rehabilitation in the BBB open field test, which plateaued in both groups at week 10. 4-MU did not enhance this spontaneous recovery. Values are mean ± SEM (n=7 animals for placebo group and n=8 animals for 4-MU group); ns > 0.05 by two-way ANOVA, Sidak's multiple comparison test (BBB, ladder-rung walking test); ns > 0.05 by two-way ANOVA, Tukey's multiple comparison test (maximum speed). (**B**) Bar graphs show sensory function scores before and after feeding and at the end of the experiment. No significant difference was found. Values are expressed as mean ± SEM (n=7 in placebo and n=8 in 4-MU); ns>0.05 by two-way ANOVA, Tukey's multiple comparison test.

4.3 Expression of alpha 9 integrin allows for the reconstruction of the sensory pathway of the spinal cord after injury

4.3.1 AAV transduces integrin and kindlin in DRG neurons

Sensory neuron transduction was assessed by immunostaining of DRGs and axons below the lesion level (Supplementary Fig. S1A). The ratio of GFP- and/or V5+ive cell bodies to βIII-tubulin+ive cell bodies was counted to determine transduction efficiency. The transduction efficiency was similar for the three vectors and ranged from 28 to 38% for the single vectors and from 20 to 25% for the co-transduction with both the alpha 9 and the kindlin-1 vectors. To compensate for the greater length of the integrin gene, the kindlin-1 vector was injected at a 1:3 ratio. Tab. 6 and Fig. 28 show the transduction efficiencies.

In order to confirm that the transduced sensory neurons are located throughout the DRG and not just locally, we imaged the transduced DRGs using 3D light sheet microscopy 13 weeks after the injection of AAVs (Supplementary Fig. S1C). Furthermore, immunostaining showed that AAV1-α9-V5 and AAV1-kindlin-1-GFP transduced all three sensory neuron types located in the DRGs: large-diameter mechanoreceptors (NF200+ive), medium-diameter nociceptors (IBA4+ive) and small-diameter thermoreceptors (CGRP+ive) (Fig. 28).

Tab. 6. Sensory neuron transducing efficiencies after direct DRG injection. Data are expressed as mean ± SEM, n = 20 - 24 per group.

VIRAL VECTORS	L4, L5 DRGs (%)
AAV1-GFP	36.59 ± 2.838
AAV1-kindlin-1-GFP	39.06 ± 2.973
AAV1-α9-V5	32.94 ± 1.575
% βIII tubulin +ve neurons co-transduced with AAV1-α9-V5 + AAV1-kindlin-1-GFP (injected in 3:1 ratio)	23.37 ± 1.589
% α9 neurons also +ve for kindlin	68.48 ± 2.537

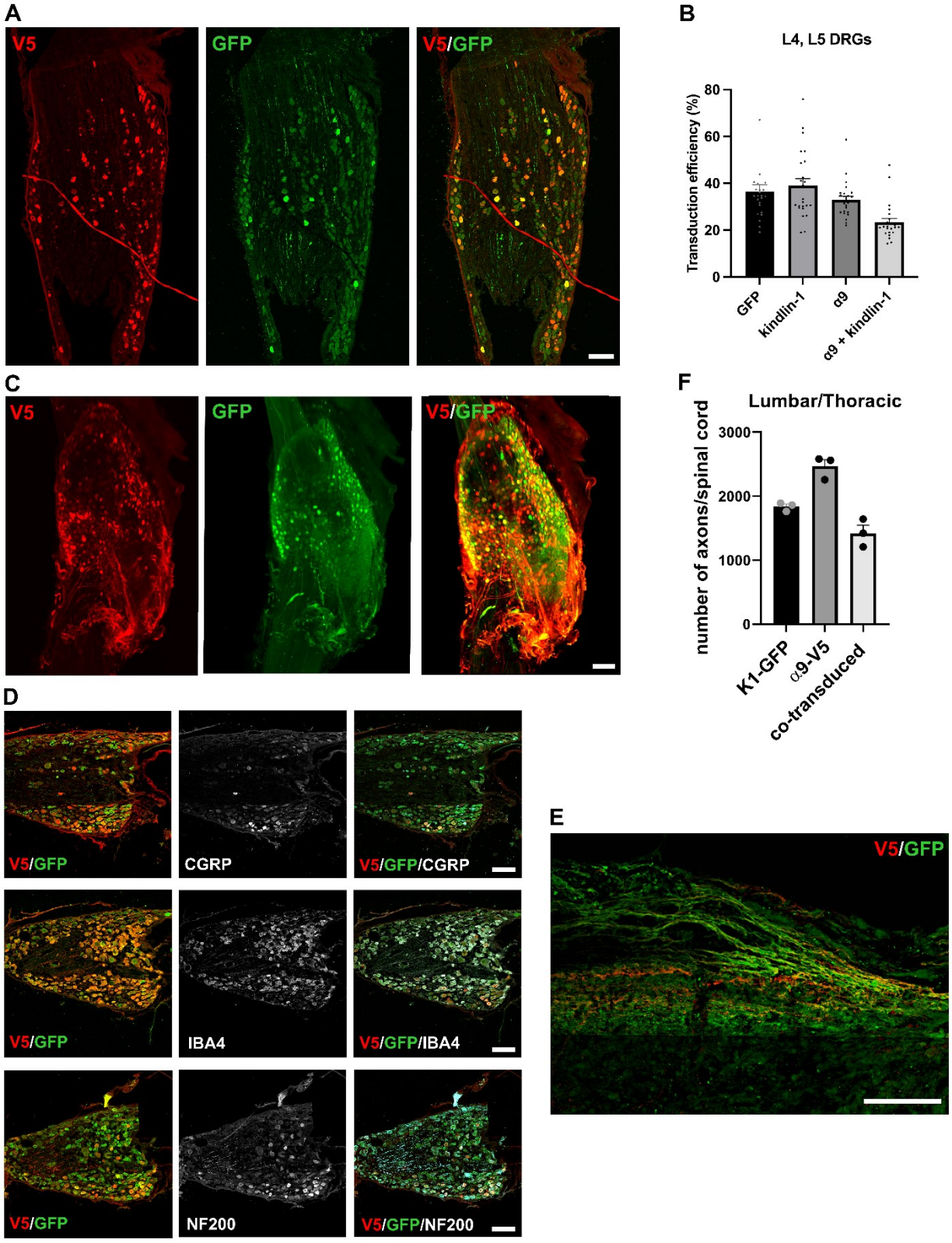

Fig. 28. Thirteen weeks after direct injection, expression of α9 integrin and kindlin-1 in DRG neurons and axons beneath the lesion. (**A**) A dorsal root ganglion that had been injected with AAV1-kindlin-1-GFP + AAV1-α9-V5 13 weeks before. Many neurons are yellow in the composite image below, indicating co-transduction, but some neurons are red

or indicating that they were transduced by only one of the viral vectors. Scale bar: 200 µm. (**B**) Quantification of (**A**)**.** (**C**) Light-sheet microscopy images of the DRG after direct AAV injection with AAV1-kindlin-1-GFP + AAV1-α9-V5. Sensory neurons are uniformly transduced throughout the DRG. Scale bar: 200 µm. (**D**) AAV1 vectors were used to transduce sensory neurons of the three main types. CGRP, IBA4 and NF200 immunostaining (middle column) overlaps with V5 and GFP staining. Integrin and Kindlin are shown (left and right merged columns). Scale bar: 200 µm (**E**) V5 and GFP staining of axons caudal to the lesion. Many axons contain both integrins and kindlins, although some axons stain positive for only one. Scale bar: 100 µm. (**F**) Quantification of (**E**). Bar graphs show individual data with their mean ± SEM (n= 3 animals per group).

Immunostaining was used to visualise α9-V5 and kindlin-1-GFP trafficking in sensory axons caudal to the lesion. The spinal cord was sectioned at 40µm. Every fifth section was stained for V5 and GFP. For all experiments in this study, these molecules transported from the DRGs were used as axon tracers.

The number of axons were counted using an ocular grid. The number of axons crossing a line of the grid at regular distances caudal and rostral to the lesion was counted. The number of labelled axons at that level in each spinal cord was then estimated by multiplying the sum of the values from each distance point by 5.

In both the dorsal roots and caudal to the lesion, many axons were positive for both α9-V5 and kindlin-1-GFP. However, there were also axons that were positive for only one molecule (Fig. 28). The observed average number of co-transduced axons labelled in the spinal cord below the thoracic lesion was between 1340 and 1410 (see Tab. 7).

Tab. 7. Number of V5 or GFP or co-labelled axons per spinal cord 600 µm caudal to the site of injury. Data are expressed as the mean ± SEM, n = 3 per group.

	Number of labelled axons
Kindlin-1-GFP axons	1890 ± 45
Integrin α9-V5 axons	2322 ± 109
Co-transduced axons	1375 ± 35

4.3.2 α9-K1 axons regenerate across lesions in the bridges of connective tissue

Axons from the integrin α9 + kindlin-1 group were observed to cross the lesion, re-enter CNS tissue and continue growing rostrally up the spinal cord. Within the lesions, many axons were seen in GFAP-negative connective tissue strands and bridges, and in the meningeal/connective tissue roof covering most lesions. A few regenerating axons grew around the base of the lesion. At the interface of the connective tissue with the rostral lesion edge, axons often showed axonal tangles with changes in trajectory (Fig. 29). However, once established in the CNS tissue, axons followed a fairly straight trajectory. Some axons did not have a re-entry into the CNS tissue. Instead, there was growth along the spinal cord in the meninges (Fig. 29). We measured 849 ± 64 axons 1 mm rostral to the lesion edge in the α9-K1 group.

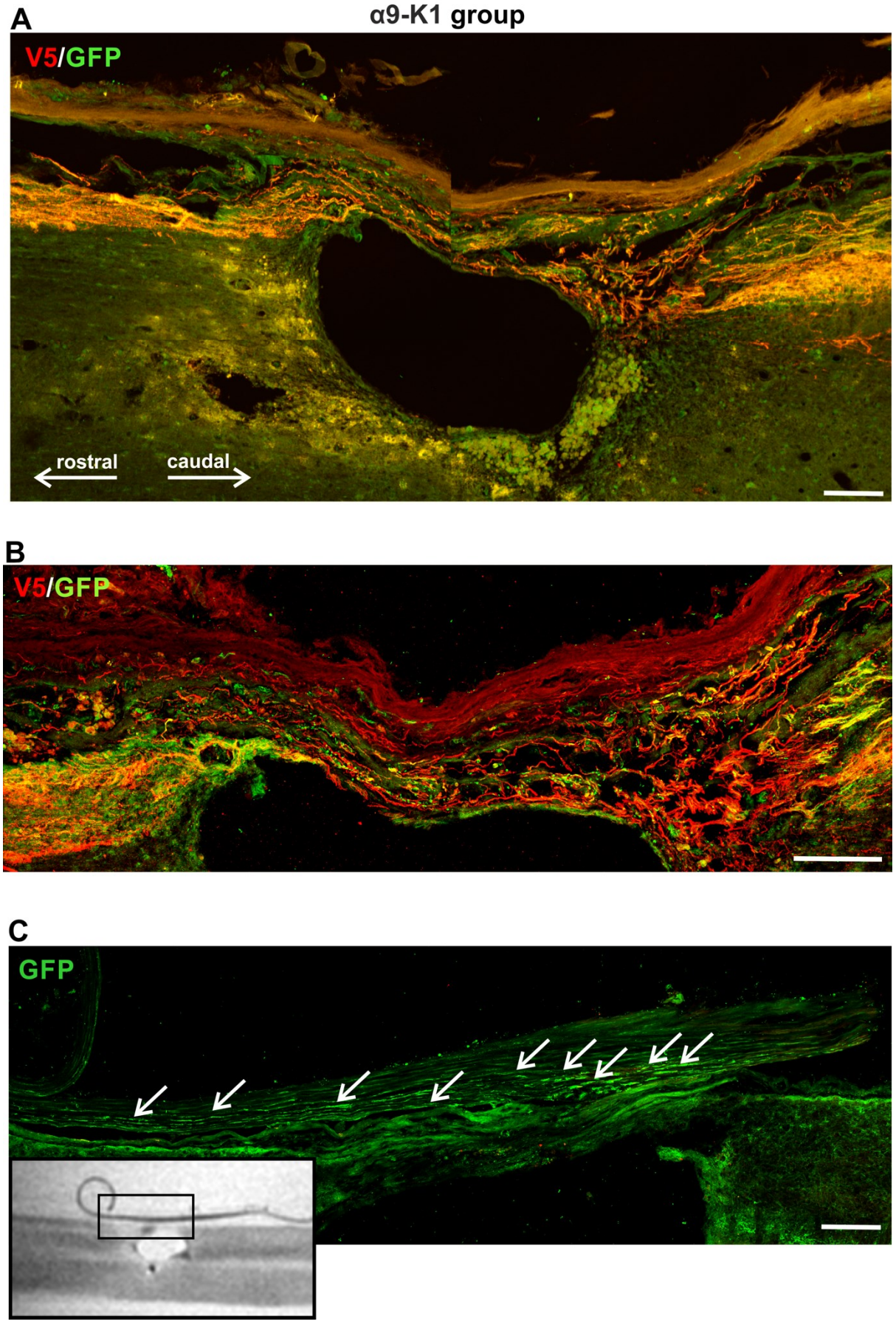
A
α9-K1 group
V5/GFP
rostral
caudal
B
V5/GFP
C
GFP

Fig. 29. Co-expressing alpha9-integrin and kindlin-1 promotes regeneration of sensory axons (**A**) An example of spinal lesions in T10 from the α9-kindlin-1 group. Approaching the lesion from the right (caudal) side are many red (α9-V5 stained) axons. Some random growth occurs when the axons enter the bridge over the top of the lesion, which consists mainly of meninges, and then the axons enter the CNS tissue again for rostral growth on the left. Scale bar: 200 μm. (**B**) An example of an axon that passes through a fine strand of connective tissue. There is a region of wandering growth as the axons re-enter CNS tissue at the rostral end (left). Scale bar: 100 μm. (**C**) Some axons continue to grow in the meninges next to the CNS tissue (white arrows) where the axons reach the point where connective tissue strands interface with the CNS tissue. Where the detail comes from is shown in the lower left MRI image. Scale bar: 50 μm.

In GFP controls (Fig. 30), a few sprouts were seen around the edge of the lesion and at the caudal edge of the lesion core, but no axons grew across the lesion. In animals expressing kindlin-1 alone, some regeneration of sensory axons was seen in the laminin+ve connective tissue within and bridging the lesion, in close contact with laminin+ve structures, but the axons did not re-enter the CNS tissue to grow beyond the lesion area (Fig. 30). At the edge of the rostral part of the lesion, the integrin a9-kindlin-1 group showed significantly more axons (819.00 ± 94) than kindlin-1 alone (413 ± 87; p=0.0012, 2way-ANOVA, n=10-12). However, no axons from the kindlin-1-only group continued to grow rostrally above the lesion, and 1 mm above the lesion there were no axons visible from either the kindlin-1-only group or the GFP controls.

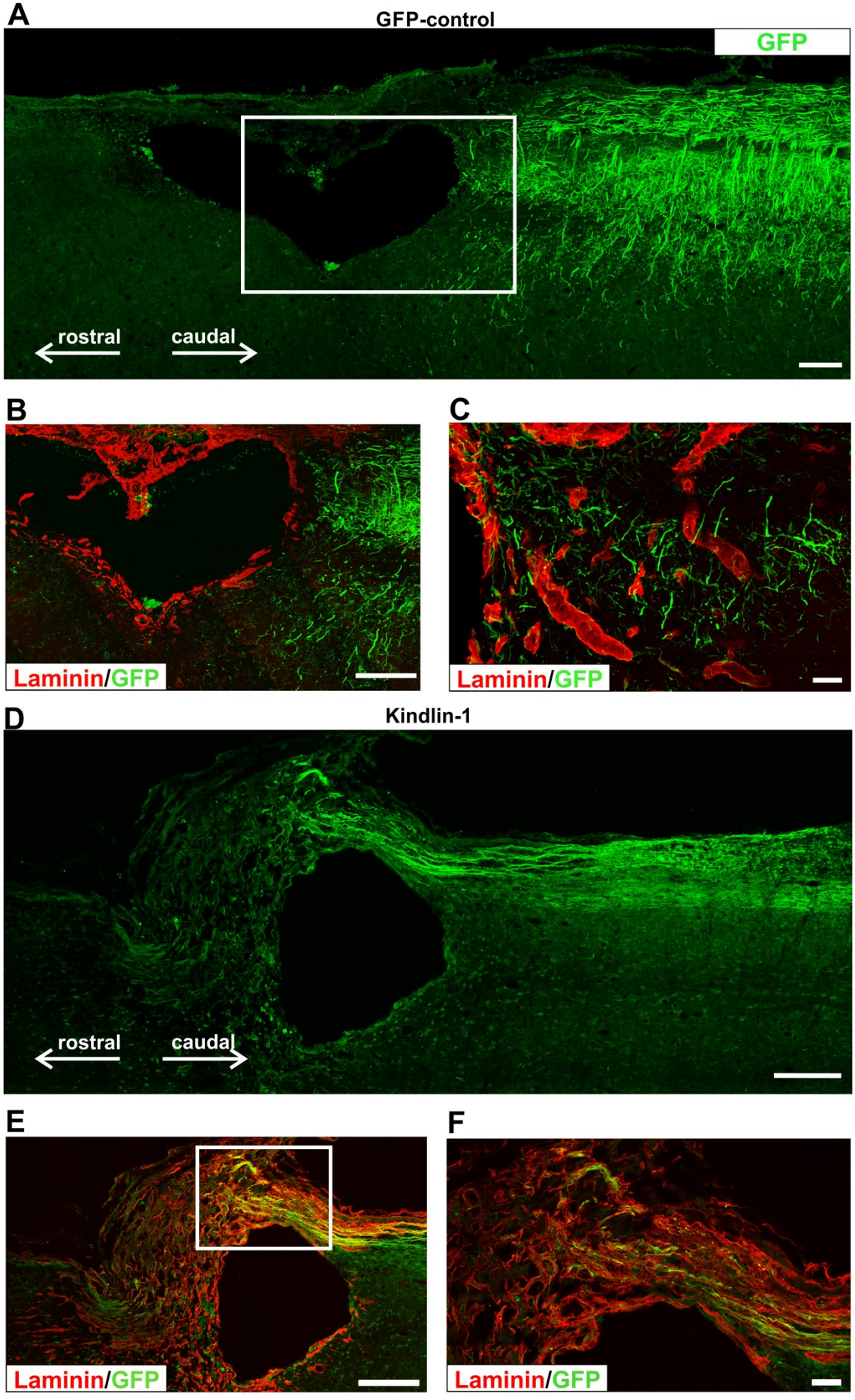
A
GFP-control
GFP
rostral
caudal
B
Laminin/GFP
C
Laminin/GFP
D
Kindlin-1
rostral
caudal
E
Laminin/GFP
F
Laminin/GFP

Fig. 30. In both the GFP and kindlin-1-only groups, no axon growth through the lesion was observed. (A) GFP immunostaining of a lesion from the GFP group. Axons are visible only caudally to the lesion (right), but none regenerated into the bridge developing over the lesion. Scale bar: 200 μm. (B) One lesion from the GFP group (inset from A), immunostained for GFP and laminin. GFP+ve axons terminate caudally of the lesion (right), however no regeneration into the laminin+ve connective tissue in the lesion. Scale bar: 200 μm. (C) A detail of the terminal axons of the GFP group, where the laminin+ve border starts to form. On the laminin+ve ECM the axons do not grow. Scale bar: 50 μm. (D) Example of axon regeneration from the kindlin-1 group. Scale bar: 200 μm. (E) Axon regeneration in the laminin+ve connective tissue in the bridge region over the lesion, closely associated with laminin+ve processes. There is no axon outgrowth from the connective tissue back into the CNS tissue. Scale bar: 200 μm. (F) A magnified inset of (E). Scale bar: 50 μm.

4.3.3 α9-K1 axons regenerate to the brain stem

Regenerating axons were seen rostral to the T10 lesion in animals injected with both integrin α9 and kindlin-1 (α9-kindlin group). Many of these axons were seen to extend all the way up to the spinal cord. Most of the axons were seen at the grey-white matter interface at the medial edge of the dorsal horns. A smaller number of axons were seen following a wandering course within the dorsal horn white matter (Fig. 31). These regenerating axons were therefore following a different path to that of the sensory axons that had not been injured. Along this regenerating pathway, there were frequent branches that extended into the grey matter of the dorsal horn. These branches terminated in arborisations (Fig. 31). The distance of axon regeneration from the thoracic lesions was up to 5 cm. Almost all regenerating axons rostral to the lesion stained for both α9-V5 and kindlin-1-GFP (Fig. 32). This contrasts with axons caudal to the lesion, where there was a significant proportion of single-stained axons (Fig. 32). The implication is that only axons with both alpha9 and kindlin-1 were capable of regeneration through the lesion. Regeneration index 5mm above lesion was approximately 0.5 for thoracic SCI and 0.2 for T10 group 5cm above lesion. See Tab. 8 for detailed information on the number of axons regenerating through the T10 lesion.

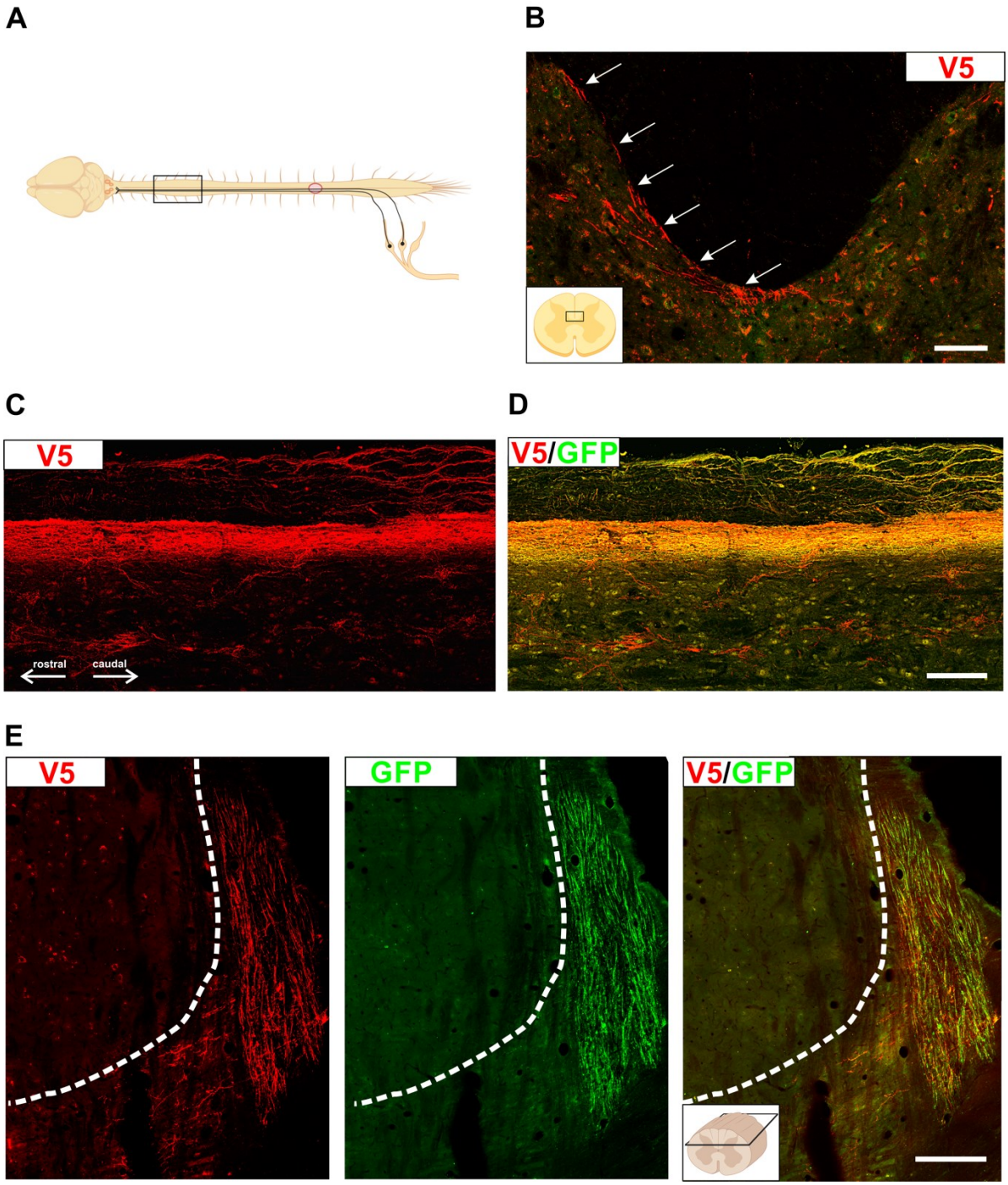

Fig. 31. α9-K1 axon regeneration to the brainstem. (**A**) Diagram showing the spinal cord segment from which the following sections (**B**, **C**, **D**) were taken. Created with BioRender.com. (**B**) α9-V5 labelled axons in a cross section of the spinal cord (C3). The source of the detail is shown in the diagram on the bottom left. BioRender.com was used to create the diagram. Scale bar: 50 µm. The axons at the edge between the dorsal horn and the dorsal column are indicated by white arrows.

(**C**) C3 level axons labelled for V5 only. Axons follow a path at the edge between the dorsal horn branches. Numerous axons can be seen in the layer between the dorsal horn and the white matter of the dorsal column, and several axons can be seen in the white matter of the dorsal horn. (**D**) Axons rostral to the lesion were double stained for α9-V5 and kindlin-1-GFP. Colocalisation of both markers was observed. Scale bar: 100 μm. (**E**) Longitudinal section of the spinal cord, dual staining for alpha9-V5 and kindlin-1-GFP, with the sensory nucleus above. The bundle of axons is approaching the edge of the nucleus and some of them are growing up to the nucleus but not into the nucleus. The absence of labelled axons in the nucleus indicates the absence of unbranched sensory axons. Scale bar of longitudinal section: 100 μm.

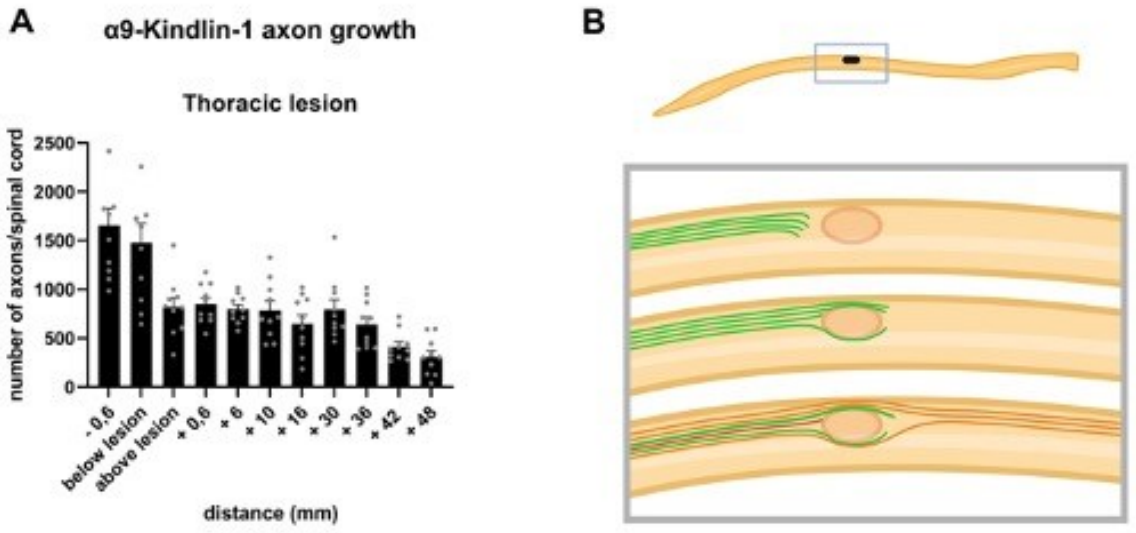

Fig. 32. Distant regeneration in the spinal cord co-expressing alpha9 integrin and kindlin-1. (**A**) Bar graphs show the number of axons after thoracic injury with L4, L5 DRG injections. In the α9-kindlin group, approximately 900 sensory axons grew into the rostral spinal cord, with a slight decrease in the number of axons as they approached the hindbrain. Regenerated axons were observed at a distance of 5 cm from the thoracic lesion to the medulla. Bar graphs show data with mean ± SEM (n= 7-12 animals per group). (B) Schematic representation of key results of Aim 2. Only the α9-Kindlin group showed substantial regeneration beyond the lesion into the rostral cord. Axons in the laminin-containing connective tissue at the core of the lesion regenerated in the kindlin group. Created with BioRender.com.

Tab. 8. GFP, kindlin-1 and α9-kindlin-1 group axon number and regeneration index.
Data are expressed as mean ± SEM, n = 7-10 (animals/group) NA = not available.

	Thoracic SCI								
	GFP			kindlin-1			integrin α9 + kindlin-1		
distance (mm)	number of axons	SEM	RI	number of axons	SEM	RI	number of axons	SEM	RI
- 0.6	1519.45	134.81	N/A	1257.73	143.65	N/A	1653.5	173.54	N/A
below lesion	0	0	N/A	1049.1	139.67	N/A	1475.5	201.48	N/A
above lesion	0	0	0	412.73	86.6	0.33	819	94.34	0.50
+ 0.6	0	0	0	0	0	0	850.5	61.61	0.51
1	0	0	0	0	0	0	849.5	64.16	0.51
6	0	0	0	0	0	0	796.5	44.83	0.48
10	0	0	0	0	0	0	784.5	93.55	0.47
16	0	0	0	0	0	0	647.5	91.02	0.39
30	0	0	0	0	0	0	793	99.54	0.48
36	0	0	0	0	0	0	640	76.33	0.39
42	0	0	0	0	0	0	413.5	47.53	0.25
48	0	0	0	0	0	0	309.2	60.2	0.19

4.3.4 α9-K1 axons regenerate through tenascin-C containing tissue

Immunolabelling for GFAP, laminin and tenascin-C was performed to examine the substrate on which α9-kindlin-1 V5- positive axons were growing. The connective tissue strands and the roof in lesions through which axons regenerated were totally or partially GFAP negative. There was usually a clear border with GFAP positive CNS tissue. Laminin and tenascin-C staining was seen in the connective tissue through which axons grew across the lesions. The boundary between the connective tissue and the CNS was less clear with tenascin staining. This is because the perilesional CNS tissue also expresses tenascin (Fig. 33). In the kindlin-1 group, GFP+ive regenerated axons were observed in association with the laminin+ve connective tissue substrate. However, they were not able to grow back into the CNS tissue (Fig. 33). In summary, within the lesion, axons expressing a9-V5 and kindlin-1 appeared to regenerate preferentially through laminin and tenascin-C positive connective tissue structures and were then able to re-enter and grow within tenascin-C expressing CNS tissue. Axons expressing kindlin-1 alone contained activated forms of the integrins (α4,5,6,7) expressed endogenously by sensory neurons, which are laminin and fibronectin receptors. These axons grew where laminin was present but did not re-enter the laminin negative CNS tissue.

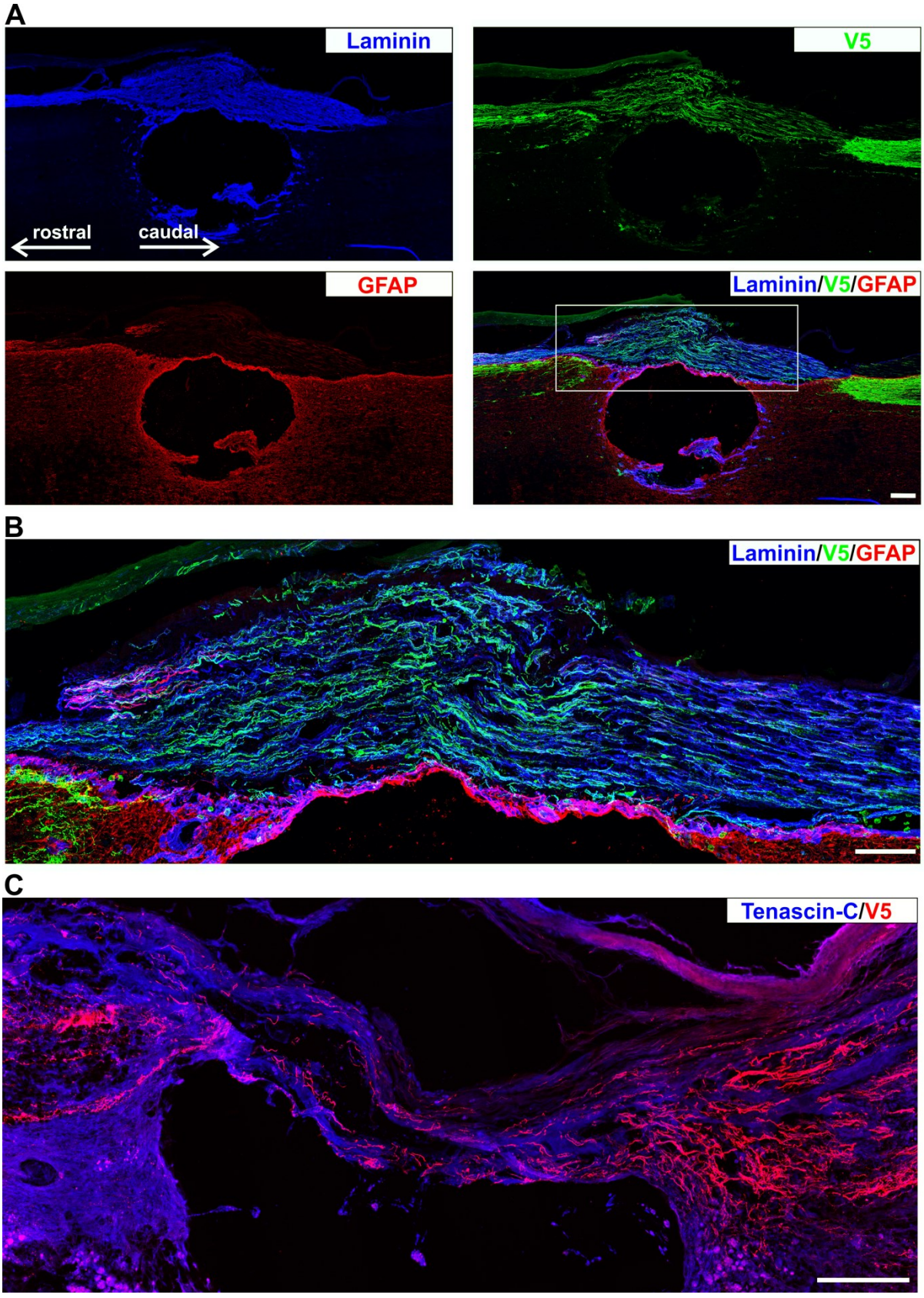
A
Laminin
V5
rostral
caudal
GFAP
Laminin/V5/GFAP
B
Laminin/V5/GFAP
C
Tenascin-C/V5

Fig. 33. α9-integrin kindlin-1 axon regeneration by laminin-111 isoform and tenascin-C positive tissues. (**A**) The GFAP-ve and tenascin+ve laminin+ve bridge that develops over the lesions is mostly derived from connective and/or meningeal tissue. Within the connective tissue bridge, tangled axons and axons crossing the lesion from the α9-kindlin group can be seen. Scale bar: 200 μm. (**B**) The detailed image shows the bridge region with growing axons with morphology typical of regenerating axons, and partially with the retracting bulb. Scale bar: 50 μm. (**C**) Growth of axons in the α9 kindlin group through strands of connective tissue that are stained for tenascin-C. A large number of axons with a typical regenerated morphology can be seen within the strands, which then enter the CNS tissue rostral to the lesion on the left side. Scale bar: 200 μm.

In summary, within the lesion, axons expressing α9-V5 and kindlin-1 appeared to regenerate preferentially through laminin- and tenascin-C+ive connective tissue structures, and were then able to re-enter and grow within tenascin-C-expressing CNS tissue. Axons expressing kindlin-1 alone contained activated forms of the integrins (α4,5,6,7) expressed endogenously by sensory neurons, which are laminin and fibronectin receptors. These axons grew where laminin was present but did not re-enter the laminin negative CNS tissue.

4.3.5 Completeness of dorsal column crush

In order to verify the completeness of the lesion in our model of dorsal column crush injury, we used 7T MRI. Sagittal and transverse sections (Fig. 34) were taken of all dissected spinal cords. The sections were then compared with the rat anatomical atlas. Lesions that were too wide, too deep or too small were excluded. Based on the MRI results, no animal was excluded from the study. Staining of the sensory nuclei also allowed us to demonstrate lesion completeness. Regenerating axons are excluded (Fig. 34), whereas non-lesioned axons innervate the nuclei (Cheah et al. 2016; Massey et al. 2008). Thus, the lesion would be considered incomplete if V5 or GFP positive axons were observed in the sensory nuclei.

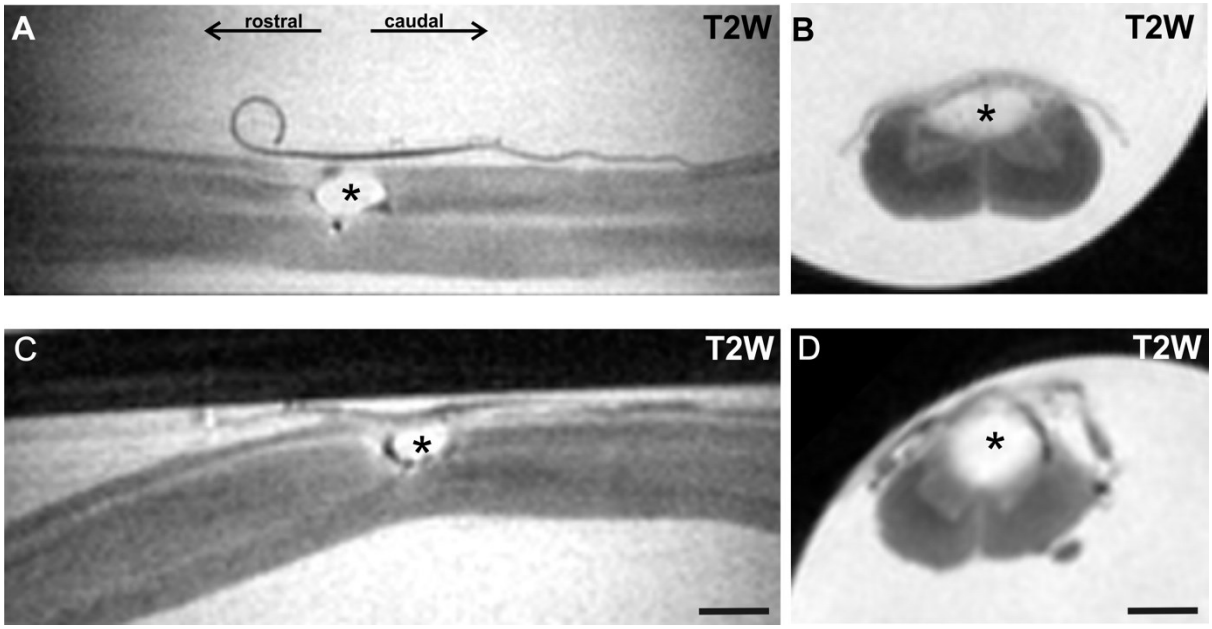

Fig. 34. Dorsal column crush completeness. Typical lesion shown in longitudinal (**A, C**) and transverse (**B, D**) T2-weighted MRI images. These images were obtained from spinal cords collected from animals after fixation at week 13. The stars indicate the lesion. (**A, B**) shows one lesion and (**C, D**) another lesion. Scale bar: 600 μm.

4.3.6 Regenerating axons form a functional synapse across the lesion

To assess functional connectivity across the lesion, spinal cFOS expression was visualised after electrical stimulation of the sciatic nerves. cFOS is an immediate early gene and a well-established marker of neuronal activity induced transcription (Fig. 35).

The Cell Counter plugin in ImageJ (Schindelin et al. 2012) was used to quantify the total number of cFOS+ nuclei in the dorsal horns below the lesion (at the L1 level) and above the lesion (at the Th8 level). Three adjacent sections below and above the lesion were analysed for each animal. The mean value of each of the subsets was then calculated. Results are presented as percentage ratio of number of cFOS+ive cells above lesion to number of cFOS+ive cells below lesion. Compared to the GFP (7.754 ± 1.334% after thoracic SCI) and kindlin-1 (9.650 ± 1.313% after thoracic SCI) groups, a higher percentage of cFOS+ive cells was observed in the α9 - kindlin-1 group (44.380 ± 2.684% after thoracic SCI) (Fig. 35). The differences between the α9 - kindlin-1 group and the GFP group were significant ($P < 0.0001$). Between the GFP and kindlin-1 groups, no significance was observed.

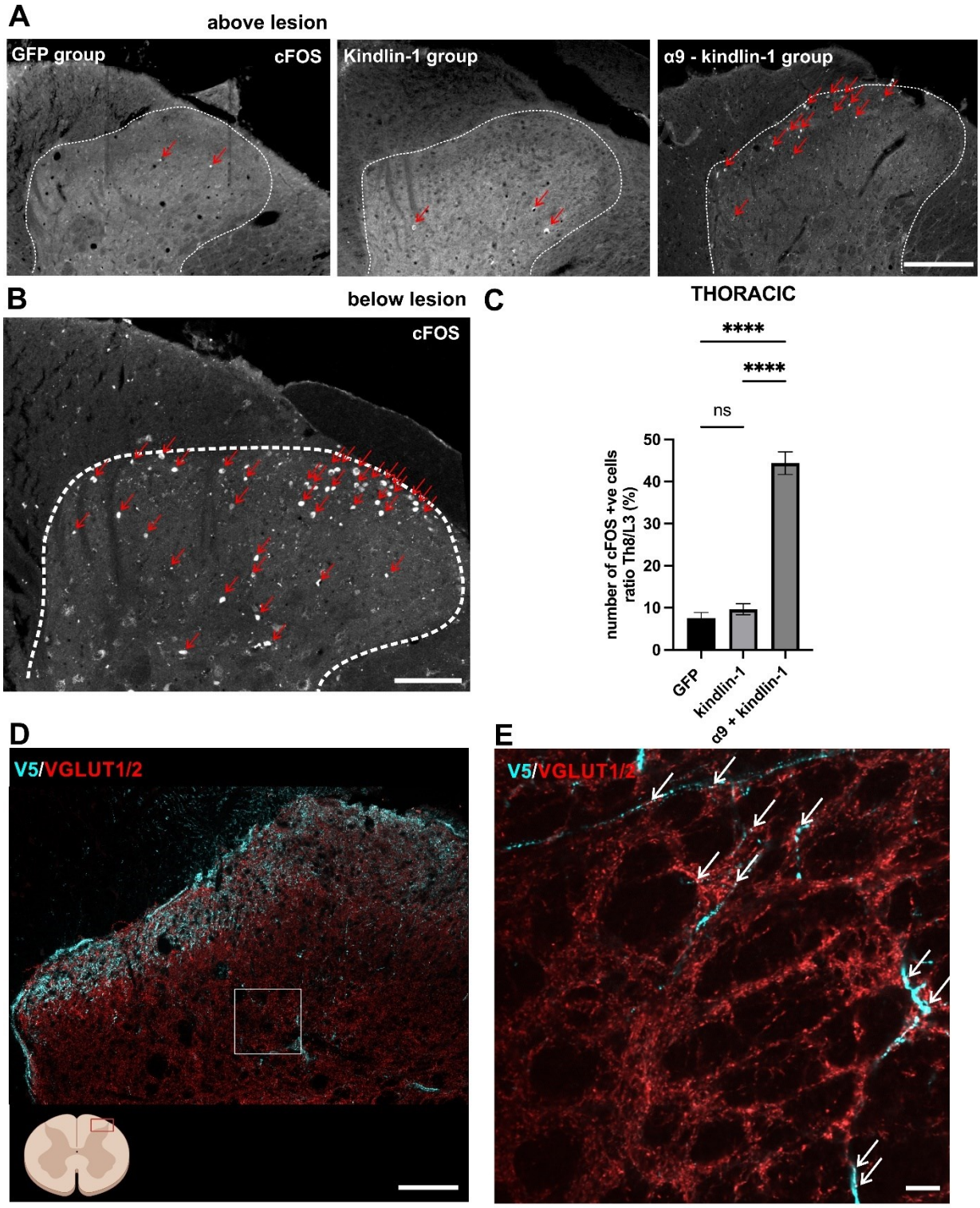

Fig. 35. Above the lesion, regenerating axons form a functional synapse. (A, B) Staining of c-Fos from the dorsal horn of the spinal cord (white dotted lines mark the border of the dorsal horn) after stimulation of the peripheral nerve.

(**B**) Activation of numerous neurons (red arrows) below the lesion. Scale bar: 100 μm. (A) 2 segments rostral to the lesion, few neurons are activated in the GFP and kindlin-1 groups (red arrows), but many more are activated in the α9 kindlin group (red arrows). This indicates that functional connections have been made. Scale bar: 200 μm. (**C**) Quantification of (**A, B**). Number of cFOS+ive cells expressed as ratio of positive cells below and above lesion. Data show mean ± SEM (n=3 animals per group). ns $p \geq 0.05$, **** $p < 0.0001$, one-way ANOVA, Tukey's multiple comparison test. (**D**) Representative confocal images showing the dorsal horn 1cm rostral to the lesion from the alpha9-Kindlin group. Blue V5+ive axons can be seen extending into the grey matter. They show swellings that also stain red for VGLUT1/2. Scale bar: 100 μm. (**E**) High-resolution single-plane images of dorsal horn detail (indicated by white rectangle in (**D**)) showing cyan V5+ive axons growing into grey matter with swellings also staining red for VGLUT1/2. Scale bar: 20 μm.

Using super-resolution, V5+ive sensory axon terminals were observed to colocalise with VGLUT1/2 puncta in the spinal coronal slice taken above the lesion, indicating functional synaptic connectivity (Fig. 35). These data show that the regenerated axons in the α9 - kindlin-1 group were able to establish functional synapses in the rostral side of the lesions.

4.3.7 α9-K1 restores sensory function

To investigate the recovery of sensory behaviour,hindlimb function tests were performed in animals with T10 lesions/DRG lumbar injections. Soft mechanical pressure (Von Frey), heat (plantar/Hargreaves) and tape removal tests were used (Fig. 36). The tests started 2 weeks before surgery (pre-test period). This was to obtain reference values for healthy animals and also to allow the animals to learn the required task. The week following surgery was a break in testing. This allowed the animals to adapt to the new pathophysiological conditions. Animals were tested every two weeks for 12 weeks from the second week of viral expression.

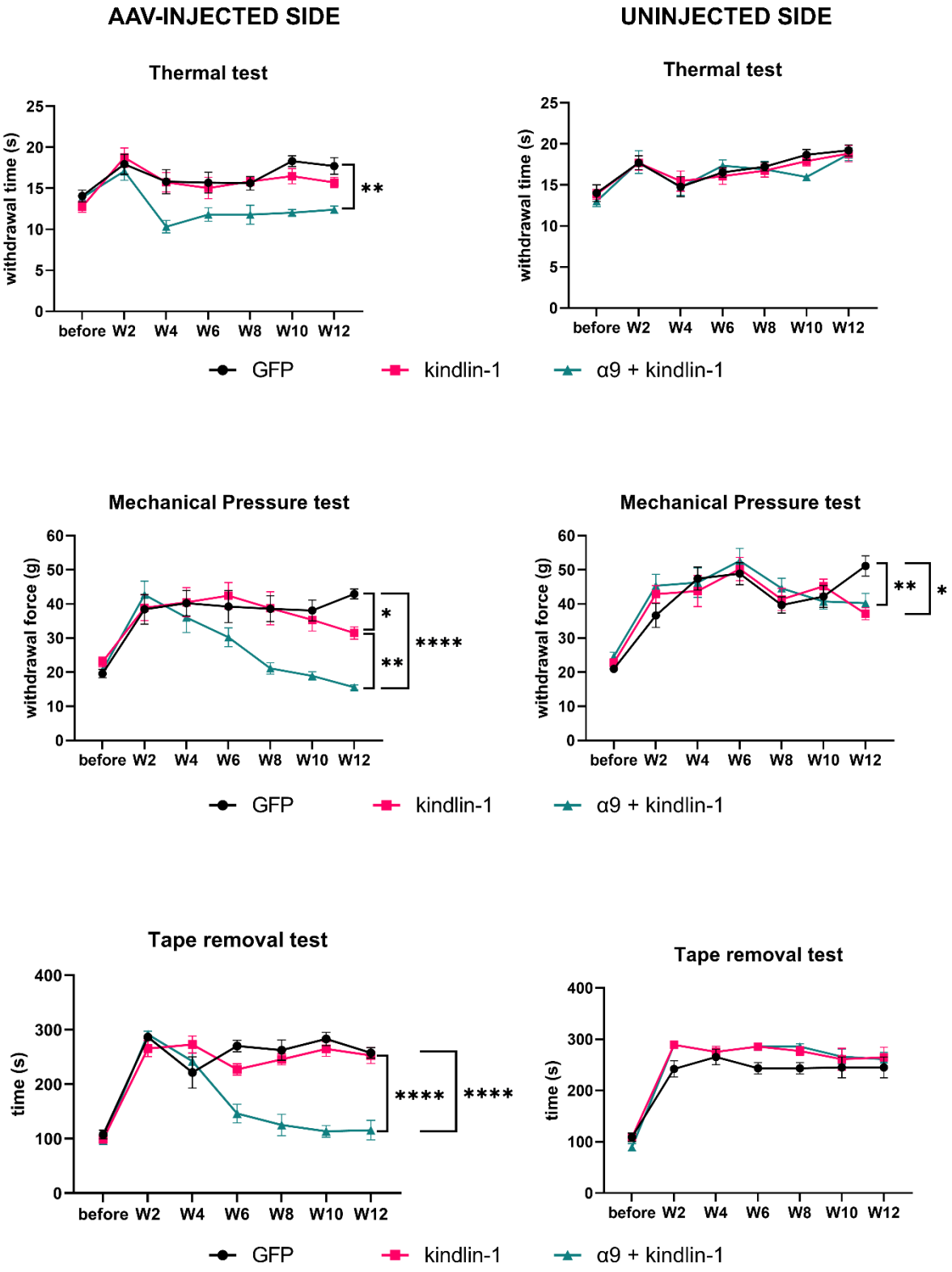
AAV-INJECTED SIDE
UNINJECTED SIDE
Thermal test
withdrawal time (s)
before W2 W4 W6 W8 W10 W12
**
Mechanical Pressure test
withdrawal force (g)
*
**
****
Tape removal test
time (s)
GFP
kindlin-1
α9 + kindlin-1

Fig. 36. α9-K1 led to recovery of sensory functions. After thoracic lesions, only in the α9-Kindlin group and only on the treated side, there was a recovery of heat sensation, pressure sensation and tape removal. Data show mean ± SEM (n=10-12 animals per group). ns $p \geq 0.05$, *$p < 0.05$, **$p < 0.01$, **** $p < 0.0001$, two-way ANOVA, Tukey's multiple comparison test.

During the first week of testing, the experimental left paw and the internal control right paw showed a significant sensory deficit compared to reference values after the thoracic level of injury. The sensory deficit was manifested by a greater force requirement to elicit withdrawal in the mechanical pressure test, a longer withdrawal time in the heat test and a longer delay time with tape in the tape removal test.

In the mechanical pressure test, the integrin a9-kindlin-1 group started to show a significant recovery compared to the GFP group from week 8 onwards ($p = 0.0006$, two-way ANOVA, n = 10-12). No significant recovery was observed in the other 2 groups (GFP and kindlin-1 only) after thoracic SCI.

In the heat test, after thoracic SCI, only the integrin α9 - kindlin-1 group showed a significant recovery compared to the GFP control group from week 4 ($p = 0.0002$, two-way ANOVA, n = 10-12). There was no recovery in the other groups.

In the tape removal test, significant recovery was only observed in the integrin α9 - kindlin-1 group ($p < 0.0001$, two-way ANOVA, n = 10-12) in comparison to the GFP control group.

In conclusion, these results indicate that the integrin a9-kindlin-1 group showed superior sensory recovery in the mechanical pressure and heat tests after thoracic SCI. They also performed well in the tape removal test after thoracic SCI.

5. DISCUSSION

5.1. 4-MU treatment at a dose of 1.2 g/kg/day is safe for long-term usage in rats

The first objective was to assess systemic effects after long-term treatment with 4-MU followed by a 9-week wash-out period. The results showed that there was a reduction in the levels of HA and CSPGs. There was a significant increase in bile acids, consistent with the choleretic activity of 4-MU. There was also an increase in blood glucose and protein a few weeks after 4-MU administration. In addition, levels of interleukins IL10, IL12p70 and IFN gamma increased significantly after 10 weeks of treatment with 4-MU. However, there were no significant differences between control and 4-MU-treated animals after the 9-week wash-out period. The results suggest that long-term treatment with 4-MU is well tolerated and does not appear to interfere with normal physiology.

4-MU has previously been identified as an inhibitor of the synthesis of HA. HA is an un-sulphated glycosaminoglycan. It consists of disaccharide repeats of D-glucuronic acid (GlcA) and N-acetyl-D-glucosamine. 4-MU inhibits HA synthesis by depletion of UDP-glucuronic acid (UDP-GlcA), an essential substrate for HA, via glucuronidation of 4-MU (Nakamura et al. 1995; Kakizaki et al. 2004; Monslow, Govindaraju, and Puré 2015). The result is a decrease in HAS mRNA levels (Vigetti et al. 2009). Here, we report that 4-MU is also an inhibitor of CS synthesis. The key building block of CS is the same monosaccharide, GlcA. As CS is a key inhibitory molecule for neural regeneration and plasticity, our results suggest that 4-MU may have potential as a novel non-invasive treatment for nervous system disorders.

In our experiments, we had a systemic route of administration. It was assumed that the whole body of the animal would be affected. We decided to look more closely at the pathophysiological changes. We investigated the systemic effect of 4-MU treatment at a dose of 1.2 kg/g/day. Our results showed no irreversible adverse effects from long-term administration of 4-MU.

5.1.1 4-MU: Clinical and experimental use

4-Methylumbeliferone (4-MU) is used in a number of European countries under the name 'Hymecromone' for the treatment of biliary diseases, based on its choleretic and anti-spasmodic activity in the biliary tract. Bile production by hepatocytes depends on active

secretion of bile salts (bile-dependent pathway) and active transport of sodium ions across canalicular membranes (bile-independent pathway), which are luminal tubular junctions between adjacent hepatocytes (Back et al. 2005). It is suggested that the choleretic activity of 4-MU is mediated by the active transport of sodium ions into the bile capillaries, thereby increasing bile flow, which is not dependent on the osmotic force of bile acids (Takeda and Aburada 1981). 4-MU increases the cation-anion gap in the bile duct by rapidly decreasing the concentration of bicarbonate and chloride ions in the bile. The conversion of 4-MU to 4-methylumbelliferyl glucuronide in the liver is thought to be responsible for this mechanism. 4-Methylumbelliferyl glucuronide, in its anionic form, is then coupled to sodium ions and actively secreted into the biliary tree, with water passively following (Takeda and Aburada 1981). In addition to its choleretic activity, 4-MU is also an inhibitor of HA synthesis (Nagy et al. 2019), and HA inhibition has been shown to be a potential treatment for a number of diseases, from reducing cancer metastasis in oncology to ischaemia-reperfusion injury and non-alcoholic steatohepatitis. In the Tab. 9 an overview of 4-MU doses, 4-MU administration time and experimental diseases treated is summarised.

Tab. 9. Overview of 4-MU dose, 4-MU dosing time and experimentally-treated diseases.

Model	Duration of the treatement	Treated condition	Dose [g/kg/day]	Digital Object Identifier (DOI)	Year
mouse	5 days	Experimental autoimmune encephalomyelitis	6.7 g/kg/day	10.1074/jbc.M114.559583	2014
	2 weeks		6 - 10 g/kg/day	10.1111/cei.12815	2016
	2 weeks	Hepatocellular carcinoma	1 g/kg/day	10.1093/glycob/cwr158	2012
	20 days		0.4 g/kg/day	10.1093/glycob/cwv023	2015
	12 months		0.0134 g/kg/day 0.134 g/kg/day 1.34 g/kg/day 6.7 g/kg/day	10.21873/invivo.11234	2018
	12 weeks		0.025 g/kg/day 0.05 g/kg/day	10.1038/s41598-019-40436-6	2019
	1 days		0.2 g/kg/day	10.1038/s41598-021-85491-0	2021
	45 days	Metastatic breast cancer stem–like cells	0.4 g/kg/day	10.1158/0008-5472.CAN-11-1678	2012
	14 days	Metastatic lesions of bone	0.0125 g/kg/day	10.1002/ijc.26014	2012
	10 days	Leukemia	0.15 g/kg/day 0.3 g/kg/day 0.45 g/kg/day	10.1016/j.leukres.2013.07.009	2013
	2 or 30 days	Renal ischaemia–reperfusion injury	10 g/kg/day	10.1093/ndt/gft314	2013
	24 days	Vascular injury	6 g/kg/day	10.1371/journal.pone.0058760	2013
	2 days	Acute Lung Injury	0.45 g/kg/day	10.3390/toxins5101814	2013
	1 week	Autoimmune type 1 diabetes	10 g/kg/day	10.1172/JCI79271	2015
	5 weeks	Type 2 diabetes	8 g/kg/day	10.1038/s41467-021-25025-4	2021
	22 weeks	Obesity and diabetes	12 g/kg/day	10.1038/s42255-019-0055-6	2019
	x	Pancreatic cancer/tumor	2 g/kg/day	10.3892/ol.2016.4930	2016
	4 weeks		2 g/kg/day	10.1097/MPA.0000000000000741	2017
	28 weeks	Prostate cancer	0.45 g/kg/day	10.1093/jnci/djv085	2015
	42 days	Chronic prostatitis	0.5 g/kg/day	10.1002/pros.24205	2021
	35 days	Bladder cancer	0.2 g/kg/day 0.4 g/kg/day	10.1038/bjc.2017.318	2017
	14 days	Pulmonary hypertension	0.02 g/kg/day	10.1111/bph.13947	2017
	6 weeks	Malignant peripheral nerve sheath tumor	0.4 - 0.5 g/kg/day	10.1002/ijc.30460	2017
	16 or 30 days	Liver fibrosis	0.6 g/mg/day	10.3390/ijms20246301	2019
	2 weeks	Non-alcoholic steatohepatitis	0.2 g/kg/day	10.1007/s12272-021-01309-7	2021
	8 weeks	Osteoarthritis	6 - 10 g/kg/day	10.1002/jor.24541	2020
	8 weeks	Myocardial hypertrophy and fibrosis	10 g/kg/day	10.1161/HYPERTENSIONAHA.120.15247	2021
	6 months	Memory enhancement	6.7 g/kg/day	10.1016/j.brainresbull.2022.01.011	2022
	15 days	Lung cancer	0.4 mg/kg/day (orally) 0.02 g/kg/day (injected IP)	10.1016/j.ijbiomac.2022.02.095	2022
rat	3 hours or 7 days	Nerve injury	0.4 g/kg/day	10.1016/j.neulet.2008.08.042	2008
	1 day	Ischemia/reperfusion injury	0.025 g/kg/day	10.1038/s41598-020-67876-9	2020
	8 weeks	Spinal cord injury	2.0 g/kg/day	https://doi.org/10.1101/2023.01.23.525137	2023
human	X	Covid-19	1.2 g/kg/day	10.1038/s41392-022-00952-w	2022

Recently, it has been proposed that 4-MU may serve as a novel plasticity treatment for CNS disorders by modulating the PNNs (Dubisova et al. 2022; Sîan F. Irvine et al. 2023, 4-; Nagy et al. 2015). These structures stabilise established neural connections, thereby limiting plasticity in the adult CNS (Sorg et al. 2016) by limiting plastic changes due to environmental adaptation (Difei Wang and Fawcett 2012). HA and CSPGs, which share a common monosaccharide residue, glucuronic acid, are key components of PNNs. The production of UDP-glucuronic acid for HA synthesis is reduced by the binding of 4-MU to glucuronic acid (Ghorbani and Yong 2021). We have previously shown that oral treatment with 4-MU reduces PNNs, thereby increasing neuroplasticity after SCI (Sîan F. Irvine et al. 2023). It also improves memory (Dubisova et al. 2022). In addition to experimental use, there are several clinical trials of 4-MU. See Tab. 10 for the conditions treated, doses and current status of the trials.

Tab. 10. Overview of the clinical trials in which the 4-MU was used. Table shows the dose and the conditions treated. Taken from https://clinicaltrials.gov (last updated 27/07/2022).

Condition	Dose [mg/day]	Duration of the treatment	Status
Respiratory disease	1200	Over 4 days of different doses	Completed
	2400		
	3600		
Primary sclerosing cholangitis	1200	6 months	Not yet recruiting
COVID-19	1200	7 days	Recruiting
Pulmonary hypertension	1600	24 weeks	Recruiting
Fabry disease	150 (q.o.d)	24 weeks and then the optional 24 weeks extension period	Completed
	150 (q.o.d)	12-week treatment period and then the optional 36-week extension period	
	150 (q.o.d), 250 (q.d) for 3 days, 4 days off per week for 2 months or 500 (q.d) for 3 days, 4 days off per week for up to 10 months	Up to 56 months	Terminated
	50 (q.o.d)	12-week treatment period and then the optional 36 weeks treatment extension period	Completed
	150 (q.o.d)		
	250 (q.o.d)		
	50 (weeks 1 and 2)	12 weeks and then the optional 1 or 2 extension periods with 50 mg for another 36 weeks.	Completed
	200 (weeks 3 and 4)		
	500 (weeks 5 and 6)		
	50 (weeks 6 – 12)		

Due to its ability to reduce PNNs, 4-MU appears to be a drug with potential in a wide range of CNS pathologies such as traumatic brain injury, memory disorders and neurodegenerative diseases (Dubisova et al. 2022; Sîan F. Irvine et al. 2023; Yong and Guoping 2008; H. F. Kuipers et al. 2016). Pharmacokinetics of 4-MU in humans and rats have been reported in cholestasis studies (Garrett et al. 1993; Morita, Sugiyama, and Hanano 1986). However, long-term administration of 4-MU at 1.2 g/kg/day, as used in the treatment of SCI, may result in undesirable side effects. It is therefore important to access the effects of long-term 4-MU treatment in other organs. Particularly when not only the PNNs are reduced after 4-

MU treatment, but also the HA, which is involved in a wide range of physiological processes and functions.

5.1.2 Physiological role of HA

HA is expressed at high levels throughout the body and is conserved throughout evolution. HA is a simple linear polysaccharide. It has a wide range of biological functions. By interacting with various molecules, HA maintains tissue homeostasis and organises the structure of the ECM. The exceptional biophysical and biomechanical properties of HA contribute to tissue hydration. It mediates the diffusion of solutes across the extracellular space and maintains tissue lubrication. As reviewed in (Dicker et al. 2014) (Fig. 37), the binding of HA to cell surface receptors activates a large number of signalling pathways that regulate cell function, tissue development, the progression of inflammation, wound healing responses and tumour biology. In the CNS, HA is a regulator of neuronal and glial cell differentiation and neuronal activity. It has a role in neurodegenerative diseases and CNS injury (for review see (Peters and Sherman 2020)). HA is also associated with the dense ECM structure that surrounds certain types of neurons in the brain and spinal cord, known as PNNs. HA forms the backbone of the PNN (Smith et al. 2015). Following treatment with 4-MU at the current dose, we observed a downregulation of HA and PNNs in the brain and spinal cord. Indeed, we have previously observed that treating adult mice with 4-MU has a beneficial effect on retaining memory (Dubisova et al. 2022). Several psychiatric disorders have recently been implicated in PNNs. Among them are schizophrenia, autistic spectrum disorders and mood disorders (Pantazopoulos and Berretta 2016). This suggests that pharmacological dose assessment is only the first step in the evaluation of the effects of 4-MU. For future clinical relevance, behavioural studies addressing the potential development of psychiatric disorders following PNN downregulation will be required.

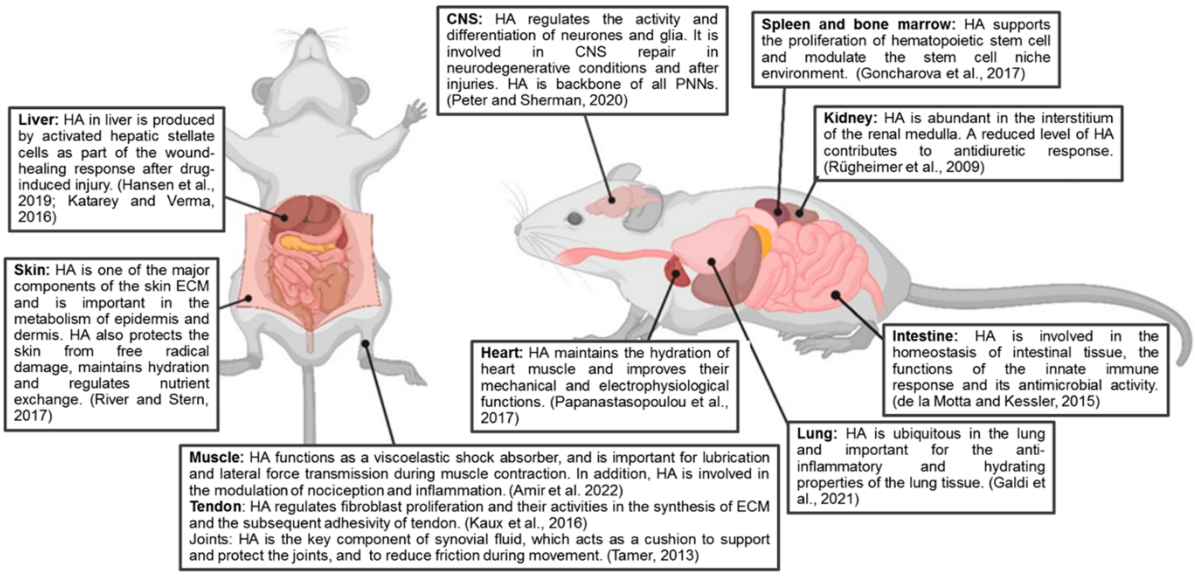

Fig. 37. Schematic illustration showing the wide range of biological functions in which HA is involved. Created with BioRender.com, Refs (Goncharova et al. 2012; Peters and Sherman 2020; de la Motte and Kessler 2015; Galdi et al. 2021; Papanastasopoulou et al. 2017; Amir et al. 2022; Kaux, Samson, and Crielaard 2015; Tamer 2013; Hansen et al. 2019; Katarey and Verma 2016; Farage, Miller, and Maibach 2017).

Outside the CNS, HA is also a regulator of physiological functions in other organs. In the lung, HA is mainly found in the pulmonary connective tissue (Kakehi, Kinoshita, and Yasueda 2003) and is involved in the formation of the viscous gel that plays a key role in tissue homeostasis, regulation of lung interstitial fluid balance and biomechanical integrity (Toole 1990). We did not observe any pathological changes in histology after treatment with 4-MU at the current dose. This suggests that administration of the current dose for 10 months does not induce structural changes in lung tissue.

HA is abundant in the heart, where it is involved in the physiological functions of the heart (Fenderson, Stamenkovic, and Aruffo 1993) as well as in pathological conditions (Tammi et al. 1978). In our study, the reduction of HA after 4-MU treatment does not indicate pathological changes in cardiac tissue, although HA is one of the key molecules in the heart that improves electrophysiological and mechanical functions.

For CD-44-mediated progenitor cell adhesion, splenic HA is important. Dysregulation of CD-44 affinity as a result of impaired HA synthesis has been associated with morphological changes in the spleen such as marked enlargement (Smadja-Joffe et al. 1996) and increased

hyaluronidase activity leading to impaired connective tissue GAG metabolism (Drózdz et al. 1988). In the histological examination of the spleen, we did not observe any significant changes in the distribution of splenic HA and/or any pathology between the groups.

The liver has been shown to be the major organ involved in the synthesis and degradation of HA (Köpke-Aguiar et al. 2002) and is also the key organ for detoxification. Glucuronidation, which requires UDP-GlcA, the major substrate for HA synthesis, is one of the major mechanisms for drug detoxification. It is through this metabolism in the liver that 4-MU administered to the body is removed. Liver function tests were performed to investigate the effect of 4-MU on the liver itself. Two enzymes were monitored: ALT and AST. There were slightly higher levels of ALT compared to the reference range in all three groups throughout the experiment. At week seven, there was also a significant increase in ALT in the wash-out group compared to the placebo group. Even under normal physiological conditions (Malakouti et al. 2017) or as a result of intense physical activity (D. R. Dufour et al. 2000), liver enzyme levels have been shown to change. Our data showed that in the case of AST, levels were within the physiological range throughout the experiment (Miura 1999).

In addition to the liver enzymes, the blood albumin, total protein, bilirubin and bile acids were analysed throughout the experiment. Albumin and total protein levels were within physiological norms throughout the experiment. The final marker monitored was bilirubin. Bilirubin is a breakdown product of red blood cells and elevated levels can also be an indication of liver damage. Our biochemical and pathological results showed no liver damage after long-term treatment with 4-MU at the current dose. This suggests that 4-MU at this dose does not cause drug-induced damage after 10 weeks of daily administration.

In the gut, HA facilitates nutrient and water absorption as well as continuous interaction with the GAG-rich interstitial ECM (Kvietys and Granger 2010). Under pathological conditions, when nutrient and water absorption is impaired, HA distribution is altered (de la Motte et al. 2003). Under pathophysiological conditions where HA synthesis is impaired, there is increased bacterial translocation and dysbiosis and permeability mediated by disrupted tight junctions. It is accompanied by mononuclear cell recruitment and increased lamina propria adhesion. We did not observe any pathophysiological changes in the intestine or other complications related to intestinal damage after long-term treatment with 4-MU.

Over the past decades, HA has emerged as a key player in nephrology and urology. It has been implicated in ECM organisation, inflammation, regeneration and pathological processes (Kaul et al. 2022). With regard to 4-MU, it has already been shown that inhibition of HA could be protective against ischaemia-reperfusion injury in the kidney (Colombaro et al. 2013). We did not observe any pathological changes after 10 weeks of 4-MU treatment, although we observed a loss of HA when staining kidney sections for HABP. Biochemical assessment of urine showed glycosuria at week 4 and proteinuria at week 7 in 4-MU-treated animals. Nephrotoxicity markers showed no evidence of renal damage. The only significant difference was observed in the levels of clusterin in the urine. A significant reduction in clusterin levels was observed in the wash-out group compared to the placebo group, which may be related to the age of the animals rather than the 4-MU treatment itself.

In mammals, approximately 27% of the total amount of HA is expressed in the skeletal and connective tissues, while only about 10% is expressed in the muscle (Fraser, Laurent, and Laurent 1997). Previous studies have shown that HA is mainly concentrated in the synovial fluid of joints, in the connective tissue of skin and muscles (Laurent et al. 1991), and in fascia and loose connective tissue (Stecco et al. 2011). HA plays a key role in lubricating as well as transmitting lateral force during muscle contraction (Purslow 2010). Behavioural tests were performed on the rotarod and grip strength to test muscle contraction and strength. There was no significant difference between the placebo and 4-MU treatment groups that would be indicative of impairment of muscle contraction or strength. Age-related changes in the neuromuscular system are probably responsible for the significant difference observed between the placebo and wash-out groups in the grip strength test (Hunter, Pereira, and Keenan 2016). Because HA is highly expressed in tendons, where it promotes fibroblast cell activity (Kaux, Samson, and Crielaard 2015), and in synovial fluid (Tamer 2013) between joints, protecting bone ends and supporting movement, we also tested tendon biomechanical properties. Our results did not show any significant changes, suggesting an adverse effect of 1.2 g/kg/day of 4-MU.

Traditionally, hyaluronan has been recognised for the role it plays in maintaining joint health. Hyaluronan is naturally synthesised at the local level by synovial cells within the joint. Once produced, it binds to collagen and elastin in the formation of articular cartilage. It is the presence of hyaluronate which makes the cartilage strong enough to resist the compression forces occurring within the joint (Seog et al. 2002). Synovial fluid also contains

unbound hyaluronan. It is the main source of lubricating fluid that allows the joint to move smoothly (Sabaratnam et al. 2005). For smooth joint movement, hyaluronan in the synovial capsule is critical: The articular cartilage encapsulates the ends of the bones and forms a smooth surface. The synovial fluid forms a lubricating film over the articular cartilage during movement. Combined, these structures protect against frictional wear (Walker et al. 1968). Within bone itself, its role in modelling and remodelling bone is the main reason for the presence of hyaluronan. Hyaluronan has been shown to regulate bone remodelling by stimulating osteoblasts and osteocytes as well as inhibiting osteoclasts (Bastow et al. 2008). Our results suggest that 4-MU-mediated reduction of HA also reduces the amount of bound water in bone. This is directly related to reduced bone toughness. With the results of our bone biomechanical tests, we have obtained results that are very similar to previous studies in which the focus was on age-related changes in the bones (X. Wang et al. 2018).

HA has been found to be responsible for the moisture content of the skin (Stern and Maibach 2008) and for the healing of wounds (Longaker et al. 1991). Both dermal and epidermal cells synthesise HA. Dermal HA is primarily responsible for skin hydration as opposed to epidermal HA. A decrease in epidermal HA is directly related to skin ageing. In contrast, dermal HA has been shown to remain constant with age (Schachtschabel and Wever 1978). Our results suggest that 4-MU treatment did not result in a down-regulation of skin HA or an alteration in biomechanical properties.

HA also plays a key role in regulating the immune response (Girish and Kemparaju 2007). Inflammation plays a key role in the body's defence against pathogens as part of the immune response. However, inappropriate activation of inflammatory processes may contribute to many pathological conditions (L. Chen et al. 2018). IFN-γ and IL10 have been described in the context of hyaluronan synthesis. Both appear to inhibit chemokine gene expression by altering mRNA stability and transcription of the MIP-1α and MIP-1β genes (Horton et al. 1998). In addition to its role in anti-inflammatory responses, IL10 also plays an important role in the regulation of HA synthesis. IL10 binds to IL10R1 and IL10R2 to form a tetrameric complex. It activates the JAK/STAT3 signalling pathway. This pathway leads to phosphorylation and nuclear translocation of STAT3. This activates genes such as hyaluronan synthase (HAS) (King et al. 2014). This could explain the significantly higher IL10 levels in 4-MU treated animals. This may be an attempt by the organism to compensate for the 4-MU-mediated inhibition of HA.

5.2 4-MU as novel therapy for chronic SCI

Then, we investigated whether a dose (1.2 g/kg/day) of 4-MU would be sufficient to reduce PNNs in the ventral horns and promote sprouting and functional recovery in chronic SCI. In a previous study, neuroplasticity for memory acquisition was enhanced by down-regulating PNNs in mice at 2.4 g/kg/day (Dubisova et al. 2022). We therefore tested whether reducing this dose to half, i.e., 1.2 g/kg/day, would be able to downregulate PNNs for potential functional recovery after SCI in rats, as the LD50 in rats is slightly lower than in mice. We found that the oral dose of 1.2 g/kg/day (4-MU) was sufficient to reduce PNNs and HA in uninjured animals, but that it was not sufficient to suppress the strong upregulation of CSPGs after SCI, so that no functional recovery was observed.

Many studies have focused on regeneration strategies after SCI in recent years. These strategies are often based on the targeting of PNNs and the manipulation of the glial scar to attenuate the inhibitory properties of its environment. Current strategies range from proteolytic manipulation of the ECM to targeting specific ECM components by synthesising inhibitory ECM molecules after SCI (Burnside and Bradbury 2014). One of the most studied approaches is enzymatic ECM modification using ChABC. By degrading CS chains to disaccharides, removing CSPG inhibition in the glial scar and removing PNNs as a brake on plasticity, ChABC benefits both acute and chronic SCI conditions (Difei Wang et al. 2011). Spinal cord injured animals show improved recovery, both anatomically and functionally, following ChABC treatment (Bradbury et al. 2002; García-Alías et al. 2009; Difei Wang et al. 2011). Functional recovery after SCI is further enhanced when restoration of plasticity is combined with rehabilitation (García-Alías et al. 2009; Difei Wang et al. 2011). However, there are several drawbacks to using ChABC. The main disadvantages of using this bacterial enzyme are its thermal instability and short half-life, which requires multiple or continuous intrathecal administrations (Nori et al. 2018), the potential for the body to develop an immune response, and the difficulty of dosing. In addition to ChABC, Keough and colleagues (Keough et al. 2016) tested a subset of 245 drugs that were known to penetrate the CNS and exhibit oral bioavailability. None of these 245 compounds was shown to have sufficient ability to overcome oligodendrocyte precursor cell inhibition of CSPG.

We therefore investigated whether the administration of 4-MU would reduce the synthesis of both HA and CS, thereby facilitating neuroplasticity. Indeed, both anatomically by

histochemistry and biochemically by GAG quantification, we observed a down-regulation of HA and CS. Our data suggest that 4-MU, in combination with daily training, is a suppressor of GAG synthesis. Administration of 4-MU resulted in removal of PNNs in the ventral horns using PNN markers including WFA and ACAN. After a wash-out period of 8 weeks, PNNs reappeared. It is likely that CS synthesis is less sensitive to UDP-GlcA deficiency, which explains why PNNs reappeared after 8 weeks of wash-out while HA levels remained low. CS is synthesised in the Golgi apparatus where UDP-GlcA sugars are transported into the Golgi lumen with high affinity. HA is synthesised directly at the cytoplasmic membrane (Nagy et al. 2015).

We used a thoracic contusion injury that mimics the most common closed SCI in humans, sparing some axons around a central cavity and ablating dorsal corticospinal tracts (CSTs) critical for human motor control (Basso 2000). In the chronic phase, starting 6 weeks after injury, 4-MU was administered (Kjell and Olson 2016). At this stage, the glial scar is well established. CSPGs are upregulated and the acute immune response has subsided (Stichel and Müller 1994; R. Hu et al. 2010). 4-MU treatment was accompanied by daily treadmill rehabilitation for consolidation of appropriate synaptic connections and pruning of others (Oudega, Bradbury, and Ramer 2012). After the 8 weeks of treatment and rehabilitation, rehabilitation was continued for a further 8 weeks as a wash-out period. This wash-out period allows the PNNs to reform and stabilise de novo synapses and consolidate anatomical plasticity (García-Alías et al. 2009; Al'joboori, Edgerton, and Ichiyama 2020; Difei Wang et al. 2011), while the continued rehabilitation prunes random connections, supports appropriate connections and removes inappropriate connections (James W. Fawcett and Curt 2009; Kanagal and Muir 2009). There was a robust reduction in the glial scar surrounding the cavity following oral administration of 1.2 g/kg/day 4-MU. Throughout the wash-out period, this reduction was sustained.

We analysed the intensity of the 5-HT signal to assess the potential of 4-MU to remove the plasticity brake formed by PNNs. Away from the lesion, we observed increased 5-HT sprouting. However, this sprouting did not result in a significant difference in synapsin immunoreactivity within the ventral horns above and below the lesion between 4-MU treated and placebo animals. The effect of 4-MU on the mediation of changes in other cellular composition was also investigated. A reduction in GFAP and nestin staining was indeed observed. This is an indication of a reduction in astrogliosis. Up-regulation of Iba-1 and NG2

staining was also observed. This is an indication of the recruitment of microglia/macrophages and OPCs to the area. It is not clear at this stage whether this recruitment is due to a direct effect of 4-MU treatment or to a 4-MU-induced modulation of the ECM. However, this is an indication that 4-MU is modulating the population of immune cells in the area of the lesion. Assessment of functional recovery using the BBB test, the maximum speed test and the ladder rung walk test showed no significant differences between the 4-MU and placebo groups, even with continued rehabilitation over the next 8 weeks. As 4-MU-mediated PNNs ablation has been demonstrated in the mouse hippocampus to improve memory in ageing mice (Dubisova et al. 2022), we hypothesised that the lack of functional recovery after SCI in this study was due to the lower dose of 4-MU administered (1.2g/kg/day versus 2.4g/kg/day) and the strong CS-GAG upregulation after injury. A higher dose of 4-MU combined with rehabilitation should be tested to see if this improves recovery after SCI.

In line with published data, the promising results we observed with 5-HT staining are encouraging. Previous studies have shown that in addition to the loss of direct muscle innervation by spinal motoneurons, there is also a loss of supraspinal tracts involved in voluntary movement initiation and a loss of descending tracts supplying neuromodulators such as 5-HT (Jacobs, Martín-Cora, and Fornal 2002; Jordan et al. 2008) to motoneurons. In the intact spinal cord, serotonergic innervation originates almost exclusively from brainstem raphe nuclei, which are lost (Murray et al. 2010; Schmidt and Jordan 2000) or severely disrupted (Hayashi et al. 2010) after SCI. The drastic and abrupt decrease in serotonin availability below the lesion results in spinal cord networks that are no longer excitable. or responsive (A. R. Harvey et al. 2006; B. Chen et al. 2018) and is a major contributor to SCI-induced paralysis (Schmidt and Jordan 2000). Barzilay and colleagues have also shown that HA is involved in serotonergic fibre propagation, thereby enhancing neuroplasticity (Barzilay et al. 2016). 5-HT acts on spinal interneurons and motor neurons to allow appropriate muscle contraction (Jacobs, Martín-Cora, and Fornal 2002; Perrier and Delgado-Lezama 2005). In acute SCI, spinal motor neurons and interneurons are deficient in 5-HT (Perrier and Hounsgaard 2003; P. J. Harvey et al. 2006) resulting in paralysis and spinal shock (Bennett et al. 1999; 2004). Therefore, despite the continued absence of 5-HT (Button et al. 2008) in chronic SCI, motor neurons partially recover their excitability. It has also been suggested that this compensatory mechanism requires activity-dependent tuning to contribute to motor activity following SCI (Murray et al. 2010). Our behavioural data also

showed spontaneous recovery of motor activity in rats with the contusion model of SCI. This spontaneous recovery is important not only in animals, but also in human patients with incomplete SCI. Some of the descending connections to the brain are spared in incomplete SCI. Animals, like humans, can learn to use these spared connections to significantly recover walking function, especially with rehabilitation training (Barbeau et al. 2002; Wirz et al. 2005; Ballermann and Fouad 2006). Therefore, understanding and promoting this plasticity in spared connections is an important focus of spinal cord research. For example, it is already known that spared corticospinal axons sprout across the injury site and form new connections, including the transmission of descending inputs around the injury site through spared propriospinal pathways (Bareyre et al. 2004; Gregoire Courtine et al. 2008; Vavrek et al. 2006). Spared descending fibres also sprout below the injury, a process shown to correlate well with recovery in animal models (Ballermann and Fouad 2006). Neurons downstream of the injury must be ready to respond to these enhanced or restored descending signals for these spared and new connections to be functional. This is likely to require compensating for lost neuromodulatory (5-HT) innervation. Serotonergic growth cones are more active than cortical growth cones when challenged with CSPG, as shown by in vitro time-lapse imaging studies. After enzymatic digestion with ChABC (Hawthorne et al. 2011), serotonergic neurons recover better. These results suggest that 4-MU may also make serotonergic fibres more responsive to treatment in vivo through its effect on CSPG expression. In the case of ChABC, studies have shown that this may be partly due to cytoskeletal or receptor differences. We speculate that even though CSPGs were not downregulated around the lesion, systemic administration of 4-MU together with general treadmill rehabilitation induced 5-HT sprouting in the spinal cord. The robust serotonin neuronal response may also be related to increased expression of GAP-43, which is implicated in axonal growth or regeneration and is normally down-regulated in adults (Skene and Willard 1981; Jacobson, Virág, and Skene 1986). Postnatally, at least in the forebrain, serotonergic neurons require GAP-43 for proper terminal arborisation (Donovan et al. 2002). In addition, serotonergic neurons continue to produce GAP -43 mRNA in adulthood (Bendotti, Servadio, and Samanin 1991)and this may increase the sensitivity of the 5-HT fibres to injury.

We evaluated the changes in mRNA expression of genes involved in HA synthesis (Has1, Has2, Has3) (Nagy et al. 2015)to determine if there is a compensatory mechanism for the loss of HA synthesis. Although their mRNA levels tended to be down-regulated, we

observed no significant difference. The expression of the has genes after treatment with 1 mM 4-MU, studied in human aortic smooth muscle cells, showed a reduction mainly in the Has1 and Has2 transcripts after treatment with 4-MU (Vigetti et al. 2009). We used histochemical staining for recombinant HABP derived from the human versican G1 domain, which binds specifically to hyaluronan and not to other glycosaminoglycans, to determine the biochemical effect of 4-MU at 1.2 g/kg/day on HA synthesis in uninjured animals (Amsbio; data sheet). We observed that HA levels remained lower than in healthy animals after a 2-month wash-out period. This may raise the question of whether the downregulation of HA after a 2-month wash-out period may cause adverse effects after treatment.

Clinical trials with 4-MU (marketed as hymecromone in Europe and Asia) have shown excellent safety parameters when administered over long periods of time at approved doses ranging from 1.2 to 3.6 g/day (Abate et al. 2001; Camarri and Marchettini 1988; Krawzak et al. 1995; Quaranta, Rossetti, and Camarri 1984; Trabucchi et al. 1986; Walter and Seidel 1979; Hoffmann et al. 2005). The longest reported duration of oral 4-MU administered to human patients was 3 months (Trabucchi et al. 1986). This is a much shorter duration based on the correlation between the ages of laboratory rats and humans (Sengupta 2013) and may be taken into account in explaining these results. The safety profile of long-term 4-MU treatment is not yet fully established (Nagy et al. 2015). However, in our recent study in healthy rats, long-term oral administration of 4-MU at a dose of 1.2 g/kg/day resulted in no serious adverse effects. If there were any deviations from the reference values, they returned to normal after a wash-out period of 9 weeks in the Wistar rats. Our results suggest that 1.2g/kg/day 4-MU could be used in long-term therapy (Štěpánková et al. 2023).

In conclusion, this study shows that the oral administration of 1.2 g/kg/day of 4-MU reduces the total amount of GAGs, decreases the glial scar and increases the number of 5-HT puncta in the chronic stage of SCI. However, these structural changes do not result in increased synaptic connections. They are not sufficient to induce functional recovery even after intensive rehabilitation. To induce functional recovery supported by synaptic plasticity, a higher dose of 4-MU may be required.

5.3 Using AAV-mediated overexpression of integrin α9 for sensory pathway reconstruction after SCI

In the last part of this thesis, we have shown that α9-K1 transduced neurons regenerated their neurons vigorously through the largely fibroblastic environment of the lesion core of the injured rat spinal cord. The axons then extended back into the CNS tissue of the spinal cord, where they regenerated down to the level of the spinal cord, a distance of more than 4 cm from the thoracic lesions. In the grey matter of the dorsal horn, where synapses were evident, many axonal branches grew. On stimulation, neurons in the dorsal part of the spinal cord upregulated cFOS, indicating that functional connections were being formed. The light touch, the heat and the removal of the tape - the full battery of behavioural tests - indicate the full recovery of the behaviour.

The sensory neurons of the DRG are capable of regeneration, as evidenced by their ability to regenerate axons within the PNS. The extensive regeneration of axons in the current study suggests that α9-K1 transduction activates mechanisms that regulate regeneration in the CNS environment. Up-regulation of the RAGs gene expression programme (Chandran et al. 2016) is associated with sensory regeneration in the PNS. Regeneration without expression of the RAGs programme is unlikely, as several of the molecules expressed in the RAGs programme are required for successful regeneration. Transduction of sensory neurons with α9-K1, even in the absence of axotomy, results in the expression of the RAGs programme, thus priming the neurons for successful regeneration (Cheah et al. 2023). However, for long-distance spinal sensory regeneration to occur, expression of the RAGs programme alone is not sufficient. Crushing peripheral nerves prior to lesioning the central sensory branch upregulates the RAGs programme and leads to increased local sprouting of severed axons, but not long-distance growth (Neumann and Woolf 1999). There is therefore a need for an additional element. The events of cell migration are dependent on growth-promoting receptors on the cell surface that bind to ligands in the environment (P. T. Caswell and Norman 2006). This receptor-ligand interaction leads to signalling, increased cytoskeletal dynamics associated with focal adhesions, which in turn lead to mechanical traction and migration (Ridley 2011). Integrins are the major cell surface adhesion molecules which are inducers of migration. Adult DRG neurons express several fibronectin- and laminin-binding integrins (α3β1, α4β1, α5β1, α6β1 and α7β1), with the laminin receptor α7β1 playing a major role in axonal regeneration in peripheral nerve (Gardiner 2011; Werner et al. 2000). However, in the acute SCI, laminin and fibronectin are found in fibroblasts in the core of the

lesion, surrounding blood vessels and in the meninges, but not in the central nervous system (Orr and Gensel 2018; Risling et al. 1993). Tenascin-C and osteopontin, which are not partners for the integrins expressed in adult DRGs, are the integrin ligands in reactive CNS tissue. The major migration-inducing integrin for tenascin-C and osteopontin is α9β1, and it is therefore not surprising that α9-K1 transduction allows axon regeneration to occur (Høye et al. 2012). Expression of kindlin-1 alone activates endogenous integrins expressed by DRG neurons. These integrins bind to laminin and fibronectin. Therefore, kindlin-1 alone allowed regeneration of sensory axons into the core region of the lesion, but not into CNS tissue containing tenascin-C, for which sensory axons have an integrin receptor but very little laminin. Only when neurons were transduced with α9-K1 to provide an activated form of this tenascin-C-osteopontin receptor, did regeneration into the lesion and on to CNS tissue occur. The uninjured axons below the lesion in the α9-K1 transduced animals expressed both α9 and K1 in most cases, but some were positive for only one of these. Only axons expressing both α9 and K1 were seen above the lesion, indicating that successful CNS regeneration requires this combination. However, in animals with lesions in the thoracic spinal cord, we observed a decrease in V5 signal in the spinal cord, which may indicate that integrin trafficking becomes weaker with distance.

The axons that regenerated through the spine lesion were associated with strands and bridges of GFAP-negative tissue that was shown to contain cells of the meninges and blood vessels, perivascular and fibroblastic origin. These cells expressed laminin and tenascin-C, providing a suitable. growth substrate for endogenously expressed kindlin-1-activated laminin-binding integrins and α9-expressing neurons. At the rostral interface of the lesion core and CNS tissue, axon growth tended to be chaotic, indicating exploratory behaviour within the disturbed tissue. Within the cord rostral to the lesion, regenerating axons in the α9-K1 group were found particularly at the dorsal column/dorsal horn border, with some axons growing wanderingly through white matter. This is different from the normal path of sensory axons and is also different from the path through the white matter that was taken by axons that regenerated after α9-K1 and a dorsal root crush (Cheah et al. 2016). Although it is not clear why the white matter/grey matter boundary should provide this, we speculate that the path disruption associated with growth through the lesion causes axons to seek a permissive path. The regenerating sensory axons did not penetrate the medullary sensory nuclei (Cheah et al. 2016; Massey et al. 2006), as in previous studies. The PNN-rich networks in these nuclei are responsible for this.

Approximately 1000 axons regenerated 2-5 cm from the lesions into the hindbrain in our study and in the previous study using dorsal root crush rather than spinal lesions (Cheah et al. 2016). Several data show that these are regenerated rather than unlesioned axons:

i) Axons in the lesion pass through GFAP negative fibroblastic tissue. Uninjured axons would be surrounded by CNS glia.

ii) Axons rostral to the lesion follow a different route than unlesioned axons.

iii) Regenerated axons avoid the sensory nuclei. There are no axons innervating the sensory nuclei (if present, these would be unlesioned axons).

iv) Regeneration progresses over time, which is well illustrated by the behavioural tests, where the very slow improvement is seen before week 8, where the sudden improvement appeared in the α9-K1 group but not in the K1-only and GFP groups, and this improvement remained until the end of the experiments, suggesting that the transduced axons only reached the particular targets after 8 weeks.

v) The controls are very clear, no axons beyond the lesion in the GFP group, axons only in the laminin+ve fibroblast tissue in the laminin-1 group, Fig. 29, 30) In our mRNA profiling study (Cheah et al. 2023) a distinct expression pattern is seen only where α9-K1 expression plus axotomy allows axon regeneration.

A large number of processes were seen to grow into the dorsal horns, taking a course perpendicular to the ascending axons. VGLUT1/2 positive swellings were seen on these processes. This is indicative of synapse formation. After stimulation of the sciatic nerve, the peripheral branch of the DRG injected with α9-K1, we tested the ability of these synapses to stimulate neurons in the spinal cord by observing the upregulation of c-FOS in propriospinal neurons. In the α9-K1-treated animals, the number of c-FOS neurons after stimulation was much higher than in the control animals, indicating connections between the regenerated axons and spinal cord neurons. This was demonstrated by sensory recovery testing. In particular, we saw eventual full recovery in fine touch, heat and tape removal tasks in the α9-K1 lumbar injected group. The time course of recovery in this and our previous experiment (Cheah et al. 2016; 2023) was similar to the time course of axon regeneration. As the animals do not appear to see the tape on their hind paws, recovery in the tape removal task is particularly informative. Instead, it appears that sensory detection triggers the removal of the tape from the hind paw. The sensation must reach the brain, which then carries out the removal process, in order to perceive that there is tape on the hind paw. This task is therefore

an example of the transmission of information to the brain by regenerating axons. It is interesting to note that this happens without re-innervating the medullary sensory nuclei. Presumably, sensory information is transmitted to the brain by propriospinal neurons. These neurons are stimulated by regenerated sensory inputs to the dorsal horn.

Almost complete reconstruction of the spinal sensory pathway has been achieved employing the strategy of using an activated integrin to induce sensory regeneration. It is important to note that in the present study, axons were able to regenerate over a length that would allow growth across a human injury, as the lesion length in human SCI varies from 1 to 7 cm (Dalkilic et al. 2018). The regeneration index, which compares the number of axons below and above the lesion, shows that 50% of the axons regenerated through the lesion area. Once through the lesion, the number of axons did not decrease significantly up to the high cervical cord. However, due to the lack of innervation of the medullary sensory nuclei, complete reconstruction was not achieved. Methods to re-innervate these nuclei have been identified using chondroitinase digestion and neurotrophin-3 expression (Massey et al. 2006; Alto et al. 2009) and could be used to achieve complete tract reconstruction. However, functional recovery, including tape removal, which requires sensory information to reach the brain, was almost complete despite the lack of innervation of the sensory nuclei. If α9-K1 could be delivered to descending spine axons, it is likely that regeneration would be possible. However, in these highly polarised neurons, integrins are restricted to the somatodendritic domain and excluded from the axons, so this repair strategy cannot currently be directly applied to descending motor pathways (Andrews et al. 2016; Franssen et al. 2015). Strategies have been identified to allow integrins to transport to motor axons, which may make it possible to reconstruct motor pathways (Petrova et al. 2020; Nieuwenhuis et al. 2020).

6. CONCLUSION

In conclusion, the results of this thesis show that the regeneration of axons in the CNS is inhibited by a large number of intrinsic and extrinsic factors. It has been shown that no single intervention is sufficient to fully regenerate damaged axons in the adult mammalian CNS because these factors act in parallel. Our aim has been to show that, in principle, there are two main therapeutic approaches to the treatment of SCI. Put simply, you could remove the inhibitory environment around the lesion site, thereby increasing plasticity, or you could use the inhibitory environment to promote regeneration by overexpressing the correct isoforms of molecules that are capable of binding to the inhibitory environment around the lesion site, thereby allowing axons to pass through the lesion. Both approaches have something in common, namely that axons in the adult CNS can be regenerated by reactivating the processes that trigger axon growth during development.

We have shown that 4-MU is safe for long-term use on rats. Furthermore, 4-MU can effectively downregulate HA throughout the body, with no detectable. side effects. We have also observed that 4-MU at a dose of 1.2 g/kg/day is effective in the downregulation of PNN (as shown by anti-aggrecan staining). The further question was whether 4-MU at the current dose would be sufficient for the promotion of anatomical plasticity and recovery after SCI.

In the next part, we focused on the chronic stage of SCI to see if 4-MU could be used to treat it. The main reason for the use of the chronic phase is that by then the scar is fully established and it is more clinically relevant for the potential future translation to the treatment of the chronic phase than is the acute phase of SCI. We hypothesised that 4-MU would not only reduce the glial scar surrounding the lesion, but also remove the PNNs around certain types of spinal neurons, thus re-opening a window of plasticity. We also expected that task-specific rehabilitation, in our case treadmill training, could remodel, adapt and reorganise axonal sprouting after training, leading to recovery of a motor skill after SCI. We investigated that 4-MU at the current dose is able to reduce the scar around the lesion, but after injury there is an upregulation in the production of CSPGs around the lesion. Despite the fact that 4-MU at the current dose reduced scar even in the chronic stage, it was not sufficient to reduce upregulated CSPGs after SCI. Thus, we did not observe functional recovery, but the 5-HT staining showed some increased sprouting in the 4-MU treated animals. These results suggest that perhaps the higher dose would lead to functional recovery. However, a further study would be needed to test this hypothesis.

As mentioned above, one way to recapitulate the developmental stage is not to remove the inhibitory (CSPGs-rich) environment. However, in attempts to achieve axon regeneration, this is not the only option available to us. During axonal pathfinding, developing axons navigate the extracellular environment, extending to postsynaptic targets to form a functional synapse. The mechanism by which they navigate is a type of classical cell migration and follows a specific set of rules. When James Fawcett's laboratory at the University of Cambridge tried to regenerate axons, they came up with a simple idea. The idea was to try to recapitulate this developmental stage in cell cultures and after dorsal root crush in the rat model by overexpressing the particular integrin isoforms that are key to axon pathfinding during development. We did a follow-up study in a rat model of SCI. The first step was to overexpress the α9 integrin with its activator kindlin-1, which was injected directly into the DRGs to try to promote sensory axon regeneration. The reason why sensory pathways were chosen for this study is simple. SCI patients have more health problems than just the inability to walk, and at the same time the neurons are in the DRGs, not at the lesion site, which gave us the idea that the sensory pathways might be a better target. In this part of the thesis, we showed that AAV-mediated overexpression of integrin α9 together with kindlin-1 can lead to partial reconstruction of sensory pathways after SCI. In addition, we observed that axons passing through the lesion were able to form functional synapses above the lesion. We also observed behavioural improvements in the treated animals. However, as the sensory axons did not reconnect in the sensory nuclei in the spinal cord, we did not achieve full pathway reconstruction with this treatment. This opens up room for follow-up studies - to use ChABC (or any other approach to locally dissolve the PNNs and CSPGs rich environment in the sensory nuclei) and then use this approach to reconstruct the sensory pathways connected to the bladder and perineum innervation (as this would be an amazing step forward for the patients if the bladder sensation would work again) and last but not least to try to reconstruct not only the sensory pathways but also the corticospinal tract.

In conclusion, this thesis has provided some insights that may change the field of axon regeneration somewhat and allow us to move forward in developing new experimental treatments that hopefully can move from the bench to patients and improve their daily lives.

7. SUMMARY

Following SCI, several developmental principles come into play to either promote or inhibit spontaneous regeneration, and manipulation of these has the potential to contribute to functional recovery. In this work, by considering not only altering the inhibitory environment of the injured spinal cord, but also forcing the overexpression of the appropriate integrin isoform that allows regenerating axons to grow onto the inhibitory scar, thereby promoting sensory tract regeneration, we have explicitly provided a novel developmental input to the field of CNS repair.

Finding an effective way to reduce the inhibitory environment is one of the key approaches in the treatment of SCI. We focused on investigating a drug that can be administered orally with a simple dosage, which has been a goal for some time - 4-MU. 4-MU is already approved for biliary therapy in humans, but only for the short term, whereas in SCI it is a long-term treatment. Long-term 4-MU treatment at a dose of 1.2g/kg/day appears to be associated with no apparent adverse effects in a rat model. However, the current dose was insufficient for effective reduction of CSPGs in the scar around the lesion.

We know that there is a remarkable communication between the growth machinery that exists during development and that which exists in the adult. When we used AAV vectors to overexpress the integrin α9 together with its activator Kindlin-1, which is crucial for developmental axon pathfinding, we were able to use the inhibitory environment around the lesion to promote axon growth to the molecules present there. We were able to partially reconstruct the sensory pathways after the dorsal column crush.

8. SOUHRN

Mícha po poranění prochází procesy, které mohou určitým způsobem připomínat vývoj CNS. Tyto procesy, pak mohou samotnou spontánní regeneraci buď podporovat nebo brzdit. Určitá manipulace s těmito mechanismy může výrazně přispět k funkčnímu zotavení. Tato disertační práce se zaměřuje na zkoumání toho, jak snížení inhibičního prostředí poraněné míchy a „znovuotevření" kritické periody ovlivňují funkční zotavení. Zároveň se zabývá otázkou, zda lze toto inhibiční prostředí, v některých případech, využít ve prospěch regenerace. V práci ukazujeme, že po vyvolání nadměrné exprese příslušné izoformy integrínu, která hraje roli při navigaci axonů během vývoje, umožňuje regenerujícím axonům růst po jinak inhibičních proteinech jizvy, kterou využívají jako lešení. Tato práce přináší nový pohled na regeneraci axonů po poranění míchy, který využívá rekapitulaci vývojového stadia.

Hledání účinného způsobu, jak snížit inhibiční prostředí, patří mezi efektivním přístupům při léčbě poranění míchy. Zaměřili jsme se na studium léku, který lze podávat perorálně s jednoduchým dávkováním - 4-MU. Tento přípravek je již schválen jako choleretikum a antispasmodikum pro krátkodobou léčbu u lidských pacientů, ale zároveň je využíváno experimentálně pro léčbu celé řady nemocí a poruch. Nicméně, v případě poranění míchy, je potřeba léčba dlouhodobější. Naše experimenty naznačují, že dlouhodobá léčba4-MU v dávce 1,2 g/kg/den nevykazuje zjevné nežádoucí účinky u potkanů. Je však nutné poznamenat, že současná dávka není dostatečná pro efektivní snížení CSPG v jizvě kolem poranění na docílení funkčního zlepšení po míšním poranění.

Víme, že existuje pozoruhodná komunikace mezi růstovým mechanismem, který funguje během vývoje, a mechanismem, který je aktivní v dospělosti. Při využití vektorů AAV k nadměrné expresi integrínu α9 spolu s jeho aktivátorem Kindlinem-1, klíčovým pro navigaci axonů během vývoje, jsme úspěšně využili inhibiční prostředí v okolí poranění k podpoře růstu axonů. Dosáhli jsme částečné rekonstrukce senzorických drah po dorsální hemisekce.

9. LITERATURE REFERENCES

1. Abate, A., V. Dimartino, P. Spina, P. L. Costa, C. Lombardo, A. Santini, M. Del Piano, and P. Alimonti. 2001. 'Hymecromone in the Treatment of Motor Disorders of the Bile Ducts: A Multicenter, Double-Blind, Placebo-Controlled Clinical Study'. *Drugs Under Experimental and Clinical Research* 27 (5–6): 223–31.
2. Abe, Namiko, Angels Almenar-Queralt, Concepcion Lillo, Zhouxin Shen, Jean Lozach, Steven P. Briggs, David S. Williams, Lawrence S. B. Goldstein, and Valeria Cavalli. 2009. 'Sunday Driver Interacts with Two Distinct Classes of Axonal Organelles'. *The Journal of Biological Chemistry* 284 (50): 34628–39. https://doi.org/10.1074/jbc.M109.035022.
3. Afshari, Fardad T., Sunil Kappagantula, and James W. Fawcett. 2009. 'Extrinsic and Intrinsic Factors Controlling Axonal Regeneration after Spinal Cord Injury'. *Expert Reviews in Molecular Medicine* 11 (December): e37. https://doi.org/10.1017/S1462399409001288.
4. Ahuja, Christopher S., Jefferson R. Wilson, Satoshi Nori, Mark R. N. Kotter, Claudia Druschel, Armin Curt, and Michael G. Fehlings. 2017. 'Traumatic Spinal Cord Injury'. *Nature Reviews. Disease Primers* 3 (April): 17018. https://doi.org/10.1038/nrdp.2017.18.
5. Al'joboori, Yazi D., V. Reggie Edgerton, and Ronaldo M. Ichiyama. 2020. 'Effects of Rehabilitation on Perineural Nets and Synaptic Plasticity Following Spinal Cord Transection'. *Brain Sciences* 10 (11): 824. https://doi.org/10.3390/brainsci10110824.
6. Almad, Akshata, F. Rezan Sahinkaya, and Dana M. McTigue. 2011. 'Oligodendrocyte Fate after Spinal Cord Injury'. *Neurotherapeutics: The Journal of the American Society for Experimental NeuroTherapeutics* 8 (2): 262–73. https://doi.org/10.1007/s13311-011-0033-5.
7. Alqahtani, Mohammed S., Mohsin Kazi, Mohammad A. Alsenaidy, and Muhammad Z. Ahmad. 2021. 'Advances in Oral Drug Delivery'. *Frontiers in Pharmacology* 12: 618411. https://doi.org/10.3389/fphar.2021.618411.
8. Alto, Laura Taylor, Leif A. Havton, James M. Conner, Edmund R. Hollis, Armin Blesch, and Mark H. Tuszynski. 2009. 'Chemotropic Guidance Facilitates Axonal Regeneration and Synapse Formation after Spinal Cord Injury'. *Nature Neuroscience* 12 (9): 1106–13. https://doi.org/10.1038/nn.2365.

9. Amir, Adam, Soo Kim, Antonio Stecco, Michael P. Jankowski, and Preeti Raghavan. 2022. 'Hyaluronan Homeostasis and Its Role in Pain and Muscle Stiffness'. *PM & R: The Journal of Injury, Function, and Rehabilitation* 14 (12): 1490–96. https://doi.org/10.1002/pmrj.12771.
10. Andrews, Melissa R., Sara Soleman, Menghon Cheah, David A. Tumbarello, Matthew R. J. Mason, Elizabeth Moloney, Joost Verhaagen, et al. 2016. 'Axonal Localization of Integrins in the CNS Is Neuronal Type and Age Dependent'. *eNeuro* 3 (4): ENEURO.0029-16.2016. https://doi.org/10.1523/ENEURO.0029-16.2016.
11. Anthis, Nicholas J., and Iain D. Campbell. 2011. 'The Tail of Integrin Activation'. *Trends in Biochemical Sciences* 36 (4): 191–98. https://doi.org/10.1016/j.tibs.2010.11.002.
12. Aruffo, A., I. Stamenkovic, M. Melnick, C. B. Underhill, and B. Seed. 1990. 'CD44 Is the Principal Cell Surface Receptor for Hyaluronate'. *Cell* 61 (7): 1303–13. https://doi.org/10.1016/0092-8674(90)90694-a.
13. Asher, R. A., R. J. Scheibe, H. D. Keiser, and A. Bignami. 1995. 'On the Existence of a Cartilage-like Proteoglycan and Link Proteins in the Central Nervous System'. *Glia* 13 (4): 294–308. https://doi.org/10.1002/glia.440130406.
14. Asher, R., G. Perides, J. J. Vanderhaeghen, and A. Bignami. 1991. 'Extracellular Matrix of Central Nervous System White Matter: Demonstration of an Hyaluronate-Protein Complex'. *Journal of Neuroscience Research* 28 (3): 410–21. https://doi.org/10.1002/jnr.490280314.
15. Askari, Janet A., Patrick A. Buckley, A. Paul Mould, and Martin J. Humphries. 2009. 'Linking Integrin Conformation to Function'. *Journal of Cell Science* 122 (Pt 2): 165–70. https://doi.org/10.1242/jcs.018556.
16. Assinck, Peggy, Greg J. Duncan, Brett J. Hilton, Jason R. Plemel, and Wolfram Tetzlaff. 2017. 'Cell Transplantation Therapy for Spinal Cord Injury'. *Nature Neuroscience* 20 (5): 637–47. https://doi.org/10.1038/nn.4541.
17. 'AXER-204 in Participants With Chronic Spinal Cord Injury (RESET)'. n.d. https://classic.clinicaltrials.gov/ct2/show/NCT03989440.
18. Back, Stephen A., Therese M. F. Tuohy, Hanqin Chen, Nicholas Wallingford, Andrew Craig, Jaime Struve, Ning Ling Luo, et al. 2005. 'Hyaluronan Accumulates in Demyelinated Lesions and Inhibits Oligodendrocyte Progenitor Maturation'. *Nature Medicine* 11 (9): 966–72. https://doi.org/10.1038/nm1279.

19. Badhiwala, Jetan H., Jefferson R. Wilson, Brian K. Kwon, Steven Casha, and Michael G. Fehlings. 2018. 'A Review of Clinical Trials in Spinal Cord Injury Including Biomarkers'. *Journal of Neurotrauma* 35 (16): 1906–17. https://doi.org/10.1089/neu.2018.5935.
20. Balakrishnan, Balaji, and Giridhara R. Jayandharan. 2014. 'Basic Biology of Adeno-Associated Virus (AAV) Vectors Used in Gene Therapy'. *Current Gene Therapy* 14 (2): 86–100. https://doi.org/10.2174/1566523214666140302193709.
21. Ballermann, Mark, and Karim Fouad. 2006. 'Spontaneous Locomotor Recovery in Spinal Cord Injured Rats Is Accompanied by Anatomical Plasticity of Reticulospinal Fibers'. *The European Journal of Neuroscience* 23 (8): 1988–96. https://doi.org/10.1111/j.1460-9568.2006.04726.x.
22. Baptiste, Darryl C., and Michael G. Fehlings. 2006. 'Pharmacological Approaches to Repair the Injured Spinal Cord'. *Journal of Neurotrauma* 23 (3–4): 318–34. https://doi.org/10.1089/neu.2006.23.318.
23. Barbeau, H., J. Fung, A. Leroux, and M. Ladouceur. 2002. 'A Review of the Adaptability and Recovery of Locomotion after Spinal Cord Injury'. *Progress in Brain Research* 137: 9–25. https://doi.org/10.1016/s0079-6123(02)37004-3.
24. Bareyre, Florence M., Martin Kerschensteiner, Olivier Raineteau, Thomas C. Mettenleiter, Oliver Weinmann, and Martin E. Schwab. 2004. 'The Injured Spinal Cord Spontaneously Forms a New Intraspinal Circuit in Adult Rats'. *Nature Neuroscience* 7 (3): 269–77. https://doi.org/10.1038/nn1195.
25. Barros, Claudia S., Santos J. Franco, and Ulrich Müller. 2011. 'Extracellular Matrix: Functions in the Nervous System'. *Cold Spring Harbor Perspectives in Biology* 3 (1): a005108. https://doi.org/10.1101/cshperspect.a005108.
26. Barzilay, R., F. Ventorp, H. Segal-Gavish, I. Aharony, A. Bieber, S. Dar, M. Vescan, et al. 2016. 'CD44 Deficiency Is Associated with Increased Susceptibility to Stress-Induced Anxiety-like Behavior in Mice'. *Journal of Molecular Neuroscience: MN* 60 (4): 548–58. https://doi.org/10.1007/s12031-016-0835-3.
27. Basso, D. M. 2000. 'Neuroanatomical Substrates of Functional Recovery after Experimental Spinal Cord Injury: Implications of Basic Science Research for Human Spinal Cord Injury'. *Physical Therapy* 80 (8): 808–17.
28. Basso, D. M., M. S. Beattie, and J. C. Bresnahan. 1995. 'A Sensitive and Reliable Locomotor Rating Scale for Open Field Testing in Rats'. *Journal of Neurotrauma* 12 (1): 1–21. https://doi.org/10.1089/neu.1995.12.1.

29. Bastow, E. R., S. Byers, S. B. Golub, C. E. Clarkin, A. A. Pitsillides, and A. J. Fosang. 2008. 'Hyaluronan Synthesis and Degradation in Cartilage and Bone'. *Cellular and Molecular Life Sciences: CMLS* 65 (3): 395–413. https://doi.org/10.1007/s00018-007-7360-z.
30. Bekku, Yoko, and Toshitaka Oohashi. 2010. 'Neurocan Contributes to the Molecular Heterogeneity of the Perinodal ECM'. *Archives of Histology and Cytology* 73 (2): 95–102. https://doi.org/10.1679/aohc.73.95.
31. Bekku, Yoko, Wei-Dong Su, Satoshi Hirakawa, Reinhard Fässler, Aiji Ohtsuka, Jeong Suk Kang, Jennifer Sanders, Takuro Murakami, Yoshifumi Ninomiya, and Toshitaka Oohashi. 2003. 'Molecular Cloning of Bral2, a Novel Brain-Specific Link Protein, and Immunohistochemical Colocalization with Brevican in Perineuronal Nets'. *Molecular and Cellular Neurosciences* 24 (1): 148–59. https://doi.org/10.1016/s1044-7431(03)00133-7.
32. Bendotti, C., M. Pende, and R. Samanin. 1994. 'Expression of GAP-43 in the Granule Cells of Rat Hippocampus after Seizure-Induced Sprouting of Mossy Fibres: In Situ Hybridization and Immunocytochemical Studies'. *The European Journal of Neuroscience* 6 (4): 509–15. https://doi.org/10.1111/j.1460-9568.1994.tb00294.x.
33. Bendotti, C., A. Servadio, and R. Samanin. 1991. 'Distribution of GAP-43 mRNA in the Brain Stem of Adult Rats as Evidenced by in Situ Hybridization: Localization within Monoaminergic Neurons'. *The Journal of Neuroscience: The Official Journal of the Society for Neuroscience* 11 (3): 600–607. https://doi.org/10.1523/JNEUROSCI.11-03-00600.1991.
34. Bennett, D. J., M. Gorassini, K. Fouad, L. Sanelli, Y. Han, and J. Cheng. 1999. 'Spasticity in Rats with Sacral Spinal Cord Injury'. *Journal of Neurotrauma* 16 (1): 69–84. https://doi.org/10.1089/neu.1999.16.69.
35. Bennett, D. J., L. Sanelli, C. L. Cooke, P. J. Harvey, and M. A. Gorassini. 2004. 'Spastic Long-Lasting Reflexes in the Awake Rat after Sacral Spinal Cord Injury'. *Journal of Neurophysiology* 91 (5): 2247–58. https://doi.org/10.1152/jn.00946.2003.
36. Berns, K. I., and R. A. Bohenzky. 1987. 'Adeno-Associated Viruses: An Update'. *Advances in Virus Research* 32: 243–306. https://doi.org/10.1016/s0065-3527(08)60479-0.
37. Blesch, Armin, and Mark H. Tuszynski. 2009. 'Spinal Cord Injury: Plasticity, Regeneration and the Challenge of Translational Drug Development'. *Trends in Neurosciences* 32 (1): 41–47. https://doi.org/10.1016/j.tins.2008.09.008.

38. Bo, Xuenong, Dongsheng Wu, John Yeh, and Yi Zhang. 2011. 'Gene Therapy Approaches for Neuroprotection and Axonal Regeneration after Spinal Cord and Spinal Root Injury'. *Current Gene Therapy* 11 (2): 101–15. https://doi.org/10.2174/156652311794940773.
39. Bojovic, Ognjen, Clive R. Bramham, and Arne Tjølsen. 2016. 'Stimulation-Induced Expression of Immediate Early Gene Proteins in the Dorsal Horn Is Increased in Neuropathy'. *Scandinavian Journal of Pain* 10 (January): 43–51. https://doi.org/10.1016/j.sjpain.2015.09.002.
40. Bourguignon, L. Y., H. Zhu, A. Chu, N. Iida, L. Zhang, and M. C. Hung. 1997. 'Interaction between the Adhesion Receptor, CD44, and the Oncogene Product, p185HER2, Promotes Human Ovarian Tumor Cell Activation'. *The Journal of Biological Chemistry* 272 (44): 27913–18. https://doi.org/10.1074/jbc.272.44.27913.
41. Bradbury, Elizabeth J., and Emily R. Burnside. 2019. 'Moving beyond the Glial Scar for Spinal Cord Repair'. *Nature Communications* 10 (1): 3879. https://doi.org/10.1038/s41467-019-11707-7.
42. Bradbury, Elizabeth J., and Lucy M. Carter. 2011. 'Manipulating the Glial Scar: Chondroitinase ABC as a Therapy for Spinal Cord Injury'. *Brain Research Bulletin* 84 (4–5): 306–16. https://doi.org/10.1016/j.brainresbull.2010.06.015.
43. Bradbury, Elizabeth J., Lawrence D. F. Moon, Reena J. Popat, Von R. King, Gavin S. Bennett, Preena N. Patel, James W. Fawcett, and Stephen B. McMahon. 2002. 'Chondroitinase ABC Promotes Functional Recovery after Spinal Cord Injury'. *Nature* 416 (6881): 636–40. https://doi.org/10.1038/416636a.
44. Bradke, Frank, James W. Fawcett, and Micha E. Spira. 2012. 'Assembly of a New Growth Cone after Axotomy: The Precursor to Axon Regeneration'. *Nature Reviews. Neuroscience* 13 (3): 183–93. https://doi.org/10.1038/nrn3176.
45. Brückner, G., K. Brauer, W. Härtig, J. R. Wolff, M. J. Rickmann, A. Derouiche, B. Delpech, N. Girard, W. H. Oertel, and A. Reichenbach. 1993. 'Perineuronal Nets Provide a Polyanionic, Glia-Associated Form of Microenvironment around Certain Neurons in Many Parts of the Rat Brain'. *Glia* 8 (3): 183–200. https://doi.org/10.1002/glia.440080306.
46. Brückner, G., W. Härtig, J. Kacza, J. Seeger, K. Welt, and K. Brauer. 1996. 'Extracellular Matrix Organization in Various Regions of Rat Brain Grey Matter'. *Journal of Neurocytology* 25 (5): 333–46. https://doi.org/10.1007/BF02284806.

47. Brückner, G., G. Seeger, K. Brauer, W. Härtig, J. Kacza, and V. Bigl. 1994. 'Cortical Areas Are Revealed by Distribution Patterns of Proteoglycan Components and Parvalbumin in the Mongolian Gerbil and Rat'. *Brain Research* 658 (1–2): 67–86. https://doi.org/10.1016/s0006-8993(09)90012-9.
48. Bu, J., N. Akhtar, and A. Nishiyama. 2001. 'Transient Expression of the NG2 Proteoglycan by a Subpopulation of Activated Macrophages in an Excitotoxic Hippocampal Lesion'. *Glia* 34 (4): 296–310. https://doi.org/10.1002/glia.1063.
49. Bukhari, Noreen, Luisa Torres, John K. Robinson, and Stella E. Tsirka. 2011. 'Axonal Regrowth after Spinal Cord Injury via Chondroitinase and the Tissue Plasminogen Activator (tPA)/Plasmin System'. *The Journal of Neuroscience: The Official Journal of the Society for Neuroscience* 31 (42): 14931–43. https://doi.org/10.1523/JNEUROSCI.3339-11.2011.
50. Burnside, E. R., and E. J. Bradbury. 2014. 'Manipulating the Extracellular Matrix and Its Role in Brain and Spinal Cord Plasticity and Repair'. *Neuropathology and Applied Neurobiology* 40 (1): 26–59. https://doi.org/10.1111/nan.12114.
51. Buss, A., G. A. Brook, B. Kakulas, D. Martin, R. Franzen, J. Schoenen, J. Noth, and A. B. Schmitt. 2004. 'Gradual Loss of Myelin and Formation of an Astrocytic Scar during Wallerian Degeneration in the Human Spinal Cord'. *Brain: A Journal of Neurology* 127 (Pt 1): 34–44. https://doi.org/10.1093/brain/awh001.
52. Buss, Armin, Katrin Pech, Byron A. Kakulas, Didier Martin, Jean Schoenen, Johannes Noth, and Gary A. Brook. 2007. 'Growth-Modulating Molecules Are Associated with Invading Schwann Cells and Not Astrocytes in Human Traumatic Spinal Cord Injury'. *Brain: A Journal of Neurology* 130 (Pt 4): 940–53. https://doi.org/10.1093/brain/awl374.
53. Button, Duane C., Jayne M. Kalmar, Kalan Gardiner, Tanguy Marqueste, Hui Zhong, Roland R. Roy, V. Reggie Edgerton, and Phillip F. Gardiner. 2008. 'Does Elimination of Afferent Input Modify the Changes in Rat Motoneurone Properties That Occur Following Chronic Spinal Cord Transection?' *The Journal of Physiology* 586 (2): 529–44. https://doi.org/10.1113/jphysiol.2007.141499.
54. Camarri, E., and G. Marchettini. 1988. '[Hymecromone in the treatment of symptoms following surgery of the bile ducts]'. *Recenti Progressi in Medicina* 79 (5): 198–202.
55. Cappella, Marisa, Chiara Ciotti, Mathilde Cohen-Tannoudji, and Maria Grazia Biferi. 2019. 'Gene Therapy for ALS-A Perspective'. *International Journal of Molecular Sciences* 20 (18). https://doi.org/10.3390/ijms20184388.

56. Carulli, Daniela, Tommaso Pizzorusso, Jessica C. F. Kwok, Elena Putignano, Andrea Poli, Serhiy Forostyak, Melissa R. Andrews, Sathyaseelan S. Deepa, Tibor T. Glant, and James W. Fawcett. 2010. 'Animals Lacking Link Protein Have Attenuated Perineuronal Nets and Persistent Plasticity'. *Brain: A Journal of Neurology* 133 (Pt 8): 2331–47. https://doi.org/10.1093/brain/awq145.
57. Carulli, Daniela, Kate E. Rhodes, and James W. Fawcett. 2007. 'Upregulation of Aggrecan, Link Protein 1, and Hyaluronan Synthases during Formation of Perineuronal Nets in the Rat Cerebellum'. *The Journal of Comparative Neurology* 501 (1): 83–94. https://doi.org/10.1002/cne.21231.
58. Caswell, Patrick, and Jim Norman. 2008. 'Endocytic Transport of Integrins during Cell Migration and Invasion'. *Trends in Cell Biology* 18 (6): 257–63. https://doi.org/10.1016/j.tcb.2008.03.004.
59. Caswell, Patrick T., and Jim C. Norman. 2006. 'Integrin Trafficking and the Control of Cell Migration'. *Traffic (Copenhagen, Denmark)* 7 (1): 14–21. https://doi.org/10.1111/j.1600-0854.2005.00362.x.
60. Celio, M. R., R. Spreafico, S. De Biasi, and L. Vitellaro-Zuccarello. 1998. 'Perineuronal Nets: Past and Present'. *Trends in Neurosciences* 21 (12): 510–15. https://doi.org/10.1016/s0166-2236(98)01298-3.
61. Chandran, Vijayendran, Giovanni Coppola, Homaira Nawabi, Takao Omura, Revital Versano, Eric A. Huebner, Alice Zhang, et al. 2016. 'A Systems-Level Analysis of the Peripheral Nerve Intrinsic Axonal Growth Program'. *Neuron* 89 (5): 956–70. https://doi.org/10.1016/j.neuron.2016.01.034.
62. Cheah, Menghon, Melissa R. Andrews, Daniel J. Chew, Elizabeth B. Moloney, Joost Verhaagen, Reinhard Fässler, and James W. Fawcett. 2016a. 'Expression of an Activated Integrin Promotes Long-Distance Sensory Axon Regeneration in the Spinal Cord'. *The Journal of Neuroscience: The Official Journal of the Society for Neuroscience* 36 (27): 7283–97. https://doi.org/10.1523/JNEUROSCI.0901-16.2016.
63. Cheah, Menghon, Yuyan Cheng, Veselina Petrova, Anda Cimpean, Pavla Jendelova, Vivek Swarup, Clifford J. Woolf, Daniel H. Geschwind, and James W. Fawcett. 2023. 'Integrin-Driven Axon Regeneration in the Spinal Cord Activates a Distinctive CNS Regeneration Program'. *The Journal of Neuroscience: The Official Journal of the Society for Neuroscience* 43 (26): 4775–94. https://doi.org/10.1523/JNEUROSCI.2076-22.2023.

64. Chen, Bo, Yi Li, Bin Yu, Zicong Zhang, Benedikt Brommer, Philip Raymond Williams, Yuanyuan Liu, et al. 2018. 'Reactivation of Dormant Relay Pathways in Injured Spinal Cord by KCC2 Manipulations'. *Cell* 174 (3): 521-535.e13. https://doi.org/10.1016/j.cell.2018.06.005.
65. Chen, Linlin, Huidan Deng, Hengmin Cui, Jing Fang, Zhicai Zuo, Junliang Deng, Yinglun Li, Xun Wang, and Ling Zhao. 2018. 'Inflammatory Responses and Inflammation-Associated Diseases in Organs'. *Oncotarget* 9 (6): 7204–18. https://doi.org/10.18632/oncotarget.23208.
66. Chen, M. S., A. B. Huber, M. E. van der Haar, M. Frank, L. Schnell, A. A. Spillmann, F. Christ, and M. E. Schwab. 2000. 'Nogo-A Is a Myelin-Associated Neurite Outgrowth Inhibitor and an Antigen for Monoclonal Antibody IN-1'. *Nature* 403 (6768): 434–39. https://doi.org/10.1038/35000219.
67. Chen, Zhenya, Ye Li, and Qipeng Yuan. 2015. 'Expression, Purification and Thermostability of MBP-Chondroitinase ABC I from Proteus Vulgaris'. *International Journal of Biological Macromolecules* 72 (January): 6–10. https://doi.org/10.1016/j.ijbiomac.2014.07.040.
68. Chen, Zhi Jiang, Micheal Negra, Angela Levine, Yvonne Ughrin, and Joel M. Levine. 2002. 'Oligodendrocyte Precursor Cells: Reactive Cells That Inhibit Axon Growth and Regeneration'. *Journal of Neurocytology* 31 (6–7): 481–95. https://doi.org/10.1023/a:1025791614468.
69. Chew, Daniel J., James W. Fawcett, and Melissa R. Andrews. 2012. 'The Challenges of Long-Distance Axon Regeneration in the Injured CNS'. *Progress in Brain Research* 201: 253–94. https://doi.org/10.1016/B978-0-444-59544-7.00013-5.
70. Chiquet-Ehrismann, Ruth. 2004. 'Tenascins'. *The International Journal of Biochemistry & Cell Biology* 36 (6): 986–90. https://doi.org/10.1016/j.biocel.2003.12.002.
71. Cho, Yongcheol, Roman Sloutsky, Kristen M. Naegle, and Valeria Cavalli. 2013. 'Injury-Induced HDAC5 Nuclear Export Is Essential for Axon Regeneration'. *Cell* 155 (4): 894–908. https://doi.org/10.1016/j.cell.2013.10.004.
72. Choi, Vivian W., Douglas M. McCarty, and R. Jude Samulski. 2006. 'Host Cell DNA Repair Pathways in Adeno-Associated Viral Genome Processing'. *Journal of Virology* 80 (21): 10346–56. https://doi.org/10.1128/JVI.00841-06.
73. Colombaro, Vanessa, Anne-Emilie Declèves, Inès Jadot, Virginie Voisin, Laetitia Giordano, Isabelle Habsch, Denis Nonclercq, Bruno Flamion, and Nathalie Caron.

2013. ‘Inhibition of Hyaluronan Is Protective against Renal Ischaemia-Reperfusion Injury’. *Nephrology, Dialysis, Transplantation: Official Publication of the European Dialysis and Transplant Association - European Renal Association* 28 (10): 2484–93. https://doi.org/10.1093/ndt/gft314.

74. Côté, Marie-Pascale, Gregory A. Azzam, Michel A. Lemay, Victoria Zhukareva, and John D. Houlé. 2011. ‘Activity-Dependent Increase in Neurotrophic Factors Is Associated with an Enhanced Modulation of Spinal Reflexes after Spinal Cord Injury’. *Journal of Neurotrauma* 28 (2): 299–309. https://doi.org/10.1089/neu.2010.1594.
75. Courtine, Grégoire, Yury Gerasimenko, Rubia van den Brand, Aileen Yew, Pavel Musienko, Hui Zhong, Bingbing Song, et al. 2009. ‘Transformation of Nonfunctional Spinal Circuits into Functional States after the Loss of Brain Input’. *Nature Neuroscience* 12 (10): 1333–42. https://doi.org/10.1038/nn.2401.
76. Courtine, Gregoire, Bingbing Song, Roland R. Roy, Hui Zhong, Julia E. Herrmann, Yan Ao, Jingwei Qi, V. Reggie Edgerton, and Michael V. Sofroniew. 2008. ‘Recovery of Supraspinal Control of Stepping via Indirect Propriospinal Relay Connections after Spinal Cord Injury’. *Nature Medicine* 14 (1): 69–74. https://doi.org/10.1038/nm1682.
77. Couto, Márcia R., Joana L. Rodrigues, and Lígia R. Rodrigues. 2022. ‘Heterologous Production of Chondroitin’. *Biotechnology Reports (Amsterdam, Netherlands)* 33 (March): e00710. https://doi.org/10.1016/j.btre.2022.e00710.
78. Curt, Armin, Hubertus J. A. Van Hedel, Daniel Klaus, Volker Dietz, and EM-SCI Study Group. 2008. ‘Recovery from a Spinal Cord Injury: Significance of Compensation, Neural Plasticity, and Repair’. *Journal of Neurotrauma* 25 (6): 677–85. https://doi.org/10.1089/neu.2007.0468.
79. Czogalla, A., and A. F. Sikorski. 2005. ‘Spectrin and Calpain: A “target” and a “Sniper” in the Pathology of Neuronal Cells’. *Cellular and Molecular Life Sciences: CMLS* 62 (17): 1913–24. https://doi.org/10.1007/s00018-005-5097-0.
80. Dalkilic, Turker, Nader Fallah, Vanessa K. Noonan, Sanam Salimi Elizei, Kevin Dong, Lise Belanger, Leanna Ritchie, et al. 2018. ‘Predicting Injury Severity and Neurological Recovery after Acute Cervical Spinal Cord Injury: A Comparison of Cerebrospinal Fluid and Magnetic Resonance Imaging Biomarkers’. *Journal of Neurotrauma* 35 (3): 435–45. https://doi.org/10.1089/neu.2017.5357.

81. Danen, Erik H. J., and Arnoud Sonnenberg. 2003. ‘Integrins in Regulation of Tissue Development and Function’. *The Journal of Pathology* 201 (4): 632–41. https://doi.org/10.1002/path.1472.
82. Davalos, Dimitrios, Jaime Grutzendler, Guang Yang, Jiyun V. Kim, Yi Zuo, Steffen Jung, Dan R. Littman, Michael L. Dustin, and Wen-Biao Gan. 2005. ‘ATP Mediates Rapid Microglial Response to Local Brain Injury in Vivo’. *Nature Neuroscience* 8 (6): 752–58. https://doi.org/10.1038/nn1472.
83. David, Stefan, and James P. Hamilton. 2010. ‘Drug-Induced Liver Injury’. *US Gastroenterology & Hepatology Review* 6 (January): 73–80.
84. Day, Joanna M., Anders I. Olin, Alan D. Murdoch, Ann Canfield, Takako Sasaki, Rupert Timpl, Timothy E. Hardingham, and Anders Aspberg. 2004. ‘Alternative Splicing in the Aggrecan G3 Domain Influences Binding Interactions with Tenascin-C and Other Extracellular Matrix Proteins’. *The Journal of Biological Chemistry* 279 (13): 12511–18. https://doi.org/10.1074/jbc.M400242200.
85. Deepa, Sarama S, Shuhei Yamada, Shigeyuki Fukui, and Kazuyuki Sugahara. 2007. ‘Structural Determination of Novel Sulfated Octasaccharides Isolated from Chondroitin Sulfate of Shark Cartilage and Their Application for Characterizing Monoclonal Antibody Epitopes’. *Glycobiology* 17 (6): 631–45. https://doi.org/10.1093/glycob/cwm021.
86. Deepa, Sarama Sathyaseelan, Daniela Carulli, Clare Galtrey, Kate Rhodes, Junko Fukuda, Tadahisa Mikami, Kazuyuki Sugahara, and James W. Fawcett. 2006. ‘Composition of Perineuronal Net Extracellular Matrix in Rat Brain: A Different Disaccharide Composition for the Net-Associated Proteoglycans’. *The Journal of Biological Chemistry* 281 (26): 17789–800. https://doi.org/10.1074/jbc.M600544200.
87. Dickendesher, Travis L., Katherine T. Baldwin, Yevgeniya A. Mironova, Yoshiki Koriyama, Stephen J. Raiker, Kim L. Askew, Andrew Wood, et al. 2012. ‘NgR1 and NgR3 Are Receptors for Chondroitin Sulfate Proteoglycans’. *Nature Neuroscience* 15 (5): 703–12. https://doi.org/10.1038/nn.3070.
88. Dicker, Kevin T., Lisa A. Gurski, Swati Pradhan-Bhatt, Robert L. Witt, Mary C. Farach-Carson, and Xinqiao Jia. 2014. ‘Hyaluronan: A Simple Polysaccharide with Diverse Biological Functions’. *Acta Biomaterialia* 10 (4): 1558–70. https://doi.org/10.1016/j.actbio.2013.12.019.

89. Dill, John, Hongyu Wang, Fengquan Zhou, and Shuxin Li. 2008. 'Inactivation of Glycogen Synthase Kinase 3 Promotes Axonal Growth and Recovery in the CNS'. *The Journal of Neuroscience: The Official Journal of the Society for Neuroscience* 28 (36): 8914–28. https://doi.org/10.1523/JNEUROSCI.1178-08.2008.
90. Ditor, David S., Sunil M. John, Josee Roy, Jeffrey C. Marx, Colin Kittmer, and Lynne C. Weaver. 2007. 'Effects of Polyethylene Glycol and Magnesium Sulfate Administration on Clinically Relevant Neurological Outcomes after Spinal Cord Injury in the Rat'. *Journal of Neuroscience Research* 85 (7): 1458–67. https://doi.org/10.1002/jnr.21283.
91. Donnelly, Christopher J., Michael Park, Mirela Spillane, Soonmoon Yoo, Almudena Pacheco, Cynthia Gomes, Deepika Vuppalanchi, et al. 2013. 'Axonally Synthesized β-Actin and GAP-43 Proteins Support Distinct Modes of Axonal Growth'. *The Journal of Neuroscience: The Official Journal of the Society for Neuroscience* 33 (8): 3311–22. https://doi.org/10.1523/JNEUROSCI.1722-12.2013.
92. Donnelly, Dustin J., and Phillip G. Popovich. 2008. 'Inflammation and Its Role in Neuroprotection, Axonal Regeneration and Functional Recovery after Spinal Cord Injury'. *Experimental Neurology* 209 (2): 378–88. https://doi.org/10.1016/j.expneurol.2007.06.009.
93. Donovan, Stacy L., Laura A. Mamounas, Anne M. Andrews, Mary E. Blue, and James S. McCasland. 2002. 'GAP-43 Is Critical for Normal Development of the Serotonergic Innervation in Forebrain'. *The Journal of Neuroscience: The Official Journal of the Society for Neuroscience* 22 (9): 3543–52. https://doi.org/10.1523/JNEUROSCI.22-09-03543.2002.
94. Dours-Zimmermann, María T., Konrad Maurer, Uwe Rauch, Wilhelm Stoffel, Reinhard Fässler, and Dieter R. Zimmermann. 2009. 'Versican V2 Assembles the Extracellular Matrix Surrounding the Nodes of Ranvier in the CNS'. *The Journal of Neuroscience: The Official Journal of the Society for Neuroscience* 29 (24): 7731–42. https://doi.org/10.1523/JNEUROSCI.4158-08.2009.
95. Drózdz, M., B. Kula, M. Wardas, and L. Weglarz. 1988. 'Hyaluronic Acid Content and Hyaluronidase Activity in Liver and Spleen of Rats with Hydralazine-Induced Collagen-like Syndrome'. *Biomedica Biochimica Acta* 47 (3): 247–50.
96. Dubisova, Jana, Jana Svobodova Burianova, Lucie Svobodova, Pavol Makovicky, Noelia Martinez-Varea, Anda Cimpean, James W. Fawcett, Jessica C. F. Kwok, and Sarka Kubinova. 2022. 'Oral Treatment of 4-Methylumbelliferone Reduced

Perineuronal Nets and Improved Recognition Memory in Mice'. *Brain Research Bulletin* 181 (April): 144–56. https://doi.org/10.1016/j.brainresbull.2022.01.011.

97. Dufour, Brett D., Catherine A. Smith, Randall L. Clark, Timothy R. Walker, and Jodi L. McBride. 2014. 'Intrajugular Vein Delivery of AAV9-RNAi Prevents Neuropathological Changes and Weight Loss in Huntington's Disease Mice'. *Molecular Therapy: The Journal of the American Society of Gene Therapy* 22 (4): 797–810. https://doi.org/10.1038/mt.2013.289.
98. Dufour, D. R., J. A. Lott, F. S. Nolte, D. R. Gretch, R. S. Koff, and L. B. Seeff. 2000. 'Diagnosis and Monitoring of Hepatic Injury. II. Recommendations for Use of Laboratory Tests in Screening, Diagnosis, and Monitoring'. *Clinical Chemistry* 46 (12): 2050–68. https://doi.org/10.1093/clinchem/46.12.2050.
99. Duncan, Greg J., Sohrab B. Manesh, Brett J. Hilton, Peggy Assinck, Jason R. Plemel, and Wolfram Tetzlaff. 2020. 'The Fate and Function of Oligodendrocyte Progenitor Cells after Traumatic Spinal Cord Injury'. *Glia* 68 (2): 227–45. https://doi.org/10.1002/glia.23706.
100. Durbeej, Madeleine. 2010. 'Laminins'. *Cell and Tissue Research* 339 (1): 259–68. https://doi.org/10.1007/s00441-009-0838-2.
101. Edgerton, V. Reggie, Niranjala J. K. Tillakaratne, Allison J. Bigbee, Ray D. de Leon, and Roland R. Roy. 2004. 'Plasticity of the Spinal Neural Circuitry after Injury'. *Annual Review of Neuroscience* 27: 145–67. https://doi.org/10.1146/annurev.neuro.27.070203.144308.
102. Ertürk, Ali, Farida Hellal, Joana Enes, and Frank Bradke. 2007. 'Disorganized Microtubules Underlie the Formation of Retraction Bulbs and the Failure of Axonal Regeneration'. *The Journal of Neuroscience: The Official Journal of the Society for Neuroscience* 27 (34): 9169–80. https://doi.org/10.1523/JNEUROSCI.0612-07.2007.
103. Eva, Richard, Melissa R. Andrews, Elske H. P. Franssen, and James W. Fawcett. 2012. 'Intrinsic Mechanisms Regulating Axon Regeneration: An Integrin Perspective'. *International Review of Neurobiology* 106: 75–104. https://doi.org/10.1016/B978-0-12-407178-0.00004-1.
104. Eva, Richard, and James Fawcett. 2014. 'Integrin Signalling and Traffic during Axon Growth and Regeneration'. *Current Opinion in Neurobiology* 27 (August): 179–85. https://doi.org/10.1016/j.conb.2014.03.018.

105. Fagoe, Nitish D., Jessica van Heest, and Joost Verhaagen. 2014. 'Spinal Cord Injury and the Neuron-Intrinsic Regeneration-Associated Gene Program'. *Neuromolecular Medicine* 16 (4): 799–813. https://doi.org/10.1007/s12017-014-8329-3.

106. Farage, Miranda A., Kenneth W. Miller, and Howard Ira Maibach. 2017. *Textbook of Aging Skin*. 2nd ed. Berlin: Springer.

107. Fawcett, J. W. 2017. 'An Integrin Approach to Axon Regeneration'. *Eye (London, England)* 31 (2): 206–8. https://doi.org/10.1038/eye.2016.293.

108. Fawcett, J. W., A. Curt, J. D. Steeves, W. P. Coleman, M. H. Tuszynski, D. Lammertse, P. F. Bartlett, et al. 2007. 'Guidelines for the Conduct of Clinical Trials for Spinal Cord Injury as Developed by the ICCP Panel: Spontaneous Recovery after Spinal Cord Injury and Statistical Power Needed for Therapeutic Clinical Trials'. *Spinal Cord* 45 (3): 190–205. https://doi.org/10.1038/sj.sc.3102007.

109. Fawcett, James W. 2020. 'The Struggle to Make CNS Axons Regenerate: Why Has It Been so Difficult?' *Neurochemical Research* 45 (1): 144–58. https://doi.org/10.1007/s11064-019-02844-y.

110. Fawcett, James W, and Richard. A Asher. 1999. 'The Glial Scar and Central Nervous System Repair'. *Brain Research Bulletin* 49 (6): 377–91. https://doi.org/10.1016/S0361-9230(99)00072-6.

111. Fawcett, James W., and Armin Curt. 2009. 'Damage Control in the Nervous System: Rehabilitation in a Plastic Environment'. *Nature Medicine* 15 (7): 735–36. https://doi.org/10.1038/nm0709-735.

112. Fawcett, James W., Martin E. Schwab, Laura Montani, Nicole Brazda, and Hans Werner Müller. 2012. 'Defeating Inhibition of Regeneration by Scar and Myelin Components'. *Handbook of Clinical Neurology* 109: 503–22. https://doi.org/10.1016/B978-0-444-52137-8.00031-0.

113. Fawcett, James W., and Joost Verhaagen. 2018. 'Intrinsic Determinants of Axon Regeneration'. *Developmental Neurobiology* 78 (10): 890–97. https://doi.org/10.1002/dneu.22637.

114. Feldblum, S., S. Arnaud, M. Simon, O. Rabin, and P. D'Arbigny. 2000. 'Efficacy of a New Neuroprotective Agent, Gacyclidine, in a Model of Rat Spinal Cord Injury'. *Journal of Neurotrauma* 17 (11): 1079–93. https://doi.org/10.1089/neu.2000.17.1079.

115. Fenderson, B. A., I. Stamenkovic, and A. Aruffo. 1993. 'Localization of Hyaluronan in Mouse Embryos during Implantation, Gastrulation and Organogenesis'. *Differentiation; Research in Biological Diversity* 54 (2): 85–98. https://doi.org/10.1111/j.1432-0436.1993.tb00711.x.

116. Filous, Angela R., and Jan M. Schwab. 2018. 'Determinants of Axon Growth, Plasticity, and Regeneration in the Context of Spinal Cord Injury'. *The American Journal of Pathology* 188 (1): 53–62. https://doi.org/10.1016/j.ajpath.2017.09.005.

117. Fischell, Jonathan M., and Paul S. Fishman. 2021. 'A Multifaceted Approach to Optimizing AAV Delivery to the Brain for the Treatment of Neurodegenerative Diseases'. *Frontiers in Neuroscience* 15: 747726. https://doi.org/10.3389/fnins.2021.747726.

118. Fisher, Daniel, Bin Xing, John Dill, Hui Li, Hai Hiep Hoang, Zhenze Zhao, Xiao-Li Yang, et al. 2011. 'Leukocyte Common Antigen-Related Phosphatase Is a Functional Receptor for Chondroitin Sulfate Proteoglycan Axon Growth Inhibitors'. *The Journal of Neuroscience: The Official Journal of the Society for Neuroscience* 31 (40): 14051–66. https://doi.org/10.1523/JNEUROSCI.1737-11.2011.

119. Fitch, Michael T., and Jerry Silver. 2008. 'CNS Injury, Glial Scars, and Inflammation: Inhibitory Extracellular Matrices and Regeneration Failure'. *Experimental Neurology* 209 (2): 294–301. https://doi.org/10.1016/j.expneurol.2007.05.014.

120. Franssen, Elske H. P., Rong-Rong Zhao, Hiroaki Koseki, Venkateswarlu Kanamarlapudi, Casper C. Hoogenraad, Richard Eva, and James W. Fawcett. 2015. 'Exclusion of Integrins from CNS Axons Is Regulated by Arf6 Activation and the AIS'. *The Journal of Neuroscience: The Official Journal of the Society for Neuroscience* 35 (21): 8359–75. https://doi.org/10.1523/JNEUROSCI.2850-14.2015.

121. Franz, Steffen, Norbert Weidner, and Armin Blesch. 2012. 'Gene Therapy Approaches to Enhancing Plasticity and Regeneration after Spinal Cord Injury'. *Experimental Neurology* 235 (1): 62–69. https://doi.org/10.1016/j.expneurol.2011.01.015.

122. Fraser, J. R., T. C. Laurent, and U. B. Laurent. 1997. 'Hyaluronan: Its Nature, Distribution, Functions and Turnover'. *Journal of Internal Medicine* 242 (1): 27–33. https://doi.org/10.1046/j.1365-2796.1997.00170.x.

123. Fry, Elizabeth J., Melanie J. Chagnon, Rubèn López-Vales, Michel L. Tremblay, and Samuel David. 2010. 'Corticospinal Tract Regeneration after Spinal Cord Injury in Receptor Protein Tyrosine Phosphatase Sigma Deficient Mice'. *Glia* 58 (4): 423–33. https://doi.org/10.1002/glia.20934.

124. Fukuchi, Ken-ichiro, Kazuki Tahara, Hong-Duck Kim, J. Adam Maxwell, Terry L. Lewis, Mary Ann Accavitti-Loper, Helen Kim, Selvarangan Ponnazhagan, and Robert Lalonde. 2006. 'Anti-Abeta Single-Chain Antibody Delivery via Adeno-Associated Virus for Treatment of Alzheimer's Disease'. *Neurobiology of Disease* 23 (3): 502–11. https://doi.org/10.1016/j.nbd.2006.04.012.

125. Galdi, Flavia, Claudio Pedone, Christopher A. McGee, Margaret George, Annette B. Rice, Shah S. Hussain, Kadambari Vijaykumar, et al. 2021. 'Inhaled High Molecular Weight Hyaluronan Ameliorates Respiratory Failure in Acute COPD Exacerbation: A Pilot Study'. *Respiratory Research* 22 (1): 30. https://doi.org/10.1186/s12931-020-01610-x.

126. Galgoczi, Erika, Florence Jeney, Monika Katko, Annamaria Erdei, Annamaria Gazdag, Livia Sira, Miklos Bodor, et al. 2020. 'Characteristics of Hyaluronan Synthesis Inhibition by 4-Methylumbelliferone in Orbital Fibroblasts'. *Investigative Ophthalmology & Visual Science* 61 (2): 27. https://doi.org/10.1167/iovs.61.2.27.

127. Galtrey, Clare M., Jessica C. F. Kwok, Daniela Carulli, Kate E. Rhodes, and James W. Fawcett. 2008. 'Distribution and Synthesis of Extracellular Matrix Proteoglycans, Hyaluronan, Link Proteins and Tenascin-R in the Rat Spinal Cord'. *The European Journal of Neuroscience* 27 (6): 1373–90. https://doi.org/10.1111/j.1460-9568.2008.06108.x.

128. García-Alías, Guillermo, Stanley Barkhuysen, Miranda Buckle, and James W. Fawcett. 2009. 'Chondroitinase ABC Treatment Opens a Window of Opportunity for Task-Specific Rehabilitation'. *Nature Neuroscience* 12 (9): 1145–51. https://doi.org/10.1038/nn.2377.

129. Gardiner, Natalie J. 2011. 'Integrins and the Extracellular Matrix: Key Mediators of Development and Regeneration of the Sensory Nervous System'. *Developmental Neurobiology* 71 (11): 1054–72. https://doi.org/10.1002/dneu.20950.

130. Garrett, E. R., J. Venitz, K. Eberst, and J. J. Cerda. 1993. 'Pharmacokinetics and Bioavailabilities of Hymecromone in Human Volunteers'. *Biopharmaceutics & Drug Disposition* 14 (1): 13–39. https://doi.org/10.1002/bdd.2510140103.

131. Geissler, Maren, Christine Gottschling, Ainhara Aguado, Uwe Rauch, Christian H. Wetzel, Hanns Hatt, and Andreas Faissner. 2013. 'Primary Hippocampal Neurons, Which Lack Four Crucial Extracellular Matrix Molecules, Display Abnormalities of Synaptic Structure and Function and Severe Deficits in Perineuronal Net Formation'. *The Journal of Neuroscience: The Official Journal of the Society for Neuroscience* 33 (18): 7742–55. https://doi.org/10.1523/JNEUROSCI.3275-12.2013.

132. Gelse, K., E. Pöschl, and T. Aigner. 2003. 'Collagens--Structure, Function, and Biosynthesis'. *Advanced Drug Delivery Reviews* 55 (12): 1531–46. https://doi.org/10.1016/j.addr.2003.08.002.

133. Ghorbani, Samira, and V. Wee Yong. 2021. 'The Extracellular Matrix as Modifier of Neuroinflammation and Remyelination in Multiple Sclerosis'. *Brain: A Journal of Neurology* 144 (7): 1958–73. https://doi.org/10.1093/brain/awab059.

134. Girish, K. S., and K. Kemparaju. 2007. 'The Magic Glue Hyaluronan and Its Eraser Hyaluronidase: A Biological Overview'. *Life Sciences* 80 (21): 1921–43. https://doi.org/10.1016/j.lfs.2007.02.037.

135. Gitler, D., and M. E. Spira. 1998. 'Real Time Imaging of Calcium-Induced Localized Proteolytic Activity after Axotomy and Its Relation to Growth Cone Formation'. *Neuron* 20 (6): 1123–35. https://doi.org/10.1016/s0896-6273(00)80494-8.

136. Gitler, Daniel, and Micha E. Spira. 2002. 'Short Window of Opportunity for Calpain Induced Growth Cone Formation after Axotomy of Aplysia Neurons'. *Journal of Neurobiology* 52 (4): 267–79. https://doi.org/10.1002/neu.10084.

137. Goldberg, Jeffrey L., Matthew P. Klassen, Ying Hua, and Ben A. Barres. 2002. 'Amacrine-Signaled Loss of Intrinsic Axon Growth Ability by Retinal Ganglion Cells'. *Science (New York, N.Y.)* 296 (5574): 1860–64. https://doi.org/10.1126/science.1068428.

138. Goncalves, Maria B., Tim Mant, Jörg Täubel, Earl Clarke, Hana Hassanin, Daryl Bendel, Henry Fok, et al. 2023. 'Phase 1 Safety, Tolerability, Pharmacokinetics and Pharmacodynamic Results of KCL-286, a Novel Retinoic Acid Receptor-β Agonist for Treatment of Spinal Cord Injury, in Male Healthy Participants'. *British Journal of Clinical Pharmacology* 89 (12): 3573–83. https://doi.org/10.1111/bcp.15854.

139. Goncharova, Valentina, Naira Serobyan, Shinji Iizuka, Ingrid Schraufstatter, Audrey de Ridder, Tatiana Povaliy, Valentina Wacker, et al. 2012. 'Hyaluronan Expressed by the Hematopoietic Microenvironment Is Required for Bone Marrow Hematopoiesis'. *The Journal of Biological Chemistry* 287 (30): 25419–33. https://doi.org/10.1074/jbc.M112.376699.

140. Göritz, Christian, David O. Dias, Nikolay Tomilin, Mariano Barbacid, Oleg Shupliakov, and Jonas Frisén. 2011. 'A Pericyte Origin of Spinal Cord Scar Tissue'. *Science (New York, N.Y.)* 333 (6039): 238–42. https://doi.org/10.1126/science.1203165.

141. GrandPré, T., F. Nakamura, T. Vartanian, and S. M. Strittmatter. 2000. 'Identification of the Nogo Inhibitor of Axon Regeneration as a Reticulon Protein'. *Nature* 403 (6768): 439–44. https://doi.org/10.1038/35000226.

142. GrandPré, Tadzia, Shuxin Li, and Stephen M. Strittmatter. 2002. 'Nogo-66 Receptor Antagonist Peptide Promotes Axonal Regeneration'. *Nature* 417 (6888): 547–51. https://doi.org/10.1038/417547a.

143. Griffin, Jarred M., and Frank Bradke. 2020. 'Therapeutic Repair for Spinal Cord Injury: Combinatory Approaches to Address a Multifaceted Problem'. *EMBO Molecular Medicine* 12 (3): e11505. https://doi.org/10.15252/emmm.201911505.

144. Guo, Wen, Xindan Zhang, Jiliang Zhai, and Jiajia Xue. 2022. 'The Roles and Applications of Neural Stem Cells in Spinal Cord Injury Repair'. *Frontiers in Bioengineering and Biotechnology* 10: 966866. https://doi.org/10.3389/fbioe.2022.966866.

145. Guo, Wenjun, and Filippo G. Giancotti. 2004. 'Integrin Signalling during Tumour Progression'. *Nature Reviews. Molecular Cell Biology* 5 (10): 816–26. https://doi.org/10.1038/nrm1490.

146. Gurtner, Geoffrey C., Sabine Werner, Yann Barrandon, and Michael T. Longaker. 2008. 'Wound Repair and Regeneration'. *Nature* 453 (7193): 314–21. https://doi.org/10.1038/nature07039.

147. Hammarberg, H., W. Wallquist, F. Piehl, M. Risling, and S. Cullheim. 2000. 'Regulation of Laminin-Associated Integrin Subunit mRNAs in Rat Spinal Motoneurons during Postnatal Development and after Axonal Injury'. *The Journal of Comparative Neurology* 428 (2): 294–304. https://doi.org/10.1002/1096-9861(20001211)428:2<294::aid-cne8>3.0.co;2-y.

148. Hampton, D. W., K. E. Rhodes, C. Zhao, R. J. M. Franklin, and J. W. Fawcett. 2004. 'The Responses of Oligodendrocyte Precursor Cells, Astrocytes and Microglia to a Cortical Stab Injury, in the Brain'. *Neuroscience* 127 (4): 813–20. https://doi.org/10.1016/j.neuroscience.2004.05.028.

149. Hansen, Janne Fuglsang, Karen Mølgaard Christiansen, Benjamin Staugaard, Belinda Klemmensen Moessner, Søren Lillevang, Aleksander Krag, and Peer Brehm Christensen. 2019. 'Combining Liver Stiffness with Hyaluronic Acid Provides Superior Prognostic Performance in Chronic Hepatitis C'. *PloS One* 14 (2): e0212036. https://doi.org/10.1371/journal.pone.0212036.

150. Hara, Hideo, Alon Monsonego, Katsutoshi Yuasa, Kayo Adachi, Xiao Xiao, Shin'ichi Takeda, Keikichi Takahashi, Howard L. Weiner, and Takeshi Tabira. 2004. 'Development of a Safe Oral Abeta Vaccine Using Recombinant Adeno-Associated Virus Vector for Alzheimer's Disease'. *Journal of Alzheimer's Disease: JAD* 6 (5): 483–88. https://doi.org/10.3233/jad-2004-6504.

151. Hardcastle, Nathan, Nicholas M. Boulis, and Thais Federici. 2018. 'AAV Gene Delivery to the Spinal Cord: Serotypes, Methods, Candidate Diseases, and Clinical Trials'. *Expert Opinion on Biological Therapy* 18 (3): 293–307. https://doi.org/10.1080/14712598.2018.1416089.

152. Harvey, Alan R., Ying Hu, Simone G. Leaver, Carla B. Mellough, Kevin Park, Joost Verhaagen, Giles W. Plant, and Qi Cui. 2006. 'Gene Therapy and Transplantation in CNS Repair: The Visual System'. *Progress in Retinal and Eye Research* 25 (5): 449–89. https://doi.org/10.1016/j.preteyeres.2006.07.002.

153. Harvey, P. J., Y. Li, X. Li, and D. J. Bennett. 2006. 'Persistent Sodium Currents and Repetitive Firing in Motoneurons of the Sacrocaudal Spinal Cord of Adult Rats'. *Journal of Neurophysiology* 96 (3): 1141–57. https://doi.org/10.1152/jn.00335.2005.

154. Hawthorne, Alicia L., Hongmei Hu, Bornali Kundu, Michael P. Steinmetz, Christi J. Wylie, Evan S. Deneris, and Jerry Silver. 2011. 'The Unusual Response of Serotonergic Neurons after CNS Injury: Lack of Axonal Dieback and Enhanced Sprouting within the Inhibitory Environment of the Glial Scar'. *The Journal of Neuroscience: The Official Journal of the Society for Neuroscience* 31 (15): 5605–16. https://doi.org/10.1523/JNEUROSCI.6663-10.2011.

155. Hayashi, Y., S. Jacob-Vadakot, E. A. Dugan, S. McBride, R. Olexa, K. Simansky, M. Murray, and J. S. Shumsky. 2010. '5-HT Precursor Loading, but Not

5-HT Receptor Agonists, Increases Motor Function after Spinal Cord Contusion in Adult Rats'. *Experimental Neurology* 221 (1): 68–78. https://doi.org/10.1016/j.expneurol.2009.10.003.

156. Hermanns, S., N. Klapka, and H. W. Müller. 2001. 'The Collagenous Lesion Scar--an Obstacle for Axonal Regeneration in Brain and Spinal Cord Injury'. *Restorative Neurology and Neuroscience* 19 (1–2): 139–48.

157. Hermens, W. T., O. ter Brake, P. A. Dijkhuizen, M. A. Sonnemans, D. Grimm, J. A. Kleinschmidt, and J. Verhaagen. 1999. 'Purification of Recombinant Adeno-Associated Virus by Iodixanol Gradient Ultracentrifugation Allows Rapid and Reproducible Preparation of Vector Stocks for Gene Transfer in the Nervous System'. *Human Gene Therapy* 10 (11): 1885–91. https://doi.org/10.1089/10430349950017563.

158. Hilton, Brett J., Eitan Anenberg, Thomas C. Harrison, Jamie D. Boyd, Timothy H. Murphy, and Wolfram Tetzlaff. 2016. 'Re-Establishment of Cortical Motor Output Maps and Spontaneous Functional Recovery via Spared Dorsolaterally Projecting Corticospinal Neurons after Dorsal Column Spinal Cord Injury in Adult Mice'. *The Journal of Neuroscience: The Official Journal of the Society for Neuroscience* 36 (14): 4080–92. https://doi.org/10.1523/JNEUROSCI.3386-15.2016.

159. Hilton, Brett J., Aaron J. Moulson, and Wolfram Tetzlaff. 2017. 'Neuroprotection and Secondary Damage Following Spinal Cord Injury: Concepts and Methods'. *Neuroscience Letters* 652 (June): 3–10. https://doi.org/10.1016/j.neulet.2016.12.004.

160. Hoffmann, R. M., G. Schwarz, C. Pohl, D. J. Ziegenhagen, and W. Kruis. 2005. '[Bile acid-independent effect of hymecromone on bile secretion and common bile duct motility]'. *Deutsche Medizinische Wochenschrift (1946)* 130 (34–35): 1938–43. https://doi.org/10.1055/s-2005-872606.

161. Hohenester, Erhard, and Peter D. Yurchenco. 2013. 'Laminins in Basement Membrane Assembly'. *Cell Adhesion & Migration* 7 (1): 56–63. https://doi.org/10.4161/cam.21831.

162. Horton, M. R., M. D. Burdick, R. M. Strieter, C. Bao, and P. W. Noble. 1998. 'Regulation of Hyaluronan-Induced Chemokine Gene Expression by IL-10 and IFN-Gamma in Mouse Macrophages'. *Journal of Immunology (Baltimore, Md.: 1950)* 160 (6): 3023–30.

163. Howell, M. D., and P. E. Gottschall. 2012. ‘Lectican Proteoglycans, Their Cleaving Metalloproteinases, and Plasticity in the Central Nervous System Extracellular Microenvironment’. *Neuroscience* 217 (August): 6–18. https://doi.org/10.1016/j.neuroscience.2012.05.034.

164. Høye, Anette M., John R. Couchman, Ulla M. Wewer, Kiyoko Fukami, and Atsuko Yoneda. 2012. ‘The Newcomer in the Integrin Family: Integrin A9 in Biology and Cancer’. *Advances in Biological Regulation* 52 (2): 326–39. https://doi.org/10.1016/j.jbior.2012.03.004.

165. Hu, Fenghua, and Stephen M. Strittmatter. 2008. ‘The N-Terminal Domain of Nogo-A Inhibits Cell Adhesion and Axonal Outgrowth by an Integrin-Specific Mechanism’. *Journal of Neuroscience* 28 (5): 1262–69. https://doi.org/10.1523/JNEUROSCI.1068-07.2008.

166. Hu, Rong, Jianjun Zhou, Chunxia Luo, Jiangkai Lin, Xianrong Wang, Xiaoguang Li, Xiuwu Bian, et al. 2010. ‘Glial Scar and Neuroregeneration: Histological, Functional, and Magnetic Resonance Imaging Analysis in Chronic Spinal Cord Injury’. *Journal of Neurosurgery. Spine* 13 (2): 169–80. https://doi.org/10.3171/2010.3.SPINE09190.

167. Hunter, Sandra K., Hugo M. Pereira, and Kevin G. Keenan. 2016. ‘The Aging Neuromuscular System and Motor Performance’. *Journal of Applied Physiology (Bethesda, Md.: 1985)* 121 (4): 982–95. https://doi.org/10.1152/japplphysiol.00475.2016.

168. Huttenlocher, Anna, and Alan Rick Horwitz. 2011. ‘Integrins in Cell Migration’. *Cold Spring Harbor Perspectives in Biology* 3 (9): a005074. https://doi.org/10.1101/cshperspect.a005074.

169. Hynes, Richard O. 2002. ‘Integrins: Bidirectional, Allosteric Signaling Machines’. *Cell* 110 (6): 673–87. https://doi.org/10.1016/s0092-8674(02)00971-6.

170. Ikpeze, Tochukwu C., and Addisu Mesfin. 2017. ‘Spinal Cord Injury in the Geriatric Population: Risk Factors, Treatment Options, and Long-Term Management’. *Geriatric Orthopaedic Surgery & Rehabilitation* 8 (2): 115–18. https://doi.org/10.1177/2151458517696680.

171. Ingham, Kenneth C., Shelesa A. Brew, and Harold P. Erickson. 2004. ‘Localization of a Cryptic Binding Site for Tenascin on Fibronectin’. *The Journal of Biological Chemistry* 279 (27): 28132–35. https://doi.org/10.1074/jbc.M312785200.

172. Iozzo, Renato V., and Liliana Schaefer. 2015. ‘Proteoglycan Form and Function: A Comprehensive Nomenclature of Proteoglycans’. *Matrix Biology: Journal of the International Society for Matrix Biology* 42 (March): 11–55. https://doi.org/10.1016/j.matbio.2015.02.003.

173. Irvine, K. A., and W. F. Blakemore. 2008. ‘Remyelination Protects Axons from Demyelination-Associated Axon Degeneration’. *Brain: A Journal of Neurology* 131 (Pt 6): 1464–77. https://doi.org/10.1093/brain/awn080.

174. Irvine, Sîan F., Sylvain Gigout, Kateřina Štěpánková, Noelia Martinez Varea, Lucia Machová Urdzíková, Pavla Jendelová, and Jessica C. F. Kwok. 2023. ‘4-Methylumbelliferone Enhances Neuroplasticity in the Central Nervous System: Potential Oral Treatment for SCI’. Preprint. Neuroscience. https://doi.org/10.1101/2023.01.23.525137.

175. Irvine, Sian F., and Jessica C. F. Kwok. 2018. ‘Perineuronal Nets in Spinal Motoneurones: Chondroitin Sulphate Proteoglycan around Alpha Motoneurones’. *International Journal of Molecular Sciences* 19 (4): 1172. https://doi.org/10.3390/ijms19041172.

176. Jacobs, Barry L., Francisco J. Martín-Cora, and Casimir A. Fornal. 2002. ‘Activity of Medullary Serotonergic Neurons in Freely Moving Animals’. *Brain Research. Brain Research Reviews* 40 (1–3): 45–52. https://doi.org/10.1016/s0165-0173(02)00187-x.

177. Jacobson, R. D., I. Virág, and J. H. Skene. 1986. ‘A Protein Associated with Axon Growth, GAP-43, Is Widely Distributed and Developmentally Regulated in Rat CNS’. *The Journal of Neuroscience: The Official Journal of the Society for Neuroscience* 6 (6): 1843–55. https://doi.org/10.1523/JNEUROSCI.06-06-01843.1986.

178. Jakovcevski, Igor, Djordje Miljkovic, Melitta Schachner, and Pavle R. Andjus. 2013. ‘Tenascins and Inflammation in Disorders of the Nervous System’. *Amino Acids* 44 (4): 1115–27. https://doi.org/10.1007/s00726-012-1446-0.

179. Jiang, Dianhua, Jiurong Liang, and Paul W. Noble. 2007. ‘Hyaluronan in Tissue Injury and Repair’. *Annual Review of Cell and Developmental Biology* 23: 435–61. https://doi.org/10.1146/annurev.cellbio.23.090506.123337.

180. John, Gareth R., Sunhee C. Lee, and Celia F. Brosnan. 2003. ‘Cytokines: Powerful Regulators of Glial Cell Activation’. *The Neuroscientist: A Review Journal*

Bringing Neurobiology, Neurology and Psychiatry 9 (1): 10–22. https://doi.org/10.1177/1073858402239587.

181. Jones, F. S., and P. L. Jones. 2000. 'The Tenascin Family of ECM Glycoproteins: Structure, Function, and Regulation during Embryonic Development and Tissue Remodeling'. *Developmental Dynamics: An Official Publication of the American Association of Anatomists* 218 (2): 235–59. https://doi.org/10.1002/(SICI)1097-0177(200006)218:2<235::AID-DVDY2>3.0.CO;2-G.

182. Jones, L. S. 1996. 'Integrins: Possible Functions in the Adult CNS'. *Trends in Neurosciences* 19 (2): 68–72. https://doi.org/10.1016/0166-2236(96)89623-8.

183. Jones, Leonard L., Richard U. Margolis, and Mark H. Tuszynski. 2003. 'The Chondroitin Sulfate Proteoglycans Neurocan, Brevican, Phosphacan, and Versican Are Differentially Regulated Following Spinal Cord Injury'. *Experimental Neurology* 182 (2): 399–411. https://doi.org/10.1016/s0014-4886(03)00087-6.

184. Jones, Leonard L., Yu Yamaguchi, William B. Stallcup, and Mark H. Tuszynski. 2002. 'NG2 Is a Major Chondroitin Sulfate Proteoglycan Produced after Spinal Cord Injury and Is Expressed by Macrophages and Oligodendrocyte Progenitors'. *The Journal of Neuroscience: The Official Journal of the Society for Neuroscience* 22 (7): 2792–2803. https://doi.org/10.1523/JNEUROSCI.22-07-02792.2002.

185. Jones, Matthew C., Patrick T. Caswell, and Jim C. Norman. 2006. 'Endocytic Recycling Pathways: Emerging Regulators of Cell Migration'. *Current Opinion in Cell Biology* 18 (5): 549–57. https://doi.org/10.1016/j.ceb.2006.08.003.

186. Jordan, Larry M., Jun Liu, Peter B. Hedlund, Turgay Akay, and Keir G. Pearson. 2008. 'Descending Command Systems for the Initiation of Locomotion in Mammals'. *Brain Research Reviews* 57 (1): 183–91. https://doi.org/10.1016/j.brainresrev.2007.07.019.

187. Kakehi, Kazuaki, Mitsuhiro Kinoshita, and Shin-ichi Yasueda. 2003. 'Hyaluronic Acid: Separation and Biological Implications'. *Journal of Chromatography. B, Analytical Technologies in the Biomedical and Life Sciences* 797 (1–2): 347–55. https://doi.org/10.1016/s1570-0232(03)00479-3.

188. Kakizaki, Ikuko, Kaoru Kojima, Keiichi Takagaki, Masahiko Endo, Reiji Kannagi, Masaki Ito, Yoshihiro Maruo, et al. 2004. 'A Novel Mechanism for the

Inhibition of Hyaluronan Biosynthesis by 4-Methylumbelliferone'. *The Journal of Biological Chemistry* 279 (32): 33281–89. https://doi.org/10.1074/jbc.M405918200.

189. Kamber, Dotan, Hadas Erez, and Micha E. Spira. 2009. 'Local Calcium-Dependent Mechanisms Determine Whether a Cut Axonal End Assembles a Retarded Endbulb or Competent Growth Cone'. *Experimental Neurology* 219 (1): 112–25. https://doi.org/10.1016/j.expneurol.2009.05.004.

190. Kanagal, Srikanth G., and Gillian D. Muir. 2009. 'Task-Dependent Compensation after Pyramidal Tract and Dorsolateral Spinal Lesions in Rats'. *Experimental Neurology* 216 (1): 193–206. https://doi.org/10.1016/j.expneurol.2008.11.028.

191. Karamanos, Nikos K., Achilleas D. Theocharis, Zoi Piperigkou, Dimitra Manou, Alberto Passi, Spyros S. Skandalis, Demitrios H. Vynios, et al. 2021. 'A Guide to the Composition and Functions of the Extracellular Matrix'. *The FEBS Journal* 288 (24): 6850–6912. https://doi.org/10.1111/febs.15776.

192. Karimi-Abdolrezaee, Soheila, and Eftekhar Eftekharpour. 2012. 'Stem Cells and Spinal Cord Injury Repair'. *Advances in Experimental Medicine and Biology* 760: 53–73. https://doi.org/10.1007/978-1-4614-4090-1_4.

193. Katarey, Dev, and Sumita Verma. 2016. 'Drug-Induced Liver Injury'. *Clinical Medicine (London, England)* 16 (Suppl 6): s104–9. https://doi.org/10.7861/clinmedicine.16-6-s104.

194. Kaul, Aditya, Kavya L. Singampalli, Umang M. Parikh, Ling Yu, Sundeep G. Keswani, and Xinyi Wang. 2022. 'Hyaluronan, a Double-Edged Sword in Kidney Diseases'. *Pediatric Nephrology (Berlin, Germany)* 37 (4): 735–44. https://doi.org/10.1007/s00467-021-05113-9.

195. Kaux, Jean-François, Antoine Samson, and Jean-Michel Crielaard. 2015. 'Hyaluronic Acid and Tendon Lesions'. *Muscles, Ligaments and Tendons Journal* 5 (4): 264–69. https://doi.org/10.11138/mltj/2015.5.4.264.

196. Keeler, Allison M., and Terence R. Flotte. 2019. 'Recombinant Adeno-Associated Virus Gene Therapy in Light of Luxturna (and Zolgensma and Glybera): Where Are We, and How Did We Get Here?' *Annual Review of Virology* 6 (1): 601–21. https://doi.org/10.1146/annurev-virology-092818-015530.

197. Keough, Michael B., James A. Rogers, Ping Zhang, Samuel K. Jensen, Erin L. Stephenson, Tieyu Chen, Mitchel G. Hurlbert, et al. 2016. 'An Inhibitor of Chondroitin Sulfate Proteoglycan Synthesis Promotes Central Nervous System

Remyelination'. *Nature Communications* 7 (April): 11312. https://doi.org/10.1038/ncomms11312.

198. Khan, Farihah Iqbal, and Zubair Ahmed. 2022. 'Experimental Treatments for Spinal Cord Injury: A Systematic Review and Meta-Analysis'. *Cells* 11 (21): 3409. https://doi.org/10.3390/cells11213409.

199. Kiani, Chris, Liwen Chen, Yao Jiong Wu, Albert J. Yee, and Burton B. Yang. 2002. 'Structure and Function of Aggrecan'. *Cell Research* 12 (1): 19–32. https://doi.org/10.1038/sj.cr.7290106.

200. King, Alice, Swathi Balaji, Louis D. Le, Timothy M. Crombleholme, and Sundeep G. Keswani. 2014. 'Regenerative Wound Healing: The Role of Interleukin-10'. *Advances in Wound Care* 3 (4): 315–23. https://doi.org/10.1089/wound.2013.0461.

201. Kjell, Jacob, and Lars Olson. 2016. 'Rat Models of Spinal Cord Injury: From Pathology to Potential Therapies'. *Disease Models & Mechanisms* 9 (10): 1125–37. https://doi.org/10.1242/dmm.025833.

202. Klapka, Nicole, Susanne Hermanns, Guido Straten, Carmen Masanneck, Simone Duis, Frank P. T. Hamers, Daniela Müller, Werner Zuschratter, and Hans Werner Müller. 2005. 'Suppression of Fibrous Scarring in Spinal Cord Injury of Rat Promotes Long-Distance Regeneration of Corticospinal Tract Axons, Rescue of Primary Motoneurons in Somatosensory Cortex and Significant Functional Recovery'. *The European Journal of Neuroscience* 22 (12): 3047–58. https://doi.org/10.1111/j.1460-9568.2005.04495.x.

203. Kobayashi, Takashi, Theerawut Chanmee, and Naoki Itano. 2020. 'Hyaluronan: Metabolism and Function'. *Biomolecules* 10 (11): 1525. https://doi.org/10.3390/biom10111525.

204. Köpke-Aguiar, L. A., J. R. M. Martins, C. C. Passerotti, C. F. Toledo, H. B. Nader, and Durval R. Borges. 2002. 'Serum Hyaluronic Acid as a Comprehensive Marker to Assess Severity of Liver Disease in Schistosomiasis'. *Acta Tropica* 84 (2): 117–26. https://doi.org/10.1016/s0001-706x(02)00136-5.

205. Koprivica, Vuk, Kin-Sang Cho, Jong Bae Park, Glenn Yiu, Jasvinder Atwal, Bryan Gore, Jieun A. Kim, et al. 2005. 'EGFR Activation Mediates Inhibition of Axon Regeneration by Myelin and Chondroitin Sulfate Proteoglycans'. *Science (New York, N.Y.)* 310 (5745): 106–10. https://doi.org/10.1126/science.1115462.

206. Krawzak, H. W., H. P. Heistermann, K. Andrejewski, and G. Hohlbach. 1995. 'Postprandial Bile-Duct Kinetics under the Influence of 4-Methylumbelliferone (Hymecromone)'. *International Journal of Clinical Pharmacology and Therapeutics* 33 (10): 569–72.

207. Kucher, Klaus, Donald Johns, Doris Maier, Rainer Abel, Andreas Badke, Hagen Baron, Roland Thietje, et al. 2018. 'First-in-Man Intrathecal Application of Neurite Growth-Promoting Anti-Nogo-A Antibodies in Acute Spinal Cord Injury'. *Neurorehabilitation and Neural Repair* 32 (6–7): 578–89. https://doi.org/10.1177/1545968318776371.

208. Kuipers, H. F., N. Nagy, S. M. Ruppert, V. G. Sunkari, P. L. Marshall, J. A. Gebe, H. D. Ishak, et al. 2016. 'The Pharmacokinetics and Dosing of Oral 4-Methylumbelliferone for Inhibition of Hyaluronan Synthesis in Mice'. *Clinical and Experimental Immunology* 185 (3): 372–81. https://doi.org/10.1111/cei.12815.

209. Kuipers, Hedwich F., Mary Rieck, Irina Gurevich, Nadine Nagy, Manish J. Butte, Robert S. Negrin, Thomas N. Wight, Lawrence Steinman, and Paul L. Bollyky. 2016. 'Hyaluronan Synthesis Is Necessary for Autoreactive T-Cell Trafficking, Activation, and Th1 Polarization'. *Proceedings of the National Academy of Sciences of the United States of America* 113 (5): 1339–44. https://doi.org/10.1073/pnas.1525086113.

210. Kultti, Anne, Sanna Pasonen-Seppänen, Marjo Jauhiainen, Kirsi J. Rilla, Riikka Kärnä, Emma Pyöriä, Raija H. Tammi, and Markku I. Tammi. 2009. '4-Methylumbelliferone Inhibits Hyaluronan Synthesis by Depletion of Cellular UDP-Glucuronic Acid and Downregulation of Hyaluronan Synthase 2 and 3'. *Experimental Cell Research* 315 (11): 1914–23. https://doi.org/10.1016/j.yexcr.2009.03.002.

211. Kvietys, Peter R., and D. Neil Granger. 2010. 'Role of Intestinal Lymphatics in Interstitial Volume Regulation and Transmucosal Water Transport'. *Annals of the New York Academy of Sciences* 1207 Suppl 1 (Suppl 1): E29-43. https://doi.org/10.1111/j.1749-6632.2010.05709.x.

212. Kwok, Jessica C. F., Daniela Carulli, and James W. Fawcett. 2010. 'In Vitro Modeling of Perineuronal Nets: Hyaluronan Synthase and Link Protein Are Necessary for Their Formation and Integrity'. *Journal of Neurochemistry* 114 (5): 1447–59. https://doi.org/10.1111/j.1471-4159.2010.06878.x.

213. Kwok, Jessica C. F., Simona Foscarin, and James W. Fawcett. 2015. 'Perineuronal Nets: A Special Structure in the Central Nervous System Extracellular Matrix'. In *Extracellular Matrix*, edited by Jennie B. Leach and Elizabeth M. Powell, 93:23–32. Neuromethods. New York, NY: Springer New York. https://doi.org/10.1007/978-1-4939-2083-9_3.

214. Laabs, Tracy L., Hang Wang, Yasuhiro Katagiri, Thomas McCann, James W. Fawcett, and Herbert M. Geller. 2007. 'Inhibiting Glycosaminoglycan Chain Polymerization Decreases the Inhibitory Activity of Astrocyte-Derived Chondroitin Sulfate Proteoglycans'. *The Journal of Neuroscience: The Official Journal of the Society for Neuroscience* 27 (52): 14494–501. https://doi.org/10.1523/JNEUROSCI.2807-07.2007.

215. Lander, C., P. Kind, M. Maleski, and S. Hockfield. 1997. 'A Family of Activity-Dependent Neuronal Cell-Surface Chondroitin Sulfate Proteoglycans in Cat Visual Cortex'. *The Journal of Neuroscience: The Official Journal of the Society for Neuroscience* 17 (6): 1928–39. https://doi.org/10.1523/JNEUROSCI.17-06-01928.1997.

216. Laurent, C., G. Johnson-Wells, S. Hellström, A. Engström-Laurent, and A. F. Wells. 1991. 'Localization of Hyaluronan in Various Muscular Tissues. A Morphological Study in the Rat'. *Cell and Tissue Research* 263 (2): 201–5. https://doi.org/10.1007/BF00318761.

217. Laywell, E. D., U. Dörries, U. Bartsch, A. Faissner, M. Schachner, and D. A. Steindler. 1992. 'Enhanced Expression of the Developmentally Regulated Extracellular Matrix Molecule Tenascin Following Adult Brain Injury'. *Proceedings of the National Academy of Sciences of the United States of America* 89 (7): 2634–38. https://doi.org/10.1073/pnas.89.7.2634.

218. Lee, Hyun Joon, Shan Bian, Igor Jakovcevski, Bin Wu, Andrey Irintchev, and Melitta Schachner. 2012. 'Delayed Applications of L1 and Chondroitinase ABC Promote Recovery after Spinal Cord Injury'. *Journal of Neurotrauma* 29 (10): 1850–63. https://doi.org/10.1089/neu.2011.2290.

219. Lee, Jae K., and Binhai Zheng. 2012. 'Role of Myelin-Associated Inhibitors in Axonal Repair after Spinal Cord Injury'. *Experimental Neurology* 235 (1): 33–42. https://doi.org/10.1016/j.expneurol.2011.05.001.

220. Leff, S. E., S. K. Spratt, R. O. Snyder, and R. J. Mandel. 1999. 'Long-Term Restoration of Striatal L-Aromatic Amino Acid Decarboxylase Activity Using

Recombinant Adeno-Associated Viral Vector Gene Transfer in a Rodent Model of Parkinson's Disease'. *Neuroscience* 92 (1): 185–96. https://doi.org/10.1016/s0306-4522(98)00741-6.

221. Lemons, Michele L., John D. Sandy, Douglas K. Anderson, and Dena R. Howland. 2003. 'Intact Aggrecan and Chondroitin Sulfate-Depleted Aggrecan Core Glycoprotein Inhibit Axon Growth in the Adult Rat Spinal Cord'. *Experimental Neurology* 184 (2): 981–90. https://doi.org/10.1016/S0014-4886(03)00383-2.

222. Levine, J. M. 1994. 'Increased Expression of the NG2 Chondroitin-Sulfate Proteoglycan after Brain Injury'. *The Journal of Neuroscience: The Official Journal of the Society for Neuroscience* 14 (8): 4716–30. https://doi.org/10.1523/JNEUROSCI.14-08-04716.1994.

223. Levine, J. M., R. Reynolds, and J. W. Fawcett. 2001. 'The Oligodendrocyte Precursor Cell in Health and Disease'. *Trends in Neurosciences* 24 (1): 39–47. https://doi.org/10.1016/s0166-2236(00)01691-x.

224. Liu, Kai, Andrea Tedeschi, Kevin Kyungsuk Park, and Zhigang He. 2011. 'Neuronal Intrinsic Mechanisms of Axon Regeneration'. *Annual Review of Neuroscience* 34: 131–52. https://doi.org/10.1146/annurev-neuro-061010-113723.

225. Livak, K. J., and T. D. Schmittgen. 2001. 'Analysis of Relative Gene Expression Data Using Real-Time Quantitative PCR and the 2(-Delta Delta C(T)) Method'. *Methods (San Diego, Calif.)* 25 (4): 402–8. https://doi.org/10.1006/meth.2001.1262.

226. Long, Katherine R., and Wieland B. Huttner. 2021. 'The Role of the Extracellular Matrix in Neural Progenitor Cell Proliferation and Cortical Folding During Human Neocortex Development'. *Frontiers in Cellular Neuroscience* 15: 804649. https://doi.org/10.3389/fncel.2021.804649.

227. Longaker, M. T., E. S. Chiu, N. S. Adzick, M. Stern, M. R. Harrison, and R. Stern. 1991. 'Studies in Fetal Wound Healing. V. A Prolonged Presence of Hyaluronic Acid Characterizes Fetal Wound Fluid'. *Annals of Surgery* 213 (4): 292–96. https://doi.org/10.1097/00000658-199104000-00003.

228. Loy, Kristina, and Florence M. Bareyre. 2019. 'Rehabilitation Following Spinal Cord Injury: How Animal Models Can Help Our Understanding of Exercise-Induced Neuroplasticity'. *Neural Regeneration Research* 14 (3): 405–12. https://doi.org/10.4103/1673-5374.245951.

229. Lundell, Anna, Anders I. Olin, Matthias Mörgelin, Salam al-Karadaghi, Anders Aspberg, and Derek T. Logan. 2004. 'Structural Basis for Interactions between Tenascins and Lectican C-Type Lectin Domains: Evidence for a Crosslinking Role for Tenascins'. *Structure (London, England: 1993)* 12 (8): 1495–1506. https://doi.org/10.1016/j.str.2004.05.021.

230. Luo, Yunhua, and Oghenerioborорue Amromanoh. 2021. 'Bone Organic-Inorganic Phase Ratio Is a Fundamental Determinant of Bone Material Quality'. *Applied Bionics and Biomechanics* 2021: 4928396. https://doi.org/10.1155/2021/4928396.

231. Lüth, H. J., J. Fischer, and M. R. Celio. 1992. 'Soybean Lectin Binding Neurons in the Visual Cortex of the Rat Contain Parvalbumin and Are Covered by Glial Nets'. *Journal of Neurocytology* 21 (3): 211–21. https://doi.org/10.1007/BF01194979.

232. Makris, Konstantinos, Nikos Markou, Effimia Evodia, Eleni Dimopoulou, Ioannis Drakopoulos, Konstantina Ntetsika, Demetrios Rizos, George Baltopoulos, and Alexander Haliassos. 2009. 'Urinary Neutrophil Gelatinase-Associated Lipocalin (NGAL) as an Early Marker of Acute Kidney Injury in Critically Ill Multiple Trauma Patients'. *Clinical Chemistry and Laboratory Medicine* 47 (1): 79–82. https://doi.org/10.1515/CCLM.2009.004.

233. Malakouti, Mazyar, Archish Kataria, Sayed K. Ali, and Steven Schenker. 2017. 'Elevated Liver Enzymes in Asymptomatic Patients - What Should I Do?' *Journal of Clinical and Translational Hepatology* 5 (4): 394–403. https://doi.org/10.14218/JCTH.2017.00027.

234. Maloney, Finn P., Jeremi Kuklewicz, Robin A. Corey, Yunchen Bi, Ruoya Ho, Lukasz Mateusiak, Els Pardon, Jan Steyaert, Phillip J. Stansfeld, and Jochen Zimmer. 2022. 'Structure, Substrate Recognition and Initiation of Hyaluronan Synthase'. *Nature* 604 (7904): 195–201. https://doi.org/10.1038/s41586-022-04534-2.

235. Mang, Cameron S., Kristin L. Campbell, Colin J. D. Ross, and Lara A. Boyd. 2013. 'Promoting Neuroplasticity for Motor Rehabilitation after Stroke: Considering the Effects of Aerobic Exercise and Genetic Variation on Brain-Derived Neurotrophic Factor'. *Physical Therapy* 93 (12): 1707–16. https://doi.org/10.2522/ptj.20130053.

236. Mao, Yilin, Tara Nguyen, Ryan S. Tonkin, Justin G. Lees, Caitlyn Warren, Simon J. O'Carroll, Louise F. B. Nicholson, Colin R. Green, Gila Moalem-Taylor, and Catherine A. Gorrie. 2017. 'Characterisation of Peptide5 Systemic Administration for Treating Traumatic Spinal Cord Injured Rats'. *Experimental Brain Research* 235 (10): 3033–48. https://doi.org/10.1007/s00221-017-5023-3.

237. Mar, Fernando M., Azad Bonni, and Mónica M. Sousa. 2014. 'Cell Intrinsic Control of Axon Regeneration'. *EMBO Reports* 15 (3): 254–63. https://doi.org/10.1002/embr.201337723.

238. Margadant, Coert, Hanneke N. Monsuur, Jim C. Norman, and Arnoud Sonnenberg. 2011. 'Mechanisms of Integrin Activation and Trafficking'. *Current Opinion in Cell Biology* 23 (5): 607–14. https://doi.org/10.1016/j.ceb.2011.08.005.

239. Massey, James M., Jeremy Amps, Mariano S. Viapiano, Russell T. Matthews, Michelle R. Wagoner, Christopher M. Whitaker, Warren Alilain, et al. 2008. 'Increased Chondroitin Sulfate Proteoglycan Expression in Denervated Brainstem Targets Following Spinal Cord Injury Creates a Barrier to Axonal Regeneration Overcome by Chondroitinase ABC and Neurotrophin-3'. *Experimental Neurology* 209 (2): 426–45. https://doi.org/10.1016/j.expneurol.2007.03.029.

240. Massey, James M., Charles H. Hubscher, Michelle R. Wagoner, Julie A. Decker, Jeremy Amps, Jerry Silver, and Stephen M. Onifer. 2006. 'Chondroitinase ABC Digestion of the Perineuronal Net Promotes Functional Collateral Sprouting in the Cuneate Nucleus after Cervical Spinal Cord Injury'. *The Journal of Neuroscience: The Official Journal of the Society for Neuroscience* 26 (16): 4406–14. https://doi.org/10.1523/JNEUROSCI.5467-05.2006.

241. Matthews, M. A., M. F. St Onge, C. L. Faciane, and J. B. Gelderd. 1979. 'Spinal Cord Transection: A Quantitative Analysis of Elements of the Connective Tissue Matrix Formed within the Site of Lesion Following Administration of Piromen, Cytoxan or Trypsin'. *Neuropathology and Applied Neurobiology* 5 (3): 161–80. https://doi.org/10.1111/j.1365-2990.1979.tb00617.x.

242. McKeon, R. J., A. Höke, and J. Silver. 1995. 'Injury-Induced Proteoglycans Inhibit the Potential for Laminin-Mediated Axon Growth on Astrocytic Scars'. *Experimental Neurology* 136 (1): 32–43. https://doi.org/10.1006/exnr.1995.1081.

243. McTigue, Dana M., Richa Tripathi, and Ping Wei. 2006. 'NG2 Colocalizes with Axons and Is Expressed by a Mixed Cell Population in Spinal Cord Lesions'.

Journal of Neuropathology and Experimental Neurology 65 (4): 406–20. https://doi.org/10.1097/01.jnen.0000218447.32320.52.

244. Means, Terry K., and Andrew D. Luster. 2010. 'Integrins Limit the Toll'. *Nature Immunology* 11 (8): 691–93. https://doi.org/10.1038/ni0810-691.

245. Mearow, K. M., Y. Kril, A. Gloster, and J. Diamond. 1994. 'Expression of NGF Receptor and GAP-43 mRNA in DRG Neurons during Collateral Sprouting and Regeneration of Dorsal Cutaneous Nerves'. *Journal of Neurobiology* 25 (2): 127–42. https://doi.org/10.1002/neu.480250205.

246. Meldrum, B. S. 2000. 'Glutamate as a Neurotransmitter in the Brain: Review of Physiology and Pathology'. *The Journal of Nutrition* 130 (4S Suppl): 1007S-15S. https://doi.org/10.1093/jn/130.4.1007S.

247. Metz, Gerlinde A., and Ian Q. Whishaw. 2009. 'The Ladder Rung Walking Task: A Scoring System and Its Practical Application'. *Journal of Visualized Experiments: JoVE*, no. 28 (June): 1204. https://doi.org/10.3791/1204.

248. Mirzadeh, Zaman, Kimberly M. Alonge, Elaine Cabrales, Vicente Herranz-Pérez, Jarrad M. Scarlett, Jenny M. Brown, Rim Hassouna, et al. 2019. 'Perineuronal Net Formation during the Critical Period for Neuronal Maturation in the Hypothalamic Arcuate Nucleus'. *Nature Metabolism* 1 (2): 212–21. https://doi.org/10.1038/s42255-018-0029-0.

249. Miura, Y. 1999. '[Aspartate aminotransferase (AST) and alanine aminotransferase (ALT)]'. *Nihon Rinsho. Japanese Journal of Clinical Medicine* 57 Suppl (August): 320–25.

250. Miyata, Shinji, Yukio Komatsu, Yumiko Yoshimura, Choji Taya, and Hiroshi Kitagawa. 2012. 'Persistent Cortical Plasticity by Upregulation of Chondroitin 6-Sulfation'. *Nature Neuroscience* 15 (3): 414–22, S1-2. https://doi.org/10.1038/nn.3023.

251. Monnier, Philippe P., Ana Sierra, Jan M. Schwab, Sigrid Henke-Fahle, and Bernhard K. Mueller. 2003. 'The Rho/ROCK Pathway Mediates Neurite Growth-Inhibitory Activity Associated with the Chondroitin Sulfate Proteoglycans of the CNS Glial Scar'. *Molecular and Cellular Neurosciences* 22 (3): 319–30. https://doi.org/10.1016/s1044-7431(02)00035-0.

252. Monslow, James, Priya Govindaraju, and Ellen Puré. 2015. 'Hyaluronan - a Functional and Structural Sweet Spot in the Tissue Microenvironment'. *Frontiers in Immunology* 6: 231. https://doi.org/10.3389/fimmu.2015.00231.

253. Moon, L. D. F., R. A. Asher, K. E. Rhodes, and J. W. Fawcett. 2002. 'Relationship between Sprouting Axons, Proteoglycans and Glial Cells Following Unilateral Nigrostriatal Axotomy in the Adult Rat'. *Neuroscience* 109 (1): 101–17. https://doi.org/10.1016/s0306-4522(01)00457-2.

254. Moretti, Marzia, Riccardo Caraffi, Luca Lorenzini, Ilaria Ottonelli, Michele Sannia, Giuseppe Alastra, Vito Antonio Baldassarro, et al. 2023. '"Combo" Multi-Target Pharmacological Therapy and New Formulations to Reduce Inflammation and Improve Endogenous Remyelination in Traumatic Spinal Cord Injury'. *Cells* 12 (9): 1331. https://doi.org/10.3390/cells12091331.

255. Morgenstern, Daniel A., Richard A. Asher, and James W. Fawcett. 2002. 'Chondroitin Sulphate Proteoglycans in the CNS Injury Response'. *Progress in Brain Research* 137: 313–32. https://doi.org/10.1016/s0079-6123(02)37024-9.

256. Morita, K., Y. Sugiyama, and M. Hanano. 1986. 'Pharmacokinetic Study of 4-Methylumbelliferone in Rats: Influence of Dose on Its First-Pass Hepatic Elimination'. *Journal of Pharmacobio-Dynamics* 9 (2): 117–24. https://doi.org/10.1248/bpb1978.9.117.

257. Moser, Markus, Kyle R. Legate, Roy Zent, and Reinhard Fässler. 2009. 'The Tail of Integrins, Talin, and Kindlins'. *Science (New York, N.Y.)* 324 (5929): 895–99. https://doi.org/10.1126/science.1163865.

258. Motte, Carol A. de la, Vincent C. Hascall, Judith Drazba, Sudip K. Bandyopadhyay, and Scott A. Strong. 2003. 'Mononuclear Leukocytes Bind to Specific Hyaluronan Structures on Colon Mucosal Smooth Muscle Cells Treated with Polyinosinic Acid:Polycytidylic Acid: Inter-Alpha-Trypsin Inhibitor Is Crucial to Structure and Function'. *The American Journal of Pathology* 163 (1): 121–33. https://doi.org/10.1016/s0002-9440(10)63636-x.

259. Motte, Carol A. de la, and Sean P. Kessler. 2015. 'The Role of Hyaluronan in Innate Defense Responses of the Intestine'. *International Journal of Cell Biology* 2015: 481301. https://doi.org/10.1155/2015/481301.

260. Murray, Katherine C., Aya Nakae, Marilee J. Stephens, Michelle Rank, Jessica D'Amico, Philip J. Harvey, Xiaole Li, et al. 2010. 'Recovery of Motoneuron and Locomotor Function after Spinal Cord Injury Depends on Constitutive Activity in 5-HT2C Receptors'. *Nature Medicine* 16 (6): 694–700. https://doi.org/10.1038/nm.2160.

261. Myers, Jonathan P., Miguel Santiago-Medina, and Timothy M. Gomez. 2011. 'Regulation of Axonal Outgrowth and Pathfinding by Integrin-ECM Interactions'. *Developmental Neurobiology* 71 (11): 901–23. https://doi.org/10.1002/dneu.20931.

262. Nagy, Nadine, Irina Gurevich, Hedwich F. Kuipers, Shannon M. Ruppert, Payton L. Marshall, Bryan J. Xie, Wenchao Sun, et al. 2019. '4-Methylumbelliferyl Glucuronide Contributes to Hyaluronan Synthesis Inhibition'. *The Journal of Biological Chemistry* 294 (19): 7864–77. https://doi.org/10.1074/jbc.RA118.006166.

263. Nagy, Nadine, Hedwich F. Kuipers, Adam R. Frymoyer, Heather D. Ishak, Jennifer B. Bollyky, Thomas N. Wight, and Paul L. Bollyky. 2015. '4-Methylumbelliferone Treatment and Hyaluronan Inhibition as a Therapeutic Strategy in Inflammation, Autoimmunity, and Cancer'. *Frontiers in Immunology* 6: 123. https://doi.org/10.3389/fimmu.2015.00123.

264. Nahmani, M., and G. G. Turrigiano. 2014. 'Adult Cortical Plasticity Following Injury: Recapitulation of Critical Period Mechanisms?' *Neuroscience* 283 (December): 4–16. https://doi.org/10.1016/j.neuroscience.2014.04.029.

265. Nakamura, T., K. Takagaki, S. Shibata, K. Tanaka, T. Higuchi, and M. Endo. 1995. 'Hyaluronic-Acid-Deficient Extracellular Matrix Induced by Addition of 4-Methylumbelliferone to the Medium of Cultured Human Skin Fibroblasts'. *Biochemical and Biophysical Research Communications* 208 (2): 470–75. https://doi.org/10.1006/bbrc.1995.1362.

266. Nave, Klaus-Armin. 2010a. 'Myelination and the Trophic Support of Long Axons'. *Nature Reviews. Neuroscience* 11 (4): 275–83. https://doi.org/10.1038/nrn2797.

267. ———. 2010b. 'Myelination and Support of Axonal Integrity by Glia'. *Nature* 468 (7321): 244–52. https://doi.org/10.1038/nature09614.

268. Neumann, S., and C. J. Woolf. 1999. 'Regeneration of Dorsal Column Fibers into and beyond the Lesion Site Following Adult Spinal Cord Injury'. *Neuron* 23 (1): 83–91. https://doi.org/10.1016/s0896-6273(00)80755-2.

269. Nicholson, C., and E. Syková. 1998. 'Extracellular Space Structure Revealed by Diffusion Analysis'. *Trends in Neurosciences* 21 (5): 207–15. https://doi.org/10.1016/s0166-2236(98)01261-2.

270. Niekerk, Erna A. van, Mark H. Tuszynski, Paul Lu, and Jennifer N. Dulin. 2016. 'Molecular and Cellular Mechanisms of Axonal Regeneration After Spinal

Cord Injury'. *Molecular & Cellular Proteomics: MCP* 15 (2): 394–408. https://doi.org/10.1074/mcp.R115.053751.

271. Nieuwenhuis, Bart, Amanda C. Barber, Rachel S. Evans, Craig S. Pearson, Joachim Fuchs, Amy R. MacQueen, Susan van Erp, et al. 2020. 'PI 3-Kinase Delta Enhances Axonal PIP3 to Support Axon Regeneration in the Adult CNS'. *EMBO Molecular Medicine* 12 (8): e11674. https://doi.org/10.15252/emmm.201911674.

272. Nieuwenhuis, Bart, Barbara Haenzi, Melissa R. Andrews, Joost Verhaagen, and James W. Fawcett. 2018. 'Integrins Promote Axonal Regeneration after Injury of the Nervous System'. *Biological Reviews of the Cambridge Philosophical Society* 93 (3): 1339–62. https://doi.org/10.1111/brv.12398.

273. Nirwane, Abhijit, and Yao Yao. 2019. 'Laminins and Their Receptors in the CNS'. *Biological Reviews of the Cambridge Philosophical Society* 94 (1): 283–306. https://doi.org/10.1111/brv.12454.

274. 'NISCI - Nogo Inhibition in Spinal Cord Injury (NISCI)'. n.d. https://clinicaltrials.gov/study/NCT03935321.

275. Norenberg, Michael D., Jon Smith, and Alex Marcillo. 2004. 'The Pathology of Human Spinal Cord Injury: Defining the Problems'. *Journal of Neurotrauma* 21 (4): 429–40. https://doi.org/10.1089/089771504323004575.

276. Nori, Satoshi, Mohamad Khazaei, Christopher S. Ahuja, Kazuya Yokota, Jan-Eric Ahlfors, Yang Liu, Jian Wang, et al. 2018. 'Human Oligodendrogenic Neural Progenitor Cells Delivered with Chondroitinase ABC Facilitate Functional Repair of Chronic Spinal Cord Injury'. *Stem Cell Reports* 11 (6): 1433–48. https://doi.org/10.1016/j.stemcr.2018.10.017.

277. Oliferenko, S., I. Kaverina, J. V. Small, and L. A. Huber. 2000. 'Hyaluronic Acid (HA) Binding to CD44 Activates Rac1 and Induces Lamellipodia Outgrowth'. *The Journal of Cell Biology* 148 (6): 1159–64. https://doi.org/10.1083/jcb.148.6.1159.

278. Orr, Michael B., and John C. Gensel. 2018. 'Spinal Cord Injury Scarring and Inflammation: Therapies Targeting Glial and Inflammatory Responses'. *Neurotherapeutics: The Journal of the American Society for Experimental NeuroTherapeutics* 15 (3): 541–53. https://doi.org/10.1007/s13311-018-0631-6.

279. Oudega, M., E. J. Bradbury, and M. S. Ramer. 2012. 'Combination Therapies'. *Handbook of Clinical Neurology* 109: 617–36. https://doi.org/10.1016/B978-0-444-52137-8.00038-3.

280. Oyinbo, Charles Aidemise. 2011. ‘Secondary Injury Mechanisms in Traumatic Spinal Cord Injury: A Nugget of This Multiply Cascade’. *Acta Neurobiologiae Experimentalis* 71 (2): 281–99.

281. Pankov, Roumen, and Kenneth M. Yamada. 2002. ‘Fibronectin at a Glance’. *Journal of Cell Science* 115 (Pt 20): 3861–63. https://doi.org/10.1242/jcs.00059.

282. Pantazopoulos, Harry, and Sabina Berretta. 2016. ‘In Sickness and in Health: Perineuronal Nets and Synaptic Plasticity in Psychiatric Disorders’. *Neural Plasticity* 2016: 9847696. https://doi.org/10.1155/2016/9847696.

283. Papanastasopoulou, Chrysanthi, Maria Papastamataki, Petros Karampatsis, Eleni Anagnostopoulou, Ioannis Papassotiriou, and Nikolaos Sitaras. 2017. ‘Cardiovascular Risk and Serum Hyaluronic Acid: A Preliminary Study in a Healthy Population of Low/Intermediate Risk’. *Journal of Clinical Laboratory Analysis* 31 (1): e22010. https://doi.org/10.1002/jcla.22010.

284. Park, Yun Kyung, and Yukiko Goda. 2016. ‘Integrins in Synapse Regulation’. *Nature Reviews. Neuroscience* 17 (12): 745–56. https://doi.org/10.1038/nrn.2016.138.

285. Parsons, J. Thomas. 2003. ‘Focal Adhesion Kinase: The First Ten Years’. *Journal of Cell Science* 116 (Pt 8): 1409–16. https://doi.org/10.1242/jcs.00373.

286. Pattali, Rithu, Yongchao Mou, and Xue-Jun Li. 2019. ‘AAV9 Vector: A Novel Modality in Gene Therapy for Spinal Muscular Atrophy’. *Gene Therapy* 26 (7–8): 287–95. https://doi.org/10.1038/s41434-019-0085-4.

287. Pellinen, Teijo, and Johanna Ivaska. 2006. ‘Integrin Traffic’. *Journal of Cell Science* 119 (Pt 18): 3723–31. https://doi.org/10.1242/jcs.03216.

288. Perrier, Jean-François, and Rodolfo Delgado-Lezama. 2005. ‘Synaptic Release of Serotonin Induced by Stimulation of the Raphe Nucleus Promotes Plateau Potentials in Spinal Motoneurons of the Adult Turtle’. *The Journal of Neuroscience: The Official Journal of the Society for Neuroscience* 25 (35): 7993–99. https://doi.org/10.1523/JNEUROSCI.1957-05.2005.

289. Perrier, Jean-François, and Jørn Hounsgaard. 2003. ‘5-HT2 Receptors Promote Plateau Potentials in Turtle Spinal Motoneurons by Facilitating an L-Type Calcium Current’. *Journal of Neurophysiology* 89 (2): 954–59. https://doi.org/10.1152/jn.00753.2002.

290. Perry, Rotem Ben-Tov, Ella Doron-Mandel, Elena Iavnilovitch, Ida Rishal, Shachar Y. Dagan, Michael Tsoory, Giovanni Coppola, et al. 2012. ‘Subcellular

Knockout of Importin B1 Perturbs Axonal Retrograde Signaling'. *Neuron* 75 (2): 294–305. https://doi.org/10.1016/j.neuron.2012.05.033.

291. Peters, Alec, and Larry S. Sherman. 2020. 'Diverse Roles for Hyaluronan and Hyaluronan Receptors in the Developing and Adult Nervous System'. *International Journal of Molecular Sciences* 21 (17): 5988. https://doi.org/10.3390/ijms21175988.

292. Petrova, Veselina, Craig S. Pearson, Jared Ching, James R. Tribble, Andrea G. Solano, Yunfei Yang, Fiona M. Love, et al. 2020. 'Protrudin Functions from the Endoplasmic Reticulum to Support Axon Regeneration in the Adult CNS'. *Nature Communications* 11 (1): 5614. https://doi.org/10.1038/s41467-020-19436-y.

293. Pinkstaff, J. K., J. Detterich, G. Lynch, and C. Gall. 1999. 'Integrin Subunit Gene Expression Is Regionally Differentiated in Adult Brain'. *The Journal of Neuroscience: The Official Journal of the Society for Neuroscience* 19 (5): 1541–56. https://doi.org/10.1523/JNEUROSCI.19-05-01541.1999.

294. Plant, G. W., M. L. Bates, and M. B. Bunge. 2001. 'Inhibitory Proteoglycan Immunoreactivity Is Higher at the Caudal than the Rostral Schwann Cell Graft-Transected Spinal Cord Interface'. *Molecular and Cellular Neurosciences* 17 (3): 471–87. https://doi.org/10.1006/mcne.2000.0948.

295. Plunet, Ward, Brian K. Kwon, and Wolfram Tetzlaff. 2002. 'Promoting Axonal Regeneration in the Central Nervous System by Enhancing the Cell Body Response to Axotomy'. *Journal of Neuroscience Research* 68 (1): 1–6. https://doi.org/10.1002/jnr.10176.

296. Prabhakar, Vikas, Ishan Capila, Carlos J. Bosques, Kevin Pojasek, and Ram Sasisekharan. 2005. 'Chondroitinase ABC I from Proteus Vulgaris: Cloning, Recombinant Expression and Active Site Identification'. *The Biochemical Journal* 386 (Pt 1): 103–12. https://doi.org/10.1042/BJ20041222.

297. Prabhakar, Vikas, Rahul Raman, Ishan Capila, Carlos J. Bosques, Kevin Pojasek, and Ram Sasisekharan. 2005. 'Biochemical Characterization of the Chondroitinase ABC I Active Site'. *The Biochemical Journal* 390 (Pt 2): 395–405. https://doi.org/10.1042/BJ20050532.

298. Purslow, Peter P. 2010. 'Muscle Fascia and Force Transmission'. *Journal of Bodywork and Movement Therapies* 14 (4): 411–17. https://doi.org/10.1016/j.jbmt.2010.01.005.

299. Quaranta, S., S. Rossetti, and E. Camarri. 1984. '[Double-blind clinical study on hymecromone and placebo in motor disorders of the bile ducts after cholecystectomy]'. *La Clinica Terapeutica* 108 (6): 513–17.

300. Rafii, Michael S., Mark H. Tuszynski, Ronald G. Thomas, David Barba, James B. Brewer, Robert A. Rissman, Joao Siffert, Paul S. Aisen, and AAV2-NGF Study Team. 2018. 'Adeno-Associated Viral Vector (Serotype 2)-Nerve Growth Factor for Patients With Alzheimer Disease: A Randomized Clinical Trial'. *JAMA Neurology* 75 (7): 834–41. https://doi.org/10.1001/jamaneurol.2018.0233.

301. Reichelt, Amy C., Dominic J. Hare, Timothy J. Bussey, and Lisa M. Saksida. 2019. 'Perineuronal Nets: Plasticity, Protection, and Therapeutic Potential'. *Trends in Neurosciences* 42 (7): 458–70. https://doi.org/10.1016/j.tins.2019.04.003.

302. Renaudin, A., M. Lehmann, J. Girault, and L. McKerracher. 1999. 'Organization of Point Contacts in Neuronal Growth Cones'. *Journal of Neuroscience Research* 55 (4): 458–71. https://doi.org/10.1002/(SICI)1097-4547(19990215)55:4<458::AID-JNR6>3.0.CO;2-D.

303. Represa, A., H. Pollard, J. Moreau, G. Ghilini, M. Khrestchatisky, and Y. Ben-Ari. 1993. 'Mossy Fiber Sprouting in Epileptic Rats Is Associated with a Transient Increased Expression of Alpha-Tubulin'. *Neuroscience Letters* 156 (1–2): 149–52. https://doi.org/10.1016/0304-3940(93)90460-3.

304. Ridley, Anne J. 2011. 'Life at the Leading Edge'. *Cell* 145 (7): 1012–22. https://doi.org/10.1016/j.cell.2011.06.010.

305. Risling, M., K. Fried, H. Linda, T. Carlstedt, and S. Cullheim. 1993. 'Regrowth of Motor Axons Following Spinal Cord Lesions: Distribution of Laminin and Collagen in the CNS Scar Tissue'. *Brain Research Bulletin* 30 (3–4): 405–14. https://doi.org/10.1016/0361-9230(93)90272-d.

306. Rowland, James W., Gregory W. J. Hawryluk, Brian Kwon, and Michael G. Fehlings. 2008. 'Current Status of Acute Spinal Cord Injury Pathophysiology and Emerging Therapies: Promise on the Horizon'. *Neurosurgical Focus* 25 (5): E2. https://doi.org/10.3171/FOC.2008.25.11.E2.

307. Sabaratnam, S., V. Arunan, P. J. Coleman, R. M. Mason, and J. R. Levick. 2005. 'Size Selectivity of Hyaluronan Molecular Sieving by Extracellular Matrix in Rabbit Synovial Joints'. *The Journal of Physiology* 567 (Pt 2): 569–81. https://doi.org/10.1113/jphysiol.2005.088906.

308. Schachtrup, Christian, Jae K. Ryu, Matthew J. Helmrick, Eirini Vagena, Dennis K. Galanakis, Jay L. Degen, Richard U. Margolis, and Katerina Akassoglou. 2010. 'Fibrinogen Triggers Astrocyte Scar Formation by Promoting the Availability of Active TGF-Beta after Vascular Damage'. *The Journal of Neuroscience: The Official Journal of the Society for Neuroscience* 30 (17): 5843–54. https://doi.org/10.1523/JNEUROSCI.0137-10.2010.

309. Schachtschabel, D. O., and J. Wever. 1978. 'Age-Related Decline in the Synthesis of Glycosaminoglycans by Cultured Human Fibroblasts (WI-38)'. *Mechanisms of Ageing and Development* 8 (4): 257–64. https://doi.org/10.1016/0047-6374(78)90025-8.

310. Schindelin, Johannes, Ignacio Arganda-Carreras, Erwin Frise, Verena Kaynig, Mark Longair, Tobias Pietzsch, Stephan Preibisch, et al. 2012. 'Fiji: An Open-Source Platform for Biological-Image Analysis'. *Nature Methods* 9 (7): 676–82. https://doi.org/10.1038/nmeth.2019.

311. Schmidt, B. J., and L. M. Jordan. 2000. 'The Role of Serotonin in Reflex Modulation and Locomotor Rhythm Production in the Mammalian Spinal Cord'. *Brain Research Bulletin* 53 (5): 689–710. https://doi.org/10.1016/s0361-9230(00)00402-0.

312. Schwab, J. M., R. Beschorner, T. D. Nguyen, R. Meyermann, and H. J. Schluesener. 2001. 'Differential Cellular Accumulation of Connective Tissue Growth Factor Defines a Subset of Reactive Astrocytes, Invading Fibroblasts, and Endothelial Cells Following Central Nervous System Injury in Rats and Humans'. *Journal of Neurotrauma* 18 (4): 377–88. https://doi.org/10.1089/089771501750170930.

313. Schwarzbauer, J. E. 1991. 'Identification of the Fibronectin Sequences Required for Assembly of a Fibrillar Matrix'. *The Journal of Cell Biology* 113 (6): 1463–73. https://doi.org/10.1083/jcb.113.6.1463.

314. Šekeljić, Vera, and Pavle R. Andjus. 2012. 'Tenascin-C and Its Functions in Neuronal Plasticity'. *The International Journal of Biochemistry & Cell Biology* 44 (6): 825–29. https://doi.org/10.1016/j.biocel.2012.02.014.

315. Sengupta, Pallav. 2013. 'The Laboratory Rat: Relating Its Age With Human's'. *International Journal of Preventive Medicine* 4 (6): 624–30.

316. Seog, J., D. Dean, A. H. K. Plaas, S. Wong-Palms, A. J. Grodzinsky, and C. Ortiz. 2002. 'Direct Measurement of Glycosaminoglycan Intermolecular Interactions

via High-Resolution Force Spectroscopy'. *Macromolecules* 35 (14): 5601–15. https://doi.org/10.1021/ma0121621.

317. Shearer, M. C., and J. W. Fawcett. 2001. 'The Astrocyte/Meningeal Cell Interface--a Barrier to Successful Nerve Regeneration?' *Cell and Tissue Research* 305 (2): 267–73. https://doi.org/10.1007/s004410100384.

318. Shen, Y., S. I. Muramatsu, K. Ikeguchi, K. I. Fujimoto, D. S. Fan, M. Ogawa, H. Mizukami, et al. 2000. 'Triple Transduction with Adeno-Associated Virus Vectors Expressing Tyrosine Hydroxylase, Aromatic-L-Amino-Acid Decarboxylase, and GTP Cyclohydrolase I for Gene Therapy of Parkinson's Disease'. *Human Gene Therapy* 11 (11): 1509–19. https://doi.org/10.1089/10430340050083243.

319. Shen, Yingjie, Alan P. Tenney, Sarah A. Busch, Kevin P. Horn, Fernando X. Cuascut, Kai Liu, Zhigang He, Jerry Silver, and John G. Flanagan. 2009. 'PTPsigma Is a Receptor for Chondroitin Sulfate Proteoglycan, an Inhibitor of Neural Regeneration'. *Science (New York, N.Y.)* 326 (5952): 592–96. https://doi.org/10.1126/science.1178310.

320. Silver, Jerry, and Jared H. Miller. 2004. 'Regeneration beyond the Glial Scar'. *Nature Reviews. Neuroscience* 5 (2): 146–56. https://doi.org/10.1038/nrn1326.

321. Singh, Purva, Cara Carraher, and Jean E. Schwarzbauer. 2010. 'Assembly of Fibronectin Extracellular Matrix'. *Annual Review of Cell and Developmental Biology* 26: 397–419. https://doi.org/10.1146/annurev-cellbio-100109-104020.

322. Sivasankaran, Rajeev, Jiong Pei, Kevin C. Wang, Yi Ping Zhang, Christopher B. Shields, Xiao-Ming Xu, and Zhigang He. 2004. 'PKC Mediates Inhibitory Effects of Myelin and Chondroitin Sulfate Proteoglycans on Axonal Regeneration'. *Nature Neuroscience* 7 (3): 261–68. https://doi.org/10.1038/nn1193.

323. Skene, J. H. 1989. 'Axonal Growth-Associated Proteins'. *Annual Review of Neuroscience* 12: 127–56. https://doi.org/10.1146/annurev.ne.12.030189.001015.

324. Skene, J. H., and M. Willard. 1981. 'Characteristics of Growth-Associated Polypeptides in Regenerating Toad Retinal Ganglion Cell Axons'. *The Journal of Neuroscience: The Official Journal of the Society for Neuroscience* 1 (4): 419–26. https://doi.org/10.1523/JNEUROSCI.01-04-00419.1981.

325. Smadja-Joffe, F., S. Legras, N. Girard, Y. Li, B. Delpech, F. Bloget, K. Morimoto, et al. 1996. 'CD44 and Hyaluronan Binding by Human Myeloid Cells'.

Leukemia & Lymphoma 21 (5–6): 407–20, color plates following 528. https://doi.org/10.3109/10428199609093438.

326. Smith, Calvin C., Rui Mauricio, Luis Nobre, Barnaby Marsh, Rob C. I. Wüst, Harry B. Rossiter, and Ronaldo M. Ichiyama. 2015. 'Differential Regulation of Perineuronal Nets in the Brain and Spinal Cord with Exercise Training'. *Brain Research Bulletin* 111 (February): 20–26. https://doi.org/10.1016/j.brainresbull.2014.12.005.

327. Smith-Thomas, L. C., J. Fok-Seang, J. Stevens, J. S. Du, E. Muir, A. Faissner, H. M. Geller, J. H. Rogers, and J. W. Fawcett. 1994. 'An Inhibitor of Neurite Outgrowth Produced by Astrocytes'. *Journal of Cell Science* 107 (Pt 6) (June): 1687–95. https://doi.org/10.1242/jcs.107.6.1687.

328. Snow, D. M., E. M. Brown, and P. C. Letourneau. 1996. 'Growth Cone Behavior in the Presence of Soluble Chondroitin Sulfate Proteoglycan (CSPG), Compared to Behavior on CSPG Bound to Laminin or Fibronectin'. *International Journal of Developmental Neuroscience: The Official Journal of the International Society for Developmental Neuroscience* 14 (3): 331–49. https://doi.org/10.1016/0736-5748(96)00017-2.

329. Soderblom, Cynthia, Xueting Luo, Ezra Blumenthal, Eric Bray, Kirill Lyapichev, Jose Ramos, Vidhya Krishnan, et al. 2013. 'Perivascular Fibroblasts Form the Fibrotic Scar after Contusive Spinal Cord Injury'. *The Journal of Neuroscience: The Official Journal of the Society for Neuroscience* 33 (34): 13882–87. https://doi.org/10.1523/JNEUROSCI.2524-13.2013.

330. Sofroniew, Michael V. 2009. 'Molecular Dissection of Reactive Astrogliosis and Glial Scar Formation'. *Trends in Neurosciences* 32 (12): 638–47. https://doi.org/10.1016/j.tins.2009.08.002.

331. Sorg, Barbara A., Sabina Berretta, Jordan M. Blacktop, James W. Fawcett, Hiroshi Kitagawa, Jessica C. F. Kwok, and Marta Miquel. 2016. 'Casting a Wide Net: Role of Perineuronal Nets in Neural Plasticity'. *The Journal of Neuroscience: The Official Journal of the Society for Neuroscience* 36 (45): 11459–68. https://doi.org/10.1523/JNEUROSCI.2351-16.2016.

332. Spicer, Andrew P., Adriane Joo, and Rodney A. Bowling. 2003. 'A Hyaluronan Binding Link Protein Gene Family Whose Members Are Physically Linked Adjacent to Chondroitin Sulfate Proteoglycan Core Protein Genes: The

Missing Links'. *The Journal of Biological Chemistry* 278 (23): 21083–91. https://doi.org/10.1074/jbc.M213100200.

333. Stallcup, William B. 2002. 'The NG2 Proteoglycan: Past Insights and Future Prospects'. *Journal of Neurocytology* 31 (6–7): 423–35. https://doi.org/10.1023/a:1025731428581.

334. Stecco, Carla, R. Stern, A. Porzionato, V. Macchi, S. Masiero, A. Stecco, and R. De Caro. 2011. 'Hyaluronan within Fascia in the Etiology of Myofascial Pain'. *Surgical and Radiologic Anatomy: SRA* 33 (10): 891–96. https://doi.org/10.1007/s00276-011-0876-9.

335. Stepankova, Katerina, Pavla Jendelova, and Lucia Machova Urdzikova. 2021. 'Planet of the AAVs: The Spinal Cord Injury Episode'. *Biomedicines* 9 (6): 613. https://doi.org/10.3390/biomedicines9060613.

336. Štěpánková, Kateřina, Dana Mareková, Kristýna Kubášová, Radek Sedláček, Karolína Turnovcová, Irena Vacková, Šárka Kubinová, et al. 2023. '4-Methylumbeliferone Treatment at a Dose of 1.2 g/Kg/Day Is Safe for Long-Term Usage in Rats'. *International Journal of Molecular Sciences* 24 (4): 3799. https://doi.org/10.3390/ijms24043799.

337. Stern, Robert, and Howard I. Maibach. 2008. 'Hyaluronan in Skin: Aspects of Aging and Its Pharmacologic Modulation'. *Clinics in Dermatology* 26 (2): 106–22. https://doi.org/10.1016/j.clindermatol.2007.09.013.

338. Stichel, C. C., and H. W. Müller. 1994. 'Extensive and Long-Lasting Changes of Glial Cells Following Transection of the Postcommissural Fornix in the Adult Rat'. *Glia* 10 (2): 89–100. https://doi.org/10.1002/glia.440100203.

339. Streit, W. J., S. A. Walter, and N. A. Pennell. 1999. 'Reactive Microgliosis'. *Progress in Neurobiology* 57 (6): 563–81. https://doi.org/10.1016/s0301-0082(98)00069-0.

340. Struve, Jaime, P. Colby Maher, Ya-Qin Li, Shawn Kinney, Michael G. Fehlings, Charles Kuntz, and Larry S. Sherman. 2005. 'Disruption of the Hyaluronan-Based Extracellular Matrix in Spinal Cord Promotes Astrocyte Proliferation'. *Glia* 52 (1): 16–24. https://doi.org/10.1002/glia.20215.

341. Sugiyama, Sayaka, Ariel A. Di Nardo, Shinichi Aizawa, Isao Matsuo, Michel Volovitch, Alain Prochiantz, and Takao K. Hensch. 2008. 'Experience-Dependent Transfer of Otx2 Homeoprotein into the Visual Cortex Activates Postnatal Plasticity'. *Cell* 134 (3): 508–20. https://doi.org/10.1016/j.cell.2008.05.054.

342. Sun, Daniel, and Tatjana C. Jakobs. 2012. 'Structural Remodeling of Astrocytes in the Injured CNS'. *The Neuroscientist: A Review Journal Bringing Neurobiology, Neurology and Psychiatry* 18 (6): 567–88. https://doi.org/10.1177/1073858411423441.

343. Taha, Masoumeh Fakhr. 2010. 'Cell Based-Gene Delivery Approaches for the Treatment of Spinal Cord Injury and Neurodegenerative Disorders'. *Current Stem Cell Research & Therapy* 5 (1): 23–36. https://doi.org/10.2174/157488810790442778.

344. Takeda, S., and M. Aburada. 1981. 'The Choleretic Mechanism of Coumarin Compounds and Phenolic Compounds'. *Journal of Pharmacobio-Dynamics* 4 (9): 724–34. https://doi.org/10.1248/bpb1978.4.724.

345. Tamer, Tamer Mahmoud. 2013. 'Hyaluronan and Synovial Joint: Function, Distribution and Healing'. *Interdisciplinary Toxicology* 6 (3): 111–25. https://doi.org/10.2478/intox-2013-0019.

346. Tammi, M., P. O. Seppälä, A. Lehtonen, and M. Möttönen. 1978. 'Connective Tissue Components in Normal and Atherosclerotic Human Coronary Arteries'. *Atherosclerosis* 29 (2): 191–94. https://doi.org/10.1016/0021-9150(78)90007-2.

347. Tan, Andrew M., Weibing Zhang, and Joel M. Levine. 2005. 'NG2: A Component of the Glial Scar That Inhibits Axon Growth'. *Journal of Anatomy* 207 (6): 717–25. https://doi.org/10.1111/j.1469-7580.2005.00452.x.

348. Tan, Chin Lik, Melissa R. Andrews, Jessica C. F. Kwok, Tristan G. P. Heintz, Laura F. Gumy, Reinhard Fässler, and James W. Fawcett. 2012. 'Kindlin-1 Enhances Axon Growth on Inhibitory Chondroitin Sulfate Proteoglycans and Promotes Sensory Axon Regeneration'. *Journal of Neuroscience* 32 (21): 7325–35. https://doi.org/10.1523/JNEUROSCI.5472-11.2012.

349. Tan, Chin Lik, Jessica C. F. Kwok, Rickie Patani, Charles Ffrench-Constant, Siddharthan Chandran, and James W. Fawcett. 2011. 'Integrin Activation Promotes Axon Growth on Inhibitory Chondroitin Sulfate Proteoglycans by Enhancing Integrin Signaling'. *The Journal of Neuroscience: The Official Journal of the Society for Neuroscience* 31 (17): 6289–95. https://doi.org/10.1523/JNEUROSCI.0008-11.2011.

350. Testa, Damien, Alain Prochiantz, and Ariel A. Di Nardo. 2019. 'Perineuronal Nets in Brain Physiology and Disease'. *Seminars in Cell & Developmental Biology* 89 (May): 125–35. https://doi.org/10.1016/j.semcdb.2018.09.011.

351. Tetzlaff, Wolfram, Elena B. Okon, Soheila Karimi-Abdolrezaee, Caitlin E. Hill, Joseph S. Sparling, Jason R. Plemel, Ward T. Plunet, et al. 2011. 'A Systematic Review of Cellular Transplantation Therapies for Spinal Cord Injury'. *Journal of Neurotrauma* 28 (8): 1611–82. https://doi.org/10.1089/neu.2009.1177.

352. Thuret, Sandrine, Lawrence D. F. Moon, and Fred H. Gage. 2006. 'Therapeutic Interventions after Spinal Cord Injury'. *Nature Reviews. Neuroscience* 7 (8): 628–43. https://doi.org/10.1038/nrn1955.

353. Tillet, E., F. Ruggiero, A. Nishiyama, and W. B. Stallcup. 1997. 'The Membrane-Spanning Proteoglycan NG2 Binds to Collagens V and VI through the Central Nonglobular Domain of Its Core Protein'. *The Journal of Biological Chemistry* 272 (16): 10769–76. https://doi.org/10.1074/jbc.272.16.10769.

354. Timpl, R., and J. C. Brown. 1996. 'Supramolecular Assembly of Basement Membranes'. *BioEssays: News and Reviews in Molecular, Cellular and Developmental Biology* 18 (2): 123–32. https://doi.org/10.1002/bies.950180208.

355. Timpl, R., H. Rohde, P. G. Robey, S. I. Rennard, J. M. Foidart, and G. R. Martin. 1979. 'Laminin--a Glycoprotein from Basement Membranes'. *The Journal of Biological Chemistry* 254 (19): 9933–37.

356. Toole, B. P. 1990. 'Hyaluronan and Its Binding Proteins, the Hyaladherins'. *Current Opinion in Cell Biology* 2 (5): 839–44. https://doi.org/10.1016/0955-0674(90)90081-o.

357. ———. 2001. 'Hyaluronan in Morphogenesis'. *Seminars in Cell & Developmental Biology* 12 (2): 79–87. https://doi.org/10.1006/scdb.2000.0244.

358. Trabucchi, E., C. Baratti, A. Centemero, M. Zuin, E. Rizzitelli, and R. Colombo. 1986. 'Controlled Study of the Effects of Tiropramide on Biliary Dyskinesia'. *Pharmatherapeutica* 4 (9): 541–50.

359. Troeberg, Linda, and Hideaki Nagase. 2012. 'Proteases Involved in Cartilage Matrix Degradation in Osteoarthritis'. *Biochimica Et Biophysica Acta* 1824 (1): 133–45. https://doi.org/10.1016/j.bbapap.2011.06.020.

360. Uchida, Kenzo, Hideaki Nakajima, Alexander Rodriguez Guerrero, William Eb Johnson, Wagih El Masri, and Hisatoshi Baba. 2014. 'Gene Therapy Strategies

for the Treatment of Spinal Cord Injury'. *Therapeutic Delivery* 5 (5): 591–607. https://doi.org/10.4155/tde.14.20.

361. Ughrin, Yvonne M., Zhi Jiang Chen, and Joel M. Levine. 2003. 'Multiple Regions of the NG2 Proteoglycan Inhibit Neurite Growth and Induce Growth Cone Collapse'. *The Journal of Neuroscience: The Official Journal of the Society for Neuroscience* 23 (1): 175–86. https://doi.org/10.1523/JNEUROSCI.23-01-00175.2003.

362. Vavrek, R., J. Girgis, W. Tetzlaff, G. W. Hiebert, and K. Fouad. 2006. 'BDNF Promotes Connections of Corticospinal Neurons onto Spared Descending Interneurons in Spinal Cord Injured Rats'. *Brain: A Journal of Neurology* 129 (Pt 6): 1534–45. https://doi.org/10.1093/brain/awl087.

363. Verdera, Helena Costa, Klaudia Kuranda, and Federico Mingozzi. 2020. 'AAV Vector Immunogenicity in Humans: A Long Journey to Successful Gene Transfer'. *Molecular Therapy: The Journal of the American Society of Gene Therapy* 28 (3): 723–46. https://doi.org/10.1016/j.ymthe.2019.12.010.

364. Verma, Poonam, Sabrina Chierzi, Amanda M. Codd, Douglas S. Campbell, Ronald L. Meyer, Christine E. Holt, and James W. Fawcett. 2005. 'Axonal Protein Synthesis and Degradation Are Necessary for Efficient Growth Cone Regeneration'. *The Journal of Neuroscience: The Official Journal of the Society for Neuroscience* 25 (2): 331–42. https://doi.org/10.1523/JNEUROSCI.3073-04.2005.

365. Vigetti, Davide, Manuela Rizzi, Manuela Viola, Eugenia Karousou, Anna Genasetti, Moira Clerici, Barbara Bartolini, Vincent C. Hascall, Giancarlo De Luca, and Alberto Passi. 2009. 'The Effects of 4-Methylumbelliferone on Hyaluronan Synthesis, MMP2 Activity, Proliferation, and Motility of Human Aortic Smooth Muscle Cells'. *Glycobiology* 19 (5): 537–46. https://doi.org/10.1093/glycob/cwp022.

366. Vogelaar, Christina Francisca, Brigitte König, Stefanie Krafft, Veronica Estrada, Nicole Brazda, Brigida Ziegler, Andreas Faissner, and Hans Werner Müller. 2015. 'Pharmacological Suppression of CNS Scarring by Deferoxamine Reduces Lesion Volume and Increases Regeneration in an In Vitro Model for Astroglial-Fibrotic Scarring and in Rat Spinal Cord Injury In Vivo'. *PloS One* 10 (7): e0134371. https://doi.org/10.1371/journal.pone.0134371.

367. Walker, P. S., D. Dowson, M. D. Longfield, and V. Wright. 1968. '"Boosted Lubrication" in Synovial Joints by Fluid Entrapment and Enrichment'. *Annals of the Rheumatic Diseases* 27 (6): 512–20. https://doi.org/10.1136/ard.27.6.512.

368. Walter, P., and W. Seidel. 1979. '[Studies on the effect of 4-methyl-umbelliferon (Hymecromone) in patients following surgical revision of the biliary pathways]'. *Der Chirurg; Zeitschrift Fur Alle Gebiete Der Operativen Medizen* 50 (7): 436–40.

369. Wang, Dan, Phillip W. L. Tai, and Guangping Gao. 2019. 'Adeno-Associated Virus Vector as a Platform for Gene Therapy Delivery'. *Nature Reviews. Drug Discovery* 18 (5): 358–78. https://doi.org/10.1038/s41573-019-0012-9.

370. Wang, Difei, and James Fawcett. 2012. 'The Perineuronal Net and the Control of CNS Plasticity'. *Cell and Tissue Research* 349 (1): 147–60. https://doi.org/10.1007/s00441-012-1375-y.

371. Wang, Difei, Ronaldo M. Ichiyama, Rongrong Zhao, Melissa R. Andrews, and James W. Fawcett. 2011. 'Chondroitinase Combined with Rehabilitation Promotes Recovery of Forelimb Function in Rats with Chronic Spinal Cord Injury'. *The Journal of Neuroscience: The Official Journal of the Society for Neuroscience* 31 (25): 9332–44. https://doi.org/10.1523/JNEUROSCI.0983-11.2011.

372. Wang, Xiaodu, Rui Hua, Abu Ahsan, Qingwen Ni, Yehong Huang, Sumin Gu, and Jean X. Jiang. 2018. 'AGE-RELATED DETERIORATION OF BONE TOUGHNESS IS RELATED TO DIMINISHING AMOUNT OF MATRIX GLYCOSAMINOGLYCANS (GAGS)'. *JBMR Plus* 2 (3): 164–73. https://doi.org/10.1002/jbm4.10030.

373. Warnock, James N., Claire Daigre, and Mohamed Al-Rubeai. 2011. 'Introduction to Viral Vectors'. *Methods in Molecular Biology (Clifton, N.J.)* 737: 1–25. https://doi.org/10.1007/978-1-61779-095-9_1.

374. Weidner, N., R. J. Grill, and M. H. Tuszynski. 1999. 'Elimination of Basal Lamina and the Collagen "Scar" after Spinal Cord Injury Fails to Augment Corticospinal Tract Regeneration'. *Experimental Neurology* 160 (1): 40–50. https://doi.org/10.1006/exnr.1999.7200.

375. Werner, A., M. Willem, L. L. Jones, G. W. Kreutzberg, U. Mayer, and G. Raivich. 2000. 'Impaired Axonal Regeneration in Alpha7 Integrin-Deficient Mice'. *The Journal of Neuroscience: The Official Journal of the Society for Neuroscience* 20 (5): 1822–30. https://doi.org/10.1523/JNEUROSCI.20-05-01822.2000.

376. Whitman, Patrick A., Marjorie V. Launico, and Oluwaseun O. Adigun. 2024. 'Anatomy, Skin, Dermatomes'. In *StatPearls*. Treasure Island (FL): StatPearls Publishing. http://www.ncbi.nlm.nih.gov/books/NBK535401/.

377. 'WHO'. n.d. https://www.who.int/news-room/fact-sheets/detail/injuries-and-violence).

378. Winter, Carla C., Zhigang He, and Anne Jacobi. 2022. 'Axon Regeneration: A Subcellular Extension in Multiple Dimensions'. *Cold Spring Harbor Perspectives in Biology* 14 (3): a040923. https://doi.org/10.1101/cshperspect.a040923.

379. Wirz, Markus, David H. Zemon, Ruediger Rupp, Anke Scheel, Gery Colombo, Volker Dietz, and T. George Hornby. 2005. 'Effectiveness of Automated Locomotor Training in Patients with Chronic Incomplete Spinal Cord Injury: A Multicenter Trial'. *Archives of Physical Medicine and Rehabilitation* 86 (4): 672–80. https://doi.org/10.1016/j.apmr.2004.08.004.

380. Ye, Feng, Chungho Kim, and Mark H. Ginsberg. 2012. 'Reconstruction of Integrin Activation'. *Blood* 119 (1): 26–33. https://doi.org/10.1182/blood-2011-04-292128.

381. Yong, Nie, and Cai Guoping. 2008. 'Upregulation of Matrix Metalloproteinase-9 Dependent on Hyaluronan Synthesis after Sciatic Nerve Injury'. *Neuroscience Letters* 444 (3): 259–63. https://doi.org/10.1016/j.neulet.2008.08.042.

382. Yoo, Soonmoon, Michael P. Nguyen, Mitsunori Fukuda, George D. Bittner, and Harvey M. Fishman. 2003. 'Plasmalemmal Sealing of Transected Mammalian Neurites Is a Gradual Process Mediated by Ca(2+)-Regulated Proteins'. *Journal of Neuroscience Research* 74 (4): 541–51. https://doi.org/10.1002/jnr.10771.

383. Yousefifard, Mahmoud, Atousa Janzadeh, Kosar Mohamed Ali, Mohammad Hossein Vazirizadeh-Mahabadi, Arash Sarveazad, Arian Madani Neishaboori, and Mostafa Hosseini. 2022. 'Chondroitinase ABC Administration in Locomotion Recovery After Spinal Cord Injury: A Systematic Review and Meta-Analysis'. *Basic and Clinical Neuroscience* 13 (5): 609–24. https://doi.org/10.32598/bcn.2021.1422.1.

384. Yudin, Dmitry, Shlomit Hanz, Soonmoon Yoo, Elena Iavnilovitch, Dianna Willis, Tal Gradus, Deepika Vuppalanchi, et al. 2008. 'Localized Regulation of Axonal RanGTPase Controls Retrograde Injury Signaling in Peripheral Nerve'. *Neuron* 59 (2): 241–52. https://doi.org/10.1016/j.neuron.2008.05.029.

385. Yurchenco, P. D., and Y. S. Cheng. 1993. 'Self-Assembly and Calcium-Binding Sites in Laminin. A Three-Arm Interaction Model'. *The Journal of Biological Chemistry* 268 (23): 17286–99.

386. Yurchenco, Peter D. 2011. 'Basement Membranes: Cell Scaffoldings and Signaling Platforms'. *Cold Spring Harbor Perspectives in Biology* 3 (2): a004911. https://doi.org/10.1101/cshperspect.a004911.

387. Zacharias, Ute, and Uwe Rauch. 2006. 'Competition and Cooperation between Tenascin-R, Lecticans and Contactin 1 Regulate Neurite Growth and Morphology'. *Journal of Cell Science* 119 (Pt 16): 3456–66. https://doi.org/10.1242/jcs.03094.

388. Zhang, Jianmin, Xiaobing Wu, Chuan Qin, Jin Qi, Shibin Ma, Huiyuan Zhang, Qingli Kong, Dongqing Chen, Denian Ba, and Wei He. 2003. 'A Novel Recombinant Adeno-Associated Virus Vaccine Reduces Behavioral Impairment and Beta-Amyloid Plaques in a Mouse Model of Alzheimer's Disease'. *Neurobiology of Disease* 14 (3): 365–79. https://doi.org/10.1016/j.nbd.2003.07.005.

389. Zhang, Xueguang, Xiangmei Chen, Quan Hong, Hongli Lin, Hanyu Zhu, Qingxin Liu, Jianzhong Wang, et al. 2006. 'TIMP-1 Promotes Age-Related Renal Fibrosis through Upregulating ICAM-1 in Human TIMP-1 Transgenic Mice'. *The Journals of Gerontology. Series A, Biological Sciences and Medical Sciences* 61 (11): 1130–43. https://doi.org/10.1093/gerona/61.11.1130.

390. Zhang, Y., J. K. Winterbottom, M. Schachner, A. R. Lieberman, and P. N. Anderson. 1997. 'Tenascin-C Expression and Axonal Sprouting Following Injury to the Spinal Dorsal Columns in the Adult Rat'. *Journal of Neuroscience Research* 49 (4): 433–50.

391. Zhao, Rong-Rong, Melissa R. Andrews, Difei Wang, Philippa Warren, Miriam Gullo, Lisa Schnell, Martin E. Schwab, and James W. Fawcett. 2013. 'Combination Treatment with Anti-Nogo-A and Chondroitinase ABC Is More Effective than Single Treatments at Enhancing Functional Recovery after Spinal Cord Injury'. *The European Journal of Neuroscience* 38 (6): 2946–61. https://doi.org/10.1111/ejn.12276.

392. Ziv, N. E., and M. E. Spira. 1995. 'Axotomy Induces a Transient and Localized Elevation of the Free Intracellular Calcium Concentration to the Millimolar Range'. *Journal of Neurophysiology* 74 (6): 2625–37. https://doi.org/10.1152/jn.1995.74.6.2625.

10. AUTHOR'S PUBLICATIONS

10.1 Dissertation-relevant publications

1. **Štěpánková K**, Mareková D, Kubášová K, Sedláček R, Turnovcová K, Vacková I, Kubinová Š, Makovický P, Petrovičová M, Kwok JCF, Jendelová P, Machová Urdzíková L. 4Methylumbeliferone Treatment at a Dose of 1.2 g/kg/Day Is Safe for Long-Term Usage in Rats. Int J Mol Sci. 2023 Feb 14;24(4):3799. doi: 10.3390/ijms24043799. PMID: 36835210; PMCID: PMC9959083. **IF: 6.208**

Student's contribution: experiments, imaging, data collection, analysis and interpretation, manuscript preparation

2. **Štepánková K*#**, Chudíčková M*, Šimková Z, Martinez-Varea N, Kubinová Š, Machová Urdzíková L#, Jendelová P#, Kwok JCF#. Low oral dose of 4-methylumbelliferone reduces glial scar but is insufficient to induce functional recovery after spinal cord injury. Sci Rep. 2023 Nov 6;13(1):19183. doi: 10.1038/s41598-023-46539-5. Erratum in: Sci Rep. 2024 Jan 8;14(1):785. PMID: 37932336; PMCID: PMC10628150. **IF: 4.6**

*** s***hared first authorship*

 # shared corresponding authorship

Student's contribution: experiments, imaging, data collection, analysis and interpretation, manuscript preparation

10.2 Dissertation-relevant publications but not included

1. Smith NJ, Doody NE, **Štěpánková K**, Fuller M, Ichiyama RM, Kwok JCF, Egginton S. Spatiotemporal microvascular changes following contusive spinal cord injury. Front Neuroanat. 2023 Mar 21;17:1152131. doi: 10.3389/fnana.2023.1152131. PMID: 37025098; PMCID: PMC10070689. **IF: 2.9**

2. Machova Urdzikova L, Cimermanova V, Karova K, Dominguez J, **Stepankova K**, Petrovicova M, Havelikova K, D Gandhi C, Jhanwar-Uniyal M, Jendelova P. The Role of Green Tea Catechin Epigallocatechin Gallate (EGCG) and Mammalian Target of Rapamycin (mTOR) Inhibitor PP242 (Torkinib) in the Treatment of Spinal Cord Injury. Antioxidants (Basel). 2023 Feb 3;12(2):363. doi: 10.3390/antiox12020363. PMID: 36829922; PMCID: PMC9952296. **IF: 7.767**

3. **Stepankova K**, Jendelova P, Machova Urdzikova L. Planet of the AAVs: The Spinal Cord Injury Episode. Biomedicines. 2021 May 28;9(6):613. doi: 10.3390/biomedicines9060613. PMID: 34071245; PMCID: PMC8228984. **IF: 4.717**

4. Krupa P, **Stepankova K**, Kwok JC, Fawcett JW, Cimermanova V, Jendelova P, Machova Urdzikova L. New Model of Ventral Spinal Cord Lesion Induced by Balloon Compression in Rats. Biomedicines. 2020 Nov 5;8(11):477. doi: 10.3390/biomedicines8110477. PMID: 33167447; PMCID: PMC7694490. **IF: 4.717**

11. APPENDIX